UNIVERSITÀ DEGLI STUDI DI MILANO

Scuola di Dottorato in Scienze Biologiche e Molecolari

XXIV Ciclo

Mechanisms preserving genome integrity in *Saccharomyces cerevisiae*

D. Novarina

PhD Thesis

Scientific tutor: Prof. Paolo Plevani

Academic year: 2011-2012

SSD: BIO/11

Thesis performed at Dipartimento di Bioscienze

Contents

Part I

Abstract

The integrity of the genome is continuously jeopardized by endogenous reactive byproducts of cellular metabolism and genotoxic insults by environmental agents, as well as by the DNA transactions (replication, transcription and recombination) required for cell survival and proliferation. Failure of the mechanisms deputed to the maintenance of genome integrity leads to genome instability, which is a hallmark of cancer and a driving force of tumorigenesis. To fully understand the mechanisms leading to genome instability and the cellular pathways counteracting them, three basic tasks must be achieved: i) identify all the genes implicated in the control of genome integrity; ii) unravel their biological role; iii) define the mechanistic molecular details of the processes in which they are implicated. This thesis describes work performed in the budding yeast *Saccharomyces cerevisiae* to explore the genome stability landscape at all these three levels. This model system is extremely useful for two main reasons: a) its high genetic tractability allows the application of genome-wide genetic screenings; b) the large conservation of the genome integrity pathways allows to extend the findings obtained in yeast to other eukaryotic organisms.

We performed a genome-wide screen, based on the overexpression of the *DDC2* DNA damage checkpoint gene in the yeast deletion collection, to identify genome stability genes on the basis of spontaneous accumulation of endogenous DNA damage in the corresponding mutant strains. Our screen identified several genes implicated in the control of genome integrity, highlighting, in particular, a key role for pathways protecting against oxidative stress. We present here the preliminary characterization of a new genome integrity gene, *VID22*.

We also investigated the mechanisms counteracting a newly discovered

source of genome instability, namely ribonucleotides (rNTPs) incorporated in genomic DNA during replication. We uncovered a role for RNase H enzymes, template switch pathways and Pol ζ translesion polymerase in protecting from misincorporated rNTPs. Given that mutations in any of the three human RNase H2 subunits were proven to cause Aicardi-Goutiéres Syndrome, these results might contribute to shed light on the complex and largely unknown pathogenetic mechanism of this rare genetic disease.

Finally, we studied the molecular details underlying the role of Rad9 mediator protein in DNA damage checkpoint activation, exploring the dynamics of Rad9 dimerization, chromatin binding, CDK-dependent phosphorylation and checkpoint activation in G1 and M phases of the cell cycle; in particular, we characterized an M-phase specific pathway for checkpoint activation which is relies on Rad9-Dpb11 interaction.

State of the art

1 Introduction: DNA damage and genome integrity maintenance

The integrity of the DNA molecules, which are the depositary of the genetic information in all living organisms, is continuously challenged by the action of multiple endogenous and exogenous agents. First of all, as a consequence of its intrinsic instability in an aqueous environment, DNA molecules can undergo spontaneous hydrolysis, which can result in depurination and subsequent formation of abasic sites, or deamination, yielding miscoding bases (Lindahl, 1993).

Second, DNA can be severely damaged by multiple byproducts of the normal cellular metabolism. Reactive oxigen and nitrogen species cause single-strand DNA breaks, formation of abasic sites and base oxidation, the most common oxidized lesion being 8-oxo-guanine (8-oxo-G). Reactive carbonil species (RCS) originating mainly during lipid peroxidation yield mispairing DNA exocyclic adducts, DNA strand breaks and DNA cross-links. Moreover, DNA alkylation by endogenous alkylating agents may result in abasic sites, replication-blocking lesions, or point mutations during replication, while estrogen and cholesterol metabolites can form depurinating DNA adducts or free radicals which cause oxidative damage (De Bont and van Larebeke, 2004). Among endogenous sources of DNA damage, also DNA replication errors should be included, resulting in dNTPs misincorporation or in accidental rNTPs incorporation in DNA (see Section *Causes of genome instability*).

Third, chemical or physical environmental agents can cause hazardous

alterations in DNA structure, above all ionizing radiation (IR) and ultraviolet (UV) component of sunlight. UV light causes bulky lesions on DNA (mainly cyclobutane pyrimidine dimers (CPDs) and 6-4 pyrimidine-pyrimidone photoproducts (6-4PPs)) which induce a distortion of the DNA helix, which represent an obstacle for replication and transcription. Moreover, near-UV light causes covalent modifications in DNA similar to those produced by oxidative damage. Instead, lesions generated by IR (X and γ rays) are mainly double-strand breaks (DSBs) and single-strand breaks (SSBs) (Lindahl and Wood, 1999). Among environmental sources of DNA damage it has to be mentioned cigarette smoke, which causes aromatic DNA adducts and oxidative damage (Phillips et al., 1988; Kiyosawa et al., 1990). Also chemotherapeutic agents can cause DNA lesions: alkylating agents such as methyl methanesulfonate (MMS) and temozolomide alkylate DNA, while crosslinking agents such as mitomycin C (MMC), cisplatin, psoralen, and nitrogen mustard introduce covalent links between the two DNA strands (interstrand crosslinks, ICLs), which block transcription and replication, or between bases of the same DNA strand (intrastrand crosslinks) (Schärer, 2005). Furthermore, topoisomerase inhibitors such as camptothecin (CPT) and etoposide, induce the formation of SSBs or DSBs by blocking topoisomerase I or II in a topoisomerase-DNA covalent complex (Pommier et al., 2010).

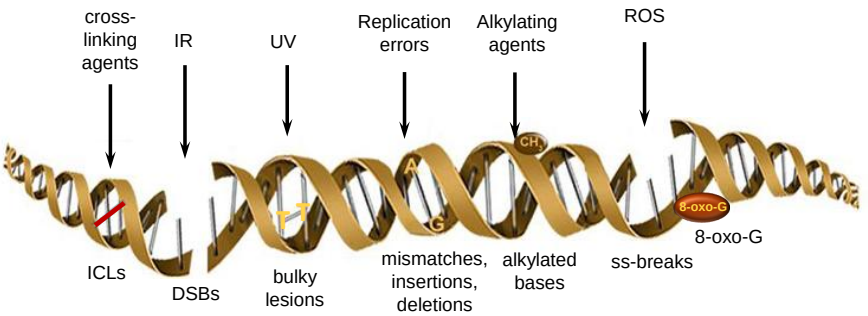

Figure 1: *The main sources of DNA damage and the most common lesions they create.*

DNA lesions are extremely harmful because they can be either mutagenic (alteration of the genetic information) or cytotoxic (impairment of cell viability). The extent of DNA damage occurring in living organisms is surprisingly high, since it was estimated that each cell experiences about 10^5DNA lesions per day (Lindahl, 1993). Therefore, a serious task posed to all cells is to maintain the integrity of the genome despite all the attacks to which it is continuously subject, in order to ensure cell survival and preserve the genetic information encoded in the DNA molecules, thus allowing the faithful transmission of the genome across generations.

2 Genomic instability and its consequences

The failure of a cell to maintain the integrity of its genetic material leads to a condition known as genomic instability, characterized by the accelerated accumulation of a wide spectrum of genetic alterations, ranging from point mutations to gross chromosomal rearrangements. Different classes of genomic instability have been described: i) instability leading to mutations (including base substitutions, micro-insertions and micro-deletions); ii) mini- and micro-satellite instability (MIN) (leading to expansion or contraction of repetitive DNA sequences); iii) gross chromosomal rearrangements (GCRs), which encompass several aberrations in chromosome structure like translocations, duplications, inversions or deletions; iv) chromosomal instability (CIN), defined as a persistently high rate of loss and gain of whole chromosomes, which results in alterations in the number of chromosomes (a state known as aneuploidy) (Aguilera and Gómez-González, 2008).

Genomic instability is present in almost all human cancers and it is considered one of the major hallmarks of cancer (Negrini et al., 2010; Hanahan and Weinberg, 2011). Not only, but due to the huge number of mutations required for tumor development, genomic instability was proposed as a key driving force in tumorigenesis (Loeb, 1991).

Cancer is a multistep process, characterized by the gradual accumulation of genetic alterations. Fig. 2 depicts an overview of the process of

tumor development modeled as a darwinian evolution according to the so-called "mutator hypothesis", in which subsequent rounds of mutation and selection drive cancer progression (Loeb, 2011). The mutator hypothesis moves from the consideration that the observed spontaneous mutation rate in somatic human cells ($\sim 2 \times 10^{-7}$ mutations/cell division) cannot account for the several genetic changes necessary for cancer development (Renan, 1993). This model proposes that at the beginning of cancerogenesis, due to endogenous or environmental DNA damage, a "mutator mutation" occurs in a gene responsible for genome integrity maintenance, resulting in an overall increase of the mutation rate. This enhanced mutagenesis will favor the occurrence of "driver mutations" in oncogenes or tumor suppressor genes (Beckman and Loeb, 2006), which provide a proliferative advantage and will thus be selected within the precancerous cell population, according to changes in the microenvironment. To a certain extent, this is expected to be a positive feedback mechanisms, since in a genetically unstable cell new mutations may occur which further increase genomic instability. Subsequent multiple rounds of selection and mutation will direct the evolution of the tumor up to a malignant cancer. Together with driver and mutator mutations, tumor cells will also acquire a number of "passenger mutations", that do not confer any growth advantage, and account for the heterogeneity within the tumor, which may be responsible for resistance to chemoterapeutic agents (Bielas et al., 2006).

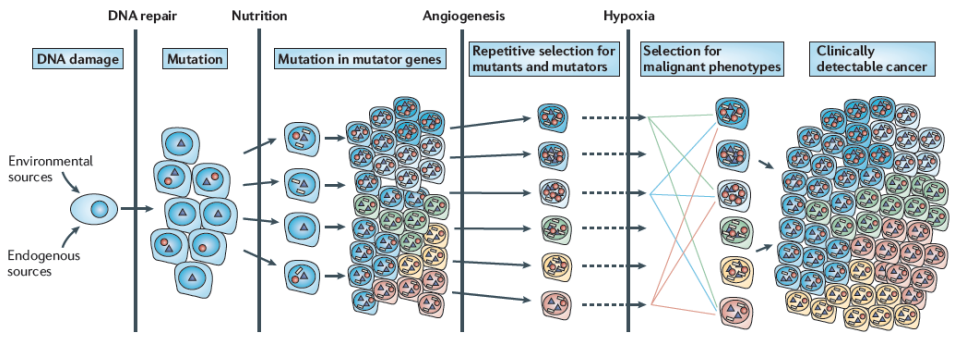

Figure 2: *Model of tumor progression according to the mutator hypothesis* (from Loeb, 2011).

The main argument against this model is that mutations in genome stability genes (also called "caretaker genes") are usually recessive. Therefore, two independent mutations inactivating both alleles are needed to get an unstable genome, and the occurrence of this event before the onset of genomic instability is expected to have a very low probability (Bodmer et al., 2008). In accordance with these considerations, high-throughput studies on cancer cell lines in many cases failed to detect mutations in known caretaker genes or to identify novel putative caretaker genes frequently mutated in tumors (Wang et al., 2004; Sjöblom et al., 2006; Wood et al., 2007; Jones et al., 2008; Parsons et al., 2008; Cancer Genome Atlas Research Network, 2008; Ding et al., 2008). Therefore, an alternative model was proposed, the so-called "oncogene-induced DNA damage model for cancer development", which still partially relies on genomic instability, but places oncogene-driven replication stress at the first stage of tumorigenesis (Halazonetis et al., 2008). This model comes from the observation that both precancerous and cancerous lesions exhibit a persistent DNA damage response indicating the presence of DSBs (Bartkova et al., 2005; Gorgoulis et al., 2005). The authors propose that the activation of a oncogene which deregulates entry into the cell cycle is the key initial step of cancer development. Activated oncogenes can induce a state of replication stress, causing frequent replication fork collapse which, in turn, leads to DSBs especially at particular chromosomal loci known as fragile sites (see Section *Causes of genome instability* for details). The genomic instability thus generated can subsequently lead to the loss of growth restrictions (typically by checkpoints, apoptosis and senescence), which marks the transition from precancerous to cancerous lesions (Fig. 3).

These two apparently conflicting models can be reconciled in a global overview of carcinogenesis which takes into account the differences between hereditary and sporadic cancers, as shown in Fig. 4 (Negrini et al., 2010). The mutator hypothesis, which places genomic instability as the earliest step of tumorigenesis, can explain very effectively the genesis of hereditary cancers: here, a germline mutation in one of the genome stability genes is already present in all the patient's cells, and therefore a single mutation

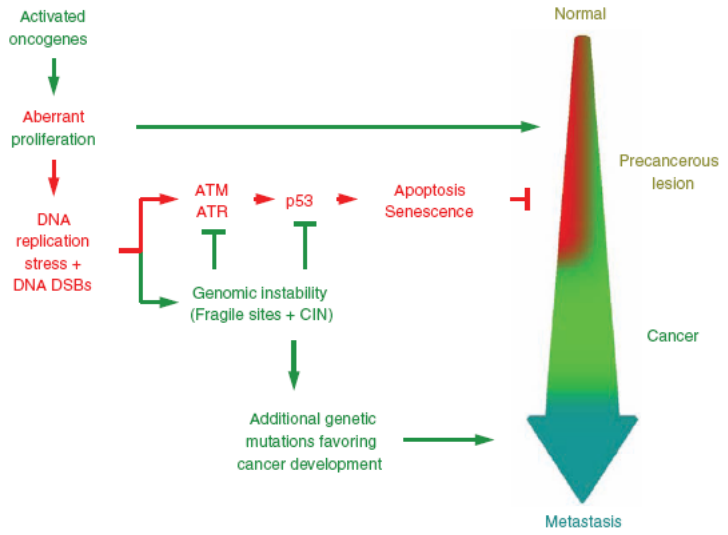

Figure 3: *The oncogene-induced DNA damage model for cancer development* (from Halazonetis et al., 2008).

is required to inactivate the other allele, resulting in genomic instability. And indeed, caretaker genes (mainly DNA repair or mitotic checkpoint genes) were often found mutated in hereditary cancers (Fishel et al., 1993; Leach et al., 1993; Al-Tassan et al., 2002; Cleaver, 2005; Ripperger et al., 2009). Instead, the oncogene-induced DNA replication stress model is best suitable to explain the mechanisms leading to sporadic cancer, not lastly due to the fact that activated oncogenes are generally dominant (Lee and Muller, 2010). In this view, deregulation of a growth-regulating gene leads to replication stress and DNA damage, which cause genomic instability and subsequently all the other cancer hallmarks. In fact, the results of high-throughput sequencing studies of human sporadic cancers are in accordance with the oncogene-induced DNA replication stress model, since the most frequently mutated or deregulated genes were found to be classical oncogenes or tumor suppressors (Sjöblom et al., 2006; Wood et al., 2007; Jones et al., 2008; Parsons et al., 2008; Cancer Genome Atlas Research Network, 2008; Ding et al., 2008). It is worth noting that, despite differing in the initial event placed at the basis of carcinogenesis, both models rely upon genomic instability as a key factor for tumor development.

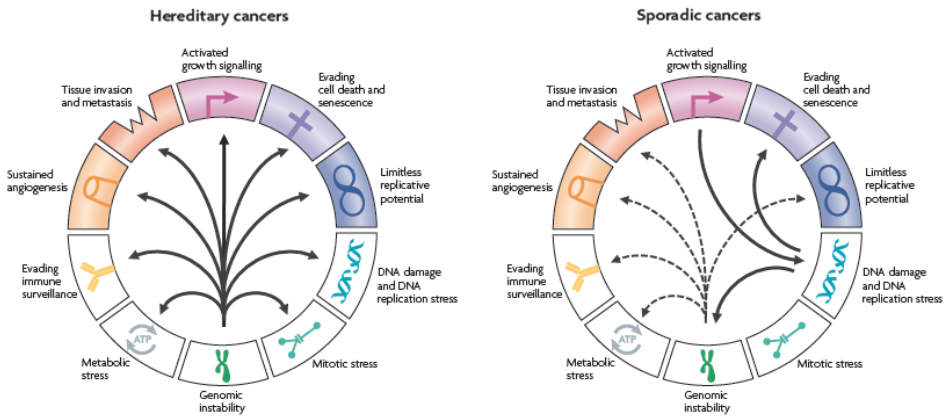

Figure 4: *The role of genomic instability in the genesis of hereditary and sporadic cancers* (modified from Negrini et al., 2010).

3 Causes of genome instability

Despite the need to maintain the integrity of the genetic material in order to guarantee the stability of the genetic information, DNA is anything but an inactive storage molecule. Instead, normal cellular metabolism entails complex DNA transactions in order to transcribe, duplicate and repair the genetic material. Therefore, apart from endogenous or environmental sources of DNA damage, a very serious threat to genome integrity comes from the DNA metabolism itself: indeed, the two main cellular processes involving DNA, namely transcription and replication, are potential sources of chromosome breakage. In accordance with the oncogene-induced DNA damage model for cancer development, replication stress and subsequent replication errors or replication failures appear to be the main origins of genome instability (Gorgoulis et al., 2005; Kunkel, 2004; Aguilera and Gómez-González, 2008; Halazonetis et al., 2008). Fragile sites and highly transcribed regions are often responsible for the impairment of replication (Durkin and Glover, 2007; Aguilera and García-Muse, 2012). Repetitive sequences, DNA secondary structures, telomere disfunction and chromosome segregation failures are additional factors contributing to the onset of genomic instability (Aguilera and Gómez-González, 2008; Bochman et al., 2012; Frias et al., 2012; Holland and Cleveland, 2012).

A comprehensive overview of the mechanisms leading to the different outcomes of genomic instability is presented in Fig. 5.

3.1 The replication fork at the center of genome instability

During replication, DNA is most vulnerable, and its integrity is jeopardised by a series of events which may perturb replication fork progression. Accordingly, replication failures emerged as one of the main sources of genomic instability, due to the generation of both ssDNA gaps and DSBs by multiple mechanisms (Aguilera and Gómez-González, 2008).

Replication of a nicked template inevitably results in the generation of a DSB (Cortés-Ledesma and Aguilera, 2006).

When a replication forks encounters an obstacle on the leading strand which prevents its progression (such obstacle may be a DNA adduct, a protein, a DNA secondary structure or the transcription machinery), uncoupling between replicative helicases and polymerases occurs and large ssDNA stretches are generated: this situation is defined as "replication fork stalling" (Carr et al., 2011). If the replisome remains associated with the stalled fork, resumption of DNA synthesis can occur after the removal of the obstacle. Conversely, if the stalled fork is not properly stabilized or the obstacle cannot be removed, the replisome can disassemble, resulting in "replication fork collapse", with the subsequent generation of ssDNA gaps and DSBs (Lopes et al., 2001; Sogo et al., 2002). Moreover, in case of replication fork stalling or uncoupling between leading-strand and lagging-strand synthesis (Pagès and Fuchs, 2003), the fork can reverse forming a Holliday junction structure known as "chicken foot" (Postow et al., 2001; Sogo et al., 2002): this structure can revert back to a normal fork, but it can also be cleaved resulting in a DSB (Jaktaji and Lloyd, 2003; Heller and Marians, 2006), or it can be processed by nucleases to generate a strech of ssDNA (Cotta-Ramusino et al., 2005).

Alternatively the replication fork can encounter a lesion on the template strand which prevents DNA synthesis without impairing fork progression.

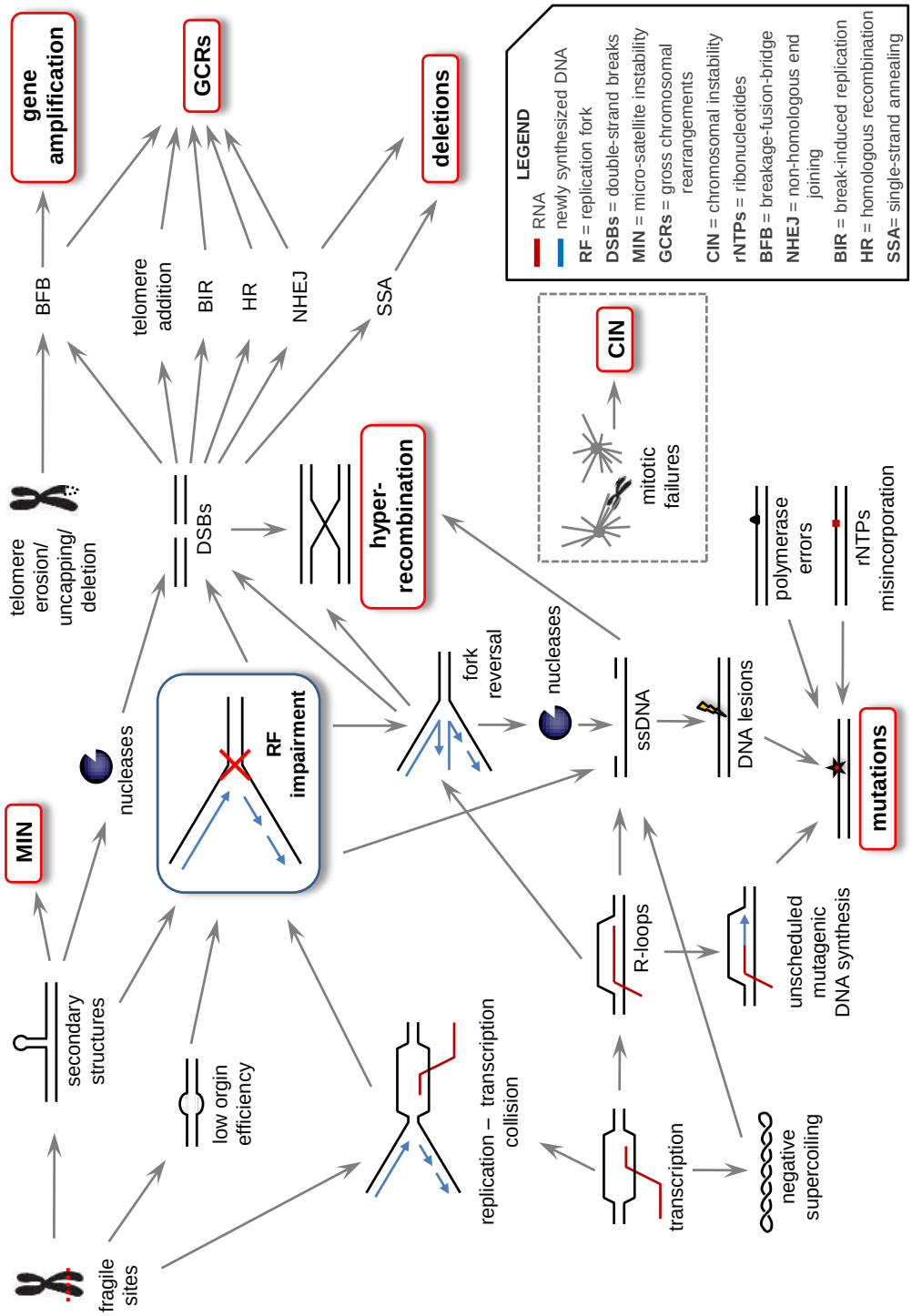

Figure 5: *An overview of the mechanisms leading to genomic instability.*

If the lesion is on the lagging strand, a ssDNA gap is left between two neighboring Okazaki fragments; if the lesion is on the leading strand DNA, synthesis can resume past the obstacle, leaving a ssDNA gap behind.

DSBs are a potential source of several GCRs (Fig. 6), according to the different ways in which they are processed and repaired (for details on the repair pathways see Section *DNA repair pathways*). Direct repair by non-homologous end joining (NHEJ) may lead to translocations, interstitial deletions, inversions or insertions; de-novo telomere addition results in a terminal deletion, while the process known as "breakage-bridge fusion" (fusion of two chromosomes resulting in a dicentric chromosome, followed by breaking during chromosome segregation) can generate translocations and gene amplification. If the DSB is processed by nucleases (resection), the break is channeled in a recombinative pathway: classical homologous recombination (HR) or synthesis-dependent strand annealing (SDSA) yield reciprocal translocations, interstitial deletions, duplications and inversions, while break-induced replication (BIR) results mainly in non-reciprocal translocations, but also interstitial deletions and inversions; repair by single-strand annealing (SSA), instead, causes interstitial deletions (Aguilera and Gómez-González, 2008).

Also ssDNA generated at the replication fork is a potential source of genomic instability. Indeed, experimental observations suggest that ssDNA itself can be recombinogenic, even without being converted to a DSB (Fabre et al., 2002; Lettier et al., 2006): therefore, the long ssDNA stretches generated as a consequence of a perturbed replication could be a source of hyper-recombination.

3.2 DNA replication fidelity

The accuracy of DNA synthesis according to the Watson-Crick base pairing rules is a key aspect in the transmission of an intact genetic information (Watson and Crick, 1953). For this reason, multiple biochemical mechanisms ensure the fidelity of replicative polymerases (eucaryotic Pol α, Pol δ and Pol ε): selectivity for the insertion of the correct nucleotide is pro-

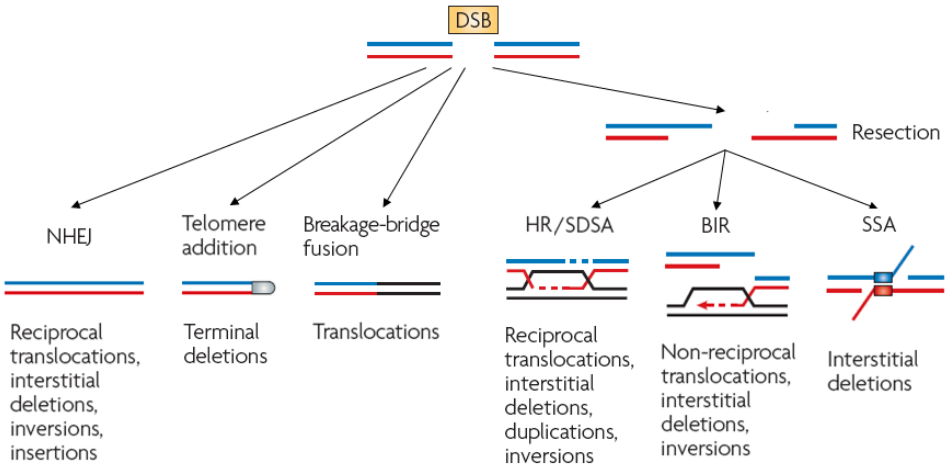

Figure 6: *Different gross chromosomal rearrangements following a double-strand break* (modified from Aguilera and Gómez-González, 2008).

vided by base-base hydrogen bonding, water exclusion from the catalitic site, and above all a steric selection on base pair shape and size within the active site (Kunkel, 2004). Moreover, many DNA polymerases possess intrinsic proofreading activity, based on a higher efficiency of these enzymes in extending a matched primer compared to an unmatched one, and on an exonuclease activity wich allows the excision of the mispaired base (Kunkel, 2004).

Despite these fidelity-ensuring systems, errors in base incorporation may occur during replication (McCulloch and Kunkel, 2008): it was estimated that base substitution error rate of replicative polymerases in vivo is in the range of 10^{-7} to 10^{-8}(Schaaper, 1993; Loeb, 1991). Furthermore, insertions or deletions of single bases may result from strand misalignement, a process which is strongly favored during replication of repetitive sequences (Streisinger et al., 1966). In addiction, to replicate past a damaged template, cells in most cases use error-prone translesion synthesis (TLS) polymerases (namely Pol ζ, Pol η, Pol ι and Pol $\varkappa$), which can accomodate helix-distorting modified bases in their active site, at the expenses of fidelity in nucleotide incorporation (Friedberg et al., 2002) (see Section *DNA*

damage tolerance mechanisms).

3.2.1 Ribonucleotide misincorporation in DNA

Recently, another potential source of genome instability linked to replication has been described. Replicative polymerases can incorporate at extremely high rates ribonucleotides (rNTPs) instead of deoxyribonucleotides (dNTPs) during DNA synthesis, mainly due to the higher rNTPs levels over dNTPs in the cell. Estimates in yeast considering the rate of discrimination against rNTPs incorporation of the different replicative polymerases and their relative contribution to genome replication, yielded a likely incorporation of 10^4 rNTPs per nuclear genome during each round of replication (Nick McElhinny et al., 2010b). Ribonucleoside monophosphates (rNMP) embedded in DNA can jeopardize genome stability in multiple ways: first of all, due to the reactive hydroxyl group at the 2' position, RNA is 100000-fold more prone to hydrolysis than DNA under physiological conditions (Li and Breaker, 1999). Moreover, the presence of rNMPs alters DNA helix parameters (Jaishree et al., 1993; DeRose et al., 2012), and this distortion may constitute an obstacle which impedes replication fork progression: indeed Pols α, δ and ε can replicate past a single ribonucleotide with reduced efficiency (Nick McElhinny et al., 2010b; Watt et al., 2011). Finally, it was directly demonstrated that increased ribonucleotide incorporation in DNA causes genomic instability, likely due to mutagenic enzimatic processing of the RNA:DNA moiety (Nick McElhinny et al., 2010a; Kim et al., 2011; Clark et al., 2011; Shen et al., 2012).

3.3 Fragile sites

Chromosomal fragile sites are defined as specific loci which undergo frequent gaps or breaks under replication stress, and are hotspots of chromosome rearrangements in tumor cells (Durkin and Glover, 2007; Lukusa and Fryns, 2008). Fragile sites are conserved from mammals to lower eukaryotes, including yeast, where many "replication slow zones" (RSZ), multiple "replication fork pausing (RFP) sites" and two "fragile sites" (FS1

and FS2) were identified (Cha and Kleckner, 2002; Lemoine et al., 2005; Ivessa et al., 2003; Admire et al., 2006).

Chromosomal fragile sites have been divided in two classes with distinct features. Rare fragile sites are observed in less than 5% of the cases and are inherited in a mendelian fashion: they are made up of microsatellite trinucleotide repeats (TNRs) or AT-rich minisatellite repeats, and are often associated with genetic diseases caused by repeat expansion (López Castel et al., 2010; Durkin and Glover, 2007). Common fragile sites (CFSs), instead, are present in all individuals, since they represent normal components of chromosome structure, and generally contain AT-rich sequences, but not nucleotide repeats (Durkin and Glover, 2007; Debatisse et al., 2012). The mechanisms underlying fragility of these sites and the genome instability outcomes differ for the two classes described.

3.3.1 Rare fragile sites

The instability of TNRs and AT-rich minisatellites relies upon their ability to form unusual secondary structures (such as hairpins, stem-loops or DNA triplexes: see Section *Unusual secondary structures*) during replication, which trigger MIN: in particular, hairpin structures at the 5´ end of a displaced Okazaki fragment during lagging strand synthesis can promote repeat expansion (Freudenreich et al., 1998; Spiro et al., 1999); similarly, secondary structures on the lagging strand can cause replication slippage events, which result in repeat deletions (Aguilera and Gómez-González, 2008).

Moreover, these secondary structures can be processed by nucleases yielding a DSB (Leach et al., 1997; Lobachev et al., 2002). Additionally, these secondary structures can perturb replication fork progression, possibly resulting in gaps or breaks (Gacy et al., 1995; Hewett et al., 1998).

3.3.2 Common fragile sites

The molecular mechanisms underlying CFSs fragility is less understood and two main models were proposed for CFSs-dependent genomic insta-

bility, which, despite being often presented as alternative models, may provide a comprehensive overview of the problem (Ozeri-Galai et al., 2012).

AT-rich sequences within CFSs are characterized by a high degree of DNA torsional flexibility, which has the potential to form secondary structures capable of impairing replication fork progression (Zlotorynski et al., 2003; Shah et al., 2010). Indeed, CFSs were described as late-replicating regions (Le Beau et al., 1998; Hellman et al., 2000; Palakodeti et al., 2004). Therefore, a first mechanism for CFSs instability envisions CFSs as slow-replication genomic regions which favor uncoupling between replicative helicases and polymerases (especially in conditions of replication stress). The subsequent generation of long ssDNA tracts allows secondary structure formation in AT-rich tracts, acting as replication fork barriers, ultimately resulting in fork stalling and/or collapse and DSBs generation (Durkin and Glover, 2007; Lukusa and Fryns, 2008).

Recent observations highlighted another feature of CFSs, that is the paucity in replication initiation. Due to the absence or low efficiency of replication origins, CFSs are often replicated from forks originating from flanking regions, resulting in incomplete replication leading to chromosome breakage under replication stress (Lemoine et al., 2008; Palumbo et al., 2010; Letessier et al., 2011; El Achkar et al., 2005). Interestingly, the density of initiation events is epigenetically determined, which accounts for cell-type differences observed in CFSs fragility (Letessier et al., 2011). Moreover, a correlation was found between the level of transcription of very large genes at CFSs and the instability of the corresponding site (Helmrich et al., 2011); this mechanism likely relies on the interference between transcription and replication (see Section *Transcription-associated genomic instability*).

Thus, both sequence features and origin efficiency can account for CFSs instability. Importantly, the mechanism of CFSs fragility is in line with the oncogene-induced DNA replication stress model for cancer development described in Section *Genomic instability and its consequences* (Halazonetis et al., 2008). During the early stages of cancer development, oncogene activation induces replication stress, which results in chromosome break-

age, deletions and rearrangements particularly at CFSs, which precede and likely drive instability in other genomic regions (Tsantoulis et al., 2008). The model is further reinforced by the finding that some CFSs lie within tumor suppressor genes, suggesting a mechanisms for inactivation of recessive tumor suppressor genes during tumor development (Bignell et al., 2010).

3.4 Unusual secondary structures

The DNA structure described by Watson and Crick is the canonical right-handed double helical structure called B-form DNA (Watson and Crick, 1953). Since then, non-B-form secondary structures have been found to occur at specific DNA sequences (Fig. 7). Hairpins can form at inverted repeats or trinucleotide repeats (TNRs), on single-stranded DNA (Nag and Petes, 1991); similarly, inverted repeats longer than 6 nucleotides can adopt a cruciform structure, which is made up of two hairpin-loop arms and a 4-way junction, resembling a Holliday junction (Palecek, 1991). Three-stranded triplex DNA structures are formed when a single-stranded DNA region binds in the major groove of purine-rich double-stranded B-DNA, leaving its complementary strand unpaired (Htun and Dahlberg, 1988). Repetitive G-rich sequences can form G-quartets, in which 4 guanines are arranged in a planar square, and multiple stacks of G-quartets yield a G-quadruplex (G4) DNA structure, which is usually stabilized by monovalent cations (Bochman et al., 2012).

These non-canonical secondary structures are hotspots for genomic instability: hairpin formation is involved in TNRs instability (López Castel et al., 2010); triplex DNA structures are intrinsically mutagenic, likely because they cause DSBs that result in translocations (Wang and Vasquez, 2004); cruciform structures formed at palindrome sequences are implicated in DSB-induced translocations (Kurahashi et al., 2006; Inagaki et al., 2009); G-quadruplexes stabilization induces DNA damage, and some rearrangement breakpoints have been mapped at sequences prone to G-quadruplex formation (Bacolla et al., 2004; Lopes et al., 2011; Rodriguez

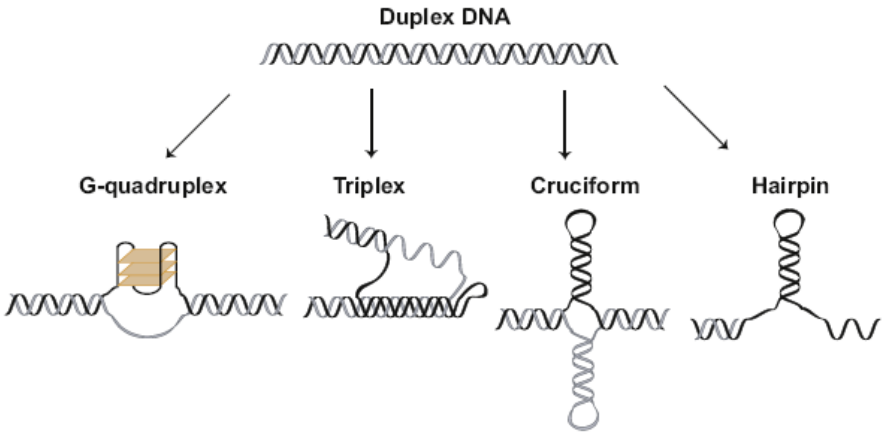

Figure 7: *The most common non-canonical DNA secondary structures* (from Saini et al., 2013).

et al., 2012).

The main mechanism through which all these unusual secondary structures jeopardize genomic stability relies on the observation that they can impair replication fork progression, inducing DSBs and ssDNA gaps (Krasilnikova and Mirkin, 2004; Mirkin and Mirkin, 2007; Voineagu et al., 2008; Lopes et al., 2011). Interestingly, non-canonical secondary structures-induced genomic instability was detected in non-proliferating cells, suggesting alternative mechanisms to replication fork impairment. DNA repair processes expose ssDNA tracts, favoring the formation of non-B-form secondary structures, which might interfere with the repair process itself, resulting in GCRs. Moreover unusual secondary structures may be recognized as helix-distorting lesions, and cleavage by the repair machinery may occur, yielding deletions and GCRs. The ssDNA which is exposed after triplex DNA formation may itself be a recombinogenic intermediate. In addition, non-canonical secondary structures seem to be more susceptible to DNA damage, likely because they impair nucleosome positioning (Wang and Vasquez, 2009).

Importantly, telomeric regions are particularly prone to secondary structure formation, which is one of the causes of telomere instability (see Section *Telomeres and genome instability*).

3.5 Transcription-associated genomic instability

In recent years, increasing amount of evidence unraveled unexpected connections between transcription and genomic instability (Aguilera, 2002): indeed, high rates of transcription at a genomic locus correlate with increased mutations, a phenomenon known as "transcription-associated mutation" (TAM) (Datta and Jinks-Robertson, 1995; Beletskii and Bhagwat, 1996). Parallely, highly transcribed regions show a greater recombination frequency, a phenomenon referred to as "transcription-associated recombination" (TAR) (Thomas and Rothstein, 1989; Nickoloff, 1992). Both outcomes are likely related to interferences between transcription and replication, as well as to the generation of ssDNA (Aguilera and Gómez-González, 2008).

As a consequence of local negative supercoiling during transcription, DNA-strand opening and ssDNA generation occurs behind an elongating RNA polymerase. Given that ssDNA is less stable and more susceptible to mutagenic damage from endogenous or environmental sources than dsDNA (Lindahl, 1993; Aguilera, 2002), this is a potential mechanism for TAM, but likely not the only one, since it cannot explain the observation that the non-transcribed strand (NTS) is more prone to mutations than the transcribed strand (TS) (Skandalis et al., 1994; Beletskii and Bhagwat, 1996). A further explanation involves the formation of R-loops (Fig. 8), a three-strand nucleic acid structure formed by annealing of the transcribed RNA on its template, resulting in an RNA:DNA hybrid plus a displaced DNA strand (ssDNA) (Aguilera and García-Muse, 2012). This structure accounts for the preferential mutagenesis of the NTS, as the displaced NTS is single-stranded, while the TS forms the RNA:DNA hybrid. Moreover, since persistent RNA:DNA hybrids can induce replication (Kogoma, 1997), it was proposed (Aguilera and García-Muse, 2012) that R-loops might trigger unscheduled DNA synthesis, which is expected to be highly mutagenic, in agreement with the finding that break-induced replication (BIR) is extremely inaccurate (Deem et al., 2011).

Instead, collisions between the replication fork and the transcription

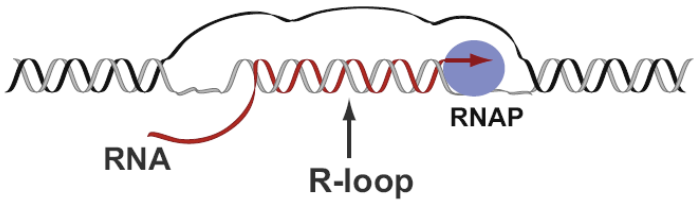

Figure 8: *R-loop structure* (from Saini et al., 2013).

machinery cause replication fork impairment, DSBs and TAR (Prado and Aguilera, 2005; Gottipati et al., 2008; Azvolinsky et al., 2009). The possible mechanisms for the induction of TAR and transcription-associated GCRs relies upon the ability of R-loops to cause replication fork blockage in multiple ways: i) unrepaired damage on the displaced strand might impede DNA polymerase progression; ii) replication fork progression could be impaired by the RNA:DNA hybrid itself, or by a RNA polymerase blocked by the R-loop; iii) R-loop formation could allow the occurrence of secondary structures on the displaced NTS, resulting in a barrier to DNA polymerase; iv) torsional stress generated in front of a R-loop could cause replication fork reversal, thus generating a highly recombinogenic "chicken foot" structure. In all the indicated cases, the final outcome would be replication fork stalling and/or collapse, with generation of DSBs or ssDNA gaps capable of triggering hyper-recombination and GCRs (Aguilera and García-Muse, 2012). Furthermore, it was suggested that the attempt to bypass a R-loop occurring between direct repeats through a template-switch mechanism, inevitably results in the deletion of the intervening region (Gómez-González et al., 2009).

3.6 Telomeres and genome instability

The ends of linear eukaryotic chromosomes, called telomeres, are made up of long tracts of repeated sequences (referred to as TG repeats), extending from few hundreds bp in yeast to several Kb in humans, and terminating in a 3' single-stranded overhang (also known as "G-tail") (Blackburn et al., 2006).

Figure 9: *Schematic representation of a human telomere* (from Palm and de Lange, 2008).

These structures pose multiple problems for genome integrity. First of all, if not properly protected, they can be mis-recognized as DSBs (discussed further). Moreover, the semi-conservative mode of replication brings about a loss of single-stranded DNA on the lagging strand at the chromosome end (a situation known as "end-replication problem") (Watson, 1972), which, together with resection of the 5' end to generate the 3' single-stranded overhang (Lingner et al., 1995), results in loss of telomeric sequences at each round of replication (telomere erosion). To overcome these threatens to genome integrity, multiple mechanisms exist to ensure proper telomere maintenance: on the one hand, a nucleoprotein structure protects the telomere from unscheduled reactions and masks it from recognition by the DNA damage response (a phenomenon defined "telomere capping"); on the other hand, a specific complex named telomerase adds short TG-rich repeats to chromosome ends, restoring proper length (Blackburn et al., 2006).

Telomere erosion actually occurs in somatic cells due to insufficient expression of telomerase (Harley et al., 1990). When a telomere shortens below a certain threshold, it looses its protective cap, it is recognized as a DSB, and accordingly repaired through the non-homologous end joining (NHEJ) pathway (see Section *DNA repair pathways*) (Smogorzewska et al., 2002; Dimitrova et al., 2008); the same effect is obtained after telomere uncapping linked to defects in telomere-capping proteins (van Steensel et al., 1998). Typically, repair of an uncapped telomere results in telomere fusion, either with the sister chromatid, or with another uncapped chromosome end; alternatively, chromosome fusion may occur between the uncapped telomere and a DSB end, producing a translocation.

These events may start a series of chromosomal aberrations through a mechanisms named breakage-fusion-bridge (BFB) (McClintock, 1941; Mieczkowski et al., 2003; Capper et al., 2007). Briefly, telomere fusion yields a dicentric chromosome, which forms a characteristic bridge between the two pools of separating chromosomes during anaphase; centromeres pulling in opposite directions results in chromosome breakage, leaving two uncapped chromosome ends which can undergo another telomere fusion event. In this way, multiple BFB cycles may occur, which not only give rise to increasing GCRs, but also result in gene amplification, a phenomenon frequently observed in cancer cell lines (O'Hagan et al., 2002).

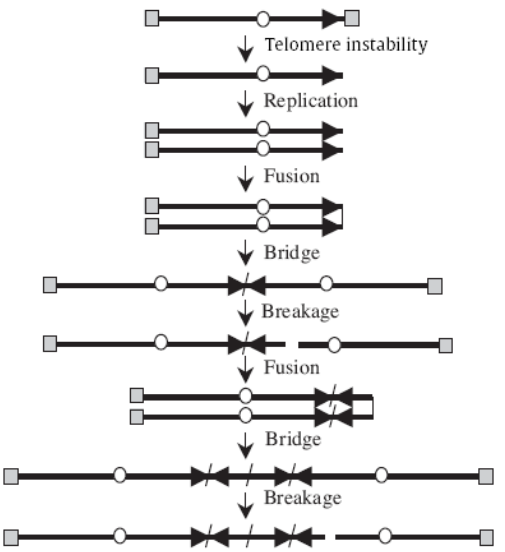

Figure 10: *Mechanism of breakage-fusion-bridge (BFB) cycles* (modified from Lo et al., 2002).

In addition to progressive telomere erosion, also sporadic telomere deletions occur, in which large tracts of telomeric repeats are lost in a single deletion event (Lustig, 2003). These events are due to the repetitive nature of telomeric sequences, and may result from unequal sister chromatin exchange or replication slippage (Baird et al., 1995). Moreover, repetitive telomeric sequences are particularly sensitive to oxidative lesions (von Zglinicki, 2002) and are prone to formation of secondary structures (Parkinson et al., 2002); both events lead to replication fork stalling, with subsequent DSBs and telomeric deletion events (Lansdorp, 2005). Furthermore, it was demonstrated that mammalian telomeric regions resemble fragile sites, which are prone to breakage upon replication stress, again resulting in telomere loss and GCRs (Sfeir et al., 2009). As in the case of telomere shortening, sporadic telomere deletions may as well trigger BFB

cycles (Lo et al., 2002).

Telomere instability is considered an important factor in tumor development, based on the observation that mouse models lacking telomerase show telomere loss, genomic instability and increased cancer incidence (Blasco et al., 1997; Rudolph et al., 1999; O'Hagan et al., 2002). The paradoxical observation that most human cancer cell lines display telomerase activation (Shay and Wright, 2005), led to a model for cancer progression envisaging a transient period of telomere loss (Fig. 11). Unprotected chromosome ends resulting from progressive telomeric shortening or sporadic telomere deletions (the latter likely occurring at telomeric fragile sites after oncogene-induces replication stress), are usually recognized as DSBs and trigger cell senescence (d'Adda di Fagagna et al., 2003). Following cell cycle checkpoints inactivation, escape from senescence occurs, and a phase named "crisis" starts, characterized by massive genomic rearrangements leading to cell death. Occasionally, some cells acquire the ability to maintain their telomeres (usually by telomerase activation), thus surviving crisis and being endowed with indefinite lifespan: these cells now display a malignant phenotype (Counter et al., 1992; Chin et al., 1999; Artandi et al., 2000). It is worth noting that telomere-driven genomic instability may still occur in these cells, although to a lower extent, due to sporadic telomere deletions (Muraki et al., 2012).

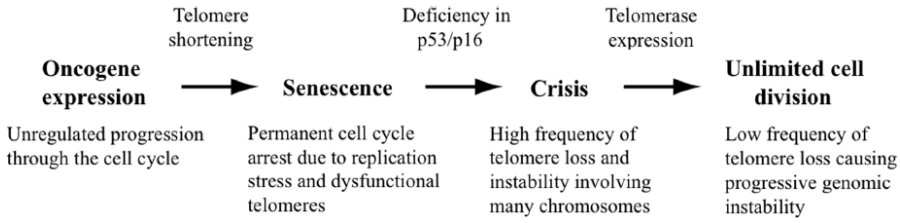

Figure 11: *Role of telomere loss in genome instability and cancer* (from Muraki et al., 2012).

3.7 Chromosome segregation and genome instability

At each division, the cell not only must faithfully replicate its genetic material, but also have to successfully distribute one copy of each chromosome into each daughter cell. Therefore, another critical step for the onset of genomic instability is chromosome partitioning during mitosis. A specific surveillance pathway called mitotic checkpoint or spindle assembly checkpoint is entrusted with ensuring accurate chromosome segregation (see Section *Mitotic checkpoint*). Failure of this pathway paves the way to chromosomal instability (CIN) (Michel et al., 2001; Iwanaga et al., 2007).

A part from mitotic checkpoint impairment, multiple mechanisms may be responsible for chromosome mis-segregation (Fig. 12). Cohesion defects are thought to be an important cause of CIN; indeed, mutations in genes involved in regulation of sister chromatin cohesion were identified in human cancers (Barber et al., 2008; Solomon et al., 2011), and altered expression of these or other genes controlling sister cromatid cohesion results in CIN (Jallepalli et al., 2001; Zhang et al., 2008; Iwaizumi et al., 2009), likely because incorrect chromatin packaging at the centrosome causes defects in chromosome orientation, and/or untimely chromatid disjunction leads to chromosome partitioning prior to establishment of proper spindle-chromosome attachment (Thompson et al., 2010). Moreover, altered kinetochore-microtubule attachment dynamics may be detrimental for faithful chromosome partitioning in mitosis. Association and dissociation of spindle microtubules from kinetochore allows correction of merotelic attachments, in which a single kinetochore attaches to microtubules arising from both spindle poles (Thompson and Compton, 2008). Destabilization of kinetochore-microtubule attachments prevents chromosome segregation (Liu et al., 2009), while hyper-stabilization of kinetochore-microtubule attachments impairs release of uncorrectly attached microtubules, reducing the efficiency of merotelic attachment correction, which results in increased kinetochore mal-orientations and chromosome mis-segregation (Bakhoum et al., 2009b,a). In addition, centrosome amplification may occur due to centriole overduplication, centrosome fragmentation or loss fo centriole co-

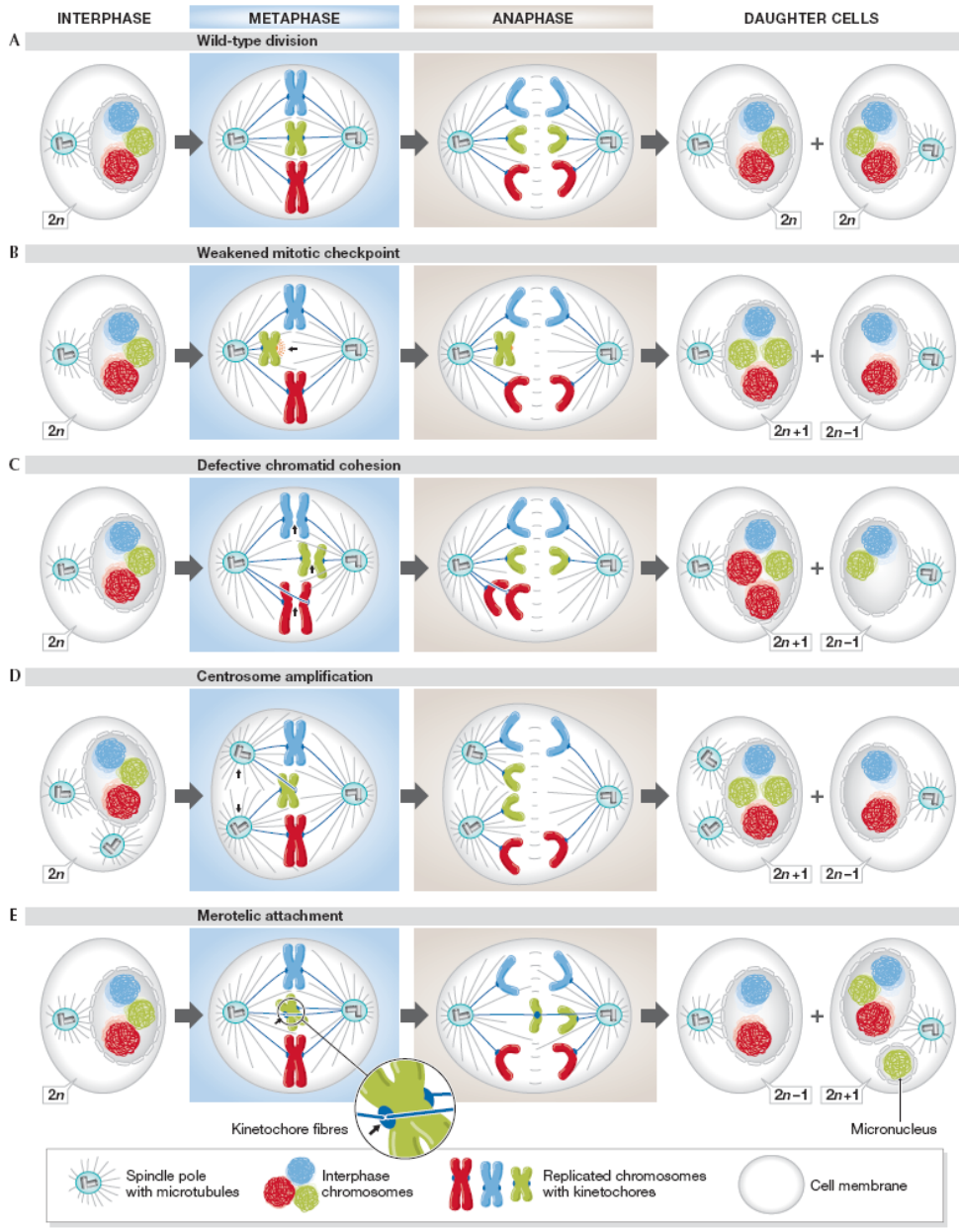

Figure 12: *Mechanisms for chromosomal instability* (from McGranahan et al., 2012).

hesion (Holland and Cleveland, 2009), yielding a cell with more than two centrosomes. This is also the outcome of tetraploidization as a consequence of cell fusion or cell divison failures (Ganem et al., 2009). The presence of extra-centrosomes induce the transient formation of multipolar spindles, resulting in a high rate of merotelic attachments leading to chromosome mis-segregation (Silkworth et al., 2009; Ganem et al., 2009).

Aneuploidy and CIN have been proposed to have a major role in tumorigenesis, based on the observation that solid tumours are aneuploid (Mitelman et al., 2012). Indeed, it was shown that, when combined with loss of p53 or other genes that restrict proliferation of aneuploid cells, CIN has a strong tumor-promoting effect (Chi et al., 2009; Li et al., 2010; Sotillo et al., 2010). Multiple mechanisms could account for this tumorigenic effect: i) loss of a chromosome may uncover a recessive mutation in a tumour suppressor gene on the homologous chromosome(Cavenee et al., 1983); ii) aneuploidy creates imbalances in the levels of proteins required for DNA replication, repair or mitosis, therefore increasing the mutation rate (Duesberg et al., 2006); iii) aneuploidy was proven to be a source of genomic instability in yeast (Sheltzer et al., 2011), and chromosome mis-segregation was found to cause DSBs and GCRs in human cells (Janssen et al., 2011); iv) recently, it was also shown that lagging anaphase chromosomes due to segregation errors are incapsulated in micronucei, where they undergo extensive fragmentation and random rejoining ('chromothripsis'), resulting in rearrangements (Stephens et al., 2011; Liu et al., 2011; Crasta et al., 2012). Importantly, due to gain or loss of whole chromosomes, CIN provides a huge phenotypic diversity, which may be the basis for tumor adaptation to microenvironment changes, when large adaptive responses are likely needed (Pavelka et al., 2010; Chen et al., 2012; Holland and Cleveland, 2012).

4 Mechanisms preserving genome integrity

4.1 Helicases, topoisomerases and nucleases meet at the fork

Given that the main challenge to genome stability derives from problems during replication (Kolodner et al., 2002; Aguilera and Gómez-González, 2008), it is not surprising that a plethora of proteins endowed with different biochemical activities are required to promote replication fork integrity (summarized in Fig. 13).

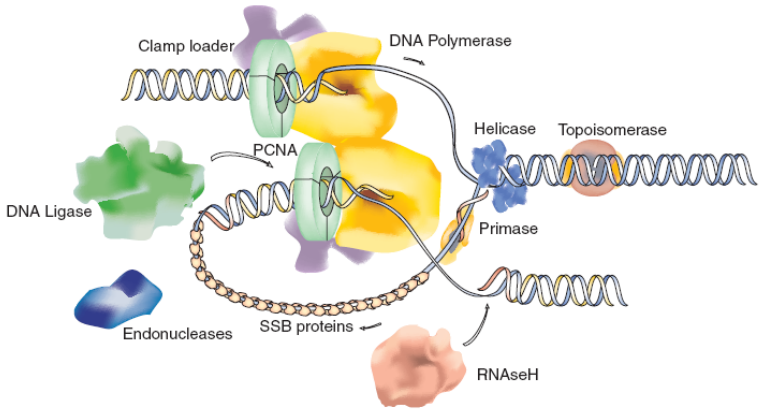

Figure 13: *Helicase, nuclease and topoisomerase activities promote replication fork progression* (from Chagin et al., 2010).

DNA duplex unwinding by replicative helicases creates torsional stress which needs to be relieved by specific topoisomerase activities: they do so by cutting one DNA strand (topoisomerase I) or both strands (topoisomerase II), thereby allowing the uncut strand to pass through the break before resealing it (Vos et al., 2011). Positive supercoiling produced in front of a traveling replication fork, at converging replication forks, or at head-on encounters between transcription and replication can be removed by either Top1 or Top2 topoisomerases. Conversely, cruciform structures (precatenanes) formed behind the replication fork or at sites of convergent replication forks are processed only by Top2 (Bermejo et al., 2007; Branzei and Foiani, 2010).

Several activities ensure proper replication fork progression under perturbed conditions or at difficult-to-replicate regions. X-shaped DNA structures resembling Holliday junctions accumulate during a perturbed replication; these likely represent recombination structures resulting from replication fork regression or recombination-mediated bypass of replication fork stalling (Liberi et al., 2005). Their processing involves the activity of Sgs1-Top3-Rmi1 complex (BLM-TOPOIIIα-RMI1 in human), which employs the concerted action of RecQ helicase BLM/Sgs1 and type IA topoisomerase TOPOIIIα/Top3. Alternatively, these structures can be cleaved by a resolvase complex made up of Mus81-Mms4 in yeast and MUS81-EME1 in human (Fabre et al., 2002; Ashton and Hickson, 2010; Hickson and Mankouri, 2011). Another helicase named Srs2, instead, directly inhibits the formation of these recombinative structures by disrupting Rad51 nucleoprotein filaments, thus preventing unwanted recombination events during replication. (Fabre et al., 2002; Pfander et al., 2005).

Other Holliday junction resolvase activities were recently detected (Svendsen and Harper, 2010), namely Slx1-Slx4 complex and GEN1/Yen1 nuclease. The Slx1-Slx4 complex is required – redundantly with Sgs1-Top3-Rmi1 complex – for resolution of stalled forks at the rDNA locus, a difficult-to-replicate region because of its highly repetitive nature (Kaliraman and Brill, 2002; Fricke and Brill, 2003). It is still unclear whether the role of the Slx1-Slx4 resolvase is required for replication of other genomic regions (Svendsen and Harper, 2010). Yen1/GEN1 nuclease, despite being involved in recombination, does not seem to be implicated in processing recombination-associated X-structures (Ip et al., 2008; Ashton et al., 2011); it was suggested that Yen1 is required in meiosis (Svendsen and Harper, 2010).

Beyond replisome-associated helicases responsible for the unwinding of the DNA duplex, Pif1 family helicases assist the replication fork by unwinding DNA secondary structures or displacing protein complexes which might impair fork progression (Bochman et al., 2010). Pif1 is involved in replication through G-quadruplex forming DNA regions, in inhibition of de-novo telomere addition through displacement of telomerase, in Okazaki

fragment maturation and in mtDNA replication (Paeschke et al., 2011; Boulé et al., 2005; Boulé and Zakian, 2007; Cheng et al., 2007); Rrm3 activity instead is implicated in disrupting non-nucleosomal protein-DNA complexes, which might constitute replication fork pausing sites, located at telomeres, rDNA locus, tRNA genes, centromeres, inactive replication origins, and transcriptional silencers (Ivessa et al., 2000, 2002, 2003). In mammalian cells only one Pif1 helicase was identified, which appears to perform the same functions as yeast Pif1 (Zhang et al., 2006b; Futami et al., 2007; George et al., 2009).

Anothey key point for genome integrity maintenance at the replication fork is the proper removal of Okazaki fragments. This task is achieved through the concerted actions of helicases and nucleases (Zheng and Shen, 2011). RNA primers on the lagging strand can be displaced by Polδ, or Pif1 helicase, thus generating a 5' flap: if the flap is shorter than 10 nt, it can be cleaved by flap-endonuclease Fen1/Rad27 (and to a lesser extent by Exo1). Conversely, longer flaps are first processed by Dna2 – which possesses ssDNA exonuclease activity – and finally cleaved by Fen1/Rad27. Importantly, Dna2 helicase activity is required for cleavage of secondary structure-forming flaps (Kang et al., 2010). If the RNA primer is not displaced, it can become a substrate of RNase H, an activity which specifically cleaves DNA:RNA hybrids (Cerritelli and Crouch, 2009).

Finally, the replication checkpoint (especially in its components Tof1 and Mrc1, which are associated with the replisome) promotes replication fork stabilization (Sogo et al., 2002; Katou et al., 2003; Hodgson et al., 2007) (see Section *DNA damage checkpoints*).

4.2 Overview of the DNA damage response

To neutralize the serious threaten to genome integrity coming from replication errors, endogenous genotoxic byproducts of cellular metabolism and environmental DNA damage, the cell has evolved a complex network of interlinked systems, collectively defined as DNA damage response (DDR): these mechanisms detect the DNA damage, signal its presence and carry

out the repair of the lesion (Fig. 14).

The DNA repair systems and the DNA damage checkpoint pathways are central for the cellular DDR. Due to the wide diversity of DNA lesions, several specialized repair pathways exist, capable of coping with the various injuries affecting the DNA molecules: some of these mechanisms are error-free, while others remove the damage at the cost of introducing mutations. DNA damage checkpoints are surveillance mechanisms which monitor the status of the genetic material throughout the cell cycle and, in the presence of DNA lesions or replication stress, temporarily halt cell cycle progression in order to provide enough time to repair the damage and faithfully complete replication. Moreover, they stimulate the repair processes both at transcriptional and post-transcriptional levels; in higher eukaryotes, in case the damage cannot be removed, they channel the cell into the apoptotic pathway (Hoeijmakers, 2001; Jackson and Bartek, 2009). These two branches of the DDR are tightly connected and share many components; processing of physically different lesions by repair mechanisms triggers checkpoint activation, which in turn modulates the repair process, by recruiting repair factors and stimulating their activity (Lazzaro et al., 2009; Novarina et al., 2011; Sertic et al., 2012).

The importance of the DDR in the maintenance of genome integrity is highlighted by the observation that defects in either DNA repair pathways or DNA damage checkpoints cause sensitivity to DNA-damaging agents and genomic instability, and inherited mutations in many DDR components are associated with cancer-predisposing syndromes (Hoeijmakers, 2001; Kennedy and D'Andrea, 2006; Kerzendorfer and O'Driscoll, 2009; Jackson and Bartek, 2009).

4.3 DNA repair pathways

DNA repair mechanisms are conventionally grouped into classes on the basis of the kind of lesion detected and the strategy carried out to remove it. In few cases, the chemical base alteration can be corrected by Direct Damage Reversal systems. Excision repair mechanisms include

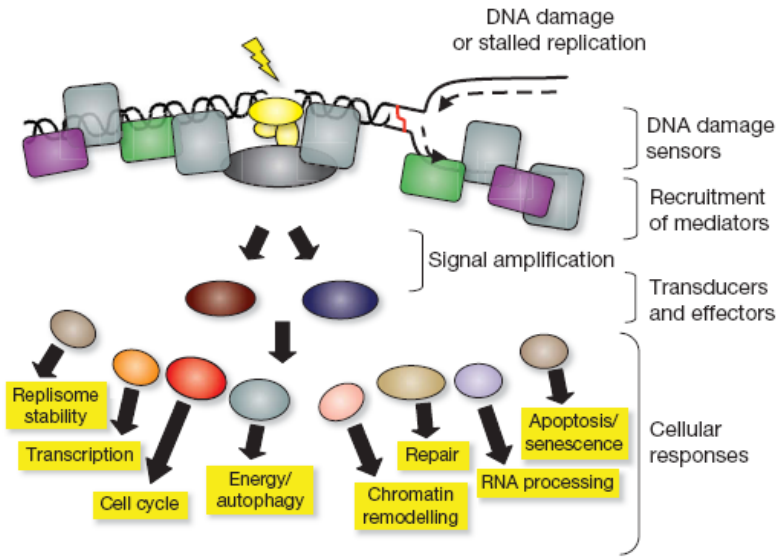

Figure 14: *Overview of the DNA damage response* (from Jackson and Bartek, 2009).

Base Excision Repair (BER), Nucleotide Excision Repair (NER) and Mismatch Repair (MMR): in all these three processes one or more nucleotides at the lesion site are eliminated forming a gap, which is filled and ligated. DSBs are instead repaired by Double Strand Break Repair (DSBR) mechanisms, namely Non-Homologous End Joining (NHEJ) and homologous recombination-based systems, which can be further divided in Homologous Recombination (HR), Synthesis-Dependent Strand Annealing (SDSA), Break-Induced Replication (BIR) and Single-Strand Annealing (SSA). Finally, DNA damage tolerance mechanisms exist, which allow the provisional lesion bypass in order to complete replication: these mechanisms include Translesion Synthesis (TLS), Post Replication Recombinational Repair (PRRR) and Replication Fork Regression (also called "template switch").

In the following brief description of the major DNA repair pathways both the human and *S. cerevisiae* names of each factor will be usually provided.

4.3.1 Direct damage reversal

Photoreactivation. Photoreactivation removes UV-induced lesion through a light-dependent mechanism: the enzyme CPD photolyase (present in many organisms from yeast to vertebrates, but absent in mammals) detects and repairs pyrimidine dimers, while the enzyme 6-4 photolyase (identified in vertebrates but not in yeast) is employed in the removal of 6-4PPs. CPD photolyase binds the DNA lesion, flips the pyrimidine dimer out of the phosphodiester backbone and breaks the chemical bound between the two nucleotides in a light-dependent electron transfer reaction (Thoma, 1999).

Demethylation. To repair some DNA lesions caused by methylation events, namely O^6-methylguanine (O^6-meG) and O^4-methylthymine (O^4-meT), the enzyme O^6-methylguanine-DNA-methyltransferase is capable of transferring the mutagenic methyl group from DNA to a cysteine residue in its active site (Sedgwick, 2004). Due to irreversible inactivation of the protein after the transfer reaction – and the subsequent requirement of a new enzyme molecule for each lesion repaired – this system seems particulary suitable for removal of infrequent but very harmful lesions, as is the case of O^6-meG (Lindahl and Wood, 1999).

4.3.2 Base excision repair

Base Excision Repair (BER) is the main system devoted to the correction of base alterations as a consequence of cellular metabolism (oxidative damage, methylation, deamination, hydroxylation). Several specialized glycosylases, each capable of recognizing a specific subset of modifications, are employed for the removal of damaged bases: when the glycosylase encounters a lesion, the modified nucleoside is flipped out from the DNA duplex in a cavity of the enzyme, where cleavage of the glycosidic bond between the base and deoxyribose occurs, resulting in an abasic site. Subsequently, an apurinic/apyrimidinic (AP) endonuclease cleaves the phosphodiester backbone and repair synthesis occurs. In short-patch BER, DNA pol β fills the

one-nucleotide gap and removes the 5'-terminal baseless sugar residue via its lyase activity, after which the nick is sealed by a ligase activity. In long-patch BER (which involves Pol δ e Pol ε) re-synthesis of 2-10 nucleotides occurs, followed by removal of the displaced flap by the flap-endonuclease FEN1/Rad27, and subsequnt nick sealing by DNA ligase (Hoeijmakers, 2001; Memisoglu and Samson, 2000).

4.3.3 Nucleotide excision repair

Nucleotide Excision Repair (NER) is a repair mechanism which recognizes a broad spectrum of helix-distorting DNA lesions, as UV-induced damage (CPDs and 6-4PPs), intrastrand and interstrand crosslinks (ICLs), and several chemical adducts. NER is divided in two sub-pathways, which differ in the lesion recognition mechanism, while the downstream steps are in common: Transcription-Coupled Repair (TC-NER), detects and repairs lesions on actively transcribed DNA, while Global Genome Repair (GG-NER) deals with non-transcribed regions and with the non-transcribed strand of transcribed genes (Thoma, 1999). It seems that lesion recognition by NER requires both DNA helix distortion and covalent base modification, while lesions producing only one of the two effects are not repaired with this system (Lindahl and Wood, 1999).

In GG-NER the lesion is recognized by XPC-hHR238B/Rad4-Rad23 complex; also human DDB and yeast Rad7-Rad16 participate in the lesion recognition step. Subsequently, XPA/Rad14, RPA complex and TFIIH transcription factor are recruited: helicases XPB/Rad25 and XPD/Rad3 of TFIIH unwind the DNA duplex in opposite directions; RPA stabilizes the ssDNA at the non-damaged strand, while XPA/Rad14 is involved in verification of the damage site. In a next step, XPG/Rad2 and XPF-ERCC1/Rad1-Rad10 nucleases are recruited, which cleave the 3' and 5' end of the open repair bubble respectively, releasing a fragment of about 30 nucleotides containing the lesion. Lastly, repair synthesis fills the gap and DNA ligase seals the nick (Thoma, 1999; Lindahl and Wood, 1999).

In TC-NER, the RNA polymerase itself is responsible for signaling the

presence of a lesion, as the helix distortion blocks polymerase progression. At this point, CSB/Rad26 and CSA/Rad28 displace RNA polymerase and recruit the other NER factors: hereafter the repair is identical to GG-NER (Hoeijmakers, 2001; Prakash and Prakash, 2000).

4.3.4 Mismatch repair

To correct mutations due to replication errors, the Mismatch Repair (MMR) system is specialized in repairing nucleotide mispaired by replicative polymerases and insertion/deletion loops (IDLs) caused by slippage during replication of repetitive sequences (Hoeijmakers, 2001). MutSα complex (Msh2/Msh6) triggers repair of base-base mismatches and IDLs of one or two nucleotides, while MutSβ (Msh2/Msh3) is specialized in recognition of longer IDLs. MutSα e MutSβ recruit heterodimeric complexes MutLα (Mlh1/Pms2) and MutLβ (Mlh1/Pms1). It seems that MutLα, based on its ability to translocate along DNA after mismatch recognition, has a key role in the discrimination of the damaged (neo-synthesized) strand, likely due to the presence of a nick: in the lagging strand the nick is provided by removal of Okazaki fragments, while it is still unclear how nicks are generated on the leading strand (Jiricny, 2006). Different mechanisms were proposed for mismatch excision and resynthesis, depending on whether the nick is upstream or downstream the lesion, based on the presence of PCNA and RFC complexes respectively at the 3' and 5'ends of the nick. If the nick is upstream the mismatch, MutS/MutLα complex translocating along DNA in a 3'-5' direction comes across RFC, displaces it and loads Exo1, which degrades the damaged strand thanks to its 5'-3' exonuxlease activity. If the nick is downstream the mismatch, MutS/MutLα complex moving in 3'-5' direction encounters PCNA; MutLα endonuclease activity, activated in a PCNA- and RFC- dependent manner, performs an incision upstream the lesion, which allows Exo1 loading and degradation of the damaged strand. In both cases the ssDNA gap generated by lesion removal is covered by RPA, DNA polymerase δ fills the gap and the remaining nick is sealed by DNA ligase (Jiricny, 2006; Li, 2008).

4.3.5 Double-strand break repair

The cell possesses two main mechanisms to repair double-strand breaks (DSBs): in Non-Homologous End Joining (NHEJ) the broken ends are juxtaposed and sealed, while in homologous recombination-based mechanisms the lesion is repaired using the genetic information on the homolog chromosome or the sister chromatid (Fig. 16). The repair pathway choice is influenced by several factors, including cell cycle phase, ploidy (in yeast), number of DSBs and features of DSB ends (Longhese et al., 2006). At the molecular level, this choice is regulated mainly by controlling nucleolytic processing of the lesion (resection). Immediately after DSB occurrence, several protein complexes are recruited at the lesion site to protect its ends (preventing unscheduled degradation and subsequent loss of genetic information), keep the ends in close proximity (limiting the possibility of chromosome rearrangements) and signal the presence of the damage to the checkpoint pathways (Fig. 15). At this stage, a key role is played by MRN/MRX and Ku complexes. MRN/MRX complex is made up of human Mre11-Rad50-Nbs1 or yeast Mre11-Rad50-Xrs2 proteins: this complex has a peculiar structure, with a globular head which binds a DSB end, and two protruding tails, which interact with the tails of the MRX/MRX complex at the other side of the break, thus ensuring a temporary tethering of the chromosome ends until effective repair occurs (Shin et al., 2004). Ku complex, composed by Ku70 and Ku80 proteins, has a toroid shape capable of hosting the DNA duplex (Hefferin and Tomkinson, 2005): it binds the DSB ends preventing their degradation, and recruits NHEJ factors; when Ku complex is inhibited (mainly by CDK activity in G2 phase), resection of the 5' strand occurs at the DSB ends, channeling lesion repair into one of the homologous recombination-based pathways (Clerici et al., 2008).

Non-homologous end joining. In NHEJ, after MRN/MRX and Ku complexes bind to DSB ends, DNA Ligase IV-XRCC4/Dnl4-Lif1 complex is recruited. In most of the DSBs caused by genotoxic agents, the broken chromosome ends are not compatible and require preliminary processing

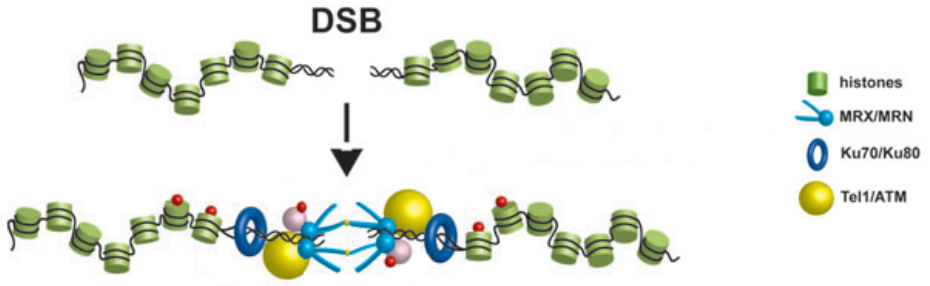

Figure 15: *Complexes formed at DSBs* (modified from Longhese et al., 2006).

through nucleolytic degradation and/or polymerization; this task in human cells is performed mainly by Artemis exonuclease, while in yeast it involves flap-endonuclease Rad27, the 3'-5' exonuclease activity of MRX complex, and DNA polymerase Pol4. It's worth noting that NHEJ is a mutagenic repair system, due to frequent loss of few nucleotides during DSB ends processing. Finally, DNA Ligase IV/Dnl4 can complete the repair by sealing the two chromosome ends (Hefferin and Tomkinson, 2005).

Homologous recombination. The key step shared by all recombination-based repair mechanisms is the exonucleolytic processing (resection) at the 5' strand of the DSB ends, with the subsequent formation of ssDNA tails at the 3' strand (Krogh and Symington, 2004). Multiple nucleases are involved in resection, namely Mre11, CtIP/Sae2 and Exo1, together with the BLM/Sgs1 helicase (Harrison and Haber, 2006; Ciccia and Elledge, 2010). The assembly of a nucleoproteic filament which is recombination-proficient is called pre-synapis: ssDNA tracts generated by resection are immediately covered by the RPA complex, which protects it from degradation and removes secondary structures which might interfere with the following recombination steps; then Rad51 replaces RPA on the nucleoproteic filament, an event favored by Rad52, while Rad55 e Rad57 are involved in nucleoproteic filament stabilization (Krogh and Symington, 2004). The synapsis step consists in the identification of the homolog donor sequence (strand invasion) and its annealing with the nucleopro-

teic filament (strand exchange), a process promoted by Rad54. Rad54 is also involved in the post-synapsis step, when it displaces Rad51 from the DNA heteroduplex, allowing the access of DNA polymerase. The subsequent DNA synthesis using the 3' end of the broken strand as a primer creates a structure known as D-loop (Li and Heyer, 2008). From this point on, the homologous recombination sub-pathways diverge according to what happens in the following step (Fig. 16). In classical HR, second end capture, DNA synthesis and ligation yield an intermediate known as double Holliday Junction (HJ) (Li and Heyer, 2008). This intermediate can be processed by MUS81-EME1/Mus81-Mms4 or GEN1/Yen1 resolvases (resolution), yielding crossover products, or by the concerted action of BLM/Sgs1 helicase and TopoIIIα/Top3 topoisomerase (dissolution), yielding non-crossover products (Symington and Holloman, 2008).

Synthesis-dependent strand annealing. If, during the post-synapsis phase, after the synthesis of a DNA stretch the invading strand dissociates form the donor sequence before second-end capture, Synthesis-Dependent Strand Annealing (SDSA) occurs: the D-loop is dissolved (likely by a helicase activity) and the neo-synthesized strand anneals back to the other resected ssDNA DSB end; repair synthesis is completed by DNA polymerase and DNA ligase (Li and Heyer, 2008). SDSA always yields non-crossover products (Fig. 16).

Break-induced replication. Sometimes it is possible that only one DSB end is capable of strand invasion on the homologue chromosome, resulting in an unidirectional replication fork which copies the donor sequence until the end of the chromosome, or until it encounters another replication fork: this mechanism is called Break-Induced Replication (BIR) (Fig. 16). In this case, the second DSB end is never captured, and the genetic information on that chromosome region is lost, resulting in loss of heterozigosity (LOH) (Longhese et al., 2006).

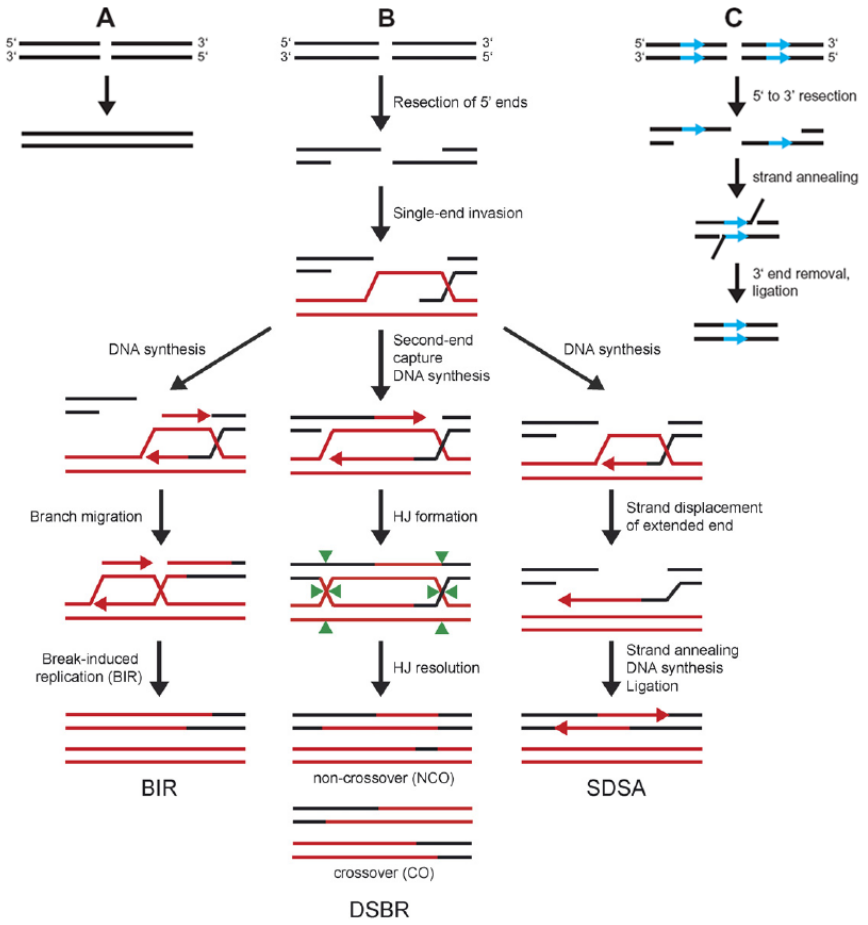

Figure 16: *Mechanisms of DSB repair.* **A)** *NHEJ;* **B)** *BIR, classical HR and SDSA;* **C)** *SSA* (modified from Longhese et al., 2006 and Longhese et al., 2008).

Single-strand annealing. When the DSB occurs between two direct repeats, repair by Single-Strand Annealing (SSA) may occur: when resection reaches the homologue sequences flanking the DSB, complementary ssDNA regions are exposed, which may anneal, leaving ssDNA flaps subsequently removed by nucleases; resulting nicks or gaps are filled by repair synthesis and ligation (Fig. 16). It is worth noting that this process entails the deletion of one of the repeats and all the region between them: this feature places SSA among mutagenic repair systems (Longhese et al., 2006).

4.4 DNA damage tolerance mechanisms

In some cases (for instance in the presence of an excessive number of DNA lesions, when they are poorly accessible, or when damage occurs during S-phase) the repair mechanisms might not be able to remove some lesions. If the lesions are capable of blocking the replication fork, the cell is exposed to a risk of fork collapse, or it might even be unable to conclude the cell cycle. To face this dangerous situation, DNA damage tolerance mechanisms exist, which allow replication past a lesion without removing it. Of course this task is fulfilled at the price of transmitting potential mutations to the next generations (Andersen et al., 2008). Replication of a damaged template may represent and extreme attempt of the cell to survive, in the hope to repair the lesion during the next cell cycle.

4.4.1 Translesion synthesis

A first DNA damage tolerance system, called Translesion Synthesis (TLS), is based on the employment of alternative DNA polymerases, capable of replicating – generally with low fidelity – past a damaged template (Fig. 17). A common feature of translesion polymerases is a looser active site conformation, capable of accommodating bulky adducts and mismatched base pairs (Friedberg, 2005). *S. cerevisiae* possesses three translesion polymerases, namely Pol η, Pol ζ e Rev1, while mammalian cells beyond these also use Pol ι and Pol $\varkappa$. Pol η can correctly insert two A nucleotides in front of a thymine dimer, while it displays low fidelity with

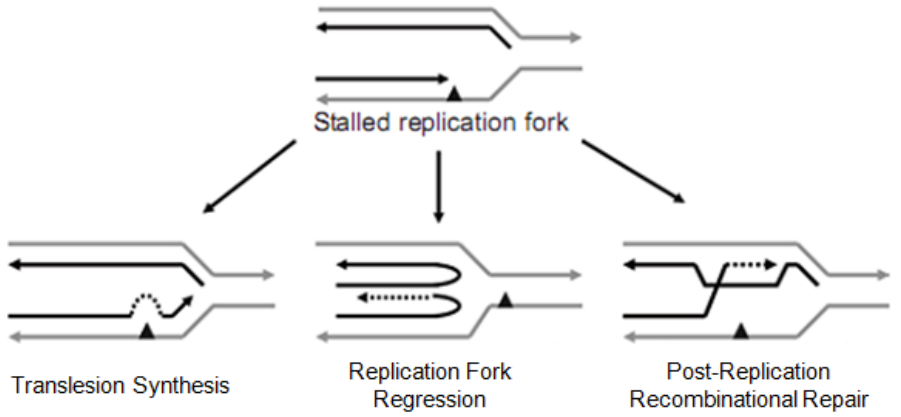

Figure 17: *DNA damage tolerance mechanisms* (modified from Andersen et al., 2008).

other lesions (Andersen et al., 2008). Pol ζ is made by a catalytic subunit and a regulatory one (Rev3 and Rev7), and has a low replication fidelity, to such an extent that it is considered the main polymerase responsible for mutagenic lesion bypass events (Gan et al., 2008). Rev1 is capable of inserting cytosines in front of an abasic site and, with lower efficiency, in front of a G or and A; moreover, it is thought to play a structural role in TLS, acting as a scaffold for the interaction between the other translesion polymerases and PCNA (Andersen et al., 2008). Pol ι has a very low processivity (it can insert bases opposite some lesions, but not extend synthesis past the damage) and is very error prone, in that preferentially inserts G opposite a template T (Lehmann et al., 2007). Pol κ is specialized in bypassing N^2-adducted dG lesions, but is prone to small insertions/deletions (Waters et al., 2009).

The PCNA complex is a key regulator of DNA damage tolerance pathway choice: damage- and Rad6-Rad18- dependent mono-ubiquitylation of PCNA-K164 promotes TLS, while poly-ubiquitylation of PCNA on the same residue by Mms2-Ubc13-Rad5 complex channels the lesion into a non-mutagenic lesion bypass mechanisms (see below) (Andersen et al., 2008). Two models, which are not mutually exclusive, have been proposed

for TLS-mediated lesion bypass. According to the "polymerase switch" model, many polymerases are associated to the replication fork, through interaction with PCNA; when the fork is blocked at a lesion, PCNA mono-ubiquitylation promotes the loading of a translesion polymerase capable of replicating past the lesion; then a second translesion polymerase extends the replicated strand (to avoid profreading activity by canonical replicative polymerases), and finally normal synthesis is resumed. According to the "gap-filling" model, when the replication fork is halted by a lesion, synthesis restarts downstream of the blocking lesion, leaving ssDNA gaps behind, which are later filled by translesion polymerases (Waters et al., 2009).

4.4.2 Post-replication recombinational repair

Post-Replication Recombinational Repair (PRRR) represents, together with Replication Fork Regression, a strategy to avoid replicating the damaged template in the immediate proximity of the lesion: both systems are therefore error-free mechanisms.

In PRRR, when the replication forks stalls at a lesion, repriming occurs about 1Kb downstream, allowing normal synthesis by replicative polymerases; the gap is repaired through homologous recombination-based lesion bypass, triggered by sister chromatid invasion: error-free synthesis takes place using the other newly-synthesized strand as a template (Fig. 17), followed by Holliday junction resolution. (Friedberg, 2005; Andersen et al., 2008).

4.4.3 Replication fork regression

Alternatively, the arrested fork may undergo a structural rearrangement, defined Replication Fork Regression, in which the template DNA partially reanneals, while the two newly-synthesized strands anneal together, resulting in a short double-stranded DNA stretch protruding in the opposite direction (Sogo et al., 2002): this transient structure at a reversed fork is defined "chicken foot" (Fig. 17). In this way the replicative polymerase can

use as a template the other newly-synthesized strand, which was already extended past the lesion, due to leading and lagging strand uncoupling. Reversal of the "chicken foot" structure restores a normal replication fork, which can carry on replication downstream of the lesion (Friedberg, 2005).

4.5 DNA damage checkpoints

At the molecular level, DNA damage checkpoints can be considered as highly conserved signal transduction cascades, mainly based on phosphorylation events, which convey the signal from damage sensors to several DDR effectors. The DNA damage checkpoint cascade is conventionally described by dividing the factors involved in: DNA damage sensors, which activate the signal transduction process; adapters and mediators, in charge of signal amplification; transducers and effectors, which phosphorylate a series of target proteins involved in the cellular response to damage (Melo and Toczyski, 2002).

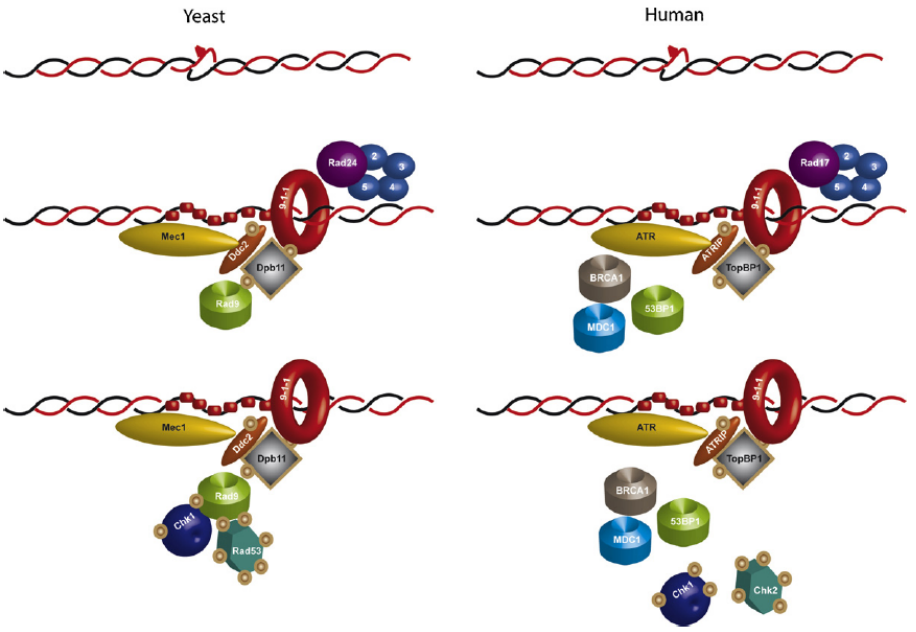

Figure 18: *A schematic overview of the DNA damage checkpoint cascade* (from Novarina et al., 2011).

For the sake of simplicity, the checkpoint cascade in yeast will be described, hinting at human proteins when necessary (Fig. 18).

4.5.1 Checkpoint activation: signals and sensors

Due to the huge plethora of different DNA lesions to which the cell needs to respond, the current model predicts that lesion processing by DNA repair mechanisms yields a common DNA intermediate, capable of activating the checkpoint response, because it is recognized by the apical checkpoint factors. Several evidences suggest that this common intermediate consists of ssDNA covered by the RPA complex (Zou and Elledge, 2003). Indeed, ssDNA tracts are generated during the incision step in NER (Giannattasio et al., 2004) and during resection at DSBs (Sugawara and Haber, 1992) and uncapped telomeres (Garvik et al., 1995); moreover, replication fork stalling displays a significant amount of ssDNA (Branzei and Foiani, 2005).

Following DNA damage, two sensor complexes are independently recruited on DNA, namely the Mec1-Ddc2 and the Rad17/Mec3/Ddc1 complex: their simultaneous presence at the damage site is needed for checkpoint activation (Melo et al., 2001). ATR/Mec1 and ATM/Tel1 are the apical checkpoint kinases; in human cells, they are equally important, with ATR mainly responding to ss-DNA exposing lesions, while ATM being directly activated by DSBs; in yeast the main kinase is Mec1, while Tel1 is redundant (Ritchie et al., 1999) and carries out only a marginal role in response to blunt (unprocessed) DSB ends (Usui et al., 2001), being instead involved in telomere length maintenance (Ritchie and Petes, 2000). Mec1 and its partner Ddc2 form a complex independently from the presence of DNA damage, and the role of Ddc2 seems to recruit Mec1 to the damage site for its activation, thus avoiding unscheduled checkpoint activation (Melo et al., 2001). The Rad17/Mec3/Ddc1 complex (9-1-1 in human) is named “PCNA-like”, due to sequence and structure similarity to PCNA; this ring-shaped complex is loaded at the 5’ ssDNA-dsDNA junctions by its “clamp loader” RFC-like complex (made up of Rad24 and Rfc2-5) (Majka et al., 2006a). Colocalization of Mec1-Ddc2 and PCNA-like complexes

is a critical step for checkpoint cascade activation (Bonilla et al., 2008). In yeast, the Ddc1 subunit of PCNA-like complex directly activates Mec1 (Majka et al., 2006b); moreover, it recruits the Mec1 activator Dpb11, which further stimulates Mec1 activity (Puddu et al., 2008; Mordes et al., 2008b); in human cells only the latter mode of ATR activation is conserved, through the action of TopBP1 protein (Mordes et al., 2008a; Navadgi-Patil and Burgers, 2009).

Once activated, Mec1 phosphorylates a series of substrates, among which Ddc2, Ddc1, Mec3, Rad24, Rpa1, Rpa2, Rad53 and Rad9. Due to its exclusive dependency from Mec1, Ddc2 phosphorylation is usually considered a biochemical marker of the apical kinase activation (Paciotti et al., 2000).

4.5.2 The signal transduction cascade: adapters and mediators

Once checkpoint is activated, the signal must be transduced down to the effectors of the cellular response to damage. A key role in this step is carried out by Rad53 and Chk1 (CHK2 and CHK1 respectively in human), two serine/theronine kinases characterized by a FHA (forkhead-associated) domain, required for interaction with checkpoint adapters. While Rad53 is absolutely required for checkpoint activation in every cell cycle phase, Chk1 seems to be involved mainly in G2/M phase, where the checkpoint cascade splits into two parallel branches controlled by Rad53 and Chk1, both under Mec1 regulation (Sanchez et al., 1999).

Activation of transducer checkpoint kinases requires the presence of adaptor proteins, among which in *S. cerevisiae* the most importan is undoubtedly Rad9. This protein, has a modular structure, characterized by conserved domains – as Tudor domain or tandem BRCT motifs – which allow its interaction with a variety of cellular factors to perform its mediator role (Toh and Lowndes, 2003). Rad9 undergoes a CDK-dependent phosphorylation in S and G2 phases, while it is phosphorylated by Mec1 (or alternatively Tel1) in response to DNA damage (Emili, 1998; Vialard et al., 1998). It appears that a partial Rad9 phosphorylation by Mec1 is required for the adaptor's localization in the lesion proximity (at least in

case of DSBs), while its complete phosphorylation allows Rad53 activation (Schwartz et al., 2002; Naiki et al., 2004): hyper-phosphorylated Rad9 can interact with the transducer kinase because Rad53 FHA domain binds a cluster of SQ/TQ motifs (SCD domain) phosphorylated by Mec1 (Sun et al., 1998; Schwartz et al., 2002).

Two models were proposed for Rad53 activation, both supported by experimental observations. According to the "solid-state catalist model" after phosphorylation Rad9 dimerizes/oligomerizes through its BRCT domains, thus creating a scaffold for Rad53: in this complex, Rad9 might act as a solid-state catalist, increasing the local Rad53 concentration, thus facilitating its in-trans autophosphorylation and subsequent activation (Soulier and Lowndes, 1999; Gilbert et al., 2001). The "adaptor-based model" suggests that Rad9's main role is to mediate recruitment of Rad53 inactive form at the lesion, where Mec1-directed phosphorylation converts it in a catalytically active kinase (Sweeney et al., 2005). As a matter of fact, the two models are not mutually exclusive. Indeed it is possible to envision a likely scenario in which Rad9 performs both the role of an adapter for Rad53-Mec1 interaction and that of a scaffold protein for Rad53 full activation. After its full phosphorylation by Mec1, Rad9 dimerizes/oligomerizes and recruits Rad53, whose auto-kinase activity is triggered by Mec1-dependent phosphorylation. Two or more Rad53 molecules, located in close proximity thanks to interaction with the Rad9 dimer/oligomer, can now autophosphorylate in-trans, resulting in full kinase activation and its release from the adapter (Pellicioli and Foiani, 2005; Sweeney et al., 2005). Once released, active Rad53 can phosphorylate all its downstream targets. Since Rad53 phosphorylation level correlates with its kinase activity, damage-dependent Rad53 phosphorylation is generally used as a marker of the signal transduction cascade activation (Pellicioli et al., 1999). Also Chk1 activation by Mec1 involves Rad9, requiring in particular its N-terminal domain named CAD (Chk1-activating domain) (Blankley and Lydall, 2004).

In S-phase Rad9 is dispensable for checkpoint activation after replicative stress, and it can be replaced by Mrc1 (human Claspin): Mec1-dependent

Mrc1 phosphorylation allows Rad53 activation (Alcasabas et al., 2001).

It's worth noting that in vertebrates Rad9 ortholog was not univocally identified, although three BRCT proteins, namely BRCA1, 53BP1 e MDC1, independently and sometimes redundantly carry out Rad9's adapter functions in human cells (Peng and Chen, 2003; Minter-Dykhouse et al., 2008; Wilson and Stern, 2008).

In recent years the importance of post-translational histone modifications for checkpoint activation was uncovered (described more in details in section *Chromatin dynamics in the DNA damage response*): in particular, some modified histone residues allow recruitment and retention of checkpoint adapters at the damage sites. In *S. cerevisiae*, Rad9 recruitment onto chromatin is mediated by interaction of its Tudor domain with methylated lysine 79 of histone H3 (H3-K79me), and of its tandem BRCT motifs with phosphorylated S129 of histone H2A: the current model suggests that the initial Rad9/H3-K79me interaction allows its localization at the damage site and its Mec1-dependent phosphorylation (Giannattasio et al., 2005; Wysocki et al., 2005); subsequently, the adapter can bind phosphorylated H2A and activate downstream checkpoint factors (Hammet et al., 2007). Interestingly, while in G1-phase disruption of the interaction between Rad9 Tudor domain and H3-K79me entails complete abolition of signal transduction, in G2/M phase checkpoint activation in these conditions is only partially defective (Giannattasio et al., 2005). Indeed, it was suggested that in this cell cycle phase an alternative pathway of Rad9 recruitment exists, mediated by Dpb11 protein, which bridges the checkpoint adapter and the PCNA-like compex (Du et al., 2006; Puddu et al., 2008).

4.5.3 The cellular response: transducers and effectors

Rad53 and Chk1 kinases transduce the checkpoint signal by phosphorylating a series of effectors which regulate the cellular response to DNA damage. In yeast three checkpoint pahways were identified, which elicit different responses according to the cell cycle phase in which the cell experiences DNA damage (Nyberg et al., 2002): G1 checkpoint prevents replica-

tion of a damaged DNA (Siede et al., 1994); intra-S checkpoint slows down S-phase progression, stabilizes the replication fork and promotes alternative replication systems (Paulovich and Hartwell, 1995); G2/M checkpoint halts the cell cycle at the metaphase-to-anaphase transition, preventing the segregation of damaged chromosomes (Weinert, 1998).

G1 checkpoint. G1 DNA damage checkpoint slows down the cell's entry into S-phase: beyond inhibiting DNA replication, it delays – in a dose-dependent manner – spindle pole body duplication, bud emergence and CDK1 activation (Fitz Gerald et al., 2002). This slowdown is due to Rad53 dependent phosphorylation of Swi6 transcription factor, resulting in inactivation of the Swi6/Swi4 complex responsible for the transcription of *CLN1* and *CLN2*: the repression of G1 cyclin genes causes a delay at the G1/S transition (Sidorova and Breeden, 1997).

S-phase checkpoint. The intra-S checkpoint responds to DNA damage experienced in S-phase, while the replication checkpoint is activated by aberrant replication forks: these two sub-pathways share many features, and can be collectively described under the name of S-phase checkpoint (Nyberg et al., 2002).

Replication fork stalling (due to dNTPs depletion or to DNA lesions) activates the S-phase checkpoint thanks to proteins associated to the fork itself, among which Sgs1 helicase, Pol2 subunit of DNA polymerase, Dpb11 and Drc1 proteins, and RFC subunits 2,3,4 and 5 (Nyberg et al., 2002); Rad53 activation in S-phase is mediated by two redundant sub-pathways, one dependent on Rad9, the other on Mrc1 and Tof1 (Alcasabas et al., 2001; Foss, 2001; Katou et al., 2003). Beyond stabilizing the replication fork, S-phase checkpoint blocks firing of late replication origins and also uncontrolled firing of latent origins; moreover, it inhibits recombination activities at the fork. Lastly, after the cause of fork arrest is removed, it allows resumption of replication (Branzei and Foiani, 2006).

G2/M checkpoint. In G2/M phase, checkpoint cascade elicits the cellular response to DNA damage through two parallel pathways under the control of Chk1 and Rad53 kinases. On the one hand, Chk1 phosphorylates Pds1, preventing its degradation, which is required for mitotic exit: Pds1 stabilization prevents chromosome segregation, promoting arrest at the metaphase-to-anaphase transition (Sanchez et al., 1999). On the other hand, Rad53 promotes Pds1 stabilization by preventing its interaction with Cdc20 and its subsequent ubiquitylation by the APC/C^{Cdc20} complex (Agarwal et al., 2003). Moreover, Rad53 inhibits mitotic exit also through an inhibitory phosphorylation on Cdc5, therefore preventing APC/C^{Cdh1} activation and the subsequent degradation of mitotic cyclins: this contributes to the maintenance of a high CDK activity (Sanchez et al., 1999).

4.5.4 Checkpoint switch-off

Cell survival to DNA damage requires not only timely checkpoint activation, but also proper shutdown of the signal transduction, which ensures resumption of cell cycle progression. Checkpoint switch-off may occur through two genetically controlled mechanisms, namely recovery and adaptation (Clémenson and Marsolier-Kergoat, 2009).

After successful lesion repair, the recovery mechanism stimulates checkpoint switch-off and re-entry into cell cycle: apart from the disappearance of the most upstream activating signal (the DNA damage), a key step in this process is Rad53 inactivation through dephosphorylation by Ptc2 and Ptc3 phosphatases (Leroy et al., 2003; O'Neill et al., 2007); however, the signaling cascade is inactivated at multiple levels, both downstream, through dephosphorylation and removal of checkpoint proteins from the damage site (Vaze et al., 2002), and upstream, as suggested by the prolonged cell cycle arrest and Rad53 phosphorylation induced by Ddc2 or Tel1 overexpression (Clerici et al., 2001).

In case the damage cannot be repaired, the adaptation mechanism allows resumption of cell cycle progression despite the persistence of unrepaired

DNA lesions, as long as this does not compromise cell survival. While in unicellular organisms like *S. cerevisiae* adaptation clearly represent an extreme attempt to survive, which relies on repair systems active in another cell cycle phase, the significance of this mechanism in multicellular organisms is less obvious, and is a source of genomic instability (Syljuåsen, 2007). Also in adaptation a key step is Rad53 dephosphorylation by Ptc2, Ptc3 and Pph3 phosphatases (Heideker et al., 2007); a major player in adaptation is Cdc5, which prevents/counteracts phosphorylation of many checkpoint factors, including Ddc2, Rad9 and Rad53 (Pellicioli et al., 2001; Donnianni et al., 2010); control of ssDNA generation is also required (Lee et al., 1998); also several recombination and chromatin remodeling proteins are involved, which regulate checkpoint factor association to the DNA damage site (Lee et al., 2001; Vaze et al., 2002; Lee et al., 2003).

4.6 Chromatin dynamics in the DNA damage response

Since in the eukaryotic nucleus the genetic material is packed into a higher order chromatin structure (Kornberg, 1977; Li and Reinberg, 2011), the elevated level of compaction might interfere with recruitment of the enzymes involved in DNA metabolism, damage repair and checkpoint signaling. As a matter of fact, chromatin is a highly dynamic structure, and in recent years multiple connections between chromatin structure and the DDR emerged, to such an extent that chromatin might be considered as an integral player in the DDR, acting as a dynamic platform for signaling and repair factors, which regulates the initiation, propagation and inactivation of the DDR (Soria et al., 2012). Besides being controlled by chromatin remodeling activities, chromatin dynamics rely on post-translational histone modifications and incorporation of histone variants, which create a so-called "histone code" for the fine-tuning of DDR (Lydall and Whitehall, 2005; Lazzaro et al., 2007; Downs et al., 2007a).

4.6.1 ATP-dependent chromatin remodeling

ATP-dependent chromatin remodeling activities are accomplished by multisubunit complexes, which employ the energy derived from ATP hydrolysis to alter histone-DNA contacts, modify the torsional degree of nucleosomal DNA, reposition nucleosomes on DNA, partially or completely remove the histone octamer from DNA, increase or decrease DNA accessibility to several proteins. Examples of key chromatin remodeling complexes involved in DDR are RSC complex, SWI/SNF complex and INO80 complex (Flaus et al., 2006; Downs et al., 2007a).

4.6.2 Post-translational histone modifications

Histones ar rich in lysine, arginine, serine and threonine residues, which are usually located at the external surface of the histone octamer; these residues undergo extensive post-translational modifications, such as phosphorylation, methylation, acetylation, ribosylation, deimination, ubiquitylation and sumoylation. Differences in electrostatic properties between the modified versus non-modified form of these residues may significantly alter histone-DNA interaction, or contacts between histones of neighbouring nucleosomes; moreover, after the identification and characterization of protein domains specialized in recognition and binding of specific modified histone residues, a picture emerged in which the different post-translational histone modifications allow recruitment of several factors onto chromatin (Costelloe et al., 2006; Kouzarides, 2007).

H2A phosphorylation. One of the earliest events occurring after DNA damage, is Mec1- and Tel1- dependent phosphorylation of the C-terminal H2A tail on serine 129 (Downs et al., 2000; Marti et al., 2006; Moore et al., 2007), a modification conserved also in human (S139 of histone variant H2AX) and in *Schizosaccharomyces pombe* (S128 and S129) (Rogakou et al., 1998; Nakamura et al., 2004). This modification, named γ-H2A(X), spreads for several Kb on chromatin adjacent to the lesion (Lowndes and Toh, 2005), and is involved in both DNA damage repair (Downs et al.,

2000) and checkpoint signaling (Celeste et al., 2003; Nakamura et al., 2004). The role of γ-H2A(X) in repair resides mainly in cohesins recruitment at DSBs, providing the sister chromatid cohesion required for recombinational repair (Unal et al., 2004). Conversely, it appears that the function of γ-H2A(X) in checkpoint consists in checkpoint signaling maintenance by stabilizing protein association to chromatin in foci, rather than directly participating in checkpoint activation through their recruitment (Celeste et al., 2003). Accordingly, it was recently found that, while initial Rad9 recruitment onto chromatin requires methylation of H3-K79 (see above), stable Rad9 accumulation at the damage site depends on H2A phosphorylation (Javaheri et al., 2006). In line with the proposed role for γ-H2A(X) in checkpoint signaling maintenance, H2A dephosphorylation by Pph3 phosphatase in yeast is needed for terminating the signaling cascade (Keogh et al., 2006). Moreover, γ-H2A(X) allows recruitment of many chromatin remodeling factors, through interaction between phospho-S129 and Arp4, a subunit shared by INO80 and SWR1 complex and by acetyltransferase NuA4 (Shen et al., 2003).

H2B ubiquitylation and H3 methylation. In recent years two histone modifications were detected which are indispensable for checkpoint signal transduction down to the effector kinases. Rad6/Bre1 complex is responsible for histone H2B ubiquitylation on lysine 123; this modification is a prerequisite for the subsequent H3 methylation on lysines 4 and 79 by methyltransferases Set1 and Dot1 respectively (Hwang et al., 2003; Krogan et al., 2002; van Leeuwen et al., 2002). H3-K79me, in particular, turned out to be necessary for damage-dependent phosphorylation of Rad9 and subsequent Rad53 activation: several works emphasized that the role of this modification lies in its ability to interact with Rad9 Tudor domain, thus recruiting the adapter protein onto chromatin and allowing its phosphorylation by Mec1 (Giannattasio et al., 2005; Wysocki et al., 2005; Grenon et al., 2007). It should be mentioned, though, that, while in G1-phase H3-K79 methylation is strictly required for checkpoint activation, in G2/M-phase a redundant pathway for Rad9 recruitment exists, dependent on

Dpb11 (Puddu et al., 2008). The same happens in *S. pombe*, where Crb2 (Rad9 ortholog) recruitment in G2/M-phase is mediated by Cut5 (Dpb11 ortholog) (Du et al., 2006). The importance of this histone mark is underlined by its conservation throughout evolution: indeed, human Rad9 ortholog 53BP1 binds H3-K79me, which mediates its recruitment at DSBs (Huyen et al., 2004); in *S. pombe*, instead, Crb2 is recruited onto chromatin my means of interaction between its Tudor domain with H4-K20 methylated by Set9 (Sanders et al., 2004; Du et al., 2006). Interestingly, this modification, absent in *S. cerevisiae*, is instead detectable in human, where it seems to contribute to 53BP1 recruitment (Botuyan et al., 2006).

It is worth noting that – both in yeast and human – H3-K79 is constitutively methylated, and no variation in its methylation levels is observed after genotoxic treatment (Feng et al., 2002; van Leeuwen et al., 2002; Huyen et al., 2004). Several hypotheses were therefore proposed to explain the involvement of this histone modification in checkpoint activation: it is possible that Rad9 interacts constitutively with H3-K79me, and is therefore immediately available for its Mec1-dependent phosphorylation; alternatively, Rad9 might be weakly bound to H3-K79me, and its damage-dependent oligomerization could allow its accumulation at the damage site. Another interpretation suggests that DNA damage causes a specific H2B ubiquitylation, therefore inducing a local increase in H3-K79me levels, which in turn is responsible for an increased Rad9 molecules concentration at the lesion. However, the most accredited interpretation suggests that, due to high chromatin compaction, constitutively methylated H3-K79 is buried inside the nucleosome, and a damage-dependent change in chromatin structure might expose the modified residue, making it accessible for its interacting proteins (Giannattasio et al., 2005; Huyen et al., 2004; Lazzaro et al., 2008). This chromatin structural alteration could result from ATP-dependent chromatin remodeling activities, or ensue just as a result of DSB-induced chromatin relaxation (Bakkenist and Kastan, 2003); in at least one case, remodeling-indendent Rad9 recruitment onto chromatin was observed, suggesting a direct role for DNA damage in disrupting nucleosome packaging (Javaheri et al., 2006). In any case,

the possibility remains open that H3-K79me exposure results from a chromatin structure change caused by other post-translational modifications of histone residues.

H3 and H4 acetylation. Several histone residues undergo acetylation, which, beyond mediating protein recruitment, results in chromatin relaxation; indeed, lysine acetylation at the N-terminal tails of histones H3 and H4 removes the positive charge on the side chain, thus destabilizing higher order chromatin structure (Downey and Durocher, 2006). In particular, H3K56 acetylation by Rtt109, and H4 acetylation by Esa1, Hat1 and Gcn5 acetyltransferases (HAT) were found important for the cellular response to DNA damage (Masumoto et al., 2005; Bird et al., 2002; Qin and Parthun, 2006; Tamburini and Tyler, 2005). Conversely, several works highlighted the involvement of histone deacetylases (HDAC) in DDR, likely required for the restoration of chromatin state during termination of repair processes and checkpoint signaling (Downs et al., 2007b).

4.6.3 Incorporation of histone variants

A third mechanism through which chromatin structure can be modulated is the substitution of one or more histones at the nucleosome core with histone variants. To date, known histone variants concern mainly histones H2A and H3; some of them are conserved from yeast to human, while others are typical of vertebrates. Incorporation of histone variants can modify the properties of nucleosome surface (defined by the exposed residues), or alter nucleosome or higher order chromatin structure stability: the function of these changes range from transcriptional regulation, to definition of functional chromatin domains, to gene silencing, to DDR (Kamakaka and Biggins, 2005).

Among the histone variants involved in DDR, H2AZ is particularly relevant. SWR complex promotes replacement of a γ-H2AX/H2B dimer with a H2AZ/H2B dimer, thus promoting DSB resection, while the INO80 complex stimulates H2AZ replacement by H2A; these dynamics are thought to

participate in restoring chromatin state at a pre-damage condition (Kalocsay et al., 2009; Papamichos-Chronakis et al., 2011).

4.7 Mitotic checkpoint

To ensure proper chromosome partitioning during mitosis, eukaryotic cells rely on sister chromatid cohesion, mediated by cohesins: these proteins form a multimeric ring-like structures which helds sister chromatids together from the end of DNA replication until the metaphase-to-anaphase transition, when they align at the center of the cell, ready for segregation. At this stage, cohesin cleavage by separase triggers anaphase and sister chromosome separation. Untimely loss of sister chromatid cohesion – detrimental for proper chromosome segregation and therefore for genome stability (see Section *Chromosome segregation and genome instability*) – is prevented by the mitotic checkpoint (also called spindle-assembly checkpoint – SAC), a feedback mechanisms which inhibits anaphase until all the chromosomes are stably attached to the spindle, an event which guarantees accurate segregation (Musacchio and Salmon, 2007; Lara-Gonzalez et al., 2012).

Briefly, mitotic checkpoint senses the presence of an unattached kinetochore through the binding of Mad1-Mad2 dimers (De Antoni et al., 2005); this event triggers the formation of the so-called "mitotic checkpoint complex" (MCC), made up of Mad2, BubR1/Mad3, Bub3, and Cdc20 (Sudakin et al., 2001; Morrow et al., 2005). Cdc20 is the APC/C co-activator required for degradative ubiquitylation of securin (the separase inhibitor) and B-type cyclins (CDK1 activators in mitosis): impairment of securin degradation maintains separase in its inactive state, thereby preventing cohesin cleavage; meanwhile inhibition of B-type cyclins degradation prolongs CDK1 activation, delaying mitotic exit until all chromosomes are correctly oriented and proper microtubule-kinetochore attachment has been established (Musacchio and Salmon, 2007). When all kinetochores are stably bound to spindle microtubules, the mitotic checkpoint is satisfied: Mad1-Mad2 and the other SAC proteins are displaced from the kinetochore

and APC/C^{Cdc20} inhibition is relieved, thereby allowing securin and B-type cyclins degradation and subsequent progression into anaphase (Musacchio and Salmon, 2007; Musacchio, 2011).

5 *Saccharomyces cerevisiae* as tool for investigating genome stability maintenance

5.1 *S. cerevisiae* as a model organism

S. cerevisiae (budding yeast) is a unicellular fungus belonging to *Ascomycota* class; its features (above all its lab tractability and the ease of its genetic manipulation) earned it a prominent position among model systems for the study eukaryotic cellular and molecular biology (Botstein and Fink, 1988). This non-pathogenic organism has a very short cell cycle (doubling time of ∼120'), and can propagate in the haploid state (useful for the study of recessive mutations) or in the diploid state (suitable for studies on dominant mutations and for complementation tests). *S. cerevisiae* has a small genome (∼13 Mb, split into 16 linear chromosomes), which was the first eukaryotic genome fully sequenced (Goffeau et al., 1996); it can be easily transformed with exogenous DNA, and its homologous recombination mechanisms can be exploited to integrate the transforming DNA fragment in a precise position within the genome. The ease of targeted deletion of a specific genetic locus allowed the creation of a nearly complete set of deletions of each budding yeast open reading frame (ORF) (Giaever et al., 2002), which – combined with the so-called 'awesome power of yeast genetics' (Forsburg, 2001) – paved the way for highly informative genome-wide scale experiments (Botstein and Fink, 2011).

In the last 10 years the most successful approach to search for functional interactors of a given gene product has been based on the concept of "synthetic lethality". This phenotype occurs when mutations in two different genes, each not lethal by itself, display a lethal phenotype when combined. Only in yeast this method can be applied on a genomic scale and it is

called "synthetic gene array" (SGA). Starting with a library of marked yeast deletion mutants and using robots to manipulate simultaneously the thousands of strains of the library, it is possible to cross a strain carrying a mutation in a query gene to all the viable deletion mutants in the library; subsequent recovery of haploid double-mutant progeny by means of haploid-specific selectable markers results in combining individually the deletions of all yeast genes with our favorite mutant strain (Baryshnikova et al., 2010): this approach yielded a highly informative genetic landscape of a eukaryotic cell (Costanzo et al., 2010).

The success of *S. cerevisiae* as a model organisms resides, on the one hand, on the high degree of evolutionary conservation of cellular pathways and molecular mechanisms from yeast to higher eukaryotes; and, on the other hand, in the lower complexity of these processes in yeast. Therefore it is reasonable to study these mechanisms in a simpler experimental system, like yeast, and later extend the acquired knowledge to increasingly complex organisms, up to human. In this respect, it is worth noting that of the nearly 5800 protein-coding *S. cerevisiae* genes, nearly 1000 (i.e., 17%) are members of orthologous gene families associated with human disease (Dolinski and Botstein, 2007; Heinicke et al., 2007).

5.2 Study of genome instability in *S. cerevisiae*

Historically, *S. cerevisiae* has been successfully employed as a heterologous host to study the functions of human DNA repair proteins and genome stability factors (Aggarwal and Brosh, 2012). Moreover, multiple assays are available in yeast to detect different forms of genomic instability, from point mutations (Foster, 2006) and instability of repeated sequences (Kelly et al., 2007; Razidlo and Lahue, 2008) to spontaneous recombination (Spell and Jinks-Robertson, 2004), chromosomal rearrangements (Motegi and Myung, 2007) and chromosome loss (Hieter et al., 1985; Spencer et al., 1990).

One of the main aims in the study of genomic instability is the systematic characterization of chromosomal rearrangements. In recent years, the development of assays which permit the identification and characterization

of a wide spectrum of genomic rearrangements (Chen and Kolodner, 1999; Schmidt et al., 2006; Cheng et al., 2012) allowed the in-depth analysis of pathways contributing to genome instability in yeast. Remarkably, these studies showed that chromosomal rearrangements observed in *S. cerevisiae* display similar frequencies and features to those detected in human cancers (Kolodner et al., 2002; Putnam et al., 2005). This observation, combined with the high degree of conservation of DNA damage checkpoints and DNA repair pathways, makes budding yeast an excellent system to study genomic instability. Moreover, the discovery that the genetic background influences dramatically the class of rearrangements generated imply that the characterization of the different classes of CGRs observed in human tumors may shed new light on the mechanisms leading to their formation, as well as on the presence of genetic defects in different kinds of cancer. These observations also suggest that the evolving genotype of cancer cells during tumor proliferation determines, at least partially, which genes are readily misregulated by genomic instability and therefore likely control carcinogenesis (Putnam et al., 2005).

Aim of the project

The maintenance of genome integrity is a key task for all living organisms, ensuring survival at the cell and organism level, and transmission of an intact genetic material to the progeny. Genome integrity can be jeopardized by a huge number of factors, which need to be counteracted by an intricate network of mechanisms deputed to maintain genome stability. The full knowledge of these mechanisms is still far from being achieved, and further investigation is required at multiple levels. The first basic task is to identify all the genes and pathways involved in controlling genome integrity. Moreover, also for the genes already known to be implicated in these controls, a deeper characterization is needed to define the mechanism(s) through which they contribute to preserve the genome. Finally, even when a genome integrity pathway has been identified, in most cases the mechanistic molecular details still wait to be clarified.

The work described in this thesis explores the genome stability landscape at all these three levels.

1 Screening the yeast deletion collection for new genome stability genes

To identify new non essential genes involved in genome integrity maintenance, a screen was designed, set up and performed in *S. cerevisiae*. The screen is based on the effect of overexpressing the *DDC2* DNA damage checkpoint gene in the yeast deletion mutant collection, which could allow the identification of mutant of strains experiencing spontaneous DNA damage.

The preliminary characterization of a new candidate genome integrity

gene is presented in this thesis.

2 Investigating the role of RNase H in genome integrity maintenance

Following the recent evidence of massive ribonucleotides (rNTPs) incorporation in genomic DNA, which was shown to promote genomic instability (Nick McElhinny et al., 2010b,a), we decided to investigate the mechanistic consequences of this rNTPs incorporation, and the biological role of yeast RNases H, whose activities in rNTPs removal from RNA:DNA moieties are essential to preserve genome integrity.

3 Characterization of the dynamics of Rad9 dimerization and chromatin binding for checkpoint activation

S. cerevisiae Rad9 is a key DNA damage checkpoint mediator, involved in the activation of the yeast checkpoint kinase Rad53 (human CHK2). Multiple mechanistic requirements for Rad9-mediated checkpoint activation have been described, namely two histone modifications promoting Rad9 recruitment onto chromatin (Giannattasio et al., 2005; Javaheri et al., 2006; Toh et al., 2006; Hammet et al., 2007; Nnakwe et al., 2009), and BRCT domain-mediated Rad9 dimerization and possibly oligomerization (Soulier and Lowndes, 1999; Usui et al., 2009). Nonetheless, the crosstalks between these molecular determinants and their functional significance are poorly understood.

We investigated the dynamics of Rad9 dimerization, chromatin binding, CDK-dependent phosphorylation and checkpoint activation in G1 and M phases of the cell cycle, exploring in particular an alternative M-phase specific branch for checkpoint activation which is dependent on Dpb11 (Puddu et al., 2008).

Main results

1 Identification of new genes and pathways important for genome stability

Yeast strains deprived of key genome stability factors often undergo spontaneous accumulation of endogenous DNA damage. This phenotype is indirectly detectable as a constitutive partial phosphorylation of the Rad53 checkpoint kinase, indicative of a chronically alerted DNA damage checkpoint response (examples can be seen in Zhang et al., 2006a; Driscoll et al., 2007; Duro et al., 2008; and Supplementary Figure 1). We designed a strategy to select these phenotypes, in order to screen the yeast deletion collection for genome integrity genes, based on accumulation of endogenous DNA damage.

1.1 *DDC2* overexpression allows the identification of genes controlling genome integrity

The rationale of our screening relies upon the overexpression of the *DDC2* gene, encoding the binding partner and activator of the DNA damage checkpoint apical kinase Mec1 (see Section *DNA damage checkpoints*). High levels of Ddc2 cause hyperactivation of the checkpoint response after DNA damage, resulting in prolonged cell cycle arrest and cell death, while no effect is visible on undamaged cells (Clerici et al., 2001). We verified that *DDC2* overexpression increases sensitivity to low doses of DNA damaging agents, and we speculated that it might also sensitize yeast cells to endogenous DNA damage. This hypothesis was confirmed by the severe

growth impairment caused by *DDC2* overexpression in some yeast strains deleted for genes coding for known players in genome integrity maintenance (Novarina et al., in preparation, Fig. S1). We exploited the Synthetic Genetic Array (SGA) automated approach (Baryshnikova et al., 2010, and Section S. cerevisiae *as a model organism*), to overexpress *DDC2* under a galactose-inducible promoter on a multicopy plasmid in the yeast haploid deletion collection, and we scored for those mutants whose fitness was reduced on galactose medium compared to the control experiment with the empty vector.

Our screen identified genes involved in several cellular pathways (Novarina et al., in preparation, Fig. 1), consistent with multiple mechanisms impacting on genome stability. Beside some already known DNA damage response genes, we found several genes involved in safeguarding cells against oxidative stress (i. e. oxidative stress response, peroxisome function and mitochondrial metabolism), many of which were not identified in previous screens. Additional genes identified belong to pathways already implicated in genome integrity maintenance, namely chromatin remodeling, modulation of transcription, cell cycle control, regulation of cytoskeleton dynamics, proteasome assembly and function and autophagy. Other pathways were more unexpected, such as protein sorting (mainly vesicular trafficking to vacuole or Golgi), ribosome biogenesis, aminoacid biosynthesis or cell wall integrity and composition. Importantly, about 20% of the ORFs identified in the screen are still uncharacterized, leaving the way open for future studies. Unespectedly, our screen also identified some strains which show increased fitness after *DDC2* overexpression, but this class of genes needs further investigation.

1.2 *VID22* is a new genome stability gene in *S. cerevisiae*

Among the genes identified, we focused on *VID22*, which was not previously implicated in genome stability, being annotated as "Glycosylated integral membrane protein localized to the plasma membrane" which "plays

a role in fructose-1,6-bisphosphatase (FBPase) degradation; involved in FBPase transport from the cytosol to Vid (vacuole import and degradation) vesicles" (Saccharomyces Genome Database). A direct involvement of *VID22* in genome integrity maintenance is suggested by the following experimental observations (Novarina et al., in preparation, Fig. 2-3-S2-S3): i) Vid22 localizes in the nucleus; ii) a *vid22Δ* strain displays a persistent partial Rad53 phosphorylation and increased levels of γH2A in unperturbed conditions, indicative of chronic accumulation of DNA damage; iii) a *vid22Δ* strain shows a higher spontaneous mutation rate at the *CAN1* locus and a greater recombination rate at the rDNA locus; iv) deletion of *VID22* displays negative genetic interactions with many genes involved in resolution of recombination intermediates arising during replication (Costanzo et al., 2010); v) *vid22Δ* cells are sensitive to genotoxic treatment.

Vid22 was found in a complex with its paralog Env11 (encoded by *YGR071C*) and with the transcription factor and telomere silencing regulator Tbf1 (Krogan et al., 2006). Strikingly, an *env11Δ* mutant was not found sensitive to any genotoxic agent examined, and did not display hallmarks of genomic instability, suggesting that *VID22* controls genome integrity at least partially independently from its role in the Vid22-Env11-Tbf1 complex. However, we could not similarly test a *tbf1Δ* mutant, since Tbf1 is an essential gene.

Bioinformatic analysis of the Vid22 protein sequence revealed two conserved domains, an N-terminal BED-finger domain and a central RNase H fold (Fig. 19). The BED-finger domain is a modified zinc finger with DNA-binding ability found in transcription factors, proteins associated with chromatin insulators, and transposases (Aravind, 2000). The RNase H fold is a structural characteristic of the catalytic core of enzymes belonging to the retroviral integrase superfamily, such as RNases H, Holliday junction resolvases, nucleases, retroviral integrases, reverse transcriptases and transposases. Despite low sequence similarity, the structure of the RNase H fold is remarkably conserved: it consists of a five-stranded β-sheet, with two key catalytic Asp residues located in the middle of the

first β-strand and at the end of the fourth strand respectively (Nowotny, 2009). However, these catalytic residues do not seem to be conserved in Vid22, as suggested by the secondary structure-based alignment between the RNase H fold of Vid22 and the highly similar RNase H fold of the Hermes transposase through the Phyre2 server (Kelley and Sternberg, 2009) (Supplementary Figure 2): thus, it seems unlikely that the RNase H fold of Vid22 is catalytically active.

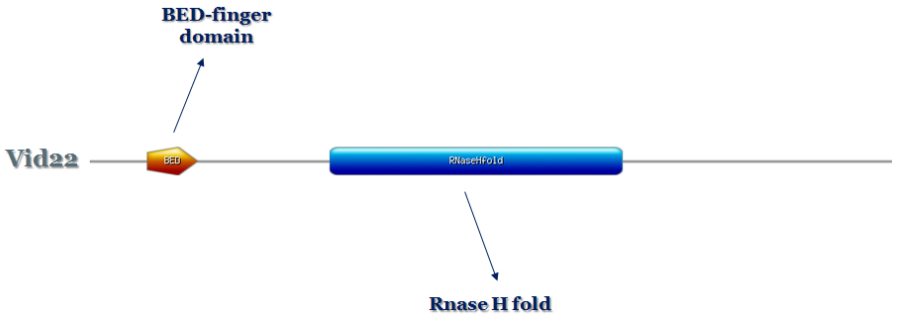

Figure 19: *Schematic representation of Vid22 conserved domains.*

FACS analysis of cell cycle progression in *vid22Δ* cells revealed a delay in S-phase, and a discrete subpopulation of cells is arrested at the G1/S transition as unbudded cells (Novarina et al., in preparation, Fig. 4). We propose that these phenotypes can be explained by the analysis of the transcriptional profiling we carried out on the *vid22Δ* mutant strain: in fact, we found that in the absence of *VID22*, several genes involved in the control of G1/S transition and S-phase progression are downregulated. These genes include: a) *CLN1* and *CLN2*, coding for G1 cyclins responsible for expression of the G1/S regulon through a positive-feedback loop (Skotheim et al., 2008); b) *CLB6*, coding for an S-phase cyclin involved in the firing of replication origins and in the initiation of DNA synthesis (Schwob and Nasmyth, 1993); c) *CDC6* and *CDC45*, whose products are required for replication initiation (Enserink and Kolodner, 2010). The experimental evidences linking deregulation of G1/S transition and replication origin firing with genomic instability (Dershowitz and Newlon, 1993; Spruck et al., 1999; Bielinsky, 2003; Enders and Maude, 2006) suggest a

model to describe the transcriptional effects of *VID22* deletion on genome integrity: reduced expression of genes encoding for cyclins and other key replication initiation factors causes a stochastic cellular arrest at the G1/S transition in a minority of cells, while the rest of the population proceeds through S phase with insufficient origin firing, leading to genomic instability (Novarina et al., in preparation, Fig. 5).

To explore a possible evolutionary conservation of *VID22*, alignment-based homology search was performed, but no significant similarity was found in higher eukaryotes. Conversely, analysis of proteins which share the same combination of BED-finger domain and RNase H fold yielded interesting results. Our attention was drawn by *Drosophila* DREF and its human ortholog ZBED1/hDREF, since both are implicated in the control of G1/S transition. DREF transcription factor regulates transcription of several genes involved in DNA replication and cell proliferation, such as the genes coding for PCNA, Orc2, Orc5, DNA primase, DNA polymerase α, RFC140, E2F and cyclin A (Yamaguchi et al., 1995; Matsukage et al., 2008). Similarly, ZBED1 targets the promoters of genes involved in DNA replication, DNA repair and cell cycle regulation. Importantly, ZBED1 silencing results in inhibition of G1/S progression, reminiscent of what we observed in *vid22Δ* cells (Ohshima et al., 2003). These findings suggest that the role of *VID22* in the control of genome integrity is likely to be conserved in higher eukaryotes.

2 RNase H and DNA damage tolerance mechanisms protect cells from ribonucleotides incorporated in DNA

Eukaryotic cells possess two RNase H activities, namely RNase H1 and RNase H2, exhibiting partially overlapping substrate specificity: while both are capable of cleaving a stretch of at least four rNMPs in an RNA:DNA hybrid, only RNase H2 can incise 5' to a single rNMP incorporated within a DNA molecule (Cerritelli and Crouch, 2009). Mammalian RNase H1 is

essential for mitochondrial DNA replication (Cerritelli et al., 2003), but this function is not conserved in budding yeast. RNase H2, which represents the major RNase H activity in eukaryotic cells, has been implicated in several cellular processes involving RNA:DNA hybrids, from Okazaki fragment processing to removal of R-loops (Qiu et al., 1999; Huertas and Aguilera, 2003). RNase H2 is a trimeric complex, made up of one catalytic and two non-catalytic subunits, encoded respectively by *RNH201*, *RNH202* and *RNH203* genes in *S. cerevisiae*; all the three subunits are required for RNase H2 activity (Jeong et al., 2004).

It was recently shown that ribonucleotides (rNTPs) are incorporated in DNA at high levels by replicative polymerases (Nick McElhinny et al., 2010b), and this incorporation constitutes a threat for genome integrity (Nick McElhinny et al., 2010a). This discovery prompted us to investigate, in collaboration with the Kunkel lab, the role of yeast RNases H and possibly other pathways in the preservation of genome integrity.

We found that the absence of both RNase H activities causes chronic checkpoint activation in untreated yeast cells, suggesting a persistent replication stress. Moreover, simultaneous knock down of RNase H1 and RNase H2 is synthetically lethal with a Polε variant (encoded by *pol2-M644G*) which incorporates rNTPs at extremely high levels , indicating that both RNase H activities are crucial for the repair of rNTPs incorporated during replication (Lazzaro et al., 2012, Fig. 1-S1). This observation reveals a previously undetected role for RNase H1 in removal of rNTPs from the chromosomes.

Unrepaired rNMPs in genomic DNA will impact on cell-cycle progression since, at the next round of DNA replication, a RNA-containing DNA template must be duplicated. Given that replicative DNA polymerases are incapable of replicating past a template ribonucleotide (Watt et al., 2011), we assume that when the replisome encounters rNMPs in the template strand, endogenous replication stress is generated. Low levels of replication stress-inducing agents (HU or MMS) are known to be toxic for cells with replication problems. And indeed, *rnh1Δ rnh201Δ* cells are highly sensitive to very low doses of HU or MMS: cells arrest in G2-M after the

bulk of genome replication has been completed, accumulate hyperphosphorylated Rad53, and exhibit massive cell lethality. Similar results were observed with the *pol2-M644G rnh201Δ* double mutant, confirming that increased rNTPs incorporation sensitizes yeast cells to replication stress (Lazzaro et al., 2012, Fig. 1-S1). We excluded that these phenotypes are due to defects in Okazaki fragment processing or R-loops removal (Lazzaro et al., 2012, Fig. S2).

Since *rnh1Δ rnh201Δ* cells are viable, we investigated the additional cellular pathways involved in the removal or tolerance of rNTPs in the genome. Our genetic analysis excludes a contribution of NER in correcting rNMPs, while a minor involvement of BER in repairing rNMP-containing chromosomes cannot be completely ruled out. We then explored a possible role of DNA damage tolerance mechanisms in the replication of rNMPs-containing chromosomes. Loss of only the template switch pathway (Post-replication recombinational repair or Replication fork regression) or only translesion DNA synthesis (TLS) has no detectable effect on *rnh1Δ rnh201Δ* cells. Conversely, simultaneous inactivation of both template switch and TLS had a striking effect in cells lacking RNAse H activities: these cells exhibit severe growth defect, G2-M arrest, cell lethality, extreme sensitivity to low HU doses, and a dramatic increase in PCNA ubiquitylation, indicative of constitutively active DNA damage tolerance pathways (Lazzaro et al., 2012, Fig. 2-5-S3). Further genetic and biochemical analyses to identify which translesion polymerases were implicated in rNMPs bypass showed that cells can use Pol ζ to replicate rNMPs-containing templates and that Rev1 likely plays a non-catalytic role to promote Pol ζ activity (Lazzaro et al., 2012, Fig. 3-4).

Altogether, these findings indicate that: i) high levels of unrepaired rNMPs in the chromosomes hinder DNA synthesis blocking replication forks, leading to replication stress; ii) RNases H1 and H2 are crucial to process misincorporated rNTPs; iii) template switch mechanisms and Pol ζ are critical to allow replication of endogenous, unrepaired rNMPs (Lazzaro et al., 2012, Fig. 6). Interestingly, the mechanistic details of single rNTPs removal from DNA were investigated *in vitro* in a following paper by the

Burgers group: they coined the definition of Ribonucleotide Excision Repair (RER), and showed that this newly characterized repair pathway relies on RNase H2 for incision, Fen1 or Exo1 for flap removal, Pol ε or Pol δ together with PCNA and RFC complexes for repair synthesis, and DNA ligase I for nick sealing (Sparks et al., 2012).

The role of RNases H in the preservation of genome integrity through rNTPs removal is conserved also in mammals (Reijns et al., 2012). This may have important implications for human health. The observation that cells depleted for RNases H are sensitive to low levels of replication stress may have consequences for cancer chemotherapy. In fact, many cancer cells are characterized by endogenous replication stress and may be thus sensitized to inhibitors of RNase H activity, which could selectively kill cells experiencing replication stress. Furthermore, mutations in any of the three subunits of human RNase H2 cause a rare genetic syndrome named Aicardi-Goutières Syndrome (AGS), an auto-inflammatory disorder mimicking a congenital viral infection that may arise from nucleic acid byproducts generated during DNA replication (Aicardi and Goutières, 1984; Crow et al., 2006; Crow and Rehwinkel, 2009). Our work may contribute to a better understanding of the mechanisms underlying the disease. In particular, the reported synthetic interactions between RNase H activities, replication stress, template switch and TLS, could facilitate the identification of modifier genes that may influence the penetrance of AGS-causing mutations in human RNase H2.

To gain further insights into the function(s) of RNAses H in eukaryotic cells, we performed a genome-wide screen to identify synthetic genetic interactions with the simultaneous loss of RNase H1 and RNase H2 in budding yeast. In fact, even though a global genetic interaction map in *S. cerevisiae* has been already published (Costanzo et al., 2010), the data obtained from digenic interactions are not always informative, due to functional redundancy in pathways of crucial importance for the cell. This is the case of RNase H1 and RNase H2, where indeed only simultaneous ablation of both activities makes cells sensitive to genotoxic treatment (Lazzaro et al., 2012). In collaboration with the Brown's and Boone's

labs in Toronto, we performed three SGA screens with a double mutant *rnh1Δ rnh201Δ* query: one was done in unperturbed conditions, while the others were performed in the presence of 10 and 25 mM HU respectively (Supplementary Figure 3). The overall results of the screens appear very promising for four main reasons: a) the large majority of the ∼50 identified interactors fall in categories that are related to likely functions of RNases H in the cell (replication/recombination/repair 62%; chromatin 10%; meiosis/mitosis 10%; mitochondria 2%; transcription 2%; uncharacterized 2%; others 12%); b) some genes were identified in all conditions, while others were specifically found in the presence of HU; c) most of the identified genes worsen the HU sensitivity of RNases H mutants, but some of them appear to ameliorate the phenotype; d) among the interactors identified we often found genes coding for subunits of the same protein complex making the likelihood of interaction more evident. The identified genes represent putative candidates for the yet unidentified AGS mutations found in human patients or may code for genes linked to the "compensatory mechanisms" observed in some AGS patients.

3 Dynamics of Rad9 dimerization and chromatin binding for checkpoint activation

S. cerevisiae Rad9 is a conserved key mediator protein of the DNA damage checkpoint cascade (see Section *DNA damage checkpoints*). As an adapter protein, it has a modular structure made of different functional domains which allow interactions with multiple partners (Fig. 20). An N-terminal Chk1 activation domain (CAD) is required for activating the Chk1 checkpoint kinase after DNA damage, likely through direct Rad9-Chk1 interaction (Blankley and Lydall, 2004; Qu et al., 2012). The [S/T]Q cluster domain (SCD), which is heavily phosphorylated in a Mec1-dependent manner after DNA damage, is bound by Rad53 FHA domain and mediates Rad53 activation (Schwartz et al., 2002). Tudor and BRCA1 carboxyl terminus (BRCT) domains, instead, have been reported to mediate Rad9

recruitment onto chromatin, via interaction with post-translationally modified histone residues. Constitutive Rad9 docking onto chromatin is mediated by interaction between its Tudor domain and H3-K79 methylated by Dot1, while the tandem BRCT motifs, which represent a single functional phospho-protein binding domain (Yu et al., 2003), allow Rad9 damage-dependent interaction with γ-H2A. Importantly, H3-K79 methylation is needed for subsequent Rad9 binding to γ-H2A, and both Rad9-histone contacts are a pre-requisite for checkpoint activation in G1-phase, and for repair in G2/M-phase, where they are instead dispensable for checkpoint activation (Giannattasio et al., 2005; Wysocki et al., 2005; Toh et al., 2006; Javaheri et al., 2006; Grenon et al., 2007; Hammet et al., 2007). Finally, BRCT domain mediates Rad9 dimerization (through a BRCT-BRCT interaction) and oligomerization (through BRCT-SCD interactions), required for a robust and sustained checkpoint activation (Soulier and Lowndes, 1999; Du et al., 2004; Usui et al., 2009). Despite this wealth of mechanistic details, the crosstalks between these molecular determinants and their functional significance remain to be elucidated.

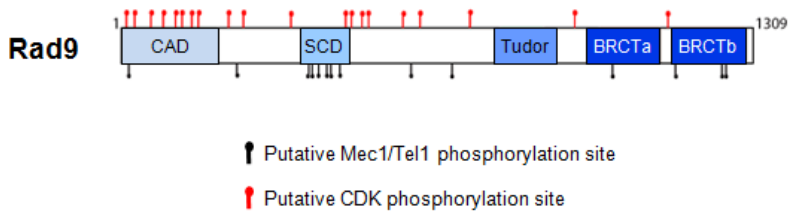

Figure 20: *Schematic representation of Rad9 domains and phosphorylatable sites.*

To gain further insights into the mechanisms underlying Rad9 function in response to DNA damage, we decided to explore the interplay between the dynamics of Rad9 multimerization and chromatin binding for checkpoint activation in G1 and M phases of the cell cycle (Granata et al., 2010).

To dissect the contribution of the different functions of Rad9 BRCT motifs, these were substituted with heterologous domains which provide a constitutive or conditional dimerization function. This analysis revealed

that BRCT-mediated Rad9 dimerization is required for Rad9 chromatin binding in G1 phase, both in untreated conditions and after genotoxic treatment: importantly, this interaction occurs via H3-K79me (Granata et al., 2010, Fig. 1-2). We suggest that, given the symmetrical structure of the histone octamer within the nucleosome core, dimerization might facilitate the correct orientation and positioning of two Rad9 molecules on the nucleosome, allowing productive interactions with modified histones (Granata et al., 2010, Fig. 9). This dynamics is conserved also in *S. pombe*, as suggested by structural modeling of a Crb2 (Rad9 ortholog) dimer on the nucleosome (Kilkenny et al., 2008), and in human, where 53BP1 self-interaction is mediated by a dimerization region outside the BRCT motifs (Ward et al., 2006; Zgheib et al., 2009).

Conversely, heterologous domain-driven dimerization could not restore Rad9 chromatin binding in M-phase, suggesting that some cell cycle-dependent phosphorylation of Rad9 may impair the chromatin association of this artificial Rad9 dimer, or that another function of the BRCT motifs is required for Rad9-chromatin interaction in mitosis. Strikingly, despite undetectable chromatin binding, Rad9 forced dimerization allowed a full checkpoint activation after DNA damage in M phase-arrested cells (Granata et al., 2010, Fig. 2-3). These findings suggest that in mitosis Rad9 docking onto chromatin may be uncoupled from its mediator function in checkpoint activation, and indeed it was proposed that in this cell cycle phase the chromatin-bound Rad9 population might be involved in repair of DNA damage (Toh et al., 2006; Grenon et al., 2007).

Previous work from our lab demonstrated that H3-K79me and γ-H2A are partially dispensable for checkpoint activation in M-phase, and identified an histone-independent branch which triggers the checkpoint cascade, hinging on Dpb11 (Puddu et al., 2008). In the light of our latest results, we hypothesized that when Rad9 cannot bind to chromatin via histone marks, Dpb11 may act as a platform for Rad9 recruitment, thus allowing efficient Rad53 activation. Moreover, given that this alternative pathway is observed specifically in M-phase, we speculated that this proposed Rad9-Dpb11 interaction could be cell-cycle regulated. We explored the molecu-

lar determinants of the Dpb11-dependent pathway through protein-protein interaction experiments and epistasis analysis. Through yeast two hybrid experiments we detected and M-phase specific interaction between Rad9 and Dpb11, which is severely reduced by deletion of Rad9 N-terminal region (NT) or by CDK1 inhibition (Granata et al., 2010, Fig. 4-6). At the same time we found that checkpoint activation in the absence of the histone-dependent pathway depends on an intact Dpb11, on Rad9 NT, and on CDK1 activity (Granata et al., 2010, Fig. 4-5). Rad9 has been shown to be a CDK1 substrate (Ubersax et al., 2003), and Rad9 N-terminal region contains 9 consensus sites for CDK-dependent phosphorylation (Fig. 20), which were mutagenized and tested, individually or in different combinations: only mutation of S11, which was found phosphorylated *in vivo* (Smolka et al., 2005), significantly affected cell cycle-dependent Rad9 phosphorylation. We then showed that the Dpb11-dependent branch for checkpoint activation needs Rad9-S11 phosphorylation; we also detected a direct Rad9-Dpb11 interaction *in vivo* by co-immunoprecipitation, which is dependent on DNA damage and Rad9-S11 phosphorylation (Granata et al., 2010, Fig. 5-S2). Finally, we explored the dynamics of Rad9 chromatin binding and checkpoint activation in the histone-dependent and the Dpb11-dependent pathways, and we found that the Dpb11-dependent pathway in M phase triggers Rad53 activation independently from Rad9 chromatin binding (Granata et al., 2010, Fig. 7).

Our working model for Rad9 dynamics predicts that checkpoint activation in G1 phase entirely relies upon Rad9 binding to histone marks: a Rad9 dimer is constitutively bound to chromatin via Tudor-H3-K79me interaction; after DNA damage, activated Rad9 may change its conformation, interacting also with γ-H2A. In M-phase an alternative way for Rad9 recruitment at DNA lesions involves its interaction with Dpb11. This factor is brought near the Mec1-Ddc2 complex via its interaction with the 9-1-1 clamp, and it binds the phosphorylated N-terminal portion of Rad9; Mec1 can thus hyper-phosphorylate Rad9, leading to Rad53 recruitment and full checkpoint activation, while the histone bound Rad9 sub-population likely mediates DNA lesion repair (Granata et al., 2010,

Fig. 9). This mechanisms are conserved in *S. pombe*, where the histone-dependent branch is governed by BRCT-directed Crb2 dimerization, Tudor domain binding to H4-K20me and BRCT domain binding to γ-H2A, while a histone-independent pathway relies upon Crb2 interaction with Dpb11 ortholog Cut5 (Du et al., 2006). Similar dynamics are observed for human Rad9 orthologs, albeit with some differences: BRCT-independent dimerization is required for 53BP1 docking onto H3-K79me (Huyen et al., 2004; Ward et al., 2006; Zgheib et al., 2009); moreover, a direct interaction between 53BP1 and TopBP1 (Dpb11 ortholog) appears to mediate recruitment of the latter to DSB sites in G1 (Cescutti et al., 2010); another Rad9 ortholog, MDC1, directly interacts with TopBP1 to promote its recruitment at stalled replication forks (Wang et al., 2011).

More recently the Diffley group re-investigated the molecular requirements for Rad9-Dpb11 interaction (Pfander and Diffley, 2011). Through in-vitro pulldown experiments with protein fragments they mapped S462 and T474 as the key Rad9 residues phosphorylated by CDK1, which seem necessary and sufficient for Rad9-Dpb11 interaction and histone-independent checkpoint activation; surprisingly, peptides containing phospho-S11 were unable to interact with Dpb11. These discrepancies are likely due to differences between *in vivo* an *in vitro* experiments: *in vitro* analysis allows a more direct exploration of some mechanistic details, at the expenses of a loss of key physiological determinants, such as full length protein folding and cellular environment. We believe that phospho-S11 may control additional Rad9-Dpb11 contacts needed for stabilization of Rad9-Dpb11 interaction. Alternatively, S11 phosphorylation by CDK1 may be a pre-requisite for S462 and T474 phosphorylation, possibly influencing the folding of the Rad9 protein.

Conclusions and future perspectives

A deep understanding of the mechanisms through which eukaryotic cells maintain the integrity of their genome is of capital importance, since failure of these pathways leads to genome instability, a driving force in tumorigenesis. The contribution of the work described in this thesis can be summarized as follows: i) we identified several novel genes possibly implicated in the control of genome stability; ii) we characterized the role of *VID22* in preserving the integrity of the genome; iii) we uncovered a new role for RNases H, template switch pathways and Pol ζ translesion polymerase in protecting the genome from misincorporated rNTPs; iv) we defined the mechanistic details of Rad9 in mediating checkpoint activation.

Each of these results raises new questions and paves the way for further investigations. Among the genes identified by the *DDC2* overexpression screen, we are particularly interested in unraveling the biological and molecular functions of the uncharacterized ORFs and we will explore the contribution of genes regulating peroxisome biology in the preservation of genome integrity. Moreover, additional experiments are required to test the model we proposed to explain the genome instability phenotype observed in the absence of *VID22*: in particular DNA combing experiments will allow direct assessment of origin firing efficiency, while aberrant recombination structures arising during replication could be detected through two-dimensional gel electrophoresis. Another issue worth investigating is whether Vid22 has also a direct role in the stabilization of replication forks or in the resolution of X-shaped molecules: techniques such as ChIP (chromatin immunoprecipitation) or iPOND (isolation of proteins on nascent

DNA) could reveal a possible Vid22 localization at the replication fork.

The unexpected interplay between cellular pathways protecting yeast cells from rNTPs incorporated in the genome, needs to be validated also in human cells: we are presently silencing the human counterparts of the genes identified in yeast. The analysis of the expression profile of these genes in lymphoblastoid cell lines derived from AGS patients will help to better understand the mechanisms regulating RNasesH production and their functional interactions with the cellular DNA damage response. Further investigation of the genetic interactors identified in yeast (and possibly in human cells) is required: the characterization of the corresponding gene products will help to clarify the function(s) of RNAsesH in the cell, and possibly to shed some light on the pathogenic mechanisms of Aicardi-Goutières Syndrome.

A paper form our lab demonstrated that the Rad9 mediator is not only responsible for transducting the checkpoint signal to the effector kinases Rad53 an Chk1, but it is also involved in the control of the DSBs processing (resection). In fact, binding of Rad9 to H3-K79me through its Tudor domain is required to inhibit resection, thus preventing excessive nucleolytic processing and ssDNA generation, which may promote genomic instability (Lazzaro et al., 2008). Our observation was later extended to human cells (Bunting et al., 2010). It will be interesting to combine domain-swapping experiments and analysis of point mutations selectively abrogating single Rad9 interactions/functions to examine the dynamics of Rad9 dimerization, chromatin binding and CDK-dependent phosphorylation in the control of resection at DSBs.

Bibliography

Admire, A., Shanks, L., Danzl, N., Wang, M., Weier, U. et al. (2006). Cycles of chromosome instability are associated with a fragile site and are increased by defects in DNA replication and checkpoint controls in yeast. Genes Dev *20*, 159–173.

Agarwal, R., Tang, Z., Yu, H., and Cohen-Fix, O. (2003). Two distinct pathways for inhibiting pds1 ubiquitination in response to DNA damage. J Biol Chem *278*, 45027–45033.

Aggarwal, M. and Brosh, R. M. (2012). Functional analyses of human DNA repair proteins important for aging and genomic stability using yeast genetics. DNA Repair (Amst) *11*, 335–348.

Aguilera, A. (2002). The connection between transcription and genomic instability. EMBO J *21*, 195–201.

Aguilera, A. and García-Muse, T. (2012). R loops: from transcription byproducts to threats to genome stability. Mol Cell *46*, 115–124.

Aguilera, A. and Gómez-González, B. (2008). Genome instability: a mechanistic view of its causes and consequences. Nat Rev Genet *9*, 204–217.

Aicardi, J. and Goutières, F. (1984). A progressive familial encephalopathy in infancy with calcifications of the basal ganglia and chronic cerebrospinal fluid lymphocytosis. Ann Neurol *15*, 49–54.

Al-Tassan, N., Chmiel, N. H., Maynard, J., Fleming, N., Livingston, A. L. et al. (2002). Inherited variants of MYH associated with somatic G:C–>T:A mutations in colorectal tumors. Nat Genet *30*, 227–232.

Alcasabas, A. A., Osborn, A. J., Bachant, J., Hu, F., Werler, P. J. et al. (2001). Mrc1 transduces signals of DNA replication stress to activate Rad53. Nat Cell Biol *3*, 958–965.

Andersen, P. L., Xu, F., and Xiao, W. (2008). Eukaryotic DNA damage tolerance and translesion synthesis through covalent modifications of PCNA. Cell Res *18*, 162–173.

Aravind, L. (2000). The BED finger, a novel DNA-binding domain in chromatin-boundary-element-binding proteins and transposases. Trends Biochem Sci *25*, 421–423.

Artandi, S. E., Chang, S., Lee, S. L., Alson, S., Gottlieb, G. J. et al. (2000). Telomere dysfunction promotes non-reciprocal translocations and epithelial cancers in mice. Nature *406*, 641–645.

Ashton, T. M. and Hickson, I. D. (2010). Yeast as a model system to study RecQ helicase function. DNA Repair (Amst) *9*, 303–314.

Ashton, T. M., Mankouri, H. W., Heidenblut, A., McHugh, P. J., and Hickson, I. D. (2011). Pathways for Holliday Junction Processing during Homologous Recombination in *Saccharomyces cerevisiae*. Mol Cell Biol *31*, 1921–1933.

Azvolinsky, A., Giresi, P. G., Lieb, J. D., and Zakian, V. A. (2009). Highly transcribed RNA polymerase II genes are impediments to replication fork progression in *Saccharomyces cerevisiae*. Mol Cell *34*, 722–734.

Bacolla, A., Jaworski, A., Larson, J. E., Jakupciak, J. P., Chuzhanova, N. et al. (2004). Breakpoints of gross deletions coincide with non-B DNA conformations. Proc Natl Acad Sci U S A *101*, 14162–14167.

Baird, D. M., Jeffreys, A. J., and Royle, N. J. (1995). Mechanisms underlying telomere repeat turnover, revealed by hypervariable variant repeat distribution patterns in the human Xp/Yp telomere. EMBO J *14*, 5433–5443.

Bakhoum, S. F., Genovese, G., and Compton, D. A. (2009a). Deviant kinetochore microtubule dynamics underlie chromosomal instability. Curr Biol *19*, 1937–1942.

Bakhoum, S. F., Thompson, S. L., Manning, A. L., and Compton, D. A. (2009b). Genome stability is ensured by temporal control of kinetochore-microtubule dynamics. Nat Cell Biol *11*, 27–35.

Bakkenist, C. J. and Kastan, M. B. (2003). DNA damage activates ATM through intermolecular autophosphorylation and dimer dissociation. Nature *421*, 499–506.

Barber, T. D., McManus, K., Yuen, K. W. Y., Reis, M., Parmigiani, G. et al. (2008). Chromatid cohesion defects may underlie chromosome instability in human colorectal cancers. Proc Natl Acad Sci U S A *105*, 3443–3448.

Bartkova, J., Horejsí, Z., Koed, K., Krämer, A., Tort, F. et al. (2005). DNA damage response as a candidate anti-cancer barrier in early human tumorigenesis. Nature *434*, 864–870.

Baryshnikova, A., Costanzo, M., Dixon, S., Vizeacoumar, F. J., Myers, C. L. et al. (2010). Synthetic genetic array (SGA) analysis in *Saccharomyces cerevisiae* and *Schizosaccharomyces pombe*. Methods Enzymol *470*, 145–179.

Beckman, R. A. and Loeb, L. A. (2006). Efficiency of carcinogenesis with and without a mutator mutation. Proc Natl Acad Sci U S A *103*, 14140–14145.

Beletskii, A. and Bhagwat, A. S. (1996). Transcription-induced mutations: increase in C to T mutations in the nontranscribed strand during transcription in Escherichia coli. Proc Natl Acad Sci U S A *93*, 13919–13924.

Bermejo, R., Doksani, Y., Capra, T., Katou, Y.-M., Tanaka, H. et al. (2007). Top1- and Top2-mediated topological transitions at replication forks ensure fork progression and stability and prevent DNA damage checkpoint activation. Genes Dev *21*, 1921–1936.

Bielas, J. H., Loeb, K. R., Rubin, B. P., True, L. D., and Loeb, L. A. (2006). Human cancers express a mutator phenotype. Proc Natl Acad Sci U S A *103*, 18238–18242.

Bielinsky, A.-K. (2003). Replication origins: why do we need so many? Cell Cycle *2*, 307–309.

Bignell, G. R., Greenman, C. D., Davies, H., Butler, A. P., Edkins, S. et al. (2010). Signatures of mutation and selection in the cancer genome. Nature *463*, 893–898.

Bird, A. W., Yu, D. Y., Pray-Grant, M. G., Qiu, Q., Harmon, K. E. et al. (2002). Acetylation of histone H4 by Esa1 is required for DNA double-strand break repair. Nature *419*, 411–415.

Blackburn, E. H., Greider, C. W., and Szostak, J. W. (2006). Telomeres and telomerase: the path from maize, Tetrahymena and yeast to human cancer and aging. Nat Med *12*, 1133–1138.

Blankley, R. T. and Lydall, D. (2004). A domain of Rad9 specifically required for activation of Chk1 in budding yeast. J Cell Sci *117*, 601–608.

Blasco, M. A., Lee, H. W., Hande, M. P., Samper, E., Lansdorp, P. M. et al. (1997). Telomere shortening and tumor formation by mouse cells lacking telomerase RNA. Cell *91*, 25–34.

Bochman, M. L., Paeschke, K., and Zakian, V. A. (2012). DNA secondary structures: stability and function of G-quadruplex structures. Nat Rev Genet *13*, 770–780.

Bochman, M. L., Sabouri, N., and Zakian, V. A. (2010). Unwinding the functions of the Pif1 family helicases. DNA Repair (Amst) *9*, 237–249.

Bodmer, W., Bielas, J. H., and Beckman, R. A. (2008). Genetic instability is not a requirement for tumor development. Cancer Res *68*, 3558–60; discussion 3560–1.

Bonilla, C. Y., Melo, J. A., and Toczyski, D. P. (2008). Colocalization of sensors is sufficient to activate the DNA damage checkpoint in the absence of damage. Mol Cell *30*, 267–276.

Botstein, D. and Fink, G. R. (1988). Yeast: an experimental organism for modern biology. Science *240*, 1439–1443.

Botstein, D. and Fink, G. R. (2011). Yeast: an experimental organism for 21st Century biology. Genetics *189*, 695–704.

Botuyan, M. V., Lee, J., Ward, I. M., Kim, J.-E., Thompson, J. R. et al. (2006). Structural basis for the methylation state-specific recognition of histone H4-K20 by 53BP1 and Crb2 in DNA repair. Cell *127*, 1361–1373.

Boulé, J.-B., Vega, L. R., and Zakian, V. A. (2005). The yeast Pif1p helicase removes telomerase from telomeric DNA. Nature *438*, 57–61.

Boulé, J.-B. and Zakian, V. A. (2007). The yeast Pif1p DNA helicase preferentially unwinds RNA DNA substrates. Nucleic Acids Res *35*, 5809–5818.

Branzei, D. and Foiani, M. (2005). The DNA damage response during DNA replication. Curr Opin Cell Biol *17*, 568–575.

Branzei, D. and Foiani, M. (2006). The Rad53 signal transduction pathway: Replication fork stabilization, DNA repair, and adaptation. Exp Cell Res *312*, 2654–2659.

Branzei, D. and Foiani, M. (2010). Maintaining genome stability at the replication fork. Nat Rev Mol Cell Biol *11*, 208–219.

Bunting, S. F., Callén, E., Wong, N., Chen, H.-T., Polato, F. et al. (2010). 53BP1 inhibits homologous recombination in Brca1-deficient cells by blocking resection of DNA breaks. Cell *141*, 243–254.

Cancer Genome Atlas Research Network (2008). Comprehensive genomic characterization defines human glioblastoma genes and core pathways. Nature *455*, 1061–1068.

Capper, R., Britt-Compton, B., Tankimanova, M., Rowson, J., Letsolo, B. et al. (2007). The nature of telomere fusion and a definition of the critical telomere length in human cells. Genes Dev *21*, 2495–2508.

Carr, A. M., Paek, A. L., and Weinert, T. (2011). DNA replication: failures and inverted fusions. Semin Cell Dev Biol *22*, 866–874.

Cavenee, W. K., Dryja, T. P., Phillips, R. A., Benedict, W. F., Godbout, R. et al. (1983). Expression of recessive alleles by chromosomal mechanisms in retinoblastoma. Nature *305*, 779–784.

Celeste, A., Fernandez-Capetillo, O., Kruhlak, M. J., Pilch, D. R., Staudt, D. W. et al. (2003). Histone H2AX phosphorylation is dispensable for the initial recognition of DNA breaks. Nat Cell Biol *5*, 675–679.

Cerritelli, S. M. and Crouch, R. J. (2009). Ribonuclease H: the enzymes in eukaryotes. FEBS J *276*, 1494–1505.

Cerritelli, S. M., Frolova, E. G., Feng, C., Grinberg, A., Love, P. E. et al. (2003). Failure to produce mitochondrial DNA results in embryonic lethality in Rnaseh1 null mice. Mol Cell *11*, 807–815.

Cescutti, R., Negrini, S., Kohzaki, M., and Halazonetis, T. D. (2010). TopBP1 functions with 53BP1 in the G1 DNA damage checkpoint. EMBO J *29*, 3723–3732.

Cha, R. S. and Kleckner, N. (2002). ATR homolog Mec1 promotes fork progression, thus averting breaks in replication slow zones. Science *297*, 602–606.

Chagin, V. O., Stear, J. H., and Cardoso, M. C. (2010). Organization of DNA replication. Cold Spring Harb Perspect Biol *2*, a000737.

Chen, C. and Kolodner, R. D. (1999). Gross chromosomal rearrangements in *Saccharomyces cerevisiae* replication and recombination defective mutants. Nat Genet *23*, 81–85.

Chen, G., Bradford, W. D., Seidel, C. W., and Li, R. (2012). Hsp90 stress potentiates rapid cellular adaptation through induction of aneuploidy. Nature *482*, 246–250.

Cheng, E., Vaisica, J. A., Ou, J., Baryshnikova, A., Lu, Y. et al. (2012). Genome Rearrangements Caused by Depletion of Essential DNA Replication Proteins in *Saccharomyces cerevisiae*. Genetics *192*, 147–160.

Cheng, X., Dunaway, S., and Ivessa, A. S. (2007). The role of Pif1p, a DNA helicase in *Saccharomyces cerevisiae*, in maintaining mitochondrial DNA. Mitochondrion *7*, 211–222.

Chi, Y.-H., Ward, J. M., Cheng, L. I., Yasunaga, J., and Jeang, K.-T. (2009). Spindle assembly checkpoint and p53 deficiencies cooperate for tumorigenesis in mice. Int J Cancer *124*, 1483–1489.

Chin, L., Artandi, S. E., Shen, Q., Tam, A., Lee, S. L. et al. (1999). p53 deficiency rescues the adverse effects of telomere loss and cooperates with telomere dysfunction to accelerate carcinogenesis. Cell *97*, 527–538.

Ciccia, A. and Elledge, S. J. (2010). The DNA damage response: making it safe to play with knives. Mol Cell *40*, 179–204.

Clark, A. B., Lujan, S. A., Kissling, G. E., and Kunkel, T. A. (2011). Mismatch repair-independent tandem repeat sequence instability resulting from ribonucleotide incorporation by DNA polymerase ε. DNA Repair (Amst) *10*, 476–482.

Cleaver, J. E. (2005). Cancer in xeroderma pigmentosum and related disorders of DNA repair. Nat Rev Cancer *5*, 564–573.

Clerici, M., Mantiero, D., Guerini, I., Lucchini, G., and Longhese, M. P. (2008). The Yku70-Yku80 complex contributes to regulate double-strand break processing and checkpoint activation during the cell cycle. EMBO Rep *9*, 810–818.

Clerici, M., Paciotti, V., Baldo, V., Romano, M., Lucchini, G. et al. (2001). Hyperactivation of the yeast DNA damage checkpoint by TEL1 and DDC2 overexpression. EMBO J *20*, 6485–6498.

Clémenson, C. and Marsolier-Kergoat, M.-C. (2009). DNA damage checkpoint inactivation: adaptation and recovery. DNA Repair (Amst) *8*, 1101–1109.

Cortés-Ledesma, F. and Aguilera, A. (2006). Double-strand breaks arising by replication through a nick are repaired by cohesin-dependent sister-chromatid exchange. EMBO Rep *7*, 919–926.

Costanzo, M., Baryshnikova, A., Bellay, J., Kim, Y., Spear, E. D. et al. (2010). The genetic landscape of a cell. Science *327*, 425–431.

Costelloe, T., Fitzgerald, J., Murphy, N. J., Flaus, A., and Lowndes, N. F. (2006). Chromatin modulation and the DNA damage response. Exp Cell Res *312*, 2677–2686.

Cotta-Ramusino, C., Fachinetti, D., Lucca, C., Doksani, Y., Lopes, M. et al. (2005). Exo1 processes stalled replication forks and counteracts fork reversal in checkpoint-defective cells. Mol Cell *17*, 153–159.

Counter, C. M., Avilion, A. A., LeFeuvre, C. E., Stewart, N. G., Greider, C. W. et al. (1992). Telomere shortening associated with chromosome instability is arrested in immortal cells which express telomerase activity. EMBO J *11*, 1921–1929.

Crasta, K., Ganem, N. J., Dagher, R., Lantermann, A. B., Ivanova, E. V. et al. (2012). DNA breaks and chromosome pulverization from errors in mitosis. Nature *482*, 53–58.

Crow, Y. J., Leitch, A., Hayward, B. E., Garner, A., Parmar, R. et al. (2006). Mutations in genes encoding ribonuclease H2 subunits cause Aicardi-Goutières syndrome and mimic congenital viral brain infection. Nat Genet *38*, 910–916.

Crow, Y. J. and Rehwinkel, J. (2009). Aicardi-Goutieres syndrome and related phenotypes: linking nucleic acid metabolism with autoimmunity. Hum Mol Genet *18*, R130–R136.

d'Adda di Fagagna, F., Reaper, P. M., Clay-Farrace, L., Fiegler, H., Carr, P. et al. (2003). A DNA damage checkpoint response in telomere-initiated senescence. Nature *426*, 194–198.

Datta, A. and Jinks-Robertson, S. (1995). Association of increased spontaneous mutation rates with high levels of transcription in yeast. Science *268*, 1616–1619.

De Antoni, A., Pearson, C. G., Cimini, D., Canman, J. C., Sala, V. et al. (2005). The Mad1/Mad2 complex as a template for Mad2 activation in the spindle assembly checkpoint. Curr Biol *15*, 214–225.

De Bont, R. and van Larebeke, N. (2004). Endogenous DNA damage in humans: a review of quantitative data. Mutagenesis *19*, 169–185.

Debatisse, M., Le Tallec, B., Letessier, A., Dutrillaux, B., and Brison, O. (2012). Common fragile sites: mechanisms of instability revisited. Trends Genet *28*, 22–32.

Deem, A., Keszthelyi, A., Blackgrove, T., Vayl, A., Coffey, B. et al. (2011). Break-induced replication is highly inaccurate. PLoS Biol *9*, e1000594.

DeRose, E. F., Perera, L., Murray, M. S., Kunkel, T. A., and London, R. E. (2012). Solution structure of the Dickerson DNA dodecamer containing a single ribonucleotide. Biochemistry *51*, 2407–2416.

Dershowitz, A. and Newlon, C. S. (1993). The effect on chromosome stability of deleting replication origins. Mol Cell Biol *13*, 391–398.

Dimitrova, N., Chen, Y.-C. M., Spector, D. L., and de Lange, T. (2008). 53BP1 promotes non-homologous end joining of telomeres by increasing chromatin mobility. Nature *456*, 524–528.

Ding, L., Getz, G., Wheeler, D. A., Mardis, E. R., McLellan, M. D. et al. (2008). Somatic mutations affect key pathways in lung adenocarcinoma. Nature *455*, 1069–1075.

Dolinski, K. and Botstein, D. (2007). Orthology and functional conservation in eukaryotes. Annu Rev Genet *41*, 465–507.

Donnianni, R. A., Ferrari, M., Lazzaro, F., Clerici, M., Nachimuthu, B. T. et al. (2010). Elevated levels of the polo kinase Cdc5 override the Mec1/ATR checkpoint in budding yeast by acting at different steps of the signaling pathway. PLoS Genet *6*, e1000763.

Downey, M. and Durocher, D. (2006). Chromatin and DNA repair: the benefits of relaxation. Nat Cell Biol *8*, 9–10.

Downs, J. A., Lowndes, N. F., and Jackson, S. P. (2000). A role for *Saccharomyces cerevisiae* histone H2A in DNA repair. Nature *408*, 1001–1004.

Downs, J. A., Nussenzweig, M. C., and Nussenzweig, A. (2007a). Chromatin dynamics and the preservation of genetic information. Nature *447*, 951–958.

Downs, J. C., Yang, H., Girkin, C., Sakata, L., Bellezza, A. et al. (2007b). Three-dimensional histomorphometry of the normal and early glaucomatous monkey optic nerve head: neural canal and subarachnoid space architecture. Invest Ophthalmol Vis Sci *48*, 3195–3208.

Driscoll, R., Hudson, A., and Jackson, S. P. (2007). Yeast Rtt109 promotes genome stability by acetylating histone H3 on lysine 56. Science *315*, 649–652.

Du, L.-L., Moser, B. A., and Russell, P. (2004). Homo-oligomerization is the essential function of the tandem BRCT domains in the checkpoint protein Crb2. J Biol Chem *279*, 38409–38414.

Du, L.-L., Nakamura, T. M., and Russell, P. (2006). Histone modification-dependent and -independent pathways for recruitment of checkpoint protein Crb2 to double-strand breaks. Genes Dev *20*, 1583–1596.

Duesberg, P., Li, R., Fabarius, A., and Hehlmann, R. (2006). Aneuploidy and cancer: from correlation to causation. Contrib Microbiol *13*, 16–44.

Durkin, S. G. and Glover, T. W. (2007). Chromosome fragile sites. Annu Rev Genet *41*, 169–192.

Duro, E., Vaisica, J. A., Brown, G. W., and Rouse, J. (2008). Budding yeast Mms22 and Mms1 regulate homologous recombination induced by replisome blockage. DNA Repair (Amst) *7*, 811–818.

El Achkar, E., Gerbault-Seureau, M., Muleris, M., Dutrillaux, B., and Debatisse, M. (2005). Premature condensation induces breaks at the interface of early and late replicating chromosome bands bearing common fragile sites. Proc Natl Acad Sci U S A *102*, 18069–18074.

Emili, A. (1998). MEC1-dependent phosphorylation of Rad9p in response to DNA damage. Mol Cell *2*, 183–189.

Enders, G. H. and Maude, S. L. (2006). Traffic safety for the cell: influence of cyclin-dependent kinase activity on genomic stability. Gene *371*, 1–6.

Enserink, J. M. and Kolodner, R. D. (2010). An overview of Cdk1-controlled targets and processes. Cell Div *5*, 11.

Fabre, F., Chan, A., Heyer, W.-D., and Gangloff, S. (2002). Alternate pathways involving Sgs1/Top3, Mus81/ Mms4, and Srs2 prevent formation of toxic recombination intermediates from single-stranded gaps created by DNA replication. Proc Natl Acad Sci U S A *99*, 16887–16892.

Feng, Q., Wang, H., Ng, H. H., Erdjument-Bromage, H., Tempst, P. et al. (2002). Methylation of H3-lysine 79 is mediated by a new family of HMTases without a SET domain. Curr Biol *12*, 1052–1058.

Fishel, R., Lescoe, M. K., Rao, M. R., Copeland, N. G., Jenkins, N. A. et al. (1993). The human mutator gene homolog MSH2 and its association with hereditary nonpolyposis colon cancer. Cell *75*, 1027–1038.

Fitz Gerald, J. N., Benjamin, J. M., and Kron, S. J. (2002). Robust G1 checkpoint arrest in budding yeast: dependence on DNA damage signaling and repair. J Cell Sci *115*, 1749–1757.

Flaus, A., Martin, D. M. A., Barton, G. J., and Owen-Hughes, T. (2006). Identification of multiple distinct Snf2 subfamilies with conserved structural motifs. Nucleic Acids Res *34*, 2887–2905.

Forsburg, S. L. (2001). The art and design of genetic screens: yeast. Nat Rev Genet *2*, 659–668.

Foss, E. J. (2001). Tof1p regulates DNA damage responses during S phase in *Saccharomyces cerevisiae*. Genetics *157*, 567–577.

Foster, P. L. (2006). Methods for determining spontaneous mutation rates. Methods Enzymol *409*, 195–213.

Freudenreich, C. H., Kantrow, S. M., and Zakian, V. A. (1998). Expansion and length-dependent fragility of CTG repeats in yeast. Science *279*, 853–856.

Frias, C., Pampalona, J., Genesca, A., and Tusell, L. (2012). Telomere dysfunction and genome instability. Front Biosci *17*, 2181–2196.

Fricke, W. M. and Brill, S. J. (2003). Slx1-Slx4 is a second structure-specific endonuclease functionally redundant with Sgs1-Top3. Genes Dev *17*, 1768–1778.

Friedberg, E. C. (2005). Suffering in silence: the tolerance of DNA damage. Nat Rev Mol Cell Biol *6*, 943–953.

Friedberg, E. C., Wagner, R., and Radman, M. (2002). Specialized DNA polymerases, cellular survival, and the genesis of mutations. Science *296*, 1627–1630.

Futami, K., Shimamoto, A., and Furuichi, Y. (2007). Mitochondrial and nuclear localization of human Pif1 helicase. Biol Pharm Bull *30*, 1685–1692.

Gacy, A. M., Goellner, G., Juranic, N., Macura, S., and McMurray, C. T. (1995). Trinucleotide repeats that expand in human disease form hairpin structures in vitro. Cell *81*, 533–540.

Gan, G. N., Wittschieben, J. P., Wittschieben, B. ., and Wood, R. D. (2008). DNA polymerase zeta (pol zeta) in higher eukaryotes. Cell Res *18*, 174–183.

Ganem, N. J., Godinho, S. A., and Pellman, D. (2009). A mechanism linking extra centrosomes to chromosomal instability. Nature *460*, 278–282.

Garvik, B., Carson, M., and Hartwell, L. (1995). Single-stranded DNA arising at telomeres in cdc13 mutants may constitute a specific signal for the RAD9 checkpoint. Mol Cell Biol *15*, 6128–6138.

George, T., Wen, Q., Griffiths, R., Ganesh, A., Meuth, M. et al. (2009). Human Pif1 helicase unwinds synthetic DNA structures resembling stalled DNA replication forks. Nucleic Acids Res *37*, 6491–6502.

Giaever, G., Chu, A. M., Ni, L., Connelly, C., Riles, L. et al. (2002). Functional profiling of the *Saccharomyces cerevisiae* genome. Nature *418*, 387–391.

Giannattasio, M., Lazzaro, F., Longhese, M. P., Plevani, P., and Muzi-Falconi, M. (2004). Physical and functional interactions between nucleotide excision repair and DNA damage checkpoint. EMBO J *23*, 429–438.

Giannattasio, M., Lazzaro, F., Plevani, P., and Muzi-Falconi, M. (2005). The DNA damage checkpoint response requires histone H2B ubiquitination by Rad6-Bre1 and H3 methylation by Dot1. J Biol Chem *280*, 9879–9886.

Gilbert, C. S., Green, C. M., and Lowndes, N. F. (2001). Budding yeast Rad9 is an ATP-dependent Rad53 activating machine. Mol Cell *8*, 129–136.

Gómez-González, B., Felipe-Abrio, I., and Aguilera, A. (2009). The S-phase checkpoint is required to respond to R-loops accumulated in THO mutants. Mol Cell Biol *29*, 5203–5213.

Goffeau, A., Barrell, B. G., Bussey, H., Davis, R. W., Dujon, B. et al. (1996). Life with 6000 genes. Science *274*, 546, 563–546, 567.

Gorgoulis, V. G., Vassiliou, L.-V. F., Karakaidos, P., Zacharatos, P., Kotsinas, A. et al. (2005). Activation of the DNA damage checkpoint and genomic instability in human precancerous lesions. Nature *434*, 907–913.

Gottipati, P., Cassel, T. N., Savolainen, L., and Helleday, T. (2008). Transcription-associated recombination is dependent on replication in Mammalian cells. Mol Cell Biol *28*, 154–164.

Granata, M., Lazzaro, F., Novarina, D., Panigada, D., Puddu, F. et al. (2010). Dynamics of Rad9 chromatin binding and checkpoint function are mediated by its dimerization and are cell cycle-regulated by CDK1 activity. PLoS Genet *6*.

Grenon, M., Costelloe, T., Jimeno, S., O'shaughnessy, A., Fitzgerald, J. et al. (2007). Docking onto chromatin via the *Saccharomyces cerevisiae* Rad9 Tudor domain. Yeast *24*, 105–119.

Halazonetis, T. D., Gorgoulis, V. G., and Bartek, J. (2008). An oncogene-induced DNA damage model for cancer development. Science *319*, 1352–1355.

Hammet, A., Magill, C., Heierhorst, J., and Jackson, S. P. (2007). Rad9 BRCT domain interaction with phosphorylated H2AX regulates the G1 checkpoint in budding yeast. EMBO Rep *8*, 851–857.

Hanahan, D. and Weinberg, R. A. (2011). Hallmarks of cancer: the next generation. Cell *144*, 646–674.

Harley, C. B., Futcher, A. B., and Greider, C. W. (1990). Telomeres shorten during ageing of human fibroblasts. Nature *345*, 458–460.

Harrison, J. C. and Haber, J. E. (2006). Surviving the breakup: the DNA damage checkpoint.

Hefferin, M. L. and Tomkinson, A. E. (2005). Mechanism of DNA double-strand break repair by non-homologous end joining. DNA Repair (Amst) *4*, 639–648.

Heideker, J., Lis, E. T., and Romesberg, F. E. (2007). Phosphatases, DNA damage checkpoints and checkpoint deactivation. Cell Cycle *6*, 3058–3064.

Heinicke, S., Livstone, M. S., Lu, C., Oughtred, R., Kang, F. et al. (2007). The Princeton Protein Orthology Database (P-POD): a comparative genomics analysis tool for biologists. PLoS One *2*, e766.

Heller, R. C. and Marians, K. J. (2006). Replisome assembly and the direct restart of stalled replication forks. Nat Rev Mol Cell Biol *7*, 932–943.

Hellman, A., Rahat, A., Scherer, S. W., Darvasi, A., Tsui, L. C. et al. (2000). Replication delay along FRA7H, a common fragile site on human chromosome 7, leads to chromosomal instability. Mol Cell Biol *20*, 4420–4427.

Helmrich, A., Ballarino, M., and Tora, L. (2011). Collisions between replication and transcription complexes cause common fragile site instability at the longest human genes. Mol Cell *44*, 966–977.

Hewett, D. R., Handt, O., Hobson, L., Mangelsdorf, M., Eyre, H. J. et al. (1998). FRA10B structure reveals common elements in repeat expansion and chromosomal fragile site genesis. Mol Cell *1*, 773–781.

Hickson, I. D. and Mankouri, H. W. (2011). Processing of homologous recombination repair intermediates by the Sgs1-Top3-Rmi1 and Mus81-Mms4 complexes. Cell Cycle *10*, 3078–3085.

Hieter, P., Mann, C., Snyder, M., and Davis, R. W. (1985). Mitotic stability of yeast chromosomes: a colony color assay that measures nondisjunction and chromosome loss. Cell *40*, 381–392.

Hodgson, B., Calzada, A., and Labib, K. (2007). Mrc1 and Tof1 regulate DNA replication forks in different ways during normal S phase. Mol Biol Cell *18*, 3894–3902.

Hoeijmakers, J. H. (2001). Genome maintenance mechanisms for preventing cancer. Nature *411*, 366–374.

Holland, A. J. and Cleveland, D. W. (2009). Boveri revisited: chromosomal instability, aneuploidy and tumorigenesis. Nat Rev Mol Cell Biol *10*, 478–487.

Holland, A. J. and Cleveland, D. W. (2012). Losing balance: the origin and impact of aneuploidy in cancer. EMBO Rep *13*, 501–514.

Htun, H. and Dahlberg, J. E. (1988). Single strands, triple strands, and kinks in H-DNA. Science *241*, 1791–1796.

Huertas, P. and Aguilera, A. (2003). Cotranscriptionally formed DNA:RNA hybrids mediate transcription elongation impairment and transcription-associated recombination. Mol Cell *12*, 711–721.

Huyen, Y., Zgheib, O., Ditullio, R. A., Gorgoulis, V. G., Zacharatos, P. et al. (2004). Methylated lysine 79 of histone H3 targets 53BP1 to DNA double-strand breaks. Nature *432*, 406–411.

Hwang, W. W., Venkatasubrahmanyam, S., Ianculescu, A. G., Tong, A., Boone, C. et al. (2003). A conserved RING finger protein required for histone H2B monoubiquitination and cell size control. Mol Cell *11*, 261–266.

Inagaki, H., Ohye, T., Kogo, H., Kato, T., Bolor, H. et al. (2009). Chromosomal instability mediated by non-B DNA: cruciform conformation and not DNA sequence is responsible for recurrent translocation in humans. Genome Res *19*, 191–198.

Ip, S. C. Y., Rass, U., Blanco, M. G., Flynn, H. R., Skehel, J. M. et al. (2008). Identification of Holliday junction resolvases from humans and yeast. Nature *456*, 357–361.

Ivessa, A. S., Lenzmeier, B. A., Bessler, J. B., Goudsouzian, L. K., Schnakenberg, S. L. et al. (2003). The *Saccharomyces cerevisiae* helicase Rrm3p facilitates replication past nonhistone protein-DNA complexes. Mol Cell *12*, 1525–1536.

Ivessa, A. S., Zhou, J.-Q., Schulz, V. P., Monson, E. K., and Zakian, V. A. (2002). Saccharomyces Rrm3p, a 5' to 3' DNA helicase that promotes replication fork progression through telomeric and subtelomeric DNA. Genes Dev *16*, 1383–1396.

Ivessa, A. S., Zhou, J. Q., and Zakian, V. A. (2000). The Saccharomyces Pif1p DNA helicase and the highly related Rrm3p have opposite effects on replication fork progression in ribosomal DNA. Cell *100*, 479–489.

Iwaizumi, M., Shinmura, K., Mori, H., Yamada, H., Suzuki, M. et al. (2009). Human Sgo1 downregulation leads to chromosomal instability in colorectal cancer. Gut *58*, 249–260.

Iwanaga, Y., Chi, Y.-H., Miyazato, A., Sheleg, S., Haller, K. et al. (2007). Heterozygous deletion of mitotic arrest-deficient protein 1 (MAD1) increases the incidence of tumors in mice. Cancer Res *67*, 160–166.

Jackson, S. P. and Bartek, J. (2009). The DNA-damage response in human biology and disease. Nature *461*, 1071–1078.

Jaishree, T. N., van der Marel, G. A., van Boom, J. H., and Wang, A. H. (1993). Structural influence of RNA incorporation in DNA: quantitative nuclear magnetic resonance refinement of d(CG)r(CG)d(CG) and d(CG)r(C)d(TAGCG). Biochemistry *32*, 4903–4911.

Jaktaji, R. P. and Lloyd, R. G. (2003). PriA supports two distinct pathways for replication restart in UV-irradiated Escherichia coli cells. Mol Microbiol *47*, 1091–1100.

Jallepalli, P. V., Waizenegger, I. C., Bunz, F., Langer, S., Speicher, M. R. et al. (2001). Securin is required for chromosomal stability in human cells. Cell *105*, 445–457.

Janssen, A., van der Burg, M., Szuhai, K., Kops, G. J. P. L., and Medema, R. H. (2011). Chromosome segregation errors as a cause of DNA damage and structural chromosome aberrations. Science *333*, 1895–1898.

Javaheri, A., Wysocki, R., Jobin-Robitaille, O., Altaf, M., Côté, J. et al. (2006). Yeast G1 DNA damage checkpoint regulation by H2A phosphorylation is independent of chromatin remodeling. Proc Natl Acad Sci U S A *103*, 13771–13776.

Jeong, H.-S., Backlund, P. S., Chen, H.-C., Karavanov, A. A., and Crouch, R. J. (2004). RNase H2 of *Saccharomyces cerevisiae* is a complex of three proteins. Nucleic Acids Res *32*, 407–414.

Jiricny, J. (2006). The multifaceted mismatch-repair system. Nat Rev Mol Cell Biol *7*, 335–346.

Jones, S., Zhang, X., Parsons, D. W., Lin, J. C.-H., Leary, R. J. et al. (2008). Core signaling pathways in human pancreatic cancers revealed by global genomic analyses. Science *321*, 1801–1806.

Kaliraman, V. and Brill, S. J. (2002). Role of SGS1 and SLX4 in maintaining rDNA structure in *Saccharomyces cerevisiae*. Curr Genet *41*, 389–400.

Kalocsay, M., Hiller, N. J., and Jentsch, S. (2009). Chromosome-wide Rad51 spreading and SUMO-H2A.Z-dependent chromosome fixation in response to a persistent DNA double-strand break. Mol Cell *33*, 335–343.

Kamakaka, R. T. and Biggins, S. (2005). Histone variants: deviants? Genes Dev *19*, 295–310.

Kang, Y.-H., Lee, C.-H., and Seo, Y.-S. (2010). Dna2 on the road to Okazaki fragment processing and genome stability in eukaryotes. Crit Rev Biochem Mol Biol *45*, 71–96.

Katou, Y., Kanoh, Y., Bando, M., Noguchi, H., Tanaka, H. et al. (2003). S-phase checkpoint proteins Tof1 and Mrc1 form a stable replication-pausing complex. Nature *424*, 1078–1083.

Kelley, L. A. and Sternberg, M. J. E. (2009). Protein structure prediction on the Web: a case study using the Phyre server. Nat Protoc *4*, 363–371.

Kelly, M. K., Jauert, P. A., Jensen, L. E., Chan, C. L., Truong, C. S. et al. (2007). Zinc regulates the stability of repetitive minisatellite DNA tracts during stationary phase. Genetics *177*, 2469–2479.

Kennedy, R. D. and D'Andrea, A. D. (2006). DNA repair pathways in clinical practice: lessons from pediatric cancer susceptibility syndromes. J Clin Oncol *24*, 3799–3808.

Keogh, M.-C., Kim, J.-A., Downey, M., Fillingham, J., Chowdhury, D. et al. (2006). A phosphatase complex that dephosphorylates gammaH2AX regulates DNA damage checkpoint recovery. Nature *439*, 497–501.

Kerzendorfer, C. and O'Driscoll, M. (2009). Human DNA damage response and repair deficiency syndromes: linking genomic instability and cell cycle checkpoint proficiency. DNA Repair (Amst) *8*, 1139–1152.

Kilkenny, M. L., Doré, A. S., Roe, S. M., Nestoras, K., Ho, J. C. Y. et al. (2008). Structural and functional analysis of the Crb2-BRCT2 domain reveals distinct roles in checkpoint signaling and DNA damage repair. Genes Dev *22*, 2034–2047.

Kim, N., Huang, S.-y. N., Williams, J. S., Li, Y. C., Clark, A. B. et al. (2011). Mutagenic processing of ribonucleotides in DNA by yeast topoisomerase I. Science *332*, 1561–1564.

Kiyosawa, H., Suko, M., Okudaira, H., Murata, K., Miyamoto, T. et al. (1990). Cigarette smoking induces formation of 8-hydroxydeoxyguanosine, one of the oxidative DNA damages in human peripheral leukocytes. Free Radic Res Commun *11*, 23–27.

Kogoma, T. (1997). Stable DNA replication: interplay between DNA replication, homologous recombination, and transcription. Microbiol Mol Biol Rev *61*, 212–238.

Kolodner, R. D., Putnam, C. D., and Myung, K. (2002). Maintenance of genome stability in *Saccharomyces cerevisiae*. Science *297*, 552–557.

Kornberg, R. D. (1977). Structure of chromatin. Annu Rev Biochem *46*, 931–954.

Kouzarides, T. (2007). Chromatin modifications and their function. Cell *128*, 693–705.

Krasilnikova, M. M. and Mirkin, S. M. (2004). Replication stalling at Friedreich's ataxia (GAA)n repeats in vivo. Mol Cell Biol *24*, 2286–2295.

Krogan, N. J., Cagney, G., Yu, H., Zhong, G., Guo, X. et al. (2006). Global landscape of protein complexes in the yeast *Saccharomyces cerevisiae*. Nature *440*, 637–643.

Krogan, N. J., Dover, J., Khorrami, S., Greenblatt, J. F., Schneider, J. et al. (2002). COMPASS, a histone H3 (Lysine 4) methyltransferase required for telomeric silencing of gene expression. J Biol Chem *277*, 10753–10755.

Krogh, B. O. and Symington, L. S. (2004). Recombination proteins in yeast. Annu Rev Genet *38*, 233–271.

Kunkel, T. A. (2004). DNA replication fidelity. J Biol Chem *279*, 16895–16898.

Kurahashi, H., Inagaki, H., Ohye, T., Kogo, H., Kato, T. et al. (2006). Palindrome-mediated chromosomal translocations in humans. DNA Repair (Amst) *5*, 1136–1145.

Lansdorp, P. M. (2005). Major cutbacks at chromosome ends. Trends Biochem Sci *30*, 388–395.

Lara-Gonzalez, P., Westhorpe, F. G., and Taylor, S. S. (2012). The spindle assembly checkpoint. Curr Biol *22*, R966–R980.

Lazzaro, F., Giannattasio, M., Muzi-Falconi, M., and Plevani, P. (2007). The interplay among chromatin dynamics, cell cycle checkpoints and repair mechanisms modulates the cellular response to DNA damage. Ital J Biochem *56*, 141–148.

Lazzaro, F., Giannattasio, M., Puddu, F., Granata, M., Pellicioli, A. et al. (2009). Checkpoint mechanisms at the intersection between DNA damage and repair. DNA Repair (Amst) *8*, 1055–1067.

Lazzaro, F., Novarina, D., Amara, F., Watt, D. L., Stone, J. E. et al. (2012). RNase H and Postreplication Repair Protect Cells from Ribonucleotides Incorporated in DNA. Mol Cell *45*, 99–110.

Lazzaro, F., Sapountzi, V., Granata, M., Pellicioli, A., Vaze, M. et al. (2008). Histone methyltransferase Dot1 and Rad9 inhibit single-stranded DNA accumulation at DSBs and uncapped telomeres. EMBO J *27*, 1502–1512.

Le Beau, M. M., Rassool, F. V., Neilly, M. E., Espinosa, 3rd, R., Glover, T. W. et al. (1998). Replication of a common fragile site, FRA3B, occurs late in S phase and is delayed further upon induction: implications for the mechanism of fragile site induction. Hum Mol Genet *7*, 755–761.

Leach, D. R., Okely, E. A., and Pinder, D. J. (1997). Repair by recombination of DNA containing a palindromic sequence. Mol Microbiol *26*, 597–606.

Leach, F. S., Nicolaides, N. C., Papadopoulos, N., Liu, B., Jen, J. et al. (1993). Mutations of a mutS homolog in hereditary nonpolyposis colorectal cancer. Cell *75*, 1215–1225.

Lee, E. Y. H. P. and Muller, W. J. (2010). Oncogenes and tumor suppressor genes. Cold Spring Harb Perspect Biol *2*, a003236.

Lee, S. E., Moore, J. K., Holmes, A., Umezu, K., Kolodner, R. D. et al. (1998). Saccharomyces Ku70, mre11/rad50 and RPA proteins regulate adaptation to G2/M arrest after DNA damage. Cell *94*, 399–409.

Lee, S. E., Pellicioli, A., Malkova, A., Foiani, M., and Haber, J. E. (2001). The Saccharomyces recombination protein Tid1p is required for adaptation from G2/M arrest induced by a double-strand break. Curr Biol *11*, 1053–1057.

Lee, S. E., Pellicioli, A., Vaze, M. B., Sugawara, N., Malkova, A. et al. (2003). Yeast Rad52 and Rad51 recombination proteins define a second pathway of DNA damage assessment in response to a single double-strand break. Mol Cell Biol *23*, 8913–8923.

Lehmann, A. R., Niimi, A., Ogi, T., Brown, S., Sabbioneda, S. et al. (2007). Translesion synthesis: Y-family polymerases and the polymerase switch. DNA Repair (Amst) *6*, 891–899.

Lemoine, F. J., Degtyareva, N. P., Kokoska, R. J., and Petes, T. D. (2008). Reduced levels of DNA polymerase delta induce chromosome fragile site instability in yeast. Mol Cell Biol *28*, 5359–5368.

Lemoine, F. J., Degtyareva, N. P., Lobachev, K., and Petes, T. D. (2005). Chromosomal translocations in yeast induced by low levels of DNA polymerase a model for chromosome fragile sites. Cell *120*, 587–598.

Leroy, C., Lee, S. E., Vaze, M. B., Ochsenbein, F., Ochsenbien, F. et al. (2003). PP2C phosphatases Ptc2 and Ptc3 are required for DNA checkpoint inactivation after a double-strand break. Mol Cell *11*, 827–835.

Letessier, A., Millot, G. A., Koundrioukoff, S., Lachagès, A.-M., Vogt, N. et al. (2011). Cell-type-specific replication initiation programs set fragility of the FRA3B fragile site. Nature *470*, 120–123.

Lettier, G., Feng, Q., de Mayolo, A. A., Erdeniz, N., Reid, R. J. D. et al. (2006). The role of DNA double-strand breaks in spontaneous homologous recombination in *S. cerevisiae*. PLoS Genet *2*, e194.

Li, G. and Reinberg, D. (2011). Chromatin higher-order structures and gene regulation. Curr Opin Genet Dev *21*, 175–186.

Li, G.-M. (2008). Mechanisms and functions of DNA mismatch repair. Cell Res *18*, 85–98.

Li, M., Fang, X., Baker, D. J., Guo, L., Gao, X. et al. (2010). The ATM-p53 pathway suppresses aneuploidy-induced tumorigenesis. Proc Natl Acad Sci U S A *107*, 14188–14193.

Li, X. and Heyer, W.-D. (2008). Homologous recombination in DNA repair and DNA damage tolerance. Cell Res *18*, 99–113.

Li, Y. and Breaker, R. R. (1999). Kinetics of RNA Degradation by Specific Base Catalysis of Transesterification Involving the 2'-Hydroxyl Group. J. Am. Chem. Soc. *121*, 5364–5372.

Liberi, G., Maffioletti, G., Lucca, C., Chiolo, I., Baryshnikova, A. et al. (2005). Rad51-dependent DNA structures accumulate at damaged replication forks in sgs1 mutants defective in the yeast ortholog of BLM RecQ helicase. Genes Dev *19*, 339–350.

Lindahl, T. (1993). Instability and decay of the primary structure of DNA. Nature *362*, 709–715.

Lindahl, T. and Wood, R. D. (1999). Quality control by DNA repair. Science *286*, 1897–1905.

Lingner, J., Cooper, J. P., and Cech, T. R. (1995). Telomerase and DNA end replication: no longer a lagging strand problem? Science *269*, 1533–1534.

Liu, D., Vader, G., Vromans, M. J. M., Lampson, M. A., and Lens, S. M. A. (2009). Sensing chromosome bi-orientation by spatial separation of aurora B kinase from kinetochore substrates. Science *323*, 1350–1353.

Liu, P., Erez, A., Nagamani, S. C. S., Dhar, S. U., Kołodziejska, K. E. et al. (2011). Chromosome catastrophes involve replication mechanisms generating complex genomic rearrangements. Cell *146*, 889–903.

Lo, A. W. I., Sabatier, L., Fouladi, B., Pottier, G., Ricoul, M. et al. (2002). DNA amplification by breakage/fusion/bridge cycles initiated by spontaneous telomere loss in a human cancer cell line. Neoplasia *4*, 531–538.

Lobachev, K. S., Gordenin, D. A., and Resnick, M. A. (2002). The Mre11 complex is required for repair of hairpin-capped double-strand breaks and prevention of chromosome rearrangements. Cell *108*, 183–193.

Loeb, L. A. (1991). Mutator phenotype may be required for multistage carcinogenesis. Cancer Res *51*, 3075–3079.

Loeb, L. A. (2011). Human cancers express mutator phenotypes: origin, consequences and targeting. Nat Rev Cancer *11*, 450–457.

Longhese, M. P., Guerini, I., Baldo, V., and Clerici, M. (2008). Surveillance mechanisms monitoring chromosome breaks during mitosis and meiosis. DNA Repair (Amst) *7*, 545–557.

Longhese, M. P., Mantiero, D., and Clerici, M. (2006). The cellular response to chromosome breakage. Mol Microbiol *60*, 1099–1108.

Lopes, J., Piazza, A., Bermejo, R., Kriegsman, B., Colosio, A. et al. (2011). G-quadruplex-induced instability during leading-strand replication. EMBO J *30*, 4033–4046.

Lopes, M., Cotta-Ramusino, C., Pellicioli, A., Liberi, G., Plevani, P. et al. (2001). The DNA replication checkpoint response stabilizes stalled replication forks. Nature *412*, 557–561.

Lowndes, N. F. and Toh, G. W.-L. (2005). DNA repair: the importance of phosphorylating histone H2AX. Curr Biol *15*, R99–R102.

López Castel, A., Cleary, J. D., and Pearson, C. E. (2010). Repeat instability as the basis for human diseases and as a potential target for therapy. Nat Rev Mol Cell Biol *11*, 165–170.

Lukusa, T. and Fryns, J. P. (2008). Human chromosome fragility. Biochim Biophys Acta *1779*, 3–16.

Lustig, A. J. (2003). Clues to catastrophic telomere loss in mammals from yeast telomere rapid deletion. Nat Rev Genet *4*, 916–923.

Lydall, D. and Whitehall, S. (2005). Chromatin and the DNA damage response. DNA Repair (Amst) *4*, 1195–1207.

Majka, J., Binz, S. K., Wold, M. S., and Burgers, P. M. (2006a). RPA directs loading of the DNA damage checkpoint clamp to 5'-DNA junctions. J Biol Chem *281*, 27855–27861.

Majka, J., Niedziela-Majka, A., and Burgers, P. M. J. (2006b). The Checkpoint Clamp Activates Mec1 Kinase during Initiation of the DNA Damage Checkpoint. Mol Cell *24*, 891–901.

Marti, T. M., Hefner, E., Feeney, L., Natale, V., and Cleaver, J. E. (2006). H2AX phosphorylation within the G1 phase after UV irradiation depends on nucleotide excision repair and not DNA double-strand breaks. Proc Natl Acad Sci U S A *103*, 9891–9896.

Masumoto, H., Hawke, D., Kobayashi, R., and Verreault, A. (2005). A role for cell-cycle-regulated histone H3 lysine 56 acetylation in the DNA damage response. Nature *436*, 294–298.

Matsukage, A., Hirose, F., Yoo, M.-A., and Yamaguchi, M. (2008). The DRE/DREF transcriptional regulatory system: a master key for cell proliferation. Biochim Biophys Acta *1779*, 81–89.

McClintock, B. (1941). The Stability of Broken Ends of Chromosomes in Zea Mays. Genetics *26*, 234–282.

McCulloch, S. D. and Kunkel, T. A. (2008). The fidelity of DNA synthesis by eukaryotic replicative and translesion synthesis polymerases. Cell Res *18*, 148–161.

McGranahan, N., Burrell, R. A., Endesfelder, D., Novelli, M. R., and Swanton, C. (2012). Cancer chromosomal instability: therapeutic and diagnostic challenges. EMBO Rep *13*, 528–538.

Melo, J. and Toczyski, D. (2002). A unified view of the DNA-damage checkpoint.

Melo, J. A., Cohen, J., and Toczyski, D. P. (2001). Two checkpoint complexes are independently recruited to sites of DNA damage in vivo. Genes Dev *15*, 2809–2821.

Memisoglu, A. and Samson, L. (2000). Base excision repair in yeast and mammals. Mutat Res *451*, 39–51.

Michel, L. S., Liberal, V., Chatterjee, A., Kirchwegger, R., Pasche, B. et al. (2001). MAD2 haplo-insufficiency causes premature anaphase and chromosome instability in mammalian cells. Nature *409*, 355–359.

Mieczkowski, P. A., Mieczkowska, J. O., Dominska, M., and Petes, T. D. (2003). Genetic regulation of telomere-telomere fusions in the yeast Saccharomyces cerevisae. Proc Natl Acad Sci U S A *100*, 10854–10859.

Minter-Dykhouse, K., Ward, I., Huen, M. S. Y., Chen, J., and Lou, Z. (2008). Distinct versus overlapping functions of MDC1 and 53BP1 in DNA damage response and tumorigenesis. J Cell Biol *181*, 727–735.

Mirkin, E. V. and Mirkin, S. M. (2007). Replication fork stalling at natural impediments. Microbiol Mol Biol Rev *71*, 13–35.

Mitelman, F., Johansson, B., and Mertens, F. (2012). Mitelman Database of Chromosome Aberrations and Gene Fusions in Cancer. http://cgap.nci.nih.gov/Chromosomes/Mitelman.

Moore, J. D., Yazgan, O., Ataian, Y., and Krebs, J. E. (2007). Diverse roles for histone H2A modifications in DNA damage response pathways in yeast. Genetics *176*, 15–25.

Mordes, D. A., Glick, G. G., Zhao, R., and Cortez, D. (2008a). TopBP1 activates ATR through ATRIP and a PIKK regulatory domain. Genes Dev *22*, 1478–1489.

Mordes, D. A., Nam, E. A., and Cortez, D. (2008b). Dpb11 activates the Mec1-Ddc2 complex. Proc Natl Acad Sci U S A *105*, 18730–18734.

Morrow, C. J., Tighe, A., Johnson, V. L., Scott, M. I. F., Ditchfield, C. et al. (2005). Bub1 and aurora B cooperate to maintain BubR1-mediated inhibition of APC/CCdc20. J Cell Sci *118*, 3639–3652.

Motegi, A. and Myung, K. (2007). Measuring the rate of gross chromosomal rearrangements in *Saccharomyces cerevisiae*: A practical approach to study genomic rearrangements observed in cancer. Methods *41*, 168–176.

Muraki, K., Nyhan, K., Han, L., and Murnane, J. P. (2012). Mechanisms of telomere loss and their consequences for chromosome instability. Front Oncol *2*, 135.

Musacchio, A. (2011). Spindle assembly checkpoint: the third decade. Philos Trans R Soc Lond B Biol Sci *366*, 3595–3604.

Musacchio, A. and Salmon, E. D. (2007). The spindle-assembly checkpoint in space and time. Nat Rev Mol Cell Biol *8*, 379–393.

Nag, D. K. and Petes, T. D. (1991). Seven-base-pair inverted repeats in DNA form stable hairpins in vivo in *Saccharomyces cerevisiae*. Genetics *129*, 669–673.

Naiki, T., Wakayama, T., Nakada, D., Matsumoto, K., and Sugimoto, K. (2004). Association of Rad9 with double-strand breaks through a Mec1-dependent mechanism. Mol Cell Biol *24*, 3277–3285.

Nakamura, T. M., Du, L.-L., Redon, C., and Russell, P. (2004). Histone H2A phosphorylation controls Crb2 recruitment at DNA breaks, maintains checkpoint arrest, and influences DNA repair in fission yeast. Mol Cell Biol *24*, 6215–6230.

Navadgi-Patil, V. M. and Burgers, P. M. (2009). A tale of two tails: activation of DNA damage checkpoint kinase Mec1/ATR by the 9-1-1 clamp and by Dpb11/TopBP1. DNA Repair (Amst) *8*, 996–1003.

Negrini, S., Gorgoulis, V. G., and Halazonetis, T. D. (2010). Genomic instability–an evolving hallmark of cancer. Nat Rev Mol Cell Biol *11*, 220–228.

Nick McElhinny, S. A., Kumar, D., Clark, A. B., Watt, D. L., Watts, B. E. et al. (2010a). Genome instability due to ribonucleotide incorporation into DNA. Nat Chem Biol *6*, 774–781.

Nick McElhinny, S. A., Watts, B. E., Kumar, D., Watt, D. L., Lundström, E.-B. et al. (2010b). Abundant ribonucleotide incorporation into DNA by yeast replicative polymerases. Proc Natl Acad Sci U S A *107*, 4949–4954.

Nickoloff, J. A. (1992). Transcription enhances intrachromosomal homologous recombination in mammalian cells. Mol Cell Biol *12*, 5311–5318.

Nnakwe, C. C., Altaf, M., Côté, J., and Kron, S. J. (2009). Dissection of Rad9 BRCT domain function in the mitotic checkpoint response to telomere uncapping. DNA Repair (Amst) *8*, 1452–1461.

Novarina, D., Amara, F., Lazzaro, F., Plevani, P., and Muzi-Falconi, M. (2011). Mind the gap: keeping UV lesions in check. DNA Repair (Amst) *10*, 751–759.

Nowotny, M. (2009). Retroviral integrase superfamily: the structural perspective. EMBO Rep *10*, 144–151.

Nyberg, K. A., Michelson, R. J., Putnam, C. W., and Weinert, T. A. (2002). Toward maintaining the genome: DNA damage and replication checkpoints. Annu Rev Genet *36*, 617–656.

O'Hagan, R. C., Chang, S., Maser, R. S., Mohan, R., Artandi, S. E. et al. (2002). Telomere dysfunction provokes regional amplification and deletion in cancer genomes. Cancer Cell *2*, 149–155.

Ohshima, N., Takahashi, M., and Hirose, F. (2003). Identification of a human homologue of the DREF transcription factor with a potential role in regulation of the histone H1 gene. J Biol Chem *278*, 22928–22938.

O'Neill, B. M., Szyjka, S. J., Lis, E. T., Bailey, A. O., Yates, J. R. et al. (2007). Pph3-Psy2 is a phosphatase complex required for Rad53 dephosphorylation and replication fork restart during recovery from DNA damage. Proc Natl Acad Sci U S A *104*, 9290–9295.

Ozeri-Galai, E., Bester, A. C., and Kerem, B. (2012). The complex basis underlying common fragile site instability in cancer. Trends Genet *28*, 295–302.

Paciotti, V., Clerici, M., Lucchini, G., and Longhese, M. P. (2000). The checkpoint protein Ddc2, functionally related to *S. pombe* Rad26, interacts with Mec1 and is regulated by Mec1-dependent phosphorylation in budding yeast. Genes Dev *14*, 2046–2059.

Paeschke, K., Capra, J. A., and Zakian, V. A. (2011). DNA replication through G-quadruplex motifs is promoted by the *Saccharomyces cerevisiae* Pif1 DNA helicase. Cell *145*, 678–691.

Pagès, V. and Fuchs, R. P. (2003). Uncoupling of leading- and lagging-strand DNA replication during lesion bypass in vivo. Science *300*, 1300–1303.

Palakodeti, A., Han, Y., Jiang, Y., and Le Beau, M. M. (2004). The role of late/slow replication of the FRA16D in common fragile site induction. Genes Chromosomes Cancer *39*, 71–76.

Palecek, E. (1991). Local supercoil-stabilized DNA structures. Crit Rev Biochem Mol Biol *26*, 151–226.

Palm, W. and de Lange, T. (2008). How shelterin protects mammalian telomeres. Annu Rev Genet *42*, 301–334.

Palumbo, E., Matricardi, L., Tosoni, E., Bensimon, A., and Russo, A. (2010). Replication dynamics at common fragile site FRA6E. Chromosoma *119*, 575–587.

Papamichos-Chronakis, M., Watanabe, S., Rando, O. J., and Peterson, C. L. (2011). Global regulation of H2A.Z localization by the INO80 chromatin-remodeling enzyme is essential for genome integrity. Cell *144*, 200–213.

Parkinson, G. N., Lee, M. P. H., and Neidle, S. (2002). Crystal structure of parallel quadruplexes from human telomeric DNA. Nature *417*, 876–880.

Parsons, D. W., Jones, S., Zhang, X., Lin, J. C.-H., Leary, R. J. et al. (2008). An integrated genomic analysis of human glioblastoma multiforme. Science *321*, 1807–1812.

Paulovich, A. G. and Hartwell, L. H. (1995). A checkpoint regulates the rate of progression through S phase in *S. cerevisiae* in response to DNA damage. Cell *82*, 841–847.

Pavelka, N., Rancati, G., Zhu, J., Bradford, W. D., Saraf, A. et al. (2010). Aneuploidy confers quantitative proteome changes and phenotypic variation in budding yeast. Nature *468*, 321–325.

Pellicioli, A. and Foiani, M. (2005). Signal transduction: how rad53 kinase is activated. Curr Biol *15*, R769–R771.

Pellicioli, A., Lee, S. E., Lucca, C., Foiani, M., and Haber, J. E. (2001). Regulation of Saccharomyces Rad53 checkpoint kinase during adaptation from DNA damage-induced G2/M arrest. Mol Cell *7*, 293–300.

Pellicioli, A., Lucca, C., Liberi, G., Marini, F., Lopes, M. et al. (1999). Activation of Rad53 kinase in response to DNA damage and its effect in modulating phosphorylation of the lagging strand DNA polymerase. EMBO J *18*, 6561–6572.

Peng, A. and Chen, P.-L. (2003). NFBD1, like 53BP1, is an early and redundant transducer mediating Chk2 phosphorylation in response to DNA damage. J Biol Chem *278*, 8873–8876.

Pfander, B. and Diffley, J. F. X. (2011). Dpb11 coordinates Mec1 kinase activation with cell cycle-regulated Rad9 recruitment. EMBO J *30*, 4897–4907.

Pfander, B., Moldovan, G.-L., Sacher, M., Hoege, C., and Jentsch, S. (2005). SUMO-modified PCNA recruits Srs2 to prevent recombination during S phase. Nature *436*, 428–433.

Phillips, D. H., Hewer, A., Martin, C. N., Garner, R. C., and King, M. M. (1988). Correlation of DNA adduct levels in human lung with cigarette smoking. Nature *336*, 790–792.

Pommier, Y., Leo, E., Zhang, H., and Marchand, C. (2010). DNA topoisomerases and their poisoning by anticancer and antibacterial drugs. Chem Biol *17*, 421–433.

Postow, L., Ullsperger, C., Keller, R. W., Bustamante, C., Vologodskii, A. V. et al. (2001). Positive torsional strain causes the formation of a four-way junction at replication forks. J Biol Chem *276*, 2790–2796.

Prado, F. and Aguilera, A. (2005). Impairment of replication fork progression mediates RNA polII transcription-associated recombination. EMBO J *24*, 1267–1276.

Prakash, S. and Prakash, L. (2000). Nucleotide excision repair in yeast. Mutat Res *451*, 13–24.

Puddu, F., Granata, M., Di Nola, L., Balestrini, A., Piergiovanni, G. et al. (2008). Phosphorylation of the budding yeast 9-1-1 complex is required for Dpb11 function in the full activation of the UV-induced DNA damage checkpoint. Mol Cell Biol *28*, 4782–4793.

Putnam, C. D., Pennaneach, V., and Kolodner, R. D. (2005). *Saccharomyces cerevisiae* as a model system to define the chromosomal instability phenotype. Mol Cell Biol *25*, 7226–7238.

Qin, S. and Parthun, M. R. (2006). Recruitment of the type B histone acetyltransferase Hat1p to chromatin is linked to DNA double-strand breaks. Mol Cell Biol *26*, 3649–3658.

Qiu, J., Qian, Y., Frank, P., Wintersberger, U., and Shen, B. (1999). *Saccharomyces cerevisiae* RNase H(35) functions in RNA primer removal during lagging-strand DNA synthesis, most efficiently in cooperation with Rad27 nuclease. Mol Cell Biol *19*, 8361–8371.

Qu, M., Yang, B., Tao, L., Yates, 3rd, J. R., Russell, P. et al. (2012). Phosphorylation-dependent interactions between Crb2 and Chk1 are essential for DNA damage checkpoint. PLoS Genet *8*, e1002817.

Razidlo, D. F. and Lahue, R. S. (2008). Mrc1, Tof1 and Csm3 inhibit CAG.CTG repeat instability by at least two mechanisms. DNA Repair (Amst) *7*, 633–640.

Reijns, M. A. M., Rabe, B., Rigby, R. E., Mill, P., Astell, K. R. et al. (2012). Enzymatic removal of ribonucleotides from DNA is essential for mammalian genome integrity and development. Cell *149*, 1008–1022.

Renan, M. J. (1993). How many mutations are required for tumorigenesis? Implications from human cancer data. Mol Carcinog *7*, 139–146.

Ripperger, T., Gadzicki, D., Meindl, A., and Schlegelberger, B. (2009). Breast cancer susceptibility: current knowledge and implications for genetic counselling. Eur J Hum Genet *17*, 722–731.

Ritchie, K. B., Mallory, J. C., and Petes, T. D. (1999). Interactions of TLC1 (which encodes the RNA subunit of telomerase), TEL1, and MEC1 in regulating telomere length in the yeast *Saccharomyces cerevisiae*. Mol Cell Biol *19*, 6065–6075.

Ritchie, K. B. and Petes, T. D. (2000). The Mre11p/Rad50p/Xrs2p complex and the Tel1p function in a single pathway for telomere maintenance in yeast. Genetics *155*, 475–479.

Rodriguez, R., Miller, K. M., Forment, J. V., Bradshaw, C. R., Nikan, M. et al. (2012). Small-molecule-induced DNA damage identifies alternative DNA structures in human genes. Nat Chem Biol *8*, 301–310.

Rogakou, E. P., Pilch, D. R., Orr, A. H., Ivanova, V. S., and Bonner, W. M. (1998). DNA double-stranded breaks induce histone H2AX phosphorylation on serine 139. J Biol Chem *273*, 5858–5868.

Rudolph, K. L., Chang, S., Lee, H. W., Blasco, M., Gottlieb, G. J. et al. (1999). Longevity, stress response, and cancer in aging telomerase-deficient mice. Cell *96*, 701–712.

Saini, N., Zhang, Y., Usdin, K., and Lobachev, K. S. (2013). When secondary comes first - The importance of non-canonical DNA structures. Biochimie *in press*.

Sanchez, Y., Bachant, J., Wang, H., Hu, F., Liu, D. et al. (1999). Control of the DNA damage checkpoint by chk1 and rad53 protein kinases through distinct mechanisms. Science *286*, 1166–1171.

Sanders, S. L., Portoso, M., Mata, J., Bähler, J., Allshire, R. C. et al. (2004). Methylation of histone H4 lysine 20 controls recruitment of Crb2 to sites of DNA damage. Cell *119*, 603–614.

Schaaper, R. M. (1993). Base selection, proofreading, and mismatch repair during DNA replication in Escherichia coli. J Biol Chem *268*, 23762–23765.

Schmidt, K. H., Pennaneach, V., Putnam, C. D., and Kolodner, R. D. (2006). Analysis of gross-chromosomal rearrangements in *Saccharomyces cerevisiae*. Methods Enzymol *409*, 462–476.

Schärer, O. D. (2005). DNA interstrand crosslinks: natural and drug-induced DNA adducts that induce unique cellular responses. Chembiochem *6*, 27–32.

Schwartz, M. F., Duong, J. K., Sun, Z., Morrow, J. S., Pradhan, D. et al. (2002). Rad9 phosphorylation sites couple Rad53 to the *Saccharomyces cerevisiae* DNA damage checkpoint. Mol Cell *9*, 1055–1065.

Schwob, E. and Nasmyth, K. (1993). CLB5 and CLB6, a new pair of B cyclins involved in DNA replication in *Saccharomyces cerevisiae*. Genes Dev *7*, 1160–1175.

Sedgwick, B. (2004). Repairing DNA-methylation damage. Nat Rev Mol Cell Biol *5*, 148–157.

Sertic, S., Pizzi, S., Lazzaro, F., Plevani, P., and Muzi-Falconi, M. (2012). NER and DDR: classical music with new instruments. Cell Cycle *11*, 668–674.

Sfeir, A., Kosiyatrakul, S. T., Hockemeyer, D., MacRae, S. L., Karlseder, J. et al. (2009). Mammalian telomeres resemble fragile sites and require TRF1 for efficient replication. Cell *138*, 90–103.

Shah, S. N., Opresko, P. L., Meng, X., Lee, M. Y. W. T., and Eckert, K. A. (2010). DNA structure and the Werner protein modulate human DNA polymerase delta-dependent replication dynamics within the common fragile site FRA16D. Nucleic Acids Res *38*, 1149–1162.

Shay, J. W. and Wright, W. E. (2005). Senescence and immortalization: role of telomeres and telomerase. Carcinogenesis *26*, 867–874.

Sheltzer, J. M., Blank, H. M., Pfau, S. J., Tange, Y., George, B. M. et al. (2011). Aneuploidy drives genomic instability in yeast. Science *333*, 1026–1030.

Shen, X., Ranallo, R., Choi, E., and Wu, C. (2003). Involvement of actin-related proteins in ATP-dependent chromatin remodeling. Mol Cell *12*, 147–155.

Shen, Y., Koh, K. D., Weiss, B., and Storici, F. (2012). Mispaired rNMPs in DNA are mutagenic and are targets of mismatch repair and RNases H. Nat Struct Mol Biol *19*, 98–104.

Shin, D. S., Chahwan, C., Huffman, J. L., and Tainer, J. A. (2004). Structure and function of the double-strand break repair machinery. DNA Repair (Amst) *3*, 863–873.

Sidorova, J. M. and Breeden, L. L. (1997). Rad53-dependent phosphorylation of Swi6 and down-regulation of CLN1 and CLN2 transcription occur in response to DNA damage in *Saccharomyces cerevisiae*. Genes Dev *11*, 3032–3045.

Siede, W., Friedberg, A. S., Dianova, I., and Friedberg, E. C. (1994). Characterization of G1 checkpoint control in the yeast Saccharomyces cerevisiae following exposure to DNA-damaging agents. Genetics *138*, 271–281.

Silkworth, W. T., Nardi, I. K., Scholl, L. M., and Cimini, D. (2009). Multipolar spindle pole coalescence is a major source of kinetochore mis-attachment and chromosome mis-segregation in cancer cells. PLoS One *4*, e6564.

Sjöblom, T., Jones, S., Wood, L. D., Parsons, D. W., Lin, J. et al. (2006). The consensus coding sequences of human breast and colorectal cancers. Science *314*, 268–274.

Skandalis, A., Ford, B. N., and Glickman, B. W. (1994). Strand bias in mutation involving 5-methylcytosine deamination in the human hprt gene. Mutat Res *314*, 21–26.

Skotheim, J. M., Talia, S. D., Siggia, E. D., and Cross, F. R. (2008). Positive feedback of G1 cyclins ensures coherent cell cycle entry. Nature *454*, 291–296.

Smogorzewska, A., Karlseder, J., Holtgreve-Grez, H., Jauch, A., and de Lange, T. (2002). DNA ligase IV-dependent NHEJ of deprotected mammalian telomeres in G1 and G2. Curr Biol *12*, 1635–1644.

Smolka, M. B., Albuquerque, C. P., Chen, S.-h., Schmidt, K. H., Wei, X. X. et al. (2005). Dynamic changes in protein-protein interaction and protein phosphorylation probed with amine-reactive isotope tag. Mol Cell Proteomics *4*, 1358–1369.

Sogo, J. M., Lopes, M., and Foiani, M. (2002). Fork reversal and ssDNA accumulation at stalled replication forks owing to checkpoint defects. Science *297*, 599–602.

Solomon, D. A., Kim, T., Diaz-Martinez, L. A., Fair, J., Elkahloun, A. G. et al. (2011). Mutational inactivation of STAG2 causes aneuploidy in human cancer. Science *333*, 1039–1043.

Soria, G., Polo, S. E., and Almouzni, G. (2012). Prime, repair, restore: the active role of chromatin in the DNA damage response. Mol Cell *46*, 722–734.

Sotillo, R., Schvartzman, J.-M., Socci, N. D., and Benezra, R. (2010). Mad2-induced chromosome instability leads to lung tumour relapse after oncogene withdrawal. Nature *464*, 436–440.

Soulier, J. and Lowndes, N. F. (1999). The BRCT domain of the *S. cerevisiae* checkpoint protein Rad9 mediates a Rad9-Rad9 interaction after DNA damage. Curr Biol *9*, 551–554.

Sparks, J. L., Chon, H., Cerritelli, S. M., Kunkel, T. A., Johansson, E. et al. (2012). RNase H2-Initiated Ribonucleotide Excision Repair. Mol Cell *47*, 980–986.

Spell, R. M. and Jinks-Robertson, S. (2004). Determination of mitotic recombination rates by fluctuation analysis in *Saccharomyces cerevisiae*. Methods Mol Biol *262*, 3–12.

Spencer, F., Gerring, S. L., Connelly, C., and Hieter, P. (1990). Mitotic chromosome transmission fidelity mutants in *Saccharomyces cerevisiae*. Genetics *124*, 237–249.

Spiro, C., Pelletier, R., Rolfsmeier, M. L., Dixon, M. J., Lahue, R. S. et al. (1999). Inhibition of FEN-1 processing by DNA secondary structure at trinucleotide repeats. Mol Cell *4*, 1079–1085.

Spruck, C. H., Won, K. A., and Reed, S. I. (1999). Deregulated cyclin E induces chromosome instability. Nature *401*, 297–300.

Stephens, P. J., Greenman, C. D., Fu, B., Yang, F., Bignell, G. R. et al. (2011). Massive genomic rearrangement acquired in a single catastrophic event during cancer development. Cell *144*, 27–40.

Streisinger, G., Okada, Y., Emrich, J., Newton, J., Tsugita, A. et al. (1966). Frameshift mutations and the genetic code. This paper is dedicated to Professor Theodosius Dobzhansky on the occasion of his 66th birthday. Cold Spring Harb Symp Quant Biol *31*, 77–84.

Sudakin, V., Chan, G. K., and Yen, T. J. (2001). Checkpoint inhibition of the APC/C in HeLa cells is mediated by a complex of BUBR1, BUB3, CDC20, and MAD2. J Cell Biol *154*, 925–936.

Sugawara, N. and Haber, J. E. (1992). Characterization of double-strand break-induced recombination: homology requirements and single-stranded DNA formation. Mol Cell Biol *12*, 563–575.

Sun, Z., Hsiao, J., Fay, D. S., and Stern, D. F. (1998). Rad53 FHA domain associated with phosphorylated Rad9 in the DNA damage checkpoint. Science *281*, 272–274.

Svendsen, J. M. and Harper, J. W. (2010). GEN1/Yen1 and the SLX4 complex: Solutions to the problem of Holliday junction resolution. Genes Dev *24*, 521–536.

Sweeney, F. D., Yang, F., Chi, A., Shabanowitz, J., Hunt, D. F. et al. (2005). *Saccharomyces cerevisiae* Rad9 acts as a Mec1 adaptor to allow Rad53 activation. Curr Biol *15*, 1364–1375.

Syljuåsen, R. G. (2007). Checkpoint adaptation in human cells. Oncogene *26*, 5833–5839.

Symington, L. S. and Holloman, W. K. (2008). Resolving resolvases: the final act? Mol Cell *32*, 603–604.

Tamburini, B. A. and Tyler, J. K. (2005). Localized histone acetylation and deacetylation triggered by the homologous recombination pathway of double-strand DNA repair. Mol Cell Biol *25*, 4903–4913.

Thoma, F. (1999). Light and dark in chromatin repair: repair of UV-induced DNA lesions by photolyase and nucleotide excision repair. EMBO J *18*, 6585–6598.

Thomas, B. J. and Rothstein, R. (1989). Elevated recombination rates in transcriptionally active DNA. Cell *56*, 619–630.

Thompson, S. L., Bakhoum, S. F., and Compton, D. A. (2010). Mechanisms of chromosomal instability. Curr Biol *20*, R285–R295.

Thompson, S. L. and Compton, D. A. (2008). Examining the link between chromosomal instability and aneuploidy in human cells. J Cell Biol *180*, 665–672.

Toh, G. W.-L. and Lowndes, N. F. (2003). Role of the *Saccharomyces cerevisiae* Rad9 protein in sensing and responding to DNA damage. Biochem Soc Trans *31*, 242–246.

Toh, G. W.-L., O'shaughnessy, A. M., Jimeno, S., Dobbie, I. M., Grenon, M. et al. (2006). Histone H2A phosphorylation and H3 methylation are required for a novel Rad9 DSB repair function following checkpoint activation. DNA Repair (Amst) *5*, 693–703.

Tsantoulis, P. K., Kotsinas, A., Sfikakis, P. P., Evangelou, K., Sideridou, M. et al. (2008). Oncogene-induced replication stress preferentially targets common fragile sites in preneoplastic lesions. A genome-wide study. Oncogene *27*, 3256–3264.

Ubersax, J. A., Woodbury, E. L., Quang, P. N., Paraz, M., Blethrow, J. D. et al. (2003). Targets of the cyclin-dependent kinase Cdk1. Nature *425*, 859–864.

Unal, E., Arbel-Eden, A., Sattler, U., Shroff, R., Lichten, M. et al. (2004). DNA damage response pathway uses histone modification to assemble a double-strand break-specific cohesin domain. Mol Cell *16*, 991–1002.

Usui, T., Foster, S. S., and Petrini, J. H. J. (2009). Maintenance of the DNA-damage checkpoint requires DNA-damage-induced mediator protein oligomerization. Mol Cell *33*, 147–159.

Usui, T., Ogawa, H., and Petrini, J. H. (2001). A DNA damage response pathway controlled by Tel1 and the Mre11 complex. Mol Cell *7*, 1255–1266.

van Leeuwen, F., Gafken, P. R., and Gottschling, D. E. (2002). Dot1p modulates silencing in yeast by methylation of the nucleosome core. Cell *109*, 745–756.

van Steensel, B., Smogorzewska, A., and de Lange, T. (1998). TRF2 protects human telomeres from end-to-end fusions. Cell *92*, 401–413.

Vaze, M. B., Pellicioli, A., Lee, S. E., Ira, G., Liberi, G. et al. (2002). Recovery from checkpoint-mediated arrest after repair of a double-strand break requires Srs2 helicase. Mol Cell *10*, 373–385.

Vialard, J. E., Gilbert, C. S., Green, C. M., and Lowndes, N. F. (1998). The budding yeast Rad9 checkpoint protein is subjected to Mec1/Tel1-dependent hyperphosphorylation and interacts with Rad53 after DNA damage. EMBO J *17*, 5679–5688.

Voineagu, I., Narayanan, V., Lobachev, K. S., and Mirkin, S. M. (2008). Replication stalling at unstable inverted repeats: interplay between

DNA hairpins and fork stabilizing proteins. Proc Natl Acad Sci U S A *105*, 9936–9941.

von Zglinicki, T. (2002). Oxidative stress shortens telomeres. Trends Biochem Sci *27*, 339–344.

Vos, S. M., Tretter, E. M., Schmidt, B. H., and Berger, J. M. (2011). All tangled up: how cells direct, manage and exploit topoisomerase function. Nat Rev Mol Cell Biol *12*, 827–841.

Wang, G. and Vasquez, K. M. (2004). Naturally occurring H-DNA-forming sequences are mutagenic in mammalian cells. Proc Natl Acad Sci U S A *101*, 13448–13453.

Wang, G. and Vasquez, K. M. (2009). Models for chromosomal replication-independent non-B DNA structure-induced genetic instability. Mol Carcinog *48*, 286–298.

Wang, J., Gong, Z., and Chen, J. (2011). MDC1 collaborates with TopBP1 in DNA replication checkpoint control. J Cell Biol *193*, 267–273.

Wang, Z., Cummins, J. M., Shen, D., Cahill, D. P., Jallepalli, P. V. et al. (2004). Three classes of genes mutated in colorectal cancers with chromosomal instability. Cancer Res *64*, 2998–3001.

Ward, I., Kim, J.-E., Minn, K., Chini, C. C., Mer, G. et al. (2006). The tandem BRCT domain of 53BP1 is not required for its repair function. J Biol Chem *281*, 38472–38477.

Waters, L. S., Minesinger, B. K., Wiltrout, M. E., D'Souza, S., Woodruff, R. V. et al. (2009). Eukaryotic translesion polymerases and their roles and regulation in DNA damage tolerance. Microbiol Mol Biol Rev *73*, 134–154.

Watson, J. D. (1972). Origin of concatemeric T7 DNA. Nat New Biol *239*, 197–201.

Watson, J. D. and Crick, F. H. (1953). Molecular structure of nucleic acids; a structure for deoxyribose nucleic acid. Nature *171*, 737–738.

Watt, D. L., Johansson, E., Burgers, P. M., and Kunkel, T. A. (2011). Replication of ribonucleotide-containing DNA templates by yeast replicative polymerases. DNA Repair (Amst) *10*, 897–902.

Weinert, T. (1998). DNA damage and checkpoint pathways: molecular anatomy and interactions with repair. Cell *94*, 555–558.

Wilson, K. A. and Stern, D. F. (2008). NFBD1/MDC1, 53BP1 and BRCA1 have both redundant and unique roles in the ATM pathway. Cell Cycle *7*, 3584–3594.

Wood, L. D., Parsons, D. W., Jones, S., Lin, J., Sjöblom, T. et al. (2007). The genomic landscapes of human breast and colorectal cancers. Science *318*, 1108–1113.

Wysocki, R., Javaheri, A., Allard, S., Sha, F., CÃ?tÃ©, J. et al. (2005). Role of Dot1-dependent histone H3 methylation in G1 and S phase DNA damage checkpoint functions of Rad9. Mol Cell Biol *25*, 8430–8443.

Yamaguchi, M., Hayashi, Y., Nishimoto, Y., Hirose, F., and Matsukage, A. (1995). A nucleotide sequence essential for the function of DRE, a common promoter element for Drosophila DNa replication-related genes. J Biol Chem *270*, 15808–15814.

Yu, X., Chini, C. C. S., He, M., Mer, G., and Chen, J. (2003). The BRCT domain is a phospho-protein binding domain. Science *302*, 639–642.

Zgheib, O., Pataky, K., Brugger, J., and Halazonetis, T. D. (2009). An oligomerized 53BP1 tudor domain suffices for recognition of DNA double-strand breaks. Mol Cell Biol *29*, 1050–1058.

Zhang, C., Roberts, T. M., Yang, J., Desai, R., and Brown, G. W. (2006a). Suppression of genomic instability by SLX5 and SLX8 in *Saccharomyces cerevisiae*. DNA Repair (Amst) *5*, 336–346.

Zhang, D.-H., Zhou, B., Huang, Y., Xu, L.-X., and Zhou, J.-Q. (2006b). The human Pif1 helicase, a potential Escherichia coli RecD homologue, inhibits telomerase activity. Nucleic Acids Res *34*, 1393–1404.

Zhang, N., Ge, G., Meyer, R., Sethi, S., Basu, D. et al. (2008). Overexpression of Separase induces aneuploidy and mammary tumorigenesis. Proc Natl Acad Sci U S A *105*, 13033–13038.

Zheng, L. and Shen, B. (2011). Okazaki fragment maturation: nucleases take centre stage. J Mol Cell Biol *3*, 23–30.

Zlotorynski, E., Rahat, A., Skaug, J., Ben-Porat, N., Ozeri, E. et al. (2003). Molecular basis for expression of common and rare fragile sites. Mol Cell Biol *23*, 7143–7151.

Zou, L. and Elledge, S. J. (2003). Sensing DNA damage through ATRIP recognition of RPA-ssDNA complexes. Science *300*, 1542–1548.

Acknowledgments

I wish to sincerely thank professor Marco Muzi-Falconi and professor Paolo-Plevani for welcoming me in their lab and supervising my PhD work; doctor Federico Lazzaro for teaching me the wonderful art of working in a molecular biology lab; all the members of the lab not only for scientific discussion, but also for congeniality and sincere friendship.

I recall with gratitude professor Grant Brown and all the Brown lab's members, as well as all the directors and residents of Ernescliff College: it is thanks to them that the months I spent in Toronto during my PhD turned out to be a wonderful experience.

I also thank all the friends which shared these years with me.

Last but not least, I wish to thank my family for the support they provided during all these years. In particular, I cannot help but thanking my brother Davide for his invaluable help in editing this thesis and in solving all the issues raised by my poor knowledge of LyX: without his patience and technical skills, this work would be never accomplished.

Part II

Published paper I

Granata, M., Lazzaro, F., Novarina, D., Panigada, D., Puddu, F., Abreu, C. M., Kumar, R., Grenon, M., Lowndes, N. F., Plevani, P. and Muzi-Falconi, M.

Dynamics of Rad9 chromatin binding and checkpoint function are mediated by its dimerization and are cell cycle-regulated by CDK1 activity.

Published in: PLoS Genetics, **2010**, 6.

OPEN ACCESS Freely available online

PLoS GENETICS

Dynamics of Rad9 Chromatin Binding and Checkpoint Function Are Mediated by Its Dimerization and Are Cell Cycle–Regulated by CDK1 Activity

Magda Granata[1☯], Federico Lazzaro[1☯], Daniele Novarina[1], Davide Panigada[1], Fabio Puddu[1], Carla Manuela Abreu[2], Ramesh Kumar[2], Muriel Grenon[2], Noel F. Lowndes[2], Paolo Plevani[1]*, Marco Muzi-Falconi[1]*

1 Dipartimento di Scienze Biomolecolari e Biotecnologie, Università degli Studi di Milano, Milano, Italy, **2** Centre for Chromosome Biology, School of Natural Science, National University of Ireland Galway, Galway, Ireland

Abstract

Saccharomyces cerevisiae Rad9 is required for an effective DNA damage response throughout the cell cycle. Assembly of Rad9 on chromatin after DNA damage is promoted by histone modifications that create docking sites for Rad9 recruitment, allowing checkpoint activation. Rad53 phosphorylation is also dependent upon BRCT-directed Rad9 oligomerization; however, the crosstalk between these molecular determinants and their functional significance are poorly understood. Here we report that, in the G1 and M phases of the cell cycle, both constitutive and DNA damage-dependent Rad9 chromatin association require its BRCT domains. In G1 cells, GST or FKBP dimerization motifs can substitute to the BRCT domains for Rad9 chromatin binding and checkpoint function. Conversely, forced Rad9 dimerization in M phase fails to promote its recruitment onto DNA, although it supports Rad9 checkpoint function. In fact, a parallel pathway, independent on histone modifications and governed by CDK1 activity, allows checkpoint activation in the absence of Rad9 chromatin binding. CDK1-dependent phosphorylation of Rad9 on Ser11 leads to specific interaction with Dpb11, allowing Rad53 activation and bypassing the requirement for the histone branch.

Citation: Granata M, Lazzaro F, Novarina D, Panigada D, Puddu F, et al. (2010) Dynamics of Rad9 Chromatin Binding and Checkpoint Function Are Mediated by Its Dimerization and Are Cell Cycle–Regulated by CDK1 Activity. PLoS Genet 6(8): e1001047. doi:10.1371/journal.pgen.1001047

Editor: Gregory P. Copenhaver, The University of North Carolina at Chapel Hill, United States of America

Received December 24, 2009; **Accepted** July 2, 2010; **Published** August 5, 2010

Funding: This work was supported by grants from AIRC and Fondazione Cariplo to PP and MM-F, the European Union FP6 Integrated Project DNA repair contract number 512113 to PP and NFL, a NUIG college fellowship to RK, and a Science Foundation Ireland Principal Investigator award 07/IN1/B958 to NFL. CMA was supported by Fundação para a Ciência e a Tecnologia (SFRH/BD/42128/2007, Portugal). The funders had no role in study design, data collection and analysis, decision to publish or preparation of the manuscript.

Competing Interests: The authors have declared that no competing interests exist.

* E-mail: marco.muzifalconi@unimi.it (MM-F); paolo.plevani@unimi.it (PP)

☯ These authors contributed equally to this work.

Introduction

The DNA damage checkpoint coordinates cell cycle progression, DNA repair, replication, recombination, apoptosis and senescence in response to genotoxic stress. Defects in this surveillance mechanism lead to increased genomic instability, cancer susceptibility, ageing and several human pathologies [1,2]. The checkpoint is organized as a signal transduction cascade, whose players have been conserved throughout evolution [3,4]. When DNA is damaged, cells are able to sense and process the lesions generating a series of phosphorylation events, which are then amplified and propagated to specific targets [3,4]. Critical checkpoint factors are phosphorylated in response to DNA damage and their order of functions in the cascade has been mainly inferred by monitoring their phosphorylation state [5]. The apical kinases in the pathway are members of a family of phosphatidylinositol 3′ kinase-like kinases (PIKKs), which includes Mec1 and Tel1 from budding yeast, as well as mammalian ATM, ATR and DNA-PK [6]. In the yeast *Saccharomyces cerevisiae* the first biochemical event in response to checkpoint activation is the Mec1-dependent phosphorylation of its interacting subunit Ddc2 [7–9]. Other critical Mec1 targets are histone H2A, the 9-1-1 complex and the Rad9 mediator which is necessary for the recruitment and activation of the main effector kinase Rad53 [10–16]. Rad53 phosphorylation is a key step in the signal transduction cascade and it is generally used as a marker to monitor full checkpoint activation [17].

In a pioneering study, *RAD9* was the first DNA damage checkpoint gene identified in yeast and it is required for proper DNA damage response in all cell cycle phases and in response to a variety of genotoxins [18–20]. Rad9 is a large protein of 148 kDa containing a tandem repeat of the BRCT (BRCA1 C-terminus) motif, which is required for Rad9 oligomerization and function [21–23]. Until recently the biochemical role of the *RAD9* gene product remained obscure. Gilbert et al., were the first to purify Rad9 complexes from undamaged and UV-treated cells; structural characterization of such complexes led to the proposal that Rad9 recruits and catalyzes the activation of Rad53, by acting as a scaffold protein bringing Rad53 molecules in close proximity, thus facilitating the Rad53 autophosphorylation reaction [14].

The Rad9 protein contains several potential target sites for CDK1/Cdc28 kinase and PIKK-directed phosphorylation [24].

Author Summary

In response to DNA damage all eukaryotic cells activate a surveillance mechanism, known as the DNA damage checkpoint, which delays cell cycle progression and modulates DNA repair. Yeast *RAD9* was the first DNA damage checkpoint gene identified. The genetic tools available in this model system allow to address relevant questions to understand the molecular mechanisms underlying the Rad9 biological function. By chromatin-binding and domain-swapping experiments, we found that Rad9 is recruited into DNA both in unperturbed and in DNA–damaging conditions, and we identified the molecular determinants required for such interaction. Moreover, the extent of chromatin-bound Rad9 is regulated during the cell cycle and influences its role in checkpoint activation. In fact, the checkpoint function of Rad9 in G1 cells is solely mediated by its interaction with modified histones, while in M phase it occurs through an additional scaffold protein, named Dpb11. Productive Rad9-Dpb11 interaction in M phase requires Rad9 phosphorylation by CDK1, and we identified the Ser11 residue as the major CDK1 target. The model of Rad9 action that we are presenting can be extended to other eukaryotic organisms, since Rad9 and Dpb11 have been conserved through evolution from yeast to mammalian cells.

Rad9 is phosphorylated in an unperturbed cell cycle and it is hyper-phosphorylated in a Mec1- and/or Tel1-dependent manner after genotoxic treatments [12,13]. This hyper-phosphorylation is a pre-requisite for Rad9-Rad53 association, which is mediated by the two forkhead associated (FHA) Rad53 domains and specific Rad9 amino acid residues that are modified in the hyper-phosphorylated Rad9 form [12,13,15,16,25–27]. Recent data confirmed that the Rad9 BRCT domains mediate Rad9 oligomerization, and these interactions are also modulated by Mec1/Tel1-dependent phosphorylation of a SQ/TQ cluster domain (SCD) in Rad9. Rad9 oligomerization is required to maintain checkpoint signaling through a feedback loop involving Rad53-dependent phosphorylation of the Rad9 BRCT domains, which attenuates BRCT-SCD interactions [27].

Despite the fundamental nature of the cellular response to DNA damage, Rad9 and its *Schizosaccharomyces pombe* and metazoan orthologs Crb2 and 53BP1 show a modest level of amino acid sequence conservation. Dimerization mediated by the BRCT domains has been shown to be essential for the biological function of both Rad9 and Crb2 [21,28], however, 53BP1 oligomerization occurs in a BRCT-independent manner [29,30]. Recent structural analysis showed that an equivalent surface is conserved to a certain degree also in 53BP1 and it provides the binding site for p53. It was thus suggested that a functional requirement for dimerization of a checkpoint mediator may have been conserved in the evolution, but in metazoan organisms it may be delivered via a second protein rather than through homotypic interactions [31].

In the last few years it became evident that chromatin remodelling activities and post-translational modifications of chromatin components, including histones, influence DNA damage checkpoint signalling and repair in all eukaryotic cells (see [32] for a recent review). Moreover, it has been recently suggested that Rad9 may also be chromatin-bound in the absence of DNA damage [22]. This dynamic interaction with chromatin appears to require the Tudor domain of Rad9 and methylated lysine 79 of histone H3 (H3-K79me). Furthermore, this interaction modulates Rad9 functions after DNA damage [22,23,33–35]. However, the Crb2 and 53BP1 orthologues of Rad9 both recognize H4 methylated at lysine 20 (H4-K20me), although human 53BP1 may also be recruited to chromatin through interactions with H3-K79me [34,36–39].

For the Rad9/Crb2/53BP1 mediator proteins, efficient recruitment seems to require additional molecular interactions. Rad9 and Crb2 interact via their BRCT domains with H2A phosphorylated at serine 129 (γH2A) at sites of DNA damage [22,31,37,40–42]. 53BP1 binding to DSBs is facilitated by phosphorylation of serine 139 of the histone variant H2AX (γH2AX) [29,43–45]. It has been reported that various oligomerization domains in 53BP1 facilitate its recruitment to damaged DNA sites [30]. Moreover, 53BP1 recruitment to chromatin is facilitated by ubiquitination of H2A and H2AX by RNF8 through a yet unidentified mechanism [46–48].

Recently, it has been shown that Dpb11 in *S. cerevisiae* and its *S. pombe* and metazoan orthologs, termed Rad4/Cut5 and TopBP1, respectively, are required for full PIKK-dependent checkpoint activation in response to DNA damage [49,50]. Moreover it has been suggested that Dpb11 orthologs may modulate checkpoint activation through interaction with mediator/adaptor proteins [37,51]. To explore the functional role and the relationship between the BRCT domains and Rad9 ability to bind chromatin, we have analyzed both Rad9 chromatin recruitment and checkpoint activation in cells engineered to express various forms of Rad9 harboring mutated BRCT domains, including point mutations, deletion and substitutions with heterologous dimerization domains. We found that the requirements for Rad9 binding to chromatin are different in G1 or in M phase cells and in damaging versus unperturbed conditions. Moreover, we tested the requirements for Rad9 chromatin binding in yeast mutants defective in either the histone-dependent and/or histone-independent pathways essential for full checkpoint activation in M phase. Importantly, we found that CDK1-dependent Rad9 phosphorylation on Ser11 modulates the Dpb11-dependent branch in the M phase of the cell cycle in a chromatin-independent manner.

Results

Rad9 BRCT domains are required for its binding to chromatin in unperturbed and DNA damaging conditions

The Rad9 checkpoint mediator protein contains a tandem repeat of the BRCT motif at its C-terminus. Previous experiments have shown that the BRCT domains are critical for the activation of the DNA damage checkpoint and two-hybrid and GST pull-down analysis indicated that the BRCT domains modulate Rad9-Rad9 interactions [21]. More recently, it has been shown that Rad9 mutations in a conserved region of the first BRCT motif affect binding to γH2A, thus altering the G1 checkpoint signaling in response to DSBs [22,40] and the G2/M response to uncapped telomeres [23]. However, the mutations analyzed did not influence Rad9 chromatin binding in unperturbed conditions [22].

The *rad9-F1104L* or the *rad9-W1280L* mutations substitute the most highly conserved amino acid residues in the two BRCT motifs and each mutation affects productive Rad9-Rad9 interactions [21]. We tested whether such *rad9* mutations impair Rad9 recruitment to chromatin both in unperturbed and DNA damaging conditions. As expected, a proportion of wild-type Rad9 migrated much more slowly under our gel running conditions after UV treatment, consistent with hyper-phosphorylation of Rad9 (Figure 1A). A relevant fraction of Rad9 was found associated to chromatin in the absence of DNA damage, both in G1- and in M-arrested cells, confirming previous observations [22]. Control experiments were routinely performed to verify the distribution of standard protein markers in the soluble and

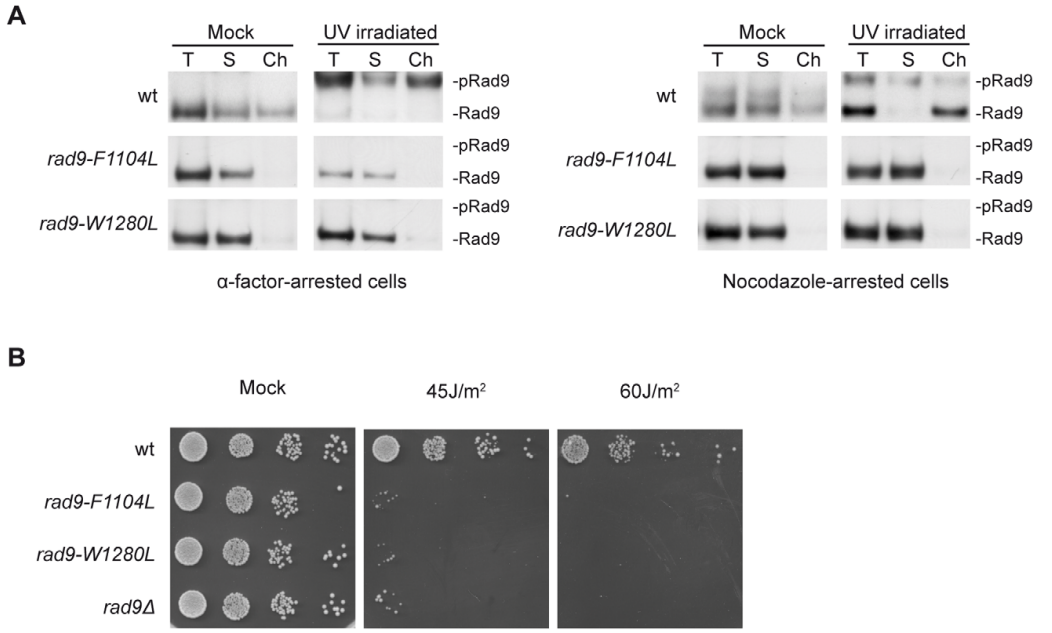

Figure 1. Rad9 chromatin binding requires an intact BRCT domains in UV–treated and in unperturbed conditions. (A) wt (K699), *rad9-F1104L* (YNOV15), *rad9-W1280L* (YNOV31) strains were arrested in G1 with α-factor or in M with nocodazole and either mock or UV irradiated (75 J/m^2). 10 min after irradiation, samples were collected and analyzed in their total (T), soluble (S) and chromatin-enriched (Ch) fractions. Blots were probed with anti-Rad9 antibodies and, after staining, the blots were cut to eliminate the Rad9-unrelated protein species migrating adjacent to the hyper-phosphorylated Rad9 isoform (Figure S1A). The positions of Rad9 and its hyper-phosphorylated isoform (pRad9) are indicated. (B) The same yeast strains analyzed in A and a *rad9Δ* strain (YMAG88) were grown overnight to log phase and serial dilutions were spotted onto YPD plates, which were then irradiated at the indicated UV doses and incubated for 3 days.
doi:10.1371/journal.pgen.1001047.g001

chromatin fractions (Figure S1B). In various experiments we consistently found that the ratio of hyper- to hypo-phosphorylated Rad9 was approximately constant in both the soluble and chromatin fractions in G1 cells. Interestingly, in M phase cells, hyper-phosphorylated Rad9 was mostly present in the soluble fraction, while chromatin was enriched in the hypo-phosphorylated form (Western blot quantitation are shown in Figure S1C). As shown in Figure 1A, any of the two BRCT mutations abolished Rad9 phosphorylation and recruitment to chromatin in G1- or M-arrested cells. As expected [21], *rad9-F1104L* and *rad9-W1280L* mutant cells were highly sensitive to UV treatments (Figure 1B).

These results indicate that BRCT domains influence not only Rad9 binding to chromatin by modulating its interaction with γH2A after DNA damage [22], but they also control Rad9 recruitment to chromatin in unperturbed conditions.

A heterologous dimerization domain restores Rad9 binding to chromatin in G1-arrested, but not M-arrested, cells

To further evaluate the relevance of Rad9-Rad9 interactions in chromatin binding, we generated a set of yeast strains in which the C-terminal region of Rad9, containing the BRCT motifs, was substituted with either a 13-MYC epitope or a GST tag (see Materials and Methods). The latter has been shown to act as a heterologous constitutive dimerization domain [28,52,53].

As shown in Figure 2A, the GST tag was capable of driving, albeit somewhat less efficiently, Rad9 chromatin binding in G1-arrested cells, both in the absence or presence of DNA damage. Importantly, Rad9ΔBRCT::GST recruitment to chromatin still occurs through its interaction with H3-K79me, as it was drastically reduced in a *dot1Δ* background, lacking the specific H3-K79 histone methyl-transferase. Rad9 dimerization through the GST tag also significantly recovered Rad9 hyper-phosphorylation after UV irradiation and full checkpoint function (Figure 2A and data not shown).

It must be underlined that addition of the GST tag to Rad9ΔBRCT, allowing Rad9 dimerization, reconstitutes chromatin binding even though Rad9ΔBRCT::GST lacks the BRCT tandem repeats and is, therefore, unable to interact with γH2A [22]. These authors suggested that, after DNA damage, Rad9 shifts from H3-K79me to phosphorylated H2A-S129, and this translocation would be deficient in *rad9ΔBRCT::GST* cells. As a consequence of its defective interaction with γH2A, binding of Rad9ΔBRCT::GST to chromatin is probably much less stable. This hypothesis may explain the finding that in the *rad9ΔBRCT::GST* strain the majority of phosphorylated Rad9 after UV irradiation in G1 is found in the soluble fraction (Figure 2A).

To further support the role of Rad9 dimerization in its chromatin binding in G1-arrested cells solely by inducing Rad9-Rad9 interactions, we tested the possibility to direct a Rad9ΔBRCT isoform to chromatin by adding to the truncated protein a FKBP

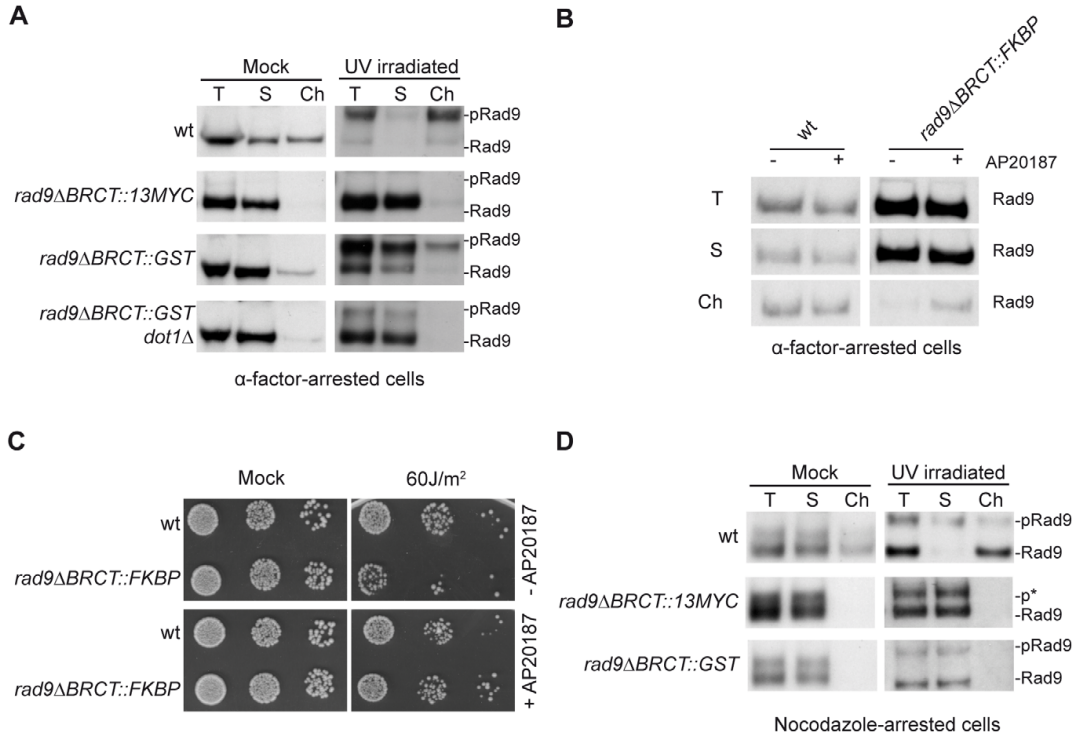

Figure 2. GST-driven Rad9 dimerization recovers its binding to chromatin in G1, but not in M phase. (A) wt (K699), *rad9ΔBRCT::13MYC* (YFL696/1b), *rad9ΔBRCT::GST* (YMAG74) and *rad9ΔBRCT::GST dot1Δ* (YFL773/2c) cells were arrested in G1 with α-factor and either mock or UV irradiated (75 J/m^2). After 10 min, samples were collected and analyzed in their total (T), soluble (S) and chromatin-enriched (Ch) fractions. Blots were probed with anti Rad9 antibodies as in the legend to Figure 1A. (B) wt (K699) and *rad9ΔBRCT::FKBP* (YFL901) cells were incubated for 6 h in the presence or in the absence of the dimerization-inducing molecule AP20187, blocked in G1 with α-factor and analyzed in their total (T), soluble (S) and chromatin-enriched (Ch) fractions. Blots were probed with anti Rad9 antibodies. (C) The same strains as in B were grown overnight to log phase and incubated for 6 h in the presence or in the absence of the dimerization-inducing molecule AP20187. Serial dilutions were spotted onto YPD plates, which were then irradiated at the indicated UV doses and incubated for 3 days. (D) Western blot analysis of the total, soluble and chromatin-enriched fractions from wt (K699), *rad9ΔBRCT::13MYC* (YFL696/1b) and *rad9ΔBRCT::GST* (YMAG74) cells arrested in M phase and either mock or UV irradiated (75 J/m^2). In all panels, the positions of Rad9 and its hyper-phosphorylated isoform (pRad9) are indicated. p* marks a partially phosphorylated Rad9 species.

doi:10.1371/journal.pgen.1001047.g002

tag, which can dimerize only in the presence of the small inducing molecule AP20187 [54]. Indeed, the presence of the FKBP tag partially rescued Rad9 chromatin binding in G1-arrested cells, but only in the presence of inducing AP20187 (Figure 2B). Importantly, addition of the dimerization inducing molecule fully recovered the UV sensitivity of *rad9DBRCT* cells (Figure 2C).

Contrary to our observations in G1-arrested cells, the heterologous GST dimerization domain did not rescue Rad9 binding to chromatin in nocodazole-arrested cells, although it restored checkpoint activation after DNA damage (Figure 2D, Figure 3A). Rad9 missing the BRCT domains only exhibits partial phosphorylation; this form can be distinguished from the hyper-phosphorylated isoform due to different electrophoretic mobility and its incapacity to activate Rad53 (see Figure 3A).

Altogether, the findings reported above indicate that dimerization is required for Rad9 to bind H3-K79me in G1-arrested cells, both with and without an exogenous DNA damaging agent. However, this is not the case in M phase-arrested cells, where GST-directed Rad9 dimerization partially recovers genotoxin-induced Rad9 hyper-phosphorylation, but fails to rescue its binding to chromatin. This may suggest that, at least in M phase, Rad9 chromatin binding is not directly linked to Rad9 hyper-phosphorylation.

GST-driven Rad9 dimerization rescues checkpoint activation and UV–sensitivity, despite undetectable chromatin binding

Although the addition of a heterologous dimerization domain to truncated Rad9ΔBRCT was not able to allow Rad9 chromatin binding in M phase-arrested cells, it rescues Rad53 activation after UV irradiation. In fact, as shown in Figure 3A, the phosphorylation state of the effector checkpoint kinase, Rad53, was found to be very different after UV-irradiation of *rad9ΔBRCT::GST* or *rad9ΔBRCT::13MYC* cells arrested with nocodazole. The hyper-phosphorylated form of Rad53 is absent in UV treated *rad9ΔBRCT::13MYC* cells, while it is clearly detectable in *rad9ΔBRCT::GST* cells. Although the extent of

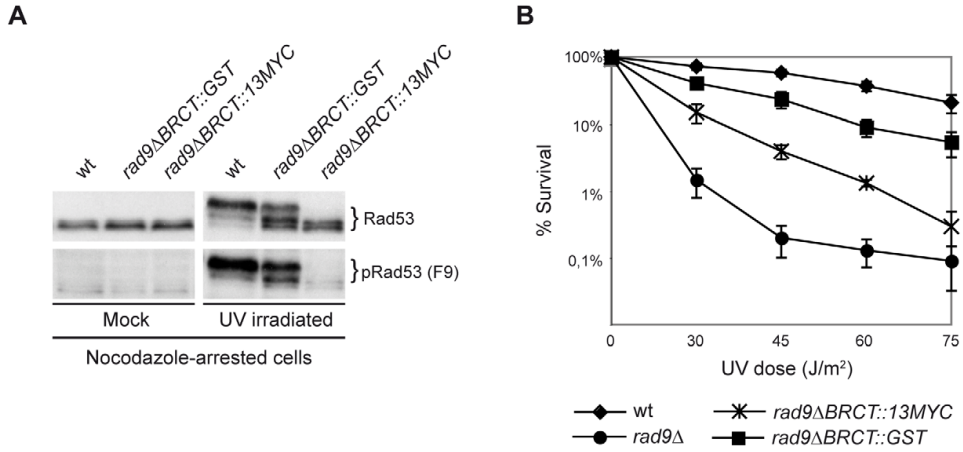

Figure 3. GST-driven Rad9 dimerization allows M checkpoint function regardless of Rad9 chromatin binding. (A) wt (K699), *rad9ΔBRCT::13MYC* (YFL696/1b), *rad9ΔBRCT::GST* (YMAG74) cells were cultured to mid-log phase, arrested in M with nocodazole, and either mock or UV irradiated (75 J/m^2); 10 min after irradiation, Rad53 phosphorylation was analyzed by SDS-PAGE and Western blotting with polyclonal Rad53 antibodies and with the F9 monoclonal antibody (Mab) recognizing only the hyper-phosphorylated active form of Rad53 to monitor checkpoint activation. (B) The same cells analyzed in A and a *rad9Δ* control strain (YMAG88) were cultured overnight, diluted and plated on YPD plates, which were irradiated with the indicated UV doses. Cell survival was assayed by determining the number of colonies grown on plates after 2 days; error bars were obtained from 3 independent experiments.
doi:10.1371/journal.pgen.1001047.g003

Rad53 phosphorylation was reduced in *rad9ΔBRCT::GST* relative to wild-type cells, the presence of the heterologous GST dimerization domain recovers the Rad9 checkpoint function, as confirmed by a direct checkpoint assay (data not shown). This conclusion is also supported by the observation that addition of the GST tag significantly rescued, although not completely, the UV sensitivity of the *rad9ΔBRCT::13MYC* strain (Figure 3B), and these findings are in agreement with previous experiments in *S.pombe* [28].

Thus far our data indicate that dimerization of Rad9 directed by an heterologous domain confers activation of the DNA damage checkpoint cascade, as well as significant resistance to UV in M phase-arrested cells, despite undetectable binding of Rad9 to chromatin (see Figure 2D).

Checkpoint activation in M phase requires CDK1 activity and is driven by Rad9–Dpb11 interaction

We have recently demonstrated that in the M phase of the cell cycle, full activation of the DNA damage checkpoint in response to various genotoxic stress is dependent upon Dpb11 [50]. Our data suggested that Dpb11 facilitates the recruitment of Rad9 proximally to DNA lesions through a mechanism independent of histone modifications. Indeed, as shown in Figure 4A, checkpoint activation after UV irradiation of nocodazole-arrested cells is only partially affected either in *dot1Δ* or in *dpb11ΔCT* cells. On the other hand, *dot1Δ dpb11ΔCT* double mutant cells are dramatically deficient in Rad53 phosphorylation since both the histone-dependent and histone-independent pathways for checkpoint activation are not functional. This finding can be interpreted by hypothesizing that when Rad9 cannot bind to chromatin via histone marks, Dpb11 may act as a platform for Rad9 recruitment in a histone-independent manner. Moreover, because the Dpb11-dependent pathway is particularly relevant in the G2 to M phases of the cell cycle [50], it was tempting to hypothesize that the proposed interaction between Rad9 and Dpb11 might be regulated by cell cycle-dependent control mechanisms [55]. Initially, we monitored this interaction using two-hybrid analysis performed at different cell cycle stages (see Materials and Methods). As shown in Figure 4B, a strong Rad9-Dpb11 interaction was observed in nocodazole-arrested cells. Several independent two-hybrid experiments showed that Rad9-Dpb11 interaction was more evident in M- rather than in G1-arrested cells. Experiments performed with a bait and a prey already known to interact by two-hybrid, indicate that the M/G1 ratio of Rad9-Dpb11 interaction was significantly higher than that found in the controls, suggesting a cell cycle-specific effect (Figure S2A). The Rad9-Dpb11 interaction was further confirmed biochemically (see below).

Since the interaction between Rad9 and Dpb11 appears to be induced in M phase, we reasoned that the Dpb11-dependent branch of the DNA damage checkpoint in M phase might be related to the increasing level of CDK1 kinase activity as cells move through the S, G2 and M phases of the cell cycle. To address this issue, we took advantage of the *cdc28-as1* mutant (in which only the Cdc28 kinase is specifically sensitive to bulky ATP analogues, such as 1NMPP1 [56]) to conditionally inactivate CDK1 in nocodazole-treated cells. Cdc28 kinase activity was inhibited or not with 1NMPP1 in nocodazole arrested cells and mitotic cells were then mock- or UV irradiated to induce DNA damage. Western blot analysis of Rad53 revealed that CDK1 inhibition abolished phosphorylation of Rad53 in the absence of the histone-dependent pathway, while no effect was observed in *DOT1* cells (Figure 4C). A similar experiment was performed by tethering checkpoint factors to DNA in the absence of damage [57]. The difference between our result and that reported by Bonilla, may be explained if, in their experimental conditions, without the addition of genotoxic agents, checkpoint activation is independent upon the Dpb11 branch.

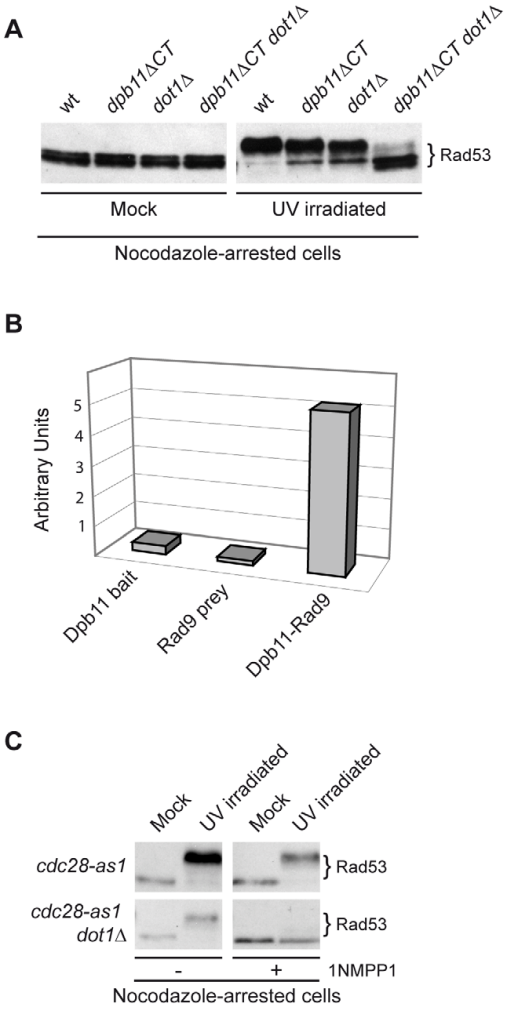

Figure 4. A cell cycle–dependent interaction between Dpb11 and Rad9 may regulate the Dpb11-dependent pathway. (A) wt (YMAG149/7B), *dpb11ΔCT* (YMAG145/20C), *dot1Δ* (YMAG150/4A) and *dpb11ΔCT dot1Δ* (YMAG148) strains were arrested in M with nocodazole and mock or UV irradiated (75 J/m^2). 10 min after irradiation, samples were taken and protein extracts were separated by SDS-PAGE. Blots were analyzed with anti Rad53 antibodies. (B) EGY42 cells, containing the pSH18-34 β-galactosidase reporter plasmid, were transformed with the Rad9 prey plasmid pMAG11.1 (pJG4-5-*RAD9*) and/or with the Dpb11 bait plasmid pFP15 (pEG202-*DPB11*). Strains were cultured overnight in -His, -Trp, -Ura medium plus raffinose and arrested in M phase by nocodazole treatment. Galactose was then added to the medium to induce bait expression. A modified version of ONPG yeast two-hybrid assay was used to determine the β-galactosidase activity in each strain, expressed in relative units. (C) *cdc28-as1* (JAU01) and *cdc28-as1 dot1Δ* (YNOV4) strains were arrested in M with nocodazole and, after incubation for 2 h in the absence or in the presence of 5 μM 1NMPP1, were either mock or UV irradiated (75 J/m^2). After 10 min, samples were collected and protein extracts were separated by SDS-PAGE. Blots were analyzed with anti-Rad53 antibodies.
doi:10.1371/journal.pgen.1001047.g004

Altogether, our results indicate that CDK1 activity is required for the function of the histone-independent branch necessary for Rad53 phosphorylation in cells arrested in mitosis.

CDK1-dependent phosphorylation of serine 11 of Rad9 modulates the Dpb11-dependent branch in M phase cells

Rad9 contains 20 potential (SP or TP) target sites for CDK-dependent phosphorylation, 9 of which conform to the canonical CDK phosphorylation site (S/T-P-x-K/R) (Figure S2B). We hypothesized that Rad9 could be a relevant CDK1 target in the histone-independent branch of the DNA damage checkpoint in M phase cells. Initially, we tested a *rad9ΔNT* mutant strain, in which the first 231 amino acids, including 9 S/T-P sites, of Rad9 are missing (Materials and Methods and [58]). As shown in Figure 5A, Rad53 phosphorylation was partially defective in both *dot1D* and *rad9DNT* mutants and essentially abolished in a *rad9ΔNT dot1Δ* double mutant strain.

All 9 potential Cdc28 phosphorylation sites in the Rad9 N-terminal region were individually mutagenized and different mutant combinations tested (Materials and Methods and data not shown). *rad9-S11A* cells displayed a detectable defect in cell cycle-regulated Rad9 phosphorylation (Figure S2C). Moreover, the *rad9-S11A* mutation recapitulates the phenotype we observed in *rad9ΔNT* cells, namely, severe loss of DNA damage-dependent Rad53 phosphorylation when combined with *dot1D* (Figure 5B). Consistently, the *rad9-S11A* mutation alone did not confer a strong sensitivity to UV irradiation (Figure 5C), while a *rad9-S11A dot1Δ* double mutant strain was synthetically sensitive to genotoxic treatment. On the other hand, a *rad9-S11A dpb11ΔCT* double mutant strain did not exhibit an increased sensitivity to UV irradiation when compared to strains harboring the single mutations, indicating that Dpb11 and Rad9-S11 phosphorylation act in the same pathway (data not shown). Phosphorylation of Rad9S11 has been reported *in vivo* [59]. In order to verify the relevance of S11 phosphorylation in our experimental conditions, we reverted the S11A mutation to Thr, another phosphorylatable residue. Figure 5D shows that Rad9 carrying a Thr at position 11 rescues the phenotype imparted by the S11A mutation, since checkpoint activation in the *rad9-S11T dot1Δ* strain is identical to that found in *dot1Δ* cells.

Interestingly, Rad9-Dpb11 interaction by two-hybrid analysis was reduced when the Rad9NT isoform, lacking the 9 potential CDK1 phosphorylation sites, was used as a prey in a wild-type background, or when Cdc28 activity was inhibited by 1NMPP1 addition in the *cdc28-as1* strain (Figure 6A). The *in vivo* interaction between Rad9 and Dpb11 was also confirmed by co-immunoprecipitation of the endogenous proteins after genotoxic treatment. As shown in Figure 6B, immunoprecipitation of MYC-tagged Dpb11 recovers the hyper-phosphorylated isoform of Rad9, and this interaction is virtually lost in the *rad9-S11A* mutant strain (Figure 6C). We also noticed that the Rad9-S11A mutant protein has slighlty less gel-mobility than its wild type counterpart, as shown in Figure 6C. This observation can be explained by either a mild defect in Mec1/Tel1-dependent hyperphosphorylation of the Rad9-S11A protein, due to the loss of Rad9-Dpb11 interaction, or a direct effect of the S11A mutation which, affecting CDK1-dependent phosphorylation of Rad9, may directly modify its migration in SDS PAGE.

Altogether, the above findings indicate that the Ser11 CDK1-consensus site on Rad9 is a relevant target to modulate Rad9-Dpb11 interaction and the CDK1-dependent checkpoint response in M phase cells.

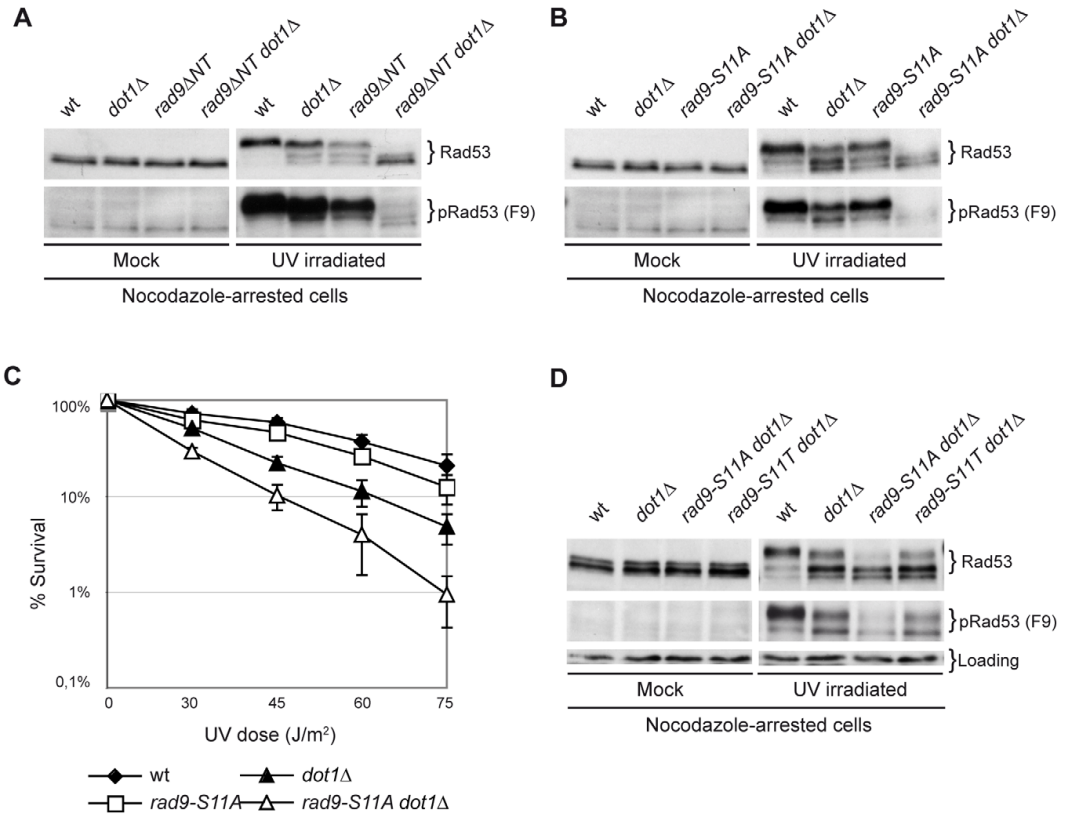

Figure 5. Phosphorylation of Rad9S11 by CDK1 is required for the establishment of an effective UV response in the absence of Dot1. (A) wt (K699), *dot1Δ* (YFL234), *rad9ΔNT* (DLY2236) and *rad9ΔNT dot1Δ* (YFP91) strains were arrested with nocodazole and either mock or UV irradiated (75 J/m^2). After 10 min samples were collected and protein extracts were separated by SDS-PAGE. Blots were analyzed with anti-Rad53 or with the F9 Mab to monitor checkpoint activation. (B) wt (K699), *dot1Δ* (YFL234), *rad9-S11A* (YMAG162) and *rad9-S11A dot1Δ* (YMAG164) strains were arrested in M, irradiated and Rad53 was detected by Western blotting as describe in panel A. (C) The same strains analyzed in B were cultured overnight, diluted and plated on YPD plates, which were irradiated with the indicated UV doses. Cell survival was assayed as described in the legend of Figure 3. (D) wt (K699), *dot1Δ* (YFL234), *rad9-S11A dot1Δ* (YMAG164) and *rad9-S11T dot1Δ* (YNOV52) strains were arrested with nocodazole and either mock or UV irradiated (75 J/m^2). After 10 min samples were collected and protein extracts were separated by SDS-PAGE. Blots were analyzed with anti-Rad53 or with the F9 Mab to monitor checkpoint activation.
doi:10.1371/journal.pgen.1001047.g005

The Dpb11-dependent branch in M phase modulates checkpoint activation in a chromatin-independent manner

To gain further insights into the mechanisms involving Rad9 and the Dpb11-dependent branch of the DNA damage checkpoint operating in nocodazole-arrested cultures, cell extracts were fractionated into soluble and chromatin fractions. Specifically, we monitored Rad9 chromatin binding and Rad53 phosphorylation in strains harbouring defects in the different branches known to regulate Rad9 checkpoint functions during M phase.

As shown in Figure 7, following DNA damage, the Dpb11 C-terminal region carrying the BRCT domain does not appear to be required for Rad9 binding to chromatin, as *dpb11DCT* cells behave as wild type. However, as expected, Rad9 chromatin recruitment is defective in *dot1Δ* and *H2A-S129A* mutant cells, as binding of Rad9 is dependent upon H3-K79me and γH2A, via its Tudor and BRCT domains respectively [22,34,60]. Checkpoint activation, as determined by Rad53 phosphorylation, was abolished in any double or triple mutant combinations carrying the *dpb11ΔCT* mutation (Figure 7). Intriguingly, even when detectable Rad9 binding to chromatin is abrogated (as in the single *dot1Δ* and *H2A-S129A* or in the double *dot1Δ H2A-S129A* mutant strains) Rad53 can be fully phosphorylated. Similar genetic dependencies were found when the various single, double and triple mutant strains were tested for checkpoint activation in response to zeocin treatment, which is known to cause DSBs (Figure S3 and data not shown).

Dpb11 is responsible for checkpoint activation in M phase cells when the Rad9 BRCT domains are replaced with a heterologous dimerization domain

We have determined (Figure 3A) that in nocodazole-arrested cells defective checkpoint activation due to the absence of the Rad9 BRCT domain can be partially rescued by adding the GST

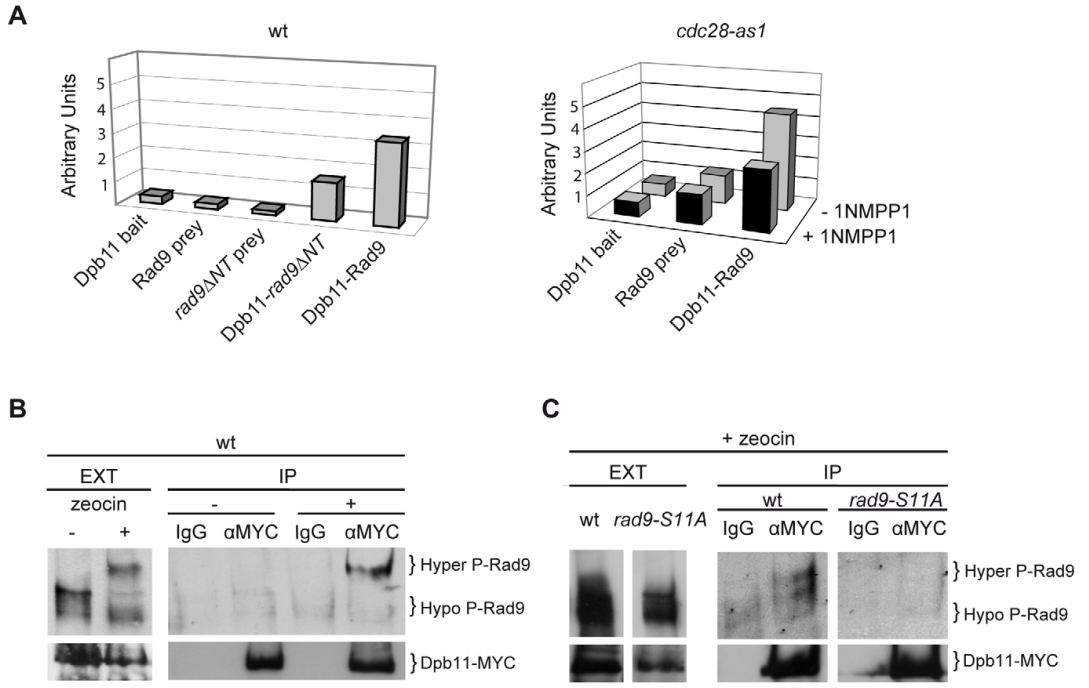

Figure 6. CDK1-dependent phosphorylation of S11-Rad9 modulates Rad9-Dpb11 interaction. (A) Two-hybrid interaction between Dpb11 and Rad9 was tested in a wt (K699) (left) or in a *cdc28-as1* (JAU01) (right) genetic background with the indicated bait and prey plasmids. Where specified 5 μM 1NMPP1 was added to the media for 1 h before bait induction and extracts preparation. (B) The *Dpb11-myc* (YFP38) strain was arrested with nocodazole and either mock treated or treated with 150 μg/ml of zeocin for 30 min. Whole cell protein extract was prepared and tagged Dpb11-MYC was immunoprecipitated either with anti-MYC antibodies or unspecific mouse IgG as described in Materials and Methods. The presence of Rad9 in the IPs was detected by Western blot analysis of the immunoprecipitates with specific anti-Rad9 antibodies. (C) Immunoprecipitations with anti-MYC antibodies were performed on extracts from nocodazole arrested cells, treated with 150 μg/ml of zeocin for 30 min, expressing Dpb11-MYC in a *RAD9* (YFP38) or *rad9S11A* (YMAG281) background. The presence of Rad9 was detected by Western blot analysis of the immunoprecipitates with specific anti-Rad9 antibodies. Lower exposure of the crude extracts lanes are shown to allow visualization of both Rad9 and Dpb11 specific bands.
doi:10.1371/journal.pgen.1001047.g006

dimerization domain. Moreover, we demonstrated that the M phase-specific DNA damage checkpoint contains a pathway based on Rad9-Dpb11 interactions and modulated via phosphorylation of the Ser11 residue of Rad9 by CDK1 (Figure 4, Figure 5, and Figure 6). As a consequence, we tested whether, in nocodazole-arrested cells, checkpoint activation supported by the heterologous dimerization motif in the *rad9ΔBRCT::GST* mutant strain was dependent upon Dpb11. To address this question, we introduced the *S11A* point mutation in the *rad9ΔBRCT::GST* strain (*rad9-S11AΔBRCT::GST*). Whilst either single mutant strain was only partially defective in Rad53 phosphorylation, in *rad9-S11AΔBRCT::GST* cells, checkpoint activation was severely impaired (Figure 8A). This result indicates that in *rad9ΔBRCT::GST* cells residual checkpoint activation depends upon an active Dpb11 branch acting through a potential CDK1 site (S11) in the amino terminus of Rad9. As expected, *rad9-S11ADBRCT::GST* cells, in which the sole Rad9 expressed contains both the point mutation and the domain swap, are more sensitive to UV irradiation than either single mutant (Figure 8B).

In conclusion, our data are consistent with the hypothesis that Rad9 plays two independent roles in checkpoint activation: the first mediated by its dimerization and binding to modified histones, the second, which involves its phosphorylation by CDK1 and interaction with Dpb11 (Figure 9).

Discussion

RAD9 was the first DNA damage checkpoint gene identified in yeast [18]; however, the precise molecular details regarding the role of the corresponding gene product, its function and regulation remain far from being fully understood. In budding yeast, Rad9 seems to act as an adaptor protein in the signal transduction checkpoint cascade, mediating the transmission of the signal from the apical PIKKs to the main primary transducer kinase, Rad53 [27,61]. Rad9 phosphorylation, mediated by Mec1, is an early event in the signal transduction cascade and this modification in G1 is mainly influenced by histone H3 methylation [22,33,60,62]. In M phase, Rad9 phosphorylation also requires Dpb11, whose role as an alternative scaffold for Rad9 activation has been unveiled only recently [50]. The dynamics of Rad9 recruitment at various cell cycle stages and the genetic dependencies controlling Rad9 interaction with DNA/chromatin and other proteins are largely unknown.

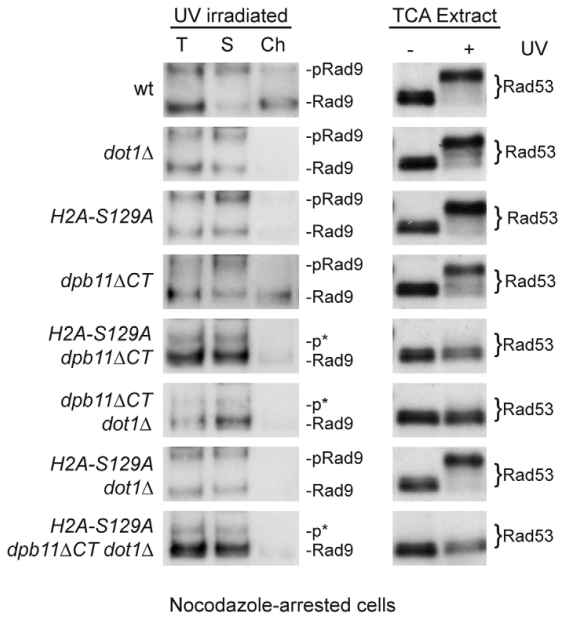

Figure 7. The Dpb11-dependent pathway in M phase modulates Rad53 activation in a chromatin-independent manner. wt (YMAG149/7B), *H2A-S129A* (YMAG168), *dpb11ΔCT* (YMAG145/20C), *dot1Δ* (YMAG150/4A), *H2A-S129A dpb11ΔCT* (YMAG155), *H2A-S129A dot1Δ* (YMAG170), *dpb11ΔCT dot1Δ* (YMAG148) and *H2A-S129A dpb11ΔCT dot1Δ* (YMAG157) strains were arrested in M with nocodazole and UV irradiated (75 J/m^2). After 10 min, samples were collected and analyzed in their total (T), soluble (S) and chromatin-enriched (Ch) fractions; blots were probed with anti-Rad9 antibodies (left panel). Protein extracts were also prepared from mock and UV treated samples and analyzed by SDS-PAGE and Western blotting with anti-Rad53 antibodies to monitor checkpoint activation (right panel). The positions of Rad9 and its hyper-phosphorylated isoform (pRad9) are indicated. p* marks partially phosphorylated Rad9 species.
doi:10.1371/journal.pgen.1001047.g007

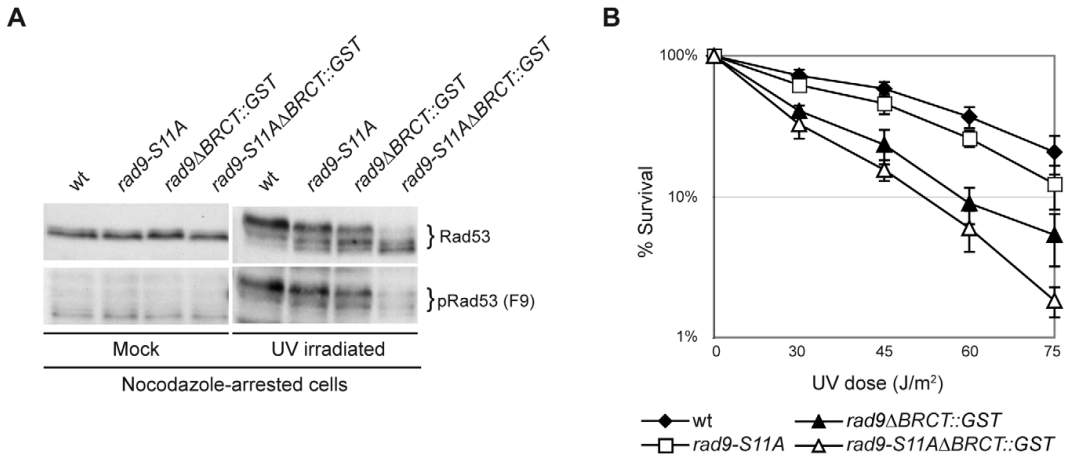

Figure 8. Partial checkpoint activation after forced Rad9 dimerization in M phase acts through the Dpb11-dependent checkpoint pathway. (A) wt (K699), *rad9-S11A* (YMAG162), *rad9ΔBRCT::GST* (YMAG74) and *rad9-S11AΔBRCT::GST* (YFL1177) strains were arrested with nocodazole and mock or UV irradiated (75 J/m^2). After 10 min, samples were collected and protein extracts were separated by SDS-PAGE. Blots were analyzed either with anti-Rad53 antibodies or with the F9 Mab to monitor checkpoint activation. (B) UV survival assay. The same strains as in A were cultured overnight and then diluted and plated on YPD plates, which were irradiated with the indicated UV doses. Cell survival was assayed as described in the legend to Figure 3.
doi:10.1371/journal.pgen.1001047.g008

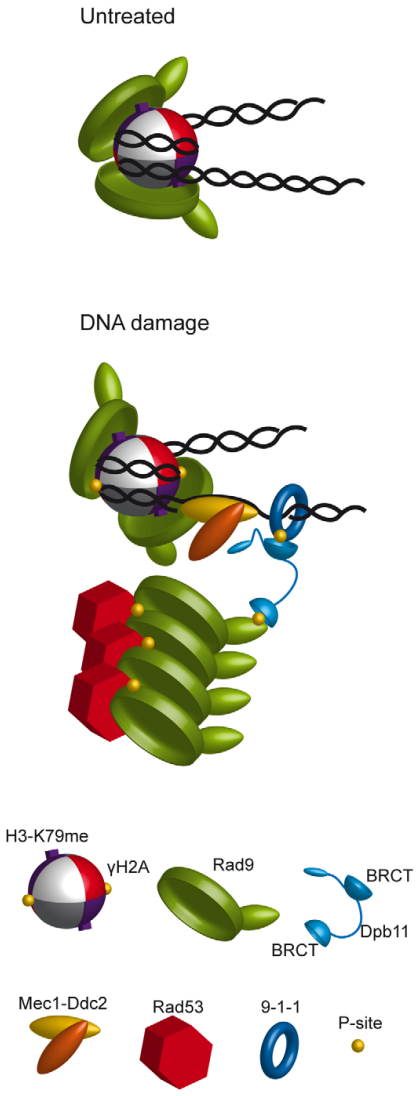

Figure 9. Possible model of the dynamics of Rad9 chromatin binding and its interaction with Dpb11 to modulate checkpoint activation in M phase. Under untreated conditions, Rad9 is chromatin bound through the interaction of its Tudor domain with H3-K79me and its BRCT-mediated dimerization. After DNA damage, activated Rad9 may change its conformation, interacting also with γ-H2A. In M-phase an alternative means of Rad9 recruitment near DNA lesions involves its interaction with Dpb11. This factor is brought near the Mec1-Ddc2 complex via its interaction with the 9-1-1 clamp, and it binds the phosphorylated N-terminal portion of Rad9 leading to full checkpoint activation.
doi:10.1371/journal.pgen.1001047.g009

Here, we show that a significant proportion of Rad9 is already chromatin-bound in unperturbed conditions throughout the cell cycle, confirming previous suggestions [22] and supporting our earlier model [14]. According to the current view, Rad9-chromatin association is controlled by interaction between its Tudor domain and H3-K79me. Constitutive, dynamic recruitment of Rad9 to chromatin may facilitate the efficiency and speed of the Rad9-dependent response to genotoxins. After DNA damage, Rad9 binding to chromatin is further strengthened through its BRCT domain, which is required to productively interact with γH2A [22,23]. In this study we found that the BRCT domain of Rad9, in addition to promoting interaction with γH2A, has a more general function in modulating Rad9 recruitment. In fact, the *rad9-F1104L* and *rad9-W1280L* mutations, affecting the folding of the whole BRCT domain [21], alter binding to chromatin also in the absence of any genotoxic treatment. The observation that *rad9-K1088M* cells are defective in Rad9 chromatin recruitment only after γ-irradiation may be explained if such mutation only prevents Rad9-γH2A interaction [22].

In G1 cells, Rad9 binding to chromatin can be achieved by substituting the BRCT repeats with a heterologous dimerization domain; such recruitment requires the activity of Dot1 histone methyl-transferase, indicating that BRCT-mediated dimerization may be a pre-requisite for constitutive interaction between the Rad9 Tudor domain and H3-K79me. Given the symmetrical structure of the histone octamer within the nucleosome core, dimerization might facilitate the correct orientation and positioning of two Rad9 molecules on the nucleosome, allowing productive interactions with modified histones (Figure 9). Such hypothesis is supported by structural modeling of a dimeric *S. pombe* Crb2 complex on a single nucleosome, where all the interactions with H4-K20me and γH2A are satisfied without changing the conformation of the histone core [31].

It is worth noting that dimerization forced by replacement of the Rad9 BRCT domains with the heterologous GST tag only restores Rad9 binding to chromatin in G1-, and not in M-arrested cells. In fact, in cells arrested with nocodazole, we observed that GST-induced dimerization can rescue Rad9 hyper-phosphorylation and DNA damage checkpoint activation, but not its stable recruitment to chromatin. It is possible that in mitosis cell cycle-dependent phosphorylation of Rad9 may interfere with the chromatin association of this artificial Rad9 dimer. Alternatively, in nocodazole-arrested cells the Rad9 BRCT motifs may play additional roles in modulating Rad9-chromatin interactions.

Several findings indicate that the cellular response to DNA damage, including the repair mechanisms themselves, are regulated differently in distinct cell cycle stages. Multiple layers of cell cycle regulation may modulate the recruitment of critical checkpoint and repair factors to damaged DNA, as well as facilitate their reciprocal cross-talk [63–67]. We have previously shown that Dpb11 is essential for full DNA damage checkpoint activation in M-arrested cells [50]. Dpb11 is held in proximity to damaged DNA through its interaction with phosphorylated 9-1-1 complex, leading to Mec1-dependent Rad9 phosphorylation. Taking advantage of the *cdc28-as1* mutation, which allows conditional turn off of CDK1 kinase activity, we have demonstrated that CDK1, targeting Rad9, is required for the function of the Dpb11-dependent branch of the checkpoint response. Indeed, yeast cells carrying a truncated Rad9 version lacking 9 putative Cdc28 phosphorylation sites in the N-terminal region, are checkpoint-defective in M phase, in the absence of the histone-dependent branch. The Ser11 residue in the Rad9 N-terminal region is the most relevant Cdc28 target site, since a *rad9-S11A* mutation recapitulates the phenotypes observed in *rad9ΔNT* cells.

By two-hybrid analysis we showed that Rad9 and Dpb11 specifically interact in M-phase arrested cells, even in the absence of DNA damage, and this interaction is stimulated by CDK1-dependent Rad9 phosphorylation. Co-immunoprecipitation exper-

iments confirmed that Rad9-Dpb11 interaction requires phosphorylation of Rad9-S11 and revealed that it depends upon genotoxic treatment, although we cannot exclude a weak/transient interaction in untreated conditions. This finding can be explained if activation of Mec1 by DNA damage facilitates or controls this interaction, e.g phosphorylating Dpb11 [50], exposing phospho-S11 or stimulating Rad9-S11 modification by CDK1. The overexpression conditions typical of the two hybrid system can easily explain why a weak interaction can be detected also in the absence of DNA damage. Interestingly, the functional interactions between Dpb11 and Rad9 in budding yeast are reminiscent of similar findings in the distantly related *S. pombe*, where histone-independent checkpoint activation is also modulated by CDK1 [37].

The Dpb11-dependent pathway does not require the histone modifications modulating Rad9 recruitment to chromatin. We found that a truncated C-terminal version of Dpb11 does not affect Rad9 recruitment to chromatin, which is instead abolished when the histone-dependent pathway is defective. Surprisingly, in a *dot1Δ H2A-S129A* double mutant strain checkpoint activation in M phase is virtually undistinguishable from that found in wild type cells, although Rad9 is not stably bound to chromatin. Only when the *dpb11ΔCT* mutation is combined with the *dot1Δ* or *H2A-S129A* mutation the checkpoint response is turned off. The working model presented in Figure 9, suggests that Dpb11 may act in M-phase as an alternative means of Rad9 recruitment. Dpb11 is located close to sites of DNA damage through its interaction with the Mec1-phosphorylated 9-1-1 complex; DNA damage leads to Mec1-dependent phosphorylation of Dpb11 [50], which interacts with S11-phosphorylated Rad9 (Figure 9). This Dpb11-dependent localization of Rad9 to sites of DNA damage allows rapid Rad9 hyper-phosphorylation by PIKKs, as suggested by the observation that the interaction between Rad9 and Dpb11 is induced by genotoxic agents and hyper-phosphorylated Rad9 is enriched in the Dpb11-bound population. Subsequently, Rad53 recruitment via its FHA domains leads to full activation of the checkpoint response. Unlike Rad9 bound via histone marks, Rad9 complexed with Dpb11 does not appear to be tightly linked to chromatin, explaining why the Dpb11-dependent branch for checkpoint activation seems to act in a chromatin-independent manner. However, we cannot rule out the possibility that the Rad9-Dpb11 complex can transiently or weakly bind to chromatin.

The model suggested here is in agreement with similar findings in the distantly related *S.pombe* fission yeast [37] as well as with recent *in vitro* data describing Dpb11 role in checkpoint activation [68], suggesting that the proposed mechanism can be extended to other eukaryotic organisms.

Materials and Methods

Strains and plasmids

All of the strains used in this work are derivatives of W303 [*MAT*a *ade2-1 trp1-1 can1-100 leu2-3,12 his3-11,15 ura3 rad5-535*]; only strains YFP91 and DLY2236 (provided by D. Lydall), are *RAD5*$^{+}$. All the strains used in this study are listed in Table S1 and further information regarding strains and plasmids is available upon request.

Plasmids pMAG11.1 and pFP15 are, respectively, the Rad9 prey and Dpb11 bait plasmids used for the yeast two-hybrid analysis. They were obtained by amplifying the relevant coding sequences from genomic DNA and by ligating the resulting fragments into pJG4-5 and pEG202 [69], respectively.

The plasmid pMAG9, which encodes the Rad9ΔNT prey, was obtained cloning the *rad9ΔNT* sequence, amplified from the yeast strain DLY2236, into pJG4-5.

Gene deletions were obtained by PCR-mediated gene replacement [70].

The YNOV15 (*rad9-F1140L*) and YNOV31 (*rad9-W1280L*) strains were obtained from YFL871. The *kanMX4* and *KlURA3* CORE cassettes, amplified from pCORE [71], were integrated in a K699 strain at position 1941 of the *RAD9* gene. Subsequently, the CORE cassette was replaced with the C-terminus of the *rad9-F1104L* or *rad9-W1280L* alleles, amplified respectively from pFL75.5 or pFL69.1, thus restoring the full-length *RAD9* open reading frame bearing the intended mutation. *RAD9* site-specific mutations on plasmids pFL75.5 and pFL69.1 were obtained by PCR with mutagenic oligonucleotides on the pFL36.1 plasmid [50]. Recombination events were selected on 5-fluoroorotic acid plates, and the strains were verified by sequencing.

The *rad9ΔBRCT::13MYC* and the *rad9ΔBRCT::GST* mutant alleles were obtained by introducing the 13-MYC or GST tags at the 984 aa, using the one-step PCR method [70], thus eliminating the whole Rad9 BRCT domain.

The *cdc28-as1* mutant allele was obtained by ClaI-directed integration of plasmid pVF6 [72] at the *CDC28* locus into the desired background. Plasmid pop-out events were selected on 5-fluoroorotic acid plates, and the presence of the *cdc28-as1* mutation was verified by assessing sensitivity to 1NMPP1 on plate.

Strains encoding the *rad9-S11A* mutant allele were obtained by MscI-directed integration of pRS306-NTRAD9^{cdk1} into the desired background. The transversion TCT-GCT causing the *rad9-S11A* mutation and the reversion GCT to ACT generating the *rad9-S11T* allele were produced by site- directed mutagenesis (Stratagene) of pGEMTeasyRAD9, containing a 2547 bp fragment from position -445 to position +2102 within the *RAD9* ORF. The 1.8 Kb BamHI-MscI fragment from the pGEMTeasyRAD9 vector was swapped with the equivalent fragment from an existing 6.3 Kb pRS306-NTRAD9 integrative vector, containing a BamHI-SpeI *RAD9* fragment from position −445 to position 1478 within the *RAD9* ORF and the presence of the mutation verified by sequencing. Plasmid pop-out events were selected on 5-fluoroorotic acid plates, and the *rad9-S11A* mutation was confirmed by PCR sequencing.

The *dpb11ΔCT* mutant allele was obtained by introducing a premature stop codon at the 583 aa and the *HPH* cassette after the codon with the one step PCR method previously described [73], thus mimicking the *dpb11-1* mutation [74].

Strain YFL921 was obtained by using the one-step PCR strategy described in Longtine 1998, using pFA6-*FKBP2x-13MYC-KanMX6*, as template. This plasmid was generated by cloning in PacI-linearized pFA6-*13MYC-KanMX6* the *FKBP2x* sequence amplified from pC4M-FV2E (ARGENT Regulated Homodimerization kit, ARIAD Pharmaceutical).

The yeast two hybrid was performed using the B42/lexA system with strain EGY42 (*MATa his3 ura3 trp1 6lexAOP-LEU2*; *lex- AOP-lacZ* reporter on plasmid pBH18-34) as the host strain [69].

Chromatin binding

To analyze chromatin binding of proteins, yeast extracts were prepared from G1- or M-arrested cells following published procedures [22].

Cell cycle blocks and DNA damage treatments

Cells were grown in YPD medium at 28°C (25°C in the experiments with strains harboring the *dpb11ΔCT* mutation) to a concentration of 6×10^6 cells/ml and arrested in G1 or M with α-factor (20 μg/ml) or nocodazole (20 μg/ml), respectively. 50 ml of cultures were centrifuged, resuspended in 500 μl of fresh YPD and plated on a Petri dish (14 cm diameter). Plates were quickly

irradiated with a Stratalinker at 75 J/m^2 and cells resuspended in 50 ml of YPD plus α-factor or nocodazole. A 25 ml sample was taken 10 min after the treatment and processed for protein extraction with trichloroacetic acid (TCA) [75]. For analysis of the double-strand breaks (DSBs) checkpoint response, cells arrested at the proper cell cycle phase were treated with 150 μg/ml of zeocin. Samples were taken 45 min after treatment and processed for protein extraction.

FKBP dimerization

To analyze FKBP-driven (FK506 binding protein) dimerization, overnight cell cultures were diluted at a concentration of 1×10^6 cells/ml and treated for 6 h with 1 μM AP20187 (ARGENT Regulated Homodimerization kit, ARIAD Pharmaceutical). UV sensitivity assays or chromatin binding analysis were performed as described elsewhere in this section.

Inactivation of the Cdc28 kinase activity

Exponentially growing cells in a *cdc28-as1* background were harvested at a concentration of 4×10^6 cells/ml and blocked in M phase as described above. To selectively inhibit Cdc28 activity [56], the ATP analogue 1NMPP1 was then added to a concentration of 5 μM to half of the cultures; after 2 h of incubation at 28°C, cells were either mock- or UV-irradiated and protein extracts were prepared.

SDS-PAGE and western blotting

TCA protein extracts or chromatin binding samples were separated by sodium dodecyl sulfate-polyacrylamide gel electrophoresis (SDS-PAGE) in 10% acrylamide gels. For the analysis of Rad9 phosphorylation, NuPAGE Tris-acetate 3% to 8% gels were used following the manufacturer's instructions. Western blotting was performed with anti-Rad9 (D. Stern), anti-Rad53 (C. Santocanale), with anti-phosphorylated Rad53 F9 Mab antibodies [76] anti-ORC2 (Abcam) and anti-tubulin (ML. Carbone), using standard techniques.

UV–sensitivity assay

To assess cell survival after UV irradiation, serials dilutions of overnight cultures were spotted onto YPD plates, which were either irradiated with different UV doses or mock-treated. For survival curves, yeast strains were cultured overnight to exponentially growing phase. Cells were diluted and approximately 500 cells/plate were plated, and then either irradiated with various UV doses or mock-treated. After 3 days, the total number of colonies formed on each plate was counted.

Yeast two-hybrid analysis

Protein interaction between Rad9 and Dpb11 in the G1 and M phase of the cell cycle was assessed by measuring β-galactosidase activity with ortho-Nitrophenyl-β-galactoside (ONPG) assay. Briefly, cells expressing Rad9 bait and/or Dpb11 prey were cultured overnight in yeast synthetic media (-Ura, -His, -Trp) with 2% (w/v) raffinose to a concentration of 5×10^6 cells/ml. Cultures were centrifuged and cells resuspended in YP plus raffinose and arrested in G1 or M phases, as described above. Galactose to a 2% w/v final concentration was added to the medium to induce prey expression. A 15 ml sample was taken after 1 h of galactose induction, centrifuged and resuspended in 250 μl of breaking buffer (100 mM Tris HCl at pH 8.0, Glycerol 10%; DTT 1 mM, 1 tablet of complete Roche antiproteolytic cocktail. Cells were lysed by using a FastPrep cell disruptor; the optical density (OD) of protein extract at 600 nm was determined using the Bio-Rad protein assay reagent. 1 ml of Z buffer (60 mM Na_2HPO_4, 40 mM NaH_2PO_4, 10 mM KCl, 1 mM $MgSO_4$, and 50 mM β-mercaptoethanol at pH 7.0) plus ONPG 4 mg/ml was aliquoted in a small glass tube for each sample. 20 μl of protein extract was added to each tube and incubated at 37°C until a yellow color developed. The reaction was stopped by adding 400 ml of 1 M $NaCO_3$ and the OD at 420 nm of each sample was measured. β - Galactosidase activity was calculated by using the formula units $= 10^3$ $OD_{420}/(OD_{600}$ x reaction time in min).

Rad9-Dpb11-MYC immunoprecipitation

1.5 l cultures of strains YFP38 and YMAG281 expressing, respectively, the tagged Dpb11-MYC fusion protein under the control of the endogenous *DPB11* promoter in a wild-type or *rad9S11A* mutant background were grown in YPD medium at a cell density of 1×10^7 cells/ml. Cells were then arrested in M phase by addition of 10 μg/ml of nocodazole and were either mock treated or treated with 150 μg/ml of zeocin for 30 min. Cells were washed twice with pre-cooled ddH_2O and once in 2× lysis buffer (300 mM KCl, 100 mM Hepes (pH 7.5), 20% glycerol, 8 mM β-mercaptethanol, 2 mM EDTA, 0.1% Tween20, 0.01% NP-40). Resuspended cells were frozen as droplets in liquid nitrogen. Aliquots of frozen cells were manually ground in a mortar in liquid nitrogen. One volume of 2× lysis buffer, containing a protein inhibitor cocktail (2.8 μM leupeptin, 8 μM pepstatin A, 4 mM PMSF, 50 mM benzamidine, 25 μM antipain, 4 μM chymostatin in ethanol) and phosphatase inhibitors (2 mM sodium fluoride, 1.2 mM β-glycerophosphate, 0.04 mM sodium vanadate, 2 mM EGTA, 10 mM sodium pyrophosphate), was added. Cell extract was clarified by a low speed centrifugation followed by additional centrifugation for 1 h at 42.000 rpm in a Beckman Sw55Ti rotor. The clarified crude extract (Ext) was adjusted to 10 mg/ml in the various immunoprecipitation experiments. 1 ml of Ext was precleared by incubation with 40 μl of 50% (v/v beads/1× lysis buffer) Protein G slurry for 1 hour at 4°C on a rotating wheel. Precleared supernatants were incubated with either 20 μg of the anti-myc Mab 9E11 or 20 μg of unspecific mouse IgG. Samples were incubated for 2 h at 4°C on a rotating wheel and centrifuged at 14.000 rpm for 15 min at 4°C. 40 μl of 50% protein G slurry were added to the supernatants, incubated on a rotating wheel for 2 h at 4°C and recovered by centrifugation. Immunoprecipitated Dpb11-MYC samples were washed four times with 1 ml of lysis buffer containing protease and phosphatase inhibitors. Beads were finally resuspended in 40 μl of 3× Laemmli buffer (IP), boiled for 5 min and released proteins separated on 6.5% (80/1 acrylamide/bisacrylamide) SDS-PAGE gels. After blotting, Rad9 was visualized with the NLO5 Rad9 polyclonal antibody [13] or the 9E11 Mab (Abcam).

Supporting Information

Figure S1 (A) wt (K699) cells were arrested in G1 with α-factor and either mock or UV irradiated (75 J/m^2). 10 min after irradiation, samples were collected and analyzed in their total (T), soluble (S) and chromatin-enriched (Ch) fractions. Blots were probed with anti Rad9 polyclonal antibodies. After UV irradiation the hyper-phosphorylated Rad9 isoform migrates and it is detected on Western blots probed with anti-Rad9 antibodies near to an aspecific protein species (mostly present in the supernatant fraction) [50]. Such band was omitted in the Western blots shown in Figure 1, Figure 2, and Figure 7 for clarity. The positions of Rad9 and its hyper-phosphorylated isoform (pRad9) are indicated; * marks the background protein species unrelated to Rad9. (B) The Western blots in which the presence of Rad9 was analyzed in

the total (T), soluble (S) and chromatin-enriched (Ch) fractions were controlled for proper fractionation of control proteins, known to remain in the soluble fraction (Tubulin) or to bind to chromatin (Orc2). The blots in S1 Panel B show the results obtained with the same protein samples analyzed in Figure 1A. (C) Quantitative analysis of the percentage of hyper-phosphorylated and hypo-phosphorylated Rad9 isoforms in the total (T), soluble (S) and chromatin-enriched (Ch) fractions in α-factor and nocodazole arrested wild-type cells. Quantification was obtained with a Versadoc (Biorad) after incubation with fluorescent secondary antibodies, and error bars were obtained from 4 independent experiments. The percentages of hyper- and hypo- phosphorylated isoforms were calculated respectively to the total amount of Rad9.
Found at: doi:10.1371/journal.pgen.1001047.s001 (1.16 MB TIF)

Figure S2 (A) The histograms show the M/G1 ratio increase in β-galactosidase activity, when the interaction between Dpb11/Rad9 or the positive controls p53 and SV40-TAg was measured by two-hybrid analysis in nocodazole (M) or α-factor (G1) arrested cells. Error bars were obtained from three independent two-hybrid experiments. (B) Amino acid sequence of the Rad9 ORF; the basic CDK1 (S/T-P) and PIKK (S/T-Q) consensus phosphorylation sites are shown in black or gray, respectively. (C) wt (K699) and *rad9-S11A* (YMAG162) strains were arrested in M with nocodazole and samples were collected to prepare protein extracts. Rad9 phosphorylation was analyzed by SDS-PAGE and Western blotting with anti-Rad9 antibodies.
Found at: doi:10.1371/journal.pgen.1001047.s002 (0.77 MB TIF)

Figure S3 wt (YMAG149/7B), *H2A-S129A* (YMAG168), *dpb11ΔCT* (YMAG145/20C), *H2A-S129A dpb11ΔCT* (YMAG155), *dot1Δ* (YMAG150/4A), *H2A-S129A dot1Δ* (YMAG170), *dpb11ΔCT dot1Δ* (YMAG148) and *H2A-S129A dpb11ΔCT dot1Δ* (YMAG157) strains were arrested in M with nocodazole and treated with zeocin (150 μg/ml). After 45 min, samples were collected and protein extracts were analyzed by SDS-PAGE and Western blotting with anti Rad53 antibodies to monitor checkpoint activation.
Found at: doi:10.1371/journal.pgen.1001047.s003 (0.76 MB TIF)

Table S1 Strains used in this study. All of the strains used in this work are derivatives of W303 [*MAT*a *ade2-1 trp1-1 can1-100 leu2-3,12 his3-11,15 ura3 rad5-535*]; only strains YFP91 and DLY2236 (provided by D. Lydall), are *RAD5*$^{+}$.
Found at: doi:10.1371/journal.pgen.1001047.s004 (0.06 MB DOC)

Acknowledgments

We thank C. Santocanale, D. Lydall, D. Stern, F. Vanoli, A. Pellicioli for the gift of antibodies, strains, and plasmids. T. Weinert and the members of our labs are acknowledged for stimulating discussions. ARIAD (www.ariad.com/regulationkits) provided the FKBP regulated homodimerization kit.

Author Contributions

Conceived and designed the experiments: M Granata, F Lazzaro, R Kumar, M Grenon, NF Lowndes, P Plevani, M Muzi-Falconi. Performed the experiments: M Granata, F Lazzaro, D Novarina, D Panigada, F Puddu, CM Abreu. Analyzed the data: M Granata, F Lazzaro, D Novarina, D Panigada, F Puddu, M Grenon, NF Lowndes, P Plevani, M Muzi-Fal. Contributed reagents/materials/analysis tools: M Granata, F Lazzaro, D Novarina, D Panigada, F Puddu. Wrote the paper: NF Lowndes, P Plevani, M Muzi-Falconi.

References

1. Lazzaro F, Giannattasio M, Puddu F, Granata M, Pellicioli A, et al. (2009) Checkpoint mechanisms at the intersection between DNA damage and repair. DNA Repair (Amst) 8: 1055–1067.
2. Kerzendorfer C, O'Driscoll M (2009) Human DNA damage response and repair deficiency syndromes: linking genomic instability and cell cycle checkpoint proficiency. DNA Repair (Amst) 8: 1139–1152.
3. Melo J, Toczyski D (2002) A unified view of the DNA-damage checkpoint. Curr Opin Cell Biol 14: 237–245.
4. Harrison JC, Haber JE (2006) Surviving the breakup: the DNA damage checkpoint. Annu Rev Genet 40: 209–235.
5. Longhese MP, Foiani M, Muzi-Falconi M, Lucchini G, Plevani P (1998) DNA damage checkpoint in budding yeast. EMBO J 17: 5525–5528.
6. Durocher D, Jackson SP (2001) DNA-PK, ATM and ATR as sensors of DNA damage: variations on a theme? Curr Opin Cell Biol 13: 225–231.
7. Paciotti V, Clerici M, Lucchini G, Longhese MP (2000) The checkpoint protein Ddc2, functionally related to S. pombe Rad26, interacts with Mec1 and is regulated by Mec1-dependent phosphorylation in budding yeast. Genes Dev 14: 2046–2059.
8. Rouse J, Jackson SP (2000) LCD1: an essential gene involved in checkpoint control and regulation of the MEC1 signalling pathway in Saccharomyces cerevisiae. EMBO J 19: 5801–5812.
9. Wakayama T, Kondo T, Ando S, Matsumoto K, Sugimoto K (2001) Pie1, a protein interacting with Mec1, controls cell growth and checkpoint responses in Saccharomyces cerevisiae. Mol Cell Biol 21: 755–764.
10. Downs JA, Lowndes NF, Jackson SP (2000) A role for Saccharomyces cerevisiae histone H2A in DNA repair. Nature 408: 1001–1004.
11. Paciotti V, Lucchini G, Plevani P, Longhese MP (1998) Mec1p is essential for phosphorylation of the yeast DNA damage checkpoint protein Ddc1p, which physically interacts with Mec3p. EMBO J 17: 4199–4209.
12. Emili A (1998) MEC1-dependent phosphorylation of Rad9p in response to DNA damage. Mol Cell 2: 183–189.
13. Vialard JE, Gilbert CS, Green CM, Lowndes NF (1998) The budding yeast Rad9 checkpoint protein is subjected to Mec1/Tel1-dependent hyperphosphorylation and interacts with Rad53 after DNA damage. EMBO J 17: 5679–5688.
14. Gilbert CS, Green CM, Lowndes NF (2001) Budding yeast Rad9 is an ATP-dependent Rad53 activating machine. Mol Cell 8: 129–136.
15. Schwartz MF, Duong JK, Sun Z, Morrow JS, Pradhan D, et al. (2002) Rad9 phosphorylation sites couple Rad53 to the Saccharomyces cerevisiae DNA damage checkpoint. Mol Cell 9: 1055–1065.
16. Sweeney FD, Yang F, Chi A, Shabanowitz J, Hunt DF, et al. (2005) Saccharomyces cerevisiae Rad9 acts as a Mec1 adaptor to allow Rad53 activation. Curr Biol 15: 1364–1375.
17. Pellicioli A, Lucca C, Liberi G, Marini F, Lopes M, et al. (1999) Activation of Rad53 kinase in response to DNA damage and its effect in modulating phosphorylation of the lagging strand DNA polymerase. EMBO J 18: 6561–6572.
18. Weinert TA, Hartwell LH (1988) The RAD9 gene controls the cell cycle response to DNA damage in Saccharomyces cerevisiae. Science 241: 317–322.
19. Weinert TA, Hartwell LH (1990) Characterization of RAD9 of Saccharomyces cerevisiae and evidence that its function acts posttranslationally in cell cycle arrest after DNA damage. Mol Cell Biol 10: 6554–6564.
20. Siede W, Friedberg AS, Friedberg EC (1993) RAD9-dependent G1 arrest defines a second checkpoint for damaged DNA in the cell cycle of Saccharomyces cerevisiae. Proc Natl Acad Sci U S A 90: 7985–7989.
21. Soulier J, Lowndes NF (1999) The BRCT domain of the S. cerevisiae checkpoint protein Rad9 mediates a Rad9-Rad9 interaction after DNA damage. Curr Biol 9: 551–554.
22. Hammet A, Magill C, Heierhorst J, Jackson SP (2007) Rad9 BRCT domain interaction with phosphorylated H2AX regulates the G1 checkpoint in budding yeast. EMBO Rep 8: 851–857.
23. Nnakwe CC, Altaf M, Cote J, Kron SJ (2009) Dissection of Rad9 BRCT domain function in the mitotic checkpoint response to telomere uncapping. DNA Repair (Amst) 8: 1452–1461.
24. Toh GW-L, Lowndes NF (2003) Role of the Saccharomyces cerevisiae Rad9 protein in sensing and responding to DNA damage. Biochem Soc Trans 31: 242–246.
25. Sun Z, Hsiao J, Fay DS, Stern DF (1998) Rad53 FHA domain associated with phosphorylated Rad9 in the DNA damage checkpoint. Science 281: 272–274.
26. Durocher D, Henckel J, Fersht AR, Jackson SP (1999) The FHA domain is a modular phosphopeptide recognition motif. Mol Cell 4: 387–394.
27. Usui T, Foster SS, Petrini JHJ (2009) Maintenance of the DNA-damage checkpoint requires DNA-damage-induced mediator protein oligomerization. Mol Cell 33: 147–159.
28. Du L-L, Moser BA, Russell P (2004) Homo-oligomerization is the essential function of the tandem BRCT domains in the checkpoint protein Crb2. J Biol Chem 279: 38409–38414.
29. Ward I, Kim J-E, Minn K, Chini CC, Mer G, et al. (2006) The tandem BRCT domain of 53BP1 is not required for its repair function. J Biol Chem 281: 38472–38477.

30. Zgheib O, Pataky K, Brugger J, Halazonetis TD (2009) An oligomerized 53BP1 tudor domain suffices for recognition of DNA double-strand breaks. Mol Cell Biol 29: 1050–1058.
31. Kilkenny ML, Doré AS, Roe SM, Nestoras K, Ho JCY, et al. (2008) Structural and functional analysis of the Crb2-BRCT2 domain reveals distinct roles in checkpoint signaling and DNA damage repair. Genes Dev 22: 2034–2047.
32. van Attikum H, Gasser SM (2009) Crosstalk between histone modifications during the DNA damage response. Trends Cell Biol 19: 207–217.
33. Giannattasio M, Lazzaro F, Plevani P, Muzi-Falconi M (2005) The DNA damage checkpoint response requires histone H2B ubiquitination by Rad6-Bre1 and H3 methylation by Dot1. J Biol Chem 280: 9879–9886.
34. Huyen Y, Zgheib O, Ditullio RA, Gorgoulis VG, Zacharatos P, et al. (2004) Methylated lysine 79 of histone H3 targets 53BP1 to DNA double-strand breaks. Nature 432: 406–411.
35. Grenon M, Magill CP, Lowndes NF, Jackson SP (2006) Double-strand breaks trigger MRX- and Mec1-dependent, but Tel1-independent, checkpoint activation. FEMS Yeast Res 6: 836–847.
36. Sanders SL, Portoso M, Mata J, Bähler J, Allshire RC, et al. (2004) Methylation of histone H4 lysine 20 controls recruitment of Crb2 to sites of DNA damage. Cell 119: 603–614.
37. Du L-L, Nakamura TM, Russell P (2006) Histone modification-dependent and -independent pathways for recruitment of checkpoint protein Crb2 to double-strand breaks. Genes Dev 20: 1583–1596.
38. Botuyan MV, Lee J, Ward IM, Kim J-E, Thompson JR, et al. (2006) Structural basis for the methylation state-specific recognition of histone H4-K20 by 53BP1 and Crb2 in DNA repair. Cell 127: 1361–1373.
39. Schotta G, Sengupta R, Kubicek S, Malin S, Kauer M, et al. (2008) A chromatin-wide transition to H4K20 monomethylation impairs genome integrity and programmed DNA rearrangements in the mouse. Genes Dev 22: 2048–2061.
40. Javaheri A, Wysocki R, Jobin-Robitaille O, Altaf M, Cote J, et al. (2006) Yeast G1 DNA damage checkpoint regulation by H2A phosphorylation is independent of chromatin remodeling. Proc Natl Acad Sci U S A 103: 13771–13776.
41. Toh GW-L, O'shaughnessy AM, Jimeno S, Dobbie IM, Grenon M, et al. (2006) Histone H2A phosphorylation and H3 methylation are required for a novel Rad9 DSB repair function following checkpoint activation. DNA Repair (Amst) 5: 693–703.
42. Nakamura TM, Du L-L, Redon C, Russell P (2004) Histone H2A phosphorylation controls Crb2 recruitment at DNA breaks, maintains checkpoint arrest, and influences DNA repair in fission yeast. Mol Cell Biol 24: 6215–6230.
43. Iwabuchi K, Basu BP, Kysela B, Kurihara T, Shibata M, et al. (2003) Potential role for 53BP1 in DNA end-joining repair through direct interaction with DNA. J Biol Chem 278: 36487–36495.
44. Pryde F, Khalili S, Robertson K, Selfridge J, Ritchie A-M, et al. (2005) 53BP1 exchanges slowly at the sites of DNA damage and appears to require RNA for its association with chromatin. J Cell Sci 118: 2043–2055.
45. Ward IM, Minn K, Jorda KG, Chen J (2003) Accumulation of checkpoint protein 53BP1 at DNA breaks involves its binding to phosphorylated histone H2AX. J Biol Chem 278: 19579–19582.
46. Huen MSY, Grant R, Manke I, Minn K, Yu X, et al. (2007) RNF8 transduces the DNA-damage signal via histone ubiquitylation and checkpoint protein assembly. Cell 131: 901–914.
47. Kolas NK, Chapman JR, Nakada S, Ylanko J, Chahwan R, et al. (2007) Orchestration of the DNA-damage response by the RNF8 ubiquitin ligase. Science 318: 1637–1640.
48. Mailand N, Bekker-Jensen S, Faustrup H, Melander F, Bartek J, et al. (2007) RNF8 ubiquitylates histones at DNA double-strand breaks and promotes assembly of repair proteins. Cell 131: 887–900.
49. Furuya K, Poitelea M, Guo L, Caspari T, Carr AM (2004) Chk1 activation requires Rad9 S/TQ-site phosphorylation to promote association with C-terminal BRCT domains of Rad4TOPBP1. Genes Dev 18: 1154–1164.
50. Puddu F, Granata M, Nola LD, Balestrini A, Piergiovanni G, et al. (2008) Phosphorylation of the budding yeast 9-1-1 complex is required for Dpb11 function in the full activation of the UV-induced DNA damage checkpoint. Mol Cell Biol 28: 4782–4793.
51. Liu S, Bekker-Jensen S, Mailand N, Lukas C, Bartek J, et al. (2006) Claspin operates downstream of TopBP1 to direct ATR signaling towards Chk1 activation. Mol Cell Biol 26: 6056–6064.
52. Walker J, Crowley P, Moreman AD, Barrett J (1993) Biochemical properties of cloned glutathione S-transferases from Schistosoma mansoni and Schistosoma japonicum. Mol Biochem Parasitol 61: 255–264.
53. Inouye C, Dhillon N, Thorner J (1997) Ste5 RING-H2 domain: role in Ste4-promoted oligomerization for yeast pheromone signaling. Science 278: 103–106.
54. Clackson T, Yang W, Rozamus LW, Hatada M, Amara JF, et al. (1998) Redesigning an FKBP-ligand interface to generate chemical dimerizers with novel specificity. Proc Natl Acad Sci U S A 95: 10437–10442.
55. Saka Y, Esashi F, Matsusaka T, Mochida S, Yanagida M (1997) Damage and replication checkpoint control in fission yeast is ensured by interactions of Crb2, a protein with BRCT motif, with Cut5 and Chk1. Genes Dev 11: 3387–3400.
56. Bishop AC, Ubersax JA, Petsch DT, Matheos DP, Gray NS, et al. (2000) A chemical switch for inhibitor-sensitive alleles of any protein kinase. Nature 407: 395–401.
57. Bonilla CY, Melo JA, Toczyski DP (2008) Colocalization of sensors is sufficient to activate the DNA damage checkpoint in the absence of damage. Mol Cell 30: 267–276.
58. Blankley RT, Lydall D (2004) A domain of Rad9 specifically required for activation of Chk1 in budding yeast. J Cell Sci 117: 601–608.
59. Smolka MB, Albuquerque CP, Chen SH, Schmidt KH, Wei XX, et al. (2005) Dynamic changes in protein-protein interaction and protein phosphorylation probed with amine-reactive isotope tag. Mol Cell Proteomics 4: 1358–1369.
60. Grenon M, Costelloe T, Jimeno S, O'shaughnessy A, Fitzgerald J, et al. (2007) Docking onto chromatin via the Saccharomyces cerevisiae Rad9 Tudor domain. Yeast 24: 105–119.
61. Pellicioli A, Foiani M (2005) Signal transduction: how rad53 kinase is activated. Curr Biol 15: R769–771.
62. Wysocki R, Javaheri A, Allard S, Sha F, Côté J, et al. (2005) Role of Dot1-dependent histone H3 methylation in G1 and S phase DNA damage checkpoint functions of Rad9. Mol Cell Biol 25: 8430–8443.
63. Ira G, Pellicioli A, Balijja A, Wang X, Fiorani S, et al. (2004) DNA end resection, homologous recombination and DNA damage checkpoint activation require CDK1. Nature 431: 1011–1017.
64. Aylon Y, Liefshitz B, Kupiec M (2004) The CDK regulates repair of double-strand breaks by homologous recombination during the cell cycle. EMBO J 23: 4868–4875.
65. Barlow JH, Lisby M, Rothstein R (2008) Differential regulation of the cellular response to DNA double-strand breaks in G1. Mol Cell 30: 73–85.
66. Branzei D, Foiani M (2008) Regulation of DNA repair throughout the cell cycle. Nat Rev Mol Cell Biol 9: 297–308.
67. Lazzaro F, Sapountzi V, Granata M, Pellicioli A, Vaze M, et al. (2008) Histone methyltransferase Dot1 and Rad9 inhibit single-stranded DNA accumulation at DSBs and uncapped telomeres. EMBO J 27: 1502–1512.
68. Navadgi-Patil VM, Burgers PM (2009) A tale of two tails: activation of DNA damage checkpoint kinase Mec1/ATR by the 9-1-1 clamp and by Dpb11/TopBP1. DNA Repair (Amst) 8: 996–1003.
69. Gyuris J, Golemis E, Chertkov H, Brent R (1993) Cdi1, a human G1 and S phase protein phosphatase that associates with Cdk2. Cell 75: 791–803.
70. Longtine MS, McKenzie A, Demarini DJ, Shah NG, Wach A, et al. (1998) Additional modules for versatile and economical PCR-based gene deletion and modification in Saccharomyces cerevisiae. Yeast 14: 953–961.
71. Storici F, Lewis LK, Resnick MA (2001) In vivo site-directed mutagenesis using oligonucleotides. Nat Biotechnol 19: 773–776.
72. Diani L, Colombelli C, Nachimuthu BT, Donnianni R, Plevani P, et al. (2009) Saccharomyces CDK1 phosphorylates Rad53 kinase in metaphase, influencing cellular morphogenesis. J Biol Chem 284: 32627–32634.
73. Goldstein AL, McCusker JH (1999) Three new dominant drug resistance cassettes for gene disruption in Saccharomyces cerevisiae. Yeast 15: 1541–1553.
74. Araki H, Leem SH, Phongdara A, Sugino A (1995) Dpb11, which interacts with DNA polymerase II(epsilon) in Saccharomyces cerevisiae, has a dual role in S-phase progression and at a cell cycle checkpoint. Proc Natl Acad Sci U S A 92: 11791–11795.
75. Muzi Falconi M, Piseri A, Ferrari M, Lucchini G, Plevani P, et al. (1993) De novo synthesis of budding yeast DNA polymerase alpha and POL1 transcription at the G1/S boundary are not required for entrance into S phase. Proc Natl Acad Sci U S A 90: 10519–10523.
76. Fiorani S, Mimun G, Caleca L, Piccini D, Pellicioli A (2008) Characterization of the activation domain of the Rad53 checkpoint kinase. Cell Cycle 7: 493–499.

Supplementary Fig.1

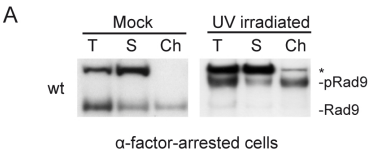

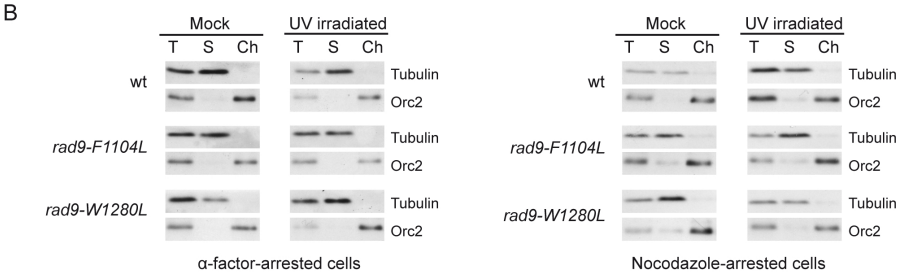

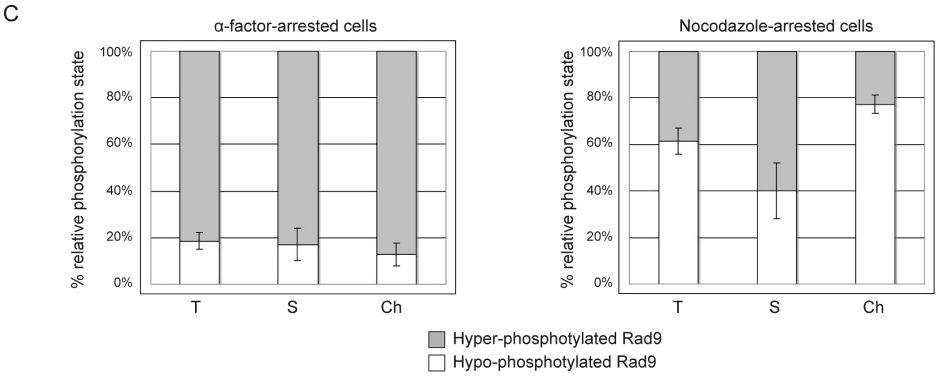

Supplementary Fig. 2

A

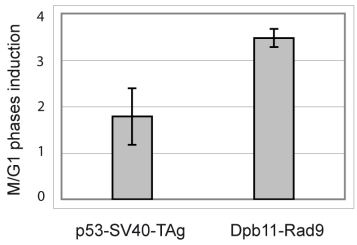

B

```
1-   MSGQLVQWKSSPDRVTQSAIKEALHSPLADGDMNEMNVPVDPLENKVNSTNIIEGSPKANPNPVKFMNTSEIFQKSLGLLDESPRHDDELNIEVGDNDRP
101- NANILHNERTPDLDRIANFFKSNRTPGKENLLTKYQSSDLEDTPLMLRKKMTFQTPTDPLEQKTFKKLKSDTGFCYYGEQNDGEENASLEVTEADATFVQ
201- MAERSADNYDCALEGIVTPKRYKDELSKSGGMQDERVQKTQIMISAESPNSISSYDKNKITGNGRTTRNVNKVFNNNEDNIGAIEEKNPVKKKSENYSSD
301- DLRERNNQIIQSNESEEINELEKNLNVSGRENDVNNLDIDINSAVSGTPSRNNAEEEMYSSESVNNREPSKKWIFRYSKDKTENNSNRSTQIVNNPRTQE
401- MPLDSISIDTQPLSKSFNTETNNELETQIIVSSLSQGISAQKGPVFHSTGQTEEIKTQIINSPEQNALNATFETPVTLSRINFEPILEVPETSSPSKNTM
501- SKPSNSSEIPKEKDTFNIHEREVETNNVFSNDIQNSSNAATRDDIIIAGSSDFNEQKEITDRIYLQLSGKQISDSGSDETERMSPNELDTKKESTIMSEV
601- ELTQELPEVEEQQDLQTSPKKLVVEEETLMEIKKSKGNSLQLHDDNKECNSDKQDGTESLDVALIEHESKGQSSELQKNLMQLFPSESQEIIQNRRTIKR
701- RQKDTIEIGEEEENRSTKTSPTKHLKRNSDLDAASIKREPSCSITIQTGETGSGKDSKEQSYVFPEGIRTADNSFLSKDDIIFGNAVWCQYTWNYKFYPG
801- ILLEVDTNQDGCWIYFETGRSLTKDEDIYYLDIRIGDAVTFDGNEYVVVGLECRSHDLNIIRCIRGYDTVHLKKKNASGLLGKRTLIKALSSISLDLSEW
901- AKRAKIILEDNEKNKGDAYRYLRHPIRGRKSMTNVLSPKKHTDDEKDINTHTEVYNNEIESSSEKKEIVKKDSRDALAEHAGAPSLLFSSGEIRTGNVFD
1001-KCIFVLTSLFENREELRQTIESQGGTVIESGFSTLFNFTHPLAKSLVNKGNTDNIRELALKLAWKPHSLFADCRFACLITKRHLRSLKYLETLALGWPTL
1101-HWKFISACIEKKRIVPHLIYQYLLPSGESFRLSLDSPSKGGIIKSNNIFSFYTQFLRGSNLRDQICGVKKMLNDYIVIVWGRSELDSFVKFAFACLSAGR
1201-MLTIDLPNIDVDDTEPLLNALDSLVPRIGSELSNRKLKFLIYANENNGKSQMKLLERLRSQISLKFKKFNYIFHTESKEWLIQTIINEDTGFHDDITDND
1301-IYNTISEVR
```

C

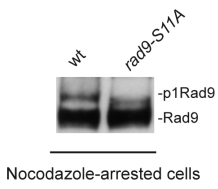

Supplementary Fig. 3

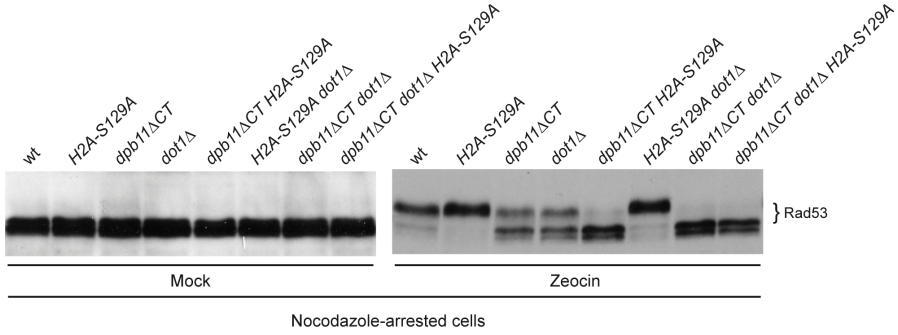

Table S1. Strains used in this study.

Strain	Relevant genotype	Source
K699	*MAT*a *ade2-1 trp1-1 leu2-3,112 his3-11 ura3 can1-100 rad5-535*	K. Nasmyth
YFL871	K699 *rad9aa1-646:kanMX4:URA3*	This work
YNOV15	K699 *rad9-F1104L*	This work
YNOV31	K699 *rad9-W1280L*	This work
YMAG88	K699 *rad9::HIS3*	This work
YFL696/1b	K699 *rad9ΔBRCT::13MYC:TRP1*	This work
YMAG74	K699 *rad9ΔBRCT::GST:kanMX6*	This work
YFL773/2c	K699 *dot1::kanMX6 rad9ΔBRCT::GST:kanMX6*	This work
YFL921	K699 *rad9ΔBRCT::2xFKBP-13MYC:kanMX6*	This work
YMAG149/7B	K699 *hta1_htb1::LEU2 hta2_htb2::TRP1* (pSAB6)	(50)
YMAG145/20C	K699 *hta1_htb1::LEU2 hta2_htb2::TRP1 dpb11ΔCT::HPH* (pSAB6)	This work
YMAG150/4A	K699 *hta1_htb1::LEU2 hta2_htb2::TRP1 dot1::kanMX6* (pSAB6)	(50)
YMAG148	K699 *hta1_htb1::LEU2 hta2_htb2::TRP1 dpb11ΔCT::HPH dot1::kanMX6* (pSAB6)	This work
EGY42	*MATα his3 ura3 trp1 leu2::6LexAop-LEU2*	R. Brent
JAU01	K699 *cdc28-as1*	(56)
YNOV4	K699 *cdc28-as1 dot1::kanMX6*	This work
YFL234	K699 *dot1::kanMX6*	(33)
DLY2236	K699 *rad9::LEU2 ura3::rad9-M232:URA3 RAD5+*	(58)
YFP91	K699 *rad9::LEU2 ura3::rad9-M232-URA3 dot1::kanMX6 RAD5+*	This work
YMAG162	K699 *rad9-S11A*	This work
YMAG164	K699 *rad9-S11A dot1::kanMX6*	This work
YMAG168	K699 *hta1_htb1::LEU2 hta2_htb2::TRP1* (pJD151)	(50)
YMAG170	K699 *hta1_htb1::LEU2 hta2_htb2::TRP1 dot1::kanMX6* (pJD151)	(50)
YMAG155	K699 *hta1_htb1::LEU2 hta2_htb2::TRP1 dpb11ΔCT::HPH* (pJD151)	This work
YMAG157	K699 *hta1_htb1::LEU2 hta2_htb2::TRP1 dpb11ΔCT::HPH dot1::kanMX6* (pJD151)	This work
YFL1177	K699 *rad9-S11AΔBRCT::GST:kanMX6*	This work

Published paper II

Novarina, D., Amara, F., Lazzaro, F., Plevani, P. and Muzi-Falconi, M.

Mind the gap: keeping UV lesions in check.

Published in: DNA Repair (Amst), **2011**, 10, 751–759.

DNA Repair 10 (2011) 751–759

Contents lists available at ScienceDirect

DNA Repair

journal homepage: www.elsevier.com/locate/dnarepair

Mini review

Mind the gap: Keeping UV lesions in check

Daniele Novarina, Flavio Amara, Federico Lazzaro, Paolo Plevani*, Marco Muzi-Falconi*

Dipartimento di Scienze Biomolecolari e Biotecnologie, Università degli Studi di Milano. Via Celoria 26, 20133 Milano, Italy

ARTICLE INFO

Article history:
Available online 23 May 2011

Keywords:
UV irradiation
DNA damage checkpoint
DNA repair

ABSTRACT

Cells respond to genotoxic insults by triggering a DNA damage checkpoint surveillance mechanism and by activating repair pathways. Recent findings indicate that the two processes are more related than originally thought. Here we discuss the mechanisms involved in responding to UV-induced lesions in different phases of the cell cycle and summarize the most recent data in a model where Nucleotide Excision Repair (NER) and exonucleolytic activities act in sequence leading to checkpoint activation in non replicating cells. The critical trigger is likely represented by problematic intermediates that cannot be completely or efficiently repaired by NER. In S phase cells, on the other hand, the replicative polymerases, blocked by bulky UV lesions, re-initiate DNA synthesis downstream of the lesions, leaving behind a ssDNA tract. If these gaps are not rapidly refilled, checkpoint kinases will be activated.

Contents

1. Introduction

Cellular DNA is constantly threatened by genotoxic events arising from cellular metabolisms (e.g., free oxygen radicals, replication errors) and induced by environmental factors (e.g., ionizing and UV radiations, chemicals). To prevent the effect of endogenous and exogenous mutagenic agents and to maintain genome integrity, cells have evolved a complex response to DNA damage (DDR), which includes repair mechanisms and regulatory circuits. A key role in this response is played by signaling pathways that we will refer to as DNA damage checkpoints, surveillance mechanisms responsible for the coordination of cell cycle progression, DNA replication, transcription with DNA repair and apoptosis. Checkpoint activation temporarily halts or delays cell cycle progression, possibly providing the cell with enough time to remove DNA lesions before these are converted in secondary and more dangerous lesions (e.g., replication through a single strand gap would generate a double strand break). The checkpoints also actively stimulate the repair processes [1–9] and, in higher eukaryotes, trigger the apoptotic response, if damage cannot be dealt with successfully [10–12].

2. DNA damage checkpoint

The importance of the DNA damage checkpoint in the maintenance of genomic stability is underlined by the existence of many syndromes linked to mutations in checkpoint genes, causing increased cancer proneness or other clinical symptoms, espe-

* Corresponding author. Tel.: +39 0250315034; fax: +39 0250315044.
E-mail addresses: paolo.plevani@unimi.it (P. Plevani), marco.muzifalconi@unimi.it (M. Muzi-Falconi).

1568-7864/$ – see front matter © 2011 Elsevier B.V. All rights reserved.
doi:10.1016/j.dnarep.2011.04.030

Table 1
Checkpoint functions are evolutionarily conserved. The table shows the correspondence between various checkpoint factors in different organisms. The upstream factors are in blue, mediators are in pink and downstream effectors are in green.

S. cerevisiae	*S. pombe*	Human	*X. laevis*
Mec1	Rad3	ATR	ATR
Ddc2	Rad26	ATRIP	ATRIP
Tel1	Tel1	ATM	ATM
Rad24	Rad17	Rad17	Rad17
Rad17	Rad1	Rad1	Rad1
Mec3	Hus1	Hus1	Hus1
Ddc1	Rad9	Rad9	Rad9
Rad9	Crb2	BRCA1, 53BP1 , MDC1	BRCA1, 53BP1
Mrc1	Mrc1	Claspin	Claspin
Dpb11	Rad4/Cut5	TopBP1	TopBP1
Rad53	Cds1	Chk2	Cds1
Chk1	Chk1	Chk1	Chk1

cially neurological defects [13,14]; it is thus not surprising that these pathways are extremely conserved throughout evolution (Table 1).

The DNA damage checkpoint response consists of a signal transduction cascade mainly based on phosphorylation events; the mechanistic details of the pathway have been recently discussed elsewhere [15,16], and will be just briefly summarized here to give a schematic picture to the reader. The first signaling event is carried out by the apical checkpoint kinases and is triggered after DNA damage detection. Two complexes are independently recruited at the lesion sites [17]: the human ATR/ATRIP or *Saccharomyces cerevisiae* Mec1/Ddc2 complex, and the 9-1-1 checkpoint clamp complex, composed of Rad9-Rad1-Hus1 in human or their orthologue subunits Rad17-Mec3-Ddc1 in yeast. The co-localization of these complexes is sufficient to trigger at least a partial checkpoint signaling even in the absence of actual DNA damage [18]. In *S. cerevisiae* the Mec1 apical kinase can be activated both by the Ddc1 subunit of the checkpoint clamp and by the adaptor protein Dpb11 which is recruited at the lesion through interaction with Ddc1 [19–23]. In human cells, the 9-1-1 complex is not able to directly activate ATR, but it is needed to recruit TopBP1 (the Dpb11 orthologue) which, in turn, stimulates ATR activity [24]. The apical kinases phosphorylate checkpoint mediators or adaptors, which are held close to the lesion by the interaction with post-translationally modified histone residues and with other checkpoint factors [25]. The mediators amplify the signaling cascade providing a platform to recruit effector kinases close to the apical kinases, and facilitating their activation. In budding yeast, Mec1 activates both Rad53 and Chk1 [26], while in human cells Chk2 is activated by ATM and Chk1 by ATR [27]. The prototype of checkpoint mediators is *S. cerevisiae* Rad9, which, once phosphorylated by the apical kinase, recruits Rad53 at the damage site allowing its phosphorylation by Mec1. Oligomerization of Rad9 seems to be critical to provide a scaffold for Rad53 binding, leading to a local increase in Rad53 molecules and stimulating its auto-phosphorylation; this event is responsible for full Rad53 activation [28,29]. Chk1 activation also requires Rad9, but the mechanism through which this mediator facilitates Chk1 phosphorylation by Mec1 is still poorly understood [30]. In human cells, the identity of the functional Rad9 orthologue is still debated: multiple candidates exist – i.e., MDC1 (mediator of DNA-damage checkpoint 1), 53BP1 (p53-binding protein 1) and BRCA1 (breast cancer 1 early-onset) – all characterized by the presence of tandem BRCT (BRCA1 C-terminal repeat) domains. Since these three proteins are involved in checkpoint signal transduction and each of them seems to carry out, separately and sometimes redundantly, some of Rad9 functions, they may be all considered as Rad9 orthologues [31]. Finally, effector kinases are responsible for the phosphorylation of a great number of targets, including cell cycle machinery factors and key proteins important for replication and repair [32,33].

The checkpoint response can act in at least three different phases of the cell cycle: in G1, to prevent chromosomes with problematic lesions from entering S phase, in S phase to control their replication, and in G2 (or M in some organisms) to avoid loss of genetic information due to mitotic segregation of severely damaged chromosomes. The general scheme of the checkpoint cascade is similar in all three cases, but significant differences can be found, depending on the nature of the DNA lesion and on the cell cycle phase in which the damage is detected [13,34–36]. Furthermore, in human cells the two apical kinases seem to be partly specialized in the response to different classes of DNA damaging agents. In fact, ATM (Ataxia Telangiectasia Mutated) is activated by double-strand breaks (DSBs) caused, for example, by ionizing radiation (IR), while ATR (ATM and Rad3-Related) is activated by ssDNA coated with the RPA heterotrimeric complex and mainly triggers checkpoint activation after UV irradiation or replication-stress. This specialization is possibly imputable to the different networks of physical interactions that these kinases participate to, and that are responsible for their recruitment at the sites of lesion [37–40]. The situation is somewhat complicated by the finding that ATR can be also recruited to DSBs and this binding depends upon ATM [41,42]. This separation of tasks is not found in budding yeast, where Mec1 (the ATR homologue) is the main player of checkpoint activation after all kind of DNA lesions, while Tel1 (the ATM homologue) is especially devoted to telomere maintenance. The redundant role of Tel1 in the DNA damage checkpoint is uncovered only in the absence of Mec1 [15,43].

In this review, we will focus our attention on UV-induced lesions and we will discuss the reciprocal interactions between NER, post replication repair (PRR), and the checkpoint pathway. In particular, we will discuss how NER plays a role in the activation of the checkpoint response after UV treatment, and how checkpoint kinases contribute to modulating the actual repair events.

Given the variety of DNA lesions the cell has to deal with, it was hypothesized that the first responders, among checkpoint factors, had to be recruited to a common DNA intermediate, which was later identified as long regions of ssDNA covered by RPA [44]. While ATRIP and Ddc2 directly bind RPA-covered ssDNA [44], loading of the 9-1-1 complex requires the activity of an RFC-like complex, that places it at the junction between dsDNA and 5′ ssDNA [45]. In the case of a single DSB, a large amount of evidence indicates that recombination factors are first recruited at the DSB, and then the 5′ ends of the DSB are processed through the concerted action of several proteins, including helicases and nucleases. This action generates long ssDNA tails that, on one hand will recruit checkpoint factors, and on the other will initiate repair through homologous recombination mechanisms [46]. On the other hand, extensive resection is not required when a DSB is repaired through a Non-Homologous End Joining (NHEJ) process [47]. For a long time, it was unclear how UV irradiation, which causes bulky lesions on DNA (mainly cyclobutane pyrimidine dimers (CPD) and 6,4 photoproducts (6-4PP)) responsible for inducing a distortion of the DNA helix [48], triggers the same checkpoint response in the absence of any DSB (Fig. 1).

3. Nucleotide excision repair

UV-induced DNA lesions are mainly removed through NER that efficiently identifies 6-4PPs and more slowly takes care of CPDs. The lesion recognition mechanism of NER depends upon the phys-

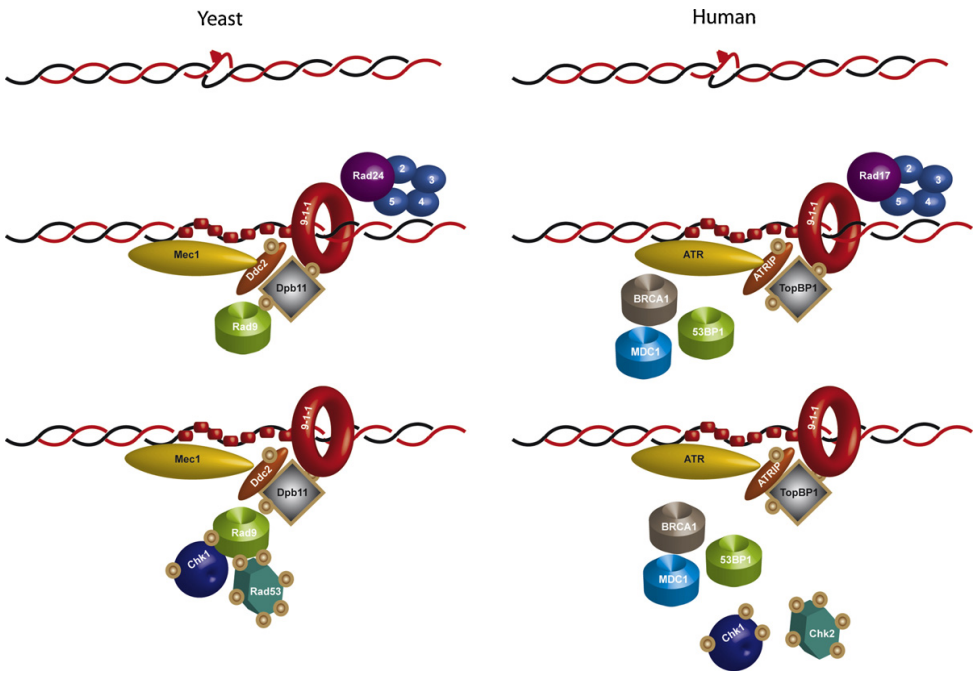

Fig. 1. The DNA damage checkpoint cascade. The DNA damage checkpoint is triggered by a ssDNA region. The left side of the figure reports the checkpoint cascade in budding yeast. RPA-covered ssDNA recruits the Mec1-Ddc2 and the 9-1-1 complexes. Phosphorylated Ddc1 interacts with Dpb11 which recruits the Rad9 mediator. Rad53 and Chk1 kinases are activated upon binding to oligomeric Rad9 and then leave chromatin to find their own targets. The right side of the figure summarizes the same signaling cascade in human cells.

ical location of the lesion, with TC-NER acting on lesions that block transcription, and GG-NER taking care of the rest of the genome [48].

NER has been reconstituted *in vitro* and the mechanism is discussed elsewhere in this issue. Briefly, once the lesion has been recognized a pre-incision complex is assembled at the damage site. Endonucleolytic incision 5′ and 3′ to the lesion produces a short gap containing ssDNA covered by RPA, which is then refilled by DNA polymerase activities.

How long this ssDNA tract is exposed for, before a DNA polymerase refills the gap is not clear, but most reports seem to agree that the refilling is extremely rapid and tightly coordinated with the incision process [49,50] (see review by Fagbemi et al. in this issue of DNA Repair).

Since UV lesions are bulky and block the progression of replicative DNA polymerases, when the replication forks collide with UV-induced lesions during the S phase of the cell cycle re-priming events may take place downstream of the lesions, leaving ssDNA gaps behind the fork. Such structures have been detected by electron microscopy on replicating UV-damaged DNA and are likely responsible for the rapid and sensitive response observed in UV-irradiated S phase cells [51]. Outside of S phase and in non cycling cells the situation is quite different. Recent analysis showed that UV lesions themselves cannot activate the checkpoint and NER plays a major role in triggering the checkpoint response, although contrasting results have also been reported [52–57].

4. NER and DNA damage checkpoint

The tight relationship between NER and the checkpoint response started to become clear when, in budding yeast, a *rad14* mutant, which is defective in assembling a competent pre-incision complex, was identified in a screen for mutations specifically inactivating the DNA damage checkpoint in response to UV irradiation, while leaving intact the DSB-induced checkpoint [55]. Furthermore, a direct interaction between Rad14 and the 9-1-1 checkpoint complex was reported, albeit its physiological significance has not been fully addressed. This work also showed that, in non cycling cells, any NER mutation affecting the incision event caused a deficient checkpoint activity, demonstrating that UV lesions *per se* are not sufficient to trigger the apical checkpoint kinase, and that their processing by a repair mechanism is necessary for recruiting the Mec1/Ddc2 and the 9-1-1 complexes to damaged chromosomes and for a prompt checkpoint response [55]. Such results are also consistent with the finding that UV irradiation in G1 of a cycling *rad14Δ* strain results in a strong arrest at the beginning of S phase [58], accompanied by the accumulation of replication-dependent ssDNA regions [51]. Altogether, it was suggested that a NER intermediate, possibly the ssDNA gapped structure generated by the double incision event may be responsible for recruiting and activating checkpoint factors. In cycling NER-deficient cells, UV irradiation would not cause a G1 delay or G2/M arrest and replication of the damaged template would lead to the accumulation of ssDNA regions resulting in Mec1 activation.

Extension of this kind of analysis to human cells derived from XP patients confirmed that lack of NER-dependent processing prevented UV-induced checkpoint activity in non cycling fibroblasts, revealing that XP cells are not only deficient in repairing UV lesions, but they are also deficient in the G1 and G2/M UV-induced checkpoint [56,57]. Interestingly, while XPC cells, defective in GG-NER, exhibit a checkpoint failure, cells obtained from Cockayne syndrome patients, which are defective in TC-NER, are instead able to activate the checkpoint, possibly thanks to the activity of GG-NER. Intriguingly, there seems to be a correlation between the capacity

of these cells to properly control G1 and G2/M transitions after UV, their genomic instability and the proneness of XP and CS patients to develop tumors [56]. In budding yeast, the analysis of mutants specifically defective in the TC-NER or in the GG-NER branches of NER, revealed that activity of either one of the sub-pathways was sufficient to trigger a checkpoint response [55]. Interestingly, although UV-induced photoproducts and DSBs are processed by different DNA repair pathways and trigger signaling responses controlled by distinct apical kinases (see above) they eventually generate the same epigenetic mark involving H2A ubiquitination [59].

The model suggesting that gapped NER intermediates are responsible for checkpoint activation in UV-irradiated cells poses a few problems: (a) the gaps are very short (~30 nt); (b) repair synthesis is very rapid, so the gaps are virtually absent; (c) it is not clear what would be the advantage of activating the checkpoint and arresting cell cycle progression, once the damage is practically repaired.

Recent work shed light on these problems, showing that normal NER-intermediates are not directly responsible for activating checkpoint kinases. In order to achieve a full and prompt checkpoint activity after UV irradiation in non cycling yeast cells, NER is necessary but not sufficient: in fact, the nuclease activity of Exo1 is also required [60,61]. Exo1 belongs to the Rad2 family of nucleases and has multiple cellular roles (see [62] for a review). This work shows that UV irradiation causes the accumulation, in yeast chromosomes, of long ssDNA regions that are dependent upon NER and Exo1 and correlate with Mec1 kinase activation. Preventing completion of repair synthesis by genetic or chemical means strongly increases accumulation of ssDNA and checkpoint activation, in agreement with a previous report [63]. The frequency of these large ssDNA gaps is much lower than the expected frequency of UV damages, suggesting that only a minor fraction of lesions undergo Exo1-dependent processing. Intriguingly, this mechanism is conserved also in human cells (Sertic et al., in preparation). These results suggest that the ~30 nt long ssDNA gaps produced by NER can be refilled by DNA polymerases or extended by Exo1; given that polymerases refill a DNA gap at a rate of about 3700 nt/min and Exo1 excises DNA at 160 nt/min, most UV lesions are normally rapidly repaired by NER. This is consistent with the observation that very low UV doses do not seem to activate the G1 checkpoint [61,64,65]; if NER can rapidly and effectively deal with a low number of lesions, there would be no point in triggering a checkpoint response. If for any reason the repair synthesis step is perturbed, Exo1 may have a kinetic opportunity to process the NER gap, generating a long ssDNA region, which recruits checkpoint factors and triggers the signaling cascade (Fig. 2). This situation may arise, for example, at higher UV doses, in case repair synthesis factors become limiting or if the refilling polymerase encounters an insurmountable block. In these conditions, repair may not be completed and the extension of the ssDNA region may meet two purposes: activating the checkpoint response and channeling the problematic lesion to a different repair pathway (e.g., recombination) [66–68].

Interestingly, translesion DNA polymerase activities (TLS) seem to counteract the generation of the UV-induced checkpoint signal [61,69]. Moreover, an unexpected role for TLS polymerases in NER was described in human cells, where DNA polymerase κ was found to be responsible for approximately 30% of the unscheduled DNA synthesis detected in UV-irradiated cells [70,71]. The actual role of TLS polymerases in NER is not completely understood and it will be interesting to determine if their activity is limited to particular regions of the genome and/or to particular configurations, such as the presence of a lesion in the template strand that may interfere with the refilling step of NER, as previously suggested in bacteria [72].

5. Closely opposing lesions

The possibility that Exo1-depedent processing may be facilitated by a polymerase blocking lesion in the template is intriguing. One instance where this might happen is when two UV lesions, one on each DNA strand, are generated in a limited region; this configuration has been defined “closely opposing UV lesions” [73–75]. Probability calculations would predict that the frequency of closely opposing lesions increases with the square of the UV dose and the chance of generating such situation in a yeast chromosome is expected to be very low. On the other hand, UV lesion formation has a strong sequence bias, and actual measurements on irradiated DNA proved that approximately 1% of all UV-induced lesions are configured as closely opposing lesions [76–78]. When NER encounters two closely spaced lesions, one on each strand, a major problem arises. NER can only process one damage at a time because the lesion needs to be in a double-stranded configuration [79]. Incision and removal of the first UV-induced dimer leaves to the refilling polymerase a gap containing a lesion in the template strand. DNA polymerase δ or ε, which normally take care of repair synthesis, cannot replicate past the template lesion and stall, strongly resembling a blocked replication fork. During S phase, such situation would be bypassed via Post Replication Repair (PRR), which entails TLS polymerases and/or template switching mechanisms. Interestingly, it was recently shown that DNA polymerase κ directly participates to NER repair synthesis in human cells [70,71] and that loss of TLS activity greatly potentiates the checkpoint response to UV irradiation in yeast G1 cells [61], suggesting that closely opposing UV lesions may indeed be at least partly responsible for checkpoint activation. These particular lesions may also contribute to explain the observation that both in wild-type yeast and bacteria cells most of the UV-induced mutagenesis depends upon a functional NER and takes place in G1 cells, while in the absence of NER the mutagenesis is S-phase specific [80,81]. Moreover, a role for TLS in G1-irradiated cells is also supported by the finding that G1 synchronized cultures of yeast mutants lacking TLS polymerases are more sensitive to UV light than asynchronous cultures, while this is not the case for strains that are TLS proficient [61].

6. Replicating UV damaged DNA

As mentioned above, in NER deficient cells, the lack of lesion removal coupled to the failure to activate the G1 DNA damage checkpoint in response to UV irradiation allows a large amount of DNA lesions to go into S phase. Here, there is no need for lesion processing to generate the checkpoint activating structures since ssDNA regions are generated by the stalling of replication forks at the polymerase blocking lesions. Blocked polymerase can leave the lesion and PCNA behind and re-initiate downstream of the lesion via a re-priming mechanism, generating numerous ssDNA gaps behind the forks, which are likely responsible for the strong activation of Mec1 during S phase in UV-irradiated cells [51,82–85]. Consistently, even at low UV doses (5 J/m^2), NER deficient yeast cells exhibit a strong cell cycle arrest at the beginning of S phase, due to Mec1 DNA damage checkpoint activation [58]. An active checkpoint leads to Rev1 phosphorylation [86,87], possibly increasing TLS activity and progressively reducing the amount of RPA-covered ssDNA, thus promoting the switch off of the checkpoint itself.

In a wild type background, elegant time lapse experiments showed that after an acute low dose of UVC light (5 J/m^2) yeast cells do not delay cell cycle progression until they proceed through S phase; for this reason this response was called post-replication checkpoint [64]. With low levels of UV-induced lesions the NER

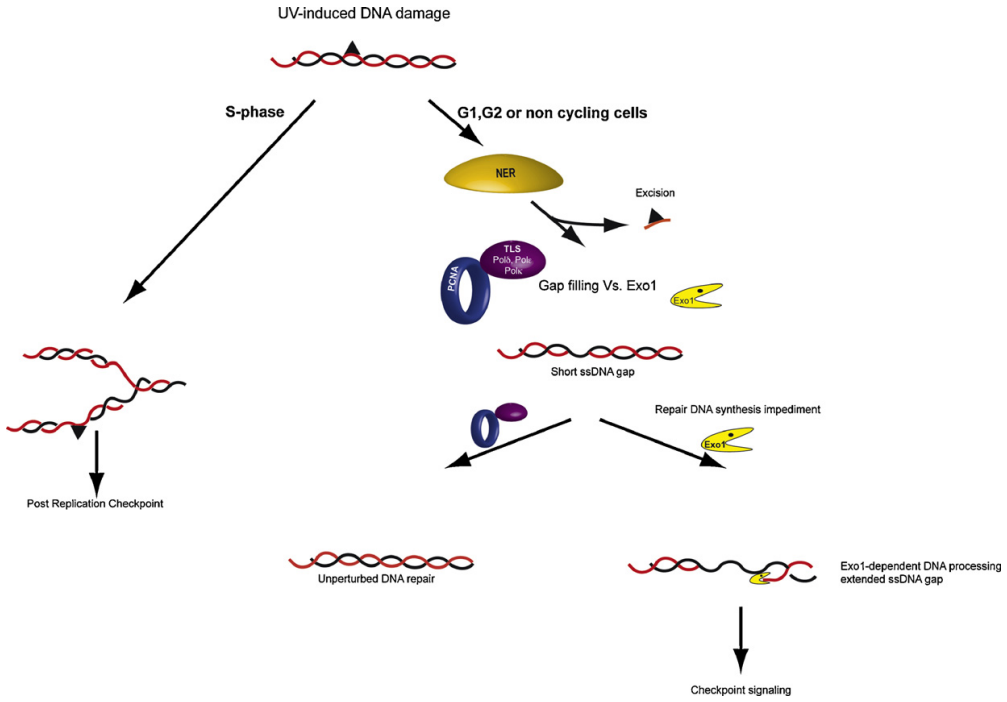

Fig. 2. UV-induced checkpoint response. In cells that are not replicating their genome (i.e., G1, G2 or non-cycling cells), NER removes UV lesions efficiently and DNA polymerases (i.e., pol δ, pol ε, TLS polymerases) begin the refilling process. If the repair reaction is impeded after the excision step, a competition between the refilling polymerases and Exo1 nuclease can take place. Problematic refilling (e.g., closely opposing lesions) allows Exo1 to further process the gapped intermediate generating long ssDNA gaps which recruit checkpoint factors and trigger the signaling. At low UV-doses G1 and G2 cells do not accumulate large ssDNA gaps since UV lesions can be efficiently removed by NER. If the damages are still present when the cell enters S phase, the replicative polymerase will be blocked by the bulky lesion and will reinitiate DNA synthesis further downstream, leaving ssDNA gaps behind the replication fork. These gaps can be refilled by post replication repair and trigger a post-replication checkpoint.

mechanism is very efficient and rapidly takes care of most lesions, so that neither the G1 or the G2 checkpoints are activated. The few lesions that are encountered by replicating polymerases in these conditions, on the other hand, block the replication fork and trigger a checkpoint response; this response may be detected in late S phase, when most replicons have completed duplication and the left-over ssDNA gaps need to be refilled (Fig. 2). An important point in this regard was made by irradiating budding yeast cells with very low ($0.18\,J\,m^{-2}\,min^{-1}$) chronic UV dose (CLUV): the only pathway necessary and sufficient to ensure cell survival was found to be the *RAD5*-dependent branch of PRR [65]. Indeed, NER deficient cells (*rad14Δ*) and DNA damage checkpoint deficient cells (*mec1Δ*) are not particularly sensitive to the CLUV treatment, contrary to the *rad18Δ* and *rad5Δ* cells, deficient in PRR [65], which irreversibly activate Mec1 DNA damage checkpoint and die in the G2 phase. In fact, S phase can be completed in the absence of PRR, but the gapped replicated DNA needs to be refilled by PRR in G2 in order to warrant cell survival [66,67].

In mammalian cells the situation is more complex, because NER acts also in S phase, where GG-NER is enhanced [88] and is stimulated by active ATR [89,90]. Indeed, ATR-deficient Seckel syndrome fibroblasts exhibit attenuation of S phase specific GG-NER and a similar effect has been detected in XPV skin fibroblasts, deficient in pol η [91]. Thus, in human cells both ATR-dependent DNA damage checkpoint and TLS influence S phase-specific GG-NER: defects in ATR or pol η may cause the abnormal persistence of ssDNA gaps opposite a template lesion and this would inhibit DNA adducts excision by GG-NER.

7. Recruitment of checkpoint factors by NER

In the last few years evidence has emerged that the role of NER in checkpoint activation is not limited to the generation of the ssDNA signal but, in addition, NER proteins seem to be involved in directly recruiting checkpoint factors to the proximity of DNA lesions.

In *S. cerevisiae*, a physical interaction was identified between Rad14 and both Ddc1 and Mec3, two subunits of the 9-1-1 checkpoint complex. Although the physiological relevance of this interaction has not been directly investigated further, association of Ddc1 and Ddc2 to UV-damaged chromosomes is lost in a *rad14Δ* strain, suggesting that the 9-1-1 complex may be initially recruited at the sites of DNA lesions by directly interacting with the key NER factor Rad14 [55].

Additional observations indicate that this mechanism is most likely conserved in higher eukaryotes. In human G1 cells the recruitment of the 9-1-1 complex onto damaged DNA is dependent on XPA and XPC proteins [92]; analogously, Cep164, a checkpoint mediator protein in the ATR signaling pathway required for Chk1 phosphorylation after UV damage, was shown to be recruited to CPD sites in a NER-dependent manner, through UV-induced physical interaction with XPA [93]. In addition, a role for NER in the activation of ATM after cisplatin treatment was discovered. Immunoprecipitation experiments revealed a physical interaction between ATM and NER factors and this association is required for ATM recruitment to DNA [94] (Fig. 3).

Combining the notion that processing of lesions by repair machineries is a pre-requisite for checkpoint activation outside of S phase, with the observation that checkpoint factors interact with

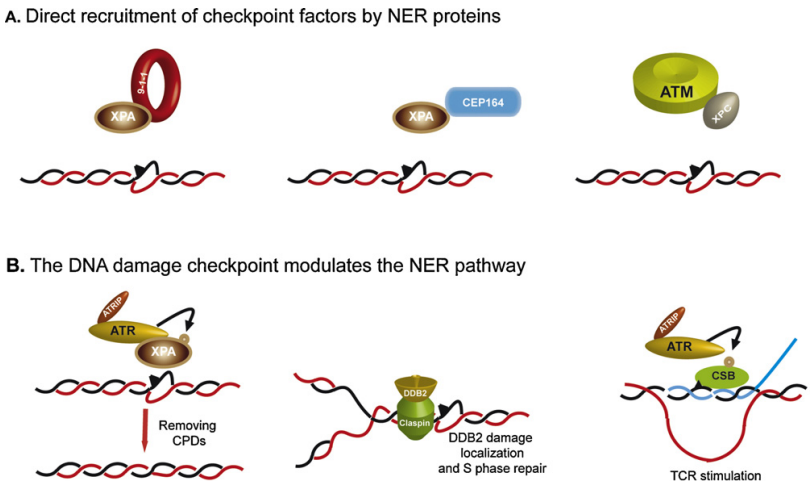

Fig. 3. Crosstalks between NER and checkpoint factors. A two-way functional interaction exists between the checkpoint machinery and the NER apparatus: some examples (discussed in the text) are shown. (A) NER factors recruit checkpoint proteins to damaged chromosomes, thus facilitating the activation of the signaling cascade. (B) DNA damage checkpoint factors modulate NER activity allowing for efficient repair of the lesions.

repair proteins depicts a model where the repair machinery, which is specialized for direct lesion recognition, increases the local concentration of checkpoint sensors on damaged chromosomal regions facilitating a robust checkpoint response.

Interestingly, a NER-independent mechanism for activating checkpoint kinases seems to exist in non cycling cells. If NER-deficient yeast cells are blocked in the G1 phase of the cell cycle, UV irradiated and held in non dividing conditions indefinitely, a delayed activation of the Mec1-dependent pathway has been reported [95,96]. Recent evidence indicates that UV-induced signaling may proceed via NER-independent mechanisms also in non-dividing mammalian cells likely through generation of DNA strand breaks [97].

8. NER modulation by checkpoint proteins

The interplay between NER and the DNA damage checkpoint is even more complex; in fact, while NER is involved in checkpoint activation, the checkpoint pathway actively stimulates NER by modulating cellular levels, localization and activity of NER factors, through transcriptional regulation, direct protein–protein interactions and post-translational modifications (Fig. 3).

The *S. cerevisiae* Rad9 gene product plays a role in the repair of both UV-damaged strands of an actively transcribed gene; this effect on NER is likely indirect and probably occurs through up-regulation of some NER genes (i.e., *RAD2*, *RAD7*, *RAD16* and *RAD23*), consistently with a previously reported Rad9-dependent stimulation of NER genes transcription [98]. Rad9 does not seem to be required for the repair of non-transcribed regions, suggesting that it is acting only when repair is coupled to transcription [8]. Along similar lines, Rad26, a NER factor critical for TC-NER, is a direct target of Mec1 kinase and its phosphorylation enhances TC-NER, possibly by stimulating its ATPase activity or by modulating its interaction with other TC-NER proteins [99]. Notably, CSB (the human orthologue of Rad26) was identified in a screen for putative ATM/ATR substrates [33], pointing to a conservation of this regulatory mechanism through evolution. Other NER factors were found in the same screening, namely XPA, XPC, RPA1 and RAD23B, but further characterization will be required to prove the significance of the interaction between ATM/ATR and the NER factors identified in the screen. Another example on the possible feedback of the checkpoint on NER is the regulation of XPA by ATR. It has been found that XPA nuclear import and its stable accumulation at nuclear foci after UV irradiation is dependent upon ATR. ATR also seems to be responsible for XPA phosphorylation after UV radiations, although this modification is not required for XPA foci formation [100–102]. Further studies will be required to firmly establish the role of ATR in the modulation of the XPA function. Finally, an S-phase specific role for the DNA damage checkpoint in regulating GG-NER was recently suggested. In particular, ATR inhibition was shown to specifically abrogate NER in S-phase, while the repair rate was unaffected in G1 and G2/M cells [89]. Another report revealed a role for the replication checkpoint mediator Claspin in regulating the DDB2 subunit of the UV-DDB factor, which is involved in the initial steps of GG-NER [103]. DDB2 is localized at the UV-induced DNA lesions, where its ubiquitination and subsequent degradation seems to control XPC recruitment and damage recognition, thus triggering the NER process [104]. Claspin knockdown affects DDB2 recruitment at damage sites and its subsequent ubiquitin-mediated degradation; in agreement with this observation, it has been shown that Claspin and DDB2 physically interact and their association is greatly enhanced upon UV irradiation [103].

9. Summary and perspectives

The complex interplay between NER and DNA damage checkpoints is not an isolate case in the DDR landscape, since in recent years a large cluster of papers highlighted the reciprocal interdependence of the checkpoint pathways and virtually all other known repair systems. It seems that, as a general rule, a two-way functional interaction exists between the checkpoint machinery and the repair apparatus. On one side, repair factors help to recruit checkpoint proteins at the damage sites onto DNA and, by modifying the primary lesions to RPA-covered ssDNA, trigger the checkpoint cascade; on the other side, once activated the checkpoint pathway stimulates the repair process mainly through direct protein–protein interactions or post-translational modifications. One of the key factors at the interface between checkpoint and repair is the 9-1-1 checkpoint clamp, and its involvement in such processes has been recently discussed [25].

The checkpoint response may be seen as a process that signals the cell that something that should have been working properly, has

instead some problem; the cell can thus deploy a set of measures to attempt to solve the problems and avoid further complications.

The data obtained with low acute UV doses suggest that if the lesions are not frequent enough to interfere with G1 or G2 processes, the cell has no way (or need) to acknowledge their presence and activate the checkpoint. Indeed, NER can easily keep these lesions under control. When these damage-containing chromosomes are replicated, though, the DNA polymerases scanning the genome will eventually detect them, and re-initiate DNA synthesis further downstream leaving behind ssDNA gaps. Since the region hosting a polymerase-blocking lesion can be almost completely replicated by an incoming fork starting from an adjacent origin, at low levels of lesions the gaps will accumulate and activate the checkpoint kinases toward the end of S phase. This event has a clear relevance since checkpoint mutants will die in this situation, and only after checkpoint activation the gaps are refilled by PRR and the lesions are actually removed from the chromosomes [61]. It has to be noted that a checkpoint response can be triggered in G1 cells, even at these low UV doses, if something interferes with completion of NER. Indeed, alterations in the refilling step of repair will sensitize G1 cells more than S phase cells [58].

At higher UV doses (>20 J/m^2), cells promptly respond also in non replicating conditions, consistently with the increased probability of repair problems arising. Repair DNA synthesis, in these situations, could be affected by the low level of dNTPs, by the formation of closely opposing lesions, by limiting level of particular factors in saturating conditions and by the higher possibility that lesions are generated in "difficult to repair" chromosomal locations. If the refilling reaction is problematic, nucleases like Exo1 have a greater chance to process the NER intermediates and elicit a checkpoint response [58].

What is surprising is what happens with chronic low UV doses (CLUV), which are supposed to best mimic sunlight exposure. Experiments performed in yeast cells have suggested that in CLUV conditions no checkpoint is activated, not even during S phase; indeed, checkpoint deficient strains do not exhibit sensitivity to CLUV treatment [62]. Even more surprisingly, NER is not important in these conditions, since NER-deficient cells are also not sensitive to CLUV. The possibility to extend these findings beyond yeast cells remains to be determined, indeed they seem to contrast with the situation observed in XP patients, who are deficient in NER and clearly hypersensitive to sunlight. In the future the actual events happening with sunlight exposure will need to be investigated.

NER is the most versatile repair system and eliminates a wide repertoire of DNA lesions, among which are UV-induced CPD and 6-4PP, that represent the main determinants in solar mutagenesis and skin cancer [105,106]. The importance of the findings summarized here may thus expand further than the problems related to exposure to UV light.

It is expected that genome-wide analysis of protein–protein interaction networks provided by high throughput screenings will progressively increase the number of known physical interactions between checkpoint proteins and repair factors, thus strengthening and expanding the model describing the functional connections between these two key genome stability pathways.

Conflicts of interest

The authors declare that there are no conflicts of interest.

Funding

Work in the authors' lab is supported by grants from AIRC, Fondazione Cariplo, MIUR and EU FP6 IP DNA Repair.

Acknowledgments

The authors apologize for the many interesting papers that they were not able to discuss or acknowledge. FP6 IP DNA Repair. F.L. is supported by Fondazione Adriano Buzzati-Traverso.

References

[1] X. Zhao, R. Rothstein, The Dun1 checkpoint kinase phosphorylates and regulates the ribonucleotide reductase inhibitor Sml1, Proc. Natl. Acad. Sci. U.S.A. 99 (2002) 3746–3751.
[2] R. Yao, Z. Zhang, et al., Subcellular localization of yeast ribonucleotide reductase regulated by the DNA replication and damage checkpoint pathways, Proc. Natl. Acad. Sci. U.S.A. 100 (2003) 6628–6633.
[3] V.I. Bashkirov, J.S. King, et al., DNA repair protein Rad55 is a terminal substrate of the DNA damage checkpoints, Mol. Cell. Biol. 20 (2000) 4393–4404.
[4] P. Ahnesorg, S.P. Jackson, The non-homologous end-joining protein Nej1p is a target of the DNA damage checkpoint, DNA Repair (Amst) 6 (2007) 190–201.
[5] S. Flott, C. Alabert, et al., Phosphorylation of Slx4 by Mec1 and Tel1 regulates the single-strand annealing mode of DNA repair in budding yeast, Mol. Cell. Biol. 27 (2007) 6433–6445.
[6] I. Morin, H.P. Ngo, et al., Checkpoint-dependent phosphorylation of Exo1 modulates the DNA damage response, EMBO J. 27 (2008) 2400–2410.
[7] W.C. Chou, H.C. Wang, et al., Chk2-dependent phosphorylation of XRCC1 in the DNA damage response promotes base excision repair, EMBO J. 27 (2008) 3140–3150.
[8] N.M. Al-Moghrabi, I.S. Al-Sharif, A. Aboussekhra, The RAD9-dependent gene trans-activation is required for excision repair of active genes but not for repair of non-transcribed DNA, Mutat. Res. 663 (2009) 60–68.
[9] A. Ciccia, S.J. Elledge, The DNA damage response: making it safe to play with knives, Mol. Cell 40 (2010) 179–204.
[10] S.W. Lowe, E.M. Schmitt, et al., p53 is required for radiation-induced apoptosis in mouse thymocytes, Nature 362 (1993) 847–849.
[11] Y. Xu, D. Baltimore, Dual roles of ATM in the cellular response to radiation and in cell growth control, Genes Dev. 10 (1996) 2401–2410.
[12] A. Hirao, Y.Y. Kong, et al., DNA damage-induced activation of p53 by the checkpoint kinase Chk2, Science 287 (2000) 1824–1827.
[13] M.B. Kastan, J. Bartek, Cell-cycle checkpoints and cancer, Nature 432 (2004) 316–323.
[14] C. Kerzendorfer, M. O'Driscoll, Human DNA damage response and repair deficiency syndromes: linking genomic instability and cell cycle checkpoint proficiency, DNA Repair (Amst) 8 (2009) 1139–1152.
[15] C.D. Putnam, E.J. Jaehnig, R.D. Kolodner, Perspectives on the DNA damage and replication checkpoint responses in *Saccharomyces cerevisiae*, DNA Repair (Amst) 8 (2009) 974–982.
[16] A. Sancar, L.A. Lindsey-Boltz, et al., Molecular mechanisms of mammalian DNA repair and the DNA damage checkpoints, Annu. Rev. Biochem. 73 (2004) 39–85.
[17] J.A. Melo, J. Cohen, D.P. Toczyski, Two checkpoint complexes are independently recruited to sites of DNA damage in vivo, Genes Dev. 15 (2001) 2809–3221.
[18] C.Y. Bonilla, J.A. Melo, D.P. Toczyski, Colocalization of sensors is sufficient to activate the DNA damage checkpoint in the absence of damage, Mol. Cell 30 (2008) 267–276.
[19] J. Majka, A. Niedziela-Majka, P.M. Burgers, The checkpoint clamp activates Mec1 kinase during initiation of the DNA damage checkpoint, Mol. Cell 24 (2006) 891–901.
[20] H. Wang, S.J. Elledge, Genetic and physical interactions between DPB11 and DDC1 in the yeast DNA damage response pathway, Genetics 160 (2002) 1295–1304.
[21] F. Puddu, M. Granata, et al., Phosphorylation of the budding yeast 9-1-1 complex is required for Dpb11 function in the full activation of the UV-induced DNA damage checkpoint, Mol. Cell. Biol. 28 (2008) 4782–4793.
[22] V.M. Navadgi-Patil, P.M. Burgers, Yeast DNA replication protein Dpb11 activates the Mec1/ATR checkpoint kinase, J. Biol. Chem. 283 (2008) 35853–35859.
[23] D.A. Mordes, E.A. Nam, D. Cortez, Dpb11 activates the Mec1-Ddc2 complex, Proc. Natl. Acad. Sci. U.S.A. 105 (2008) 18730–18734.
[24] V.M. Navadgi-Patil, P.M. Burgers, A tale of two tails: activation of DNA damage checkpoint kinase Mec1/ATR by the 9-1-1 clamp and by Dpb11/TopBP1, DNA Repair (Amst) 8 (2009) 996–1003.
[25] F. Lazzaro, M. Giannattasio, et al., Checkpoint mechanisms at the intersection between DNA damage and repair, DNA Repair (Amst) 8 (2009) 1055–1067.
[26] Y. Sanchez, J. Bachant, et al., Control of the DNA damage checkpoint by Chk1 and Rad53 protein kinases through distinct mechanisms, Science 286 (1999) 1166–1171.
[27] J. Bartek, J. Lukas, Chk1 and Chk2 kinases in checkpoint control and cancer, Cancer Cell 3 (2003) 421–429.
[28] F.D. Sweeney, F. Yang, et al., *Saccharomyces cerevisiae* Rad9 acts as a Mec1 adaptor to allow Rad53 activation, Curr. Biol. 15 (2005) 1364–1375.
[29] C.S. Gilbert, C.M. Green, N.F. Lowndes, Budding yeast Rad9 is an ATP-dependent Rad53 activating machine, Mol. Cell 8 (2001) 129–136.

[30] R.T. Blankley, D. Lydall, A domain of Rad9 specifically required for activation of Chk1 in budding yeast, J. Cell Sci. 117 (2004) 601–608.
[31] J.E. FitzGerald, M. Grenon, N.F. Lowndes, 53BP1: function and mechanisms of focal recruitment, Biochem. Soc. Trans. 37 (2009) 897–904.
[32] M.B. Smolka, C.P. Albuquerque, et al., Proteome-wide identification of in vivo targets of DNA damage checkpoint kinases, Proc. Natl. Acad. Sci. U.S.A. 104 (2007) 10364–10369.
[33] S. Matsuoka, B.A. Ballif, et al., ATM and ATR substrate analysis reveals extensive protein networks responsive to DNA damage, Science 316 (2007) 1160–1166.
[34] W. Siede, A.S. Friedberg, E.C. Friedberg, Rad9-dependent-G(1) arrest defines a second checkpoint for damaged DNA in the cell-cycle of *Saccharomyces cerevisiae*, Proc. Natl. Acad. Sci. U.S.A. 90 (1993) 7985–7989.
[35] A.G. Paulovich, L.H. Hartwell, A checkpoint regulates the rate of progression through S-phase in *Saccharomyces cerevisiae* in response to DNA-damage, Cell 82 (1995) 841–847.
[36] T.A. Weinert, L.H. Hartwell, The RAD9 gene controls the cell cycle response to DNA damage in *Saccharomyces cerevisiae*, Science 241 (1988) 317–322.
[37] K.K. Khanna, M.F. Lavin, Ionizing-radiation and UV induction of p53 protein by different pathways in ataxia–telangiectasia cells, Oncogene 8 (1993) 3307–3312.
[38] R.S. Tibbetts, K.M. Brumbaugh, et al., A role for ATR in the DNA damage-induced phosphorylation of p53, Genes Dev. 13 (1999) 152–157.
[39] C.E. Canman, D.S. Lim, et al., Activation of the ATM kinase by ionizing radiation and phosphorylation of p53, Science 281 (1998) 1677–1679.
[40] C.A. Lovejoy, D. Cortez, Common mechanisms of PIKK regulation, DNA Repair (Amst) 8 (2009) 1004–1008.
[41] A. Jazayeri, J. Falck, et al., ATM- and cell cycle-dependent regulation of ATR in response to DNA double-strand breaks, Nat. Cell Biol. 8 (2006) 37–45.
[42] K.E. Adams, A.L. Medhurst, et al., Recruitment of ATR to sites of ionising radiation-induced DNA damage requires ATM and components of the MRN protein complex, Oncogene 25 (2006) 3894–3904.
[43] D.M. Morrow, D.A. Tagle, et al., TEL1, an *S. cerevisiae* homolog of the human gene mutated in ataxia telangiectasia, is functionally related to the yeast checkpoint gene, MEC1, Cell 82 (1995) 831–840.
[44] L. Zou, S.J. Elledge, Sensing DNA damage through ATRIP recognition of RPA–ssDNA complexes, Science 300 (2003) 1542–1548.
[45] L. Zou, D. Liu, S.J. Elledge, Replication protein A-mediated recruitment and activation of Rad17 complexes, Proc. Natl. Acad. Sci. U.S.A. 100 (2003) 13827–13832.
[46] J.C. Harrison, J.E. Haber, Surviving the breakup: the DNA damage checkpoint, Annu. Rev. Genet. 40 (2006) 209–235.
[47] E. Weterings, D.J. Chen, The endless tale of non-homologous end-joining, Cell Res. 18 (2008) 114–124.
[48] E.C. Friedberg, G.C. Walker, W. Siede, DNA repair and mutagenesis, ASM Press, Washington, D.C., 2006.
[49] L. Staresincic, A.F. Fagbemi, et al., Coordination of dual incision and repair synthesis in human nucleotide excision repair, EMBO J. 28 (2009) 1111–1120.
[50] M.S. Luijsterburg, G. von Bornstaedt, et al., Stochastic and reversible assembly of a multiprotein DNA repair complex ensures accurate target site recognition and efficient repair, J. Cell Biol. 189 (2010) 445–463.
[51] M. Lopes, M. Foiani, J.M. Sogo, Multiple mechanisms control chromosome integrity after replication fork uncoupling and restart at irreparable UV lesions, Mol. Cell 21 (2006) 15–27.
[52] G. Jiang, A. Sancar, Recruitment of DNA damage checkpoint proteins to damage in transcribed and nontranscribed sequences, Mol. Cell. Biol. 26 (2006) 39–49.
[53] R.D. Bomgarden, P.J. Lupardus, et al., Opposing effects of the UV lesion repair protein XPA and UV bypass polymerase eta on ATR checkpoint signaling, EMBO J. 25 (2006) 2605–2614.
[54] M. O'Driscoll, V.L. Ruiz-Perez, et al., A splicing mutation affecting expression of ataxia–telangiectasia and Rad3-related protein (ATR) results in Seckel syndrome, Nat. Genet. 33 (2003) 497–501.
[55] M. Giannattasio, F. Lazzaro, et al., Physical and functional interactions between nucleotide excision repair and DNA damage checkpoint, EMBO J. 23 (2004) 429–438.
[56] F. Marini, T. Nardo, et al., DNA nucleotide excision repair-dependent signaling to checkpoint activation, Proc. Natl. Acad. Sci. U.S.A. 103 (2006) 17325–17330.
[57] T.M. Marti, E. Hefner, et al., H2AX phosphorylation within the G1 phase after UV irradiation depends on nucleotide excision repair and not DNA double-strand breaks, Proc. Natl. Acad. Sci. U.S.A. (2006).
[58] H. Neecke, G. Lucchini, M.P. Longhese, Cell cycle progression in the presence of irreparable DNA damage is controlled by a Mec1- and Rad53-dependent checkpoint in budding yeast, EMBO J. 18 (1999) 4485–4497.
[59] J.A. Marteijn, S. Bekker-Jensen, et al., Nucleotide excision repair-induced H2A ubiquitination is dependent on MDC1 and RNF8 and reveals a universal DNA damage response, J. Cell Biol. 186 (2009) 835–847.
[60] D. Nakada, Y. Hirano, K. Sugimoto, Requirement of the Mre11 complex and exonuclease 1 for activation of the Mec1 signaling pathway, Mol. Cell. Biol. 24 (2004) 10016–10025.
[61] M. Giannattasio, C. Follonier, et al., Exo1 competes with repair synthesis, converts NER intermediates to long ssDNA gaps, and promotes checkpoint activation, Mol. Cell 40 (2010) 50–62.
[62] P.T. Tran, N. Erdeniz, et al., EXO1-A multi-tasking eukaryotic nuclease, DNA Repair (Amst) 3 (2004) 1549–1559.
[63] M. Matsumoto, K. Yaginuma, et al., Perturbed gap-filling synthesis in nucleotide excision repair causes histone H2AX phosphorylation in human quiescent cells, J. Cell Sci. 120 (2007) 1104–1112.
[64] A.J. Callegari, T.J. Kelly, UV irradiation induces a postreplication DNA damage checkpoint, Proc. Natl. Acad. Sci. U.S.A. 103 (2006) 15877–15882.
[65] T. Hishida, Y. Kubota, et al., RAD6-RAD18-RAD5-pathway-dependent tolerance to chronic low-dose ultraviolet light, Nature 457 (2008) 612–615.
[66] G.I. Karras, S. Jentsch, The RAD6 DNA damage tolerance pathway operates uncoupled from the replication fork and is functional beyond S phase, Cell 141 (2010) 255–267.
[67] Y. Daigaku, A.A. Davies, H.D. Ulrich, Ubiquitin-dependent DNA damage bypass is separable from genome replication, Nature 465 (2010) 951–955.
[68] L. Stergiou, R. Eberhard, et al., NER and HR pathways act sequentially to promote UV-C-induced germ cell apoptosis in Caenorhabditis elegans, Cell Death Differ. 18 (2011) 897–906.
[69] A.J. Callegari, E. Clark, et al., Postreplication gaps at UV lesions are signals for checkpoint activation, Proc. Natl. Acad. Sci. U.S.A. 107 (2010) 8219–8224.
[70] T. Ogi, A.R. Lehmann, The Y-family DNA polymerase kappa (pol kappa) functions in mammalian nucleotide-excision repair, Nat. Cell Biol. 8 (2006) 640–642.
[71] T. Ogi, S. Limsirichaikul, et al., Three DNA polymerases, recruited by different mechanisms, carry out NER repair synthesis in human cells, Mol. Cell 37 (2010) 714–727.
[72] B.A. Bridges, G.M. Brown, Mutagenic DNA repair in *Escherichia coli*. XXI. A stable SOS-inducing signal persisting after excision repair of ultraviolet damage, Mutat. Res. 270 (1992) 135–144.
[73] K. Minton, E.C. Friedberg, Letter: evidence for clustering of pyrimidine dimers on opposite strands of U.V.-irradiated bacteriophage DNA, Int. J. Radiat. Biol. Relat. Stud. Phys. Chem. Med. 26 (1974) 81–85.
[74] L.H. Lam, R.J. Reynolds, Bifilar enzyme-sensitive sites in ultraviolet-irradiated DNA are indicative of closely opposed cyclobutyl pyrimidine dimers, Biophys. J. 50 (1986) 307–317.
[75] E. Sage, E. Cramb, B.W. Glickman, The distribution of UV damage in the lacI gene of *Escherichia coli* – correlation with mutation spectrum, Mutat. Res. 269 (1992) 285–299.
[76] L.H. Lam, R.J. Reynolds, A sensitive, enzymatic assay for the detection of closely opposed cyclobutyl pyrimidine dimers induced in human diploid fibroblasts, Mutat. Res. 166 (1986) 187–198.
[77] L.H. Lam, R.J. Reynolds, Repair of closely opposed cyclobutyl pyrimidine dimers in UV-sensitive human diploid fibroblasts, Mutat. Res. 166 (1986) 199–205.
[78] L.H. Lam, R.J. Reynolds, DNA sequence dependence of closely opposed cyclobutyl pyrimidine dimers induced by UV radiation, Mutat. Res. 178 (1987) 167–176.
[79] D.L. Svoboda, C.A. Smith, et al., Effect of sequence, adduct type, and opposing lesions on the binding and repair of ultraviolet photodamage by DNA photolyase and (A)BC excinuclease, J. Biol. Chem. 268 (1993) 10694–10700.
[80] F. Eckardt, S.J. Teh, R.H. Haynes, Heteroduplex repair as an intermediate step of UV mutagenesis in yeast, Genetics 95 (1980) 63–80.
[81] B.A. Bridges, R. Mottershead, $RecA^+$-dependent mutagenesis occurring before DNA replication in UV- and -γ irradiated *Escherichia coli*, Mutat. Res. 13 (1971) 1–8.
[82] W.D. Rupp, P. Howard-Flanders, Discontinuities in the DNA synthesized in an excision-defective strain of *Escherichia coli* following ultraviolet irradiation, J. Mol. Biol. 31 (1968) 291–304.
[83] A.R. Lehmann, Post-replication repair of DNA in ultraviolet-irradiated mammalian cells. No gaps in DNA synthesized late after ultraviolet irradiation, Eur. J. Biochem. 31 (1972) 438–445.
[84] L. di Caprio, B.S. Cox, DNA synthesis in UV-irradiated yeast, Mutat. Res. 82 (1981) 69–85.
[85] L. Prakash, Characterization of postreplication repair in *Saccharomyces cerevisiae* and effects of rad6, rad18, rev3 and rad52 mutations, Mol. Gen. Genet. 184 (1981) 471–478.
[86] V. Pagès, S.R. Santa Maria, et al., Role of DNA damage-induced replication checkpoint in promoting lesion bypass by translesion synthesis in yeast, Genes Dev. 23 (2009) 1438–1449.
[87] S. Sabbioneda, I. Bortolomai, et al., Yeast Rev1 is cell cycle regulated, phosphorylated in response to DNA damage and its binding to chromosomes is dependent upon MEC1, DNA Repair (Amst) 6 (2007) 121–127.
[88] A. Gospodinov, B. Anachkova, Cells synchronized in S phase show increased rate of repair of UV damaged plasmids, FEBS Lett. 572 (2004) 99–102.
[89] Y. Auclair, R. Rouget, et al., ATR kinase is required for global genomic nucleotide excision repair exclusively during S phase in human cells, Proc. Natl. Acad. Sci. U.S.A. 105 (2008) 17896–17901.
[90] Y. Auclair, R. Rouget, E.A. Drobetsky, ATR kinase as master regulator of nucleotide excision repair during S phase of the cell cycle, Cell Cycle 8 (2009) 1865–1871.
[91] Y. Auclair, R. Rouget, et al., Requirement for functional DNA polymerase eta in genome-wide repair of UV-induced DNA damage during S phase, DNA Repair (Amst) 9 (2010) 754–764.
[92] D.O. Warmerdam, R. Freire, et al., Cell cycle-dependent processing of DNA lesions controls localization of Rad9 to sites of genotoxic stress, Cell Cycle 8 (2009) 1765–1774.

[93] Y.R. Pan, E.Y. Lee, UV-dependent interaction between Cep164 and XPA mediates localization of Cep164 at sites of DNA damage and UV sensitivity, Cell Cycle 8 (2009) 655–664.
[94] S.L. Colton, X.S. Xu, et al., The involvement of ataxia–telangiectasia mutated protein activation in nucleotide excision repair-facilitated cell survival with cisplatin treatment, J. Biol. Chem. 281 (2006) 27117–27125.
[95] H. Zhang, J. Taylor, W. Siede, Checkpoint arrest signaling in response to UV damage is independent of nucleotide excision repair in *Saccharomyces cerevisiae*, J. Biol. Chem. 278 (2003) 9382–9387.
[96] M. Giannattasio, F. Lazzaro, et al., DNA decay and limited Rad53 activation after liquid holding of UV-treated nucleotide excision repair deficient *S. cerevisiae* cells, DNA Repair (Amst) 3 (2004) 1591–1599.
[97] M.G. Vrouwe, A. Pines, et al., UV-induced photolesions elicit ATR-kinase-dependent signaling in non-cycling cells through nucleotide excision repair-dependent and -independent pathways, J. Cell Sci. 124 (2011) 435–446.
[98] N.M. Al-Moghrabi, I.S. Al-Sharif, A. Aboussekhra, The *Saccharomyces cerevisiae* RAD9 cell cycle checkpoint gene is required for optimal repair of UV-induced pyrimidine dimers in both G(1) and G(2)/M phases of the cell cycle, Nucleic Acids Res. 29 (2001) 2020–2025.
[99] M. Taschner, M. Harreman, et al., A role for checkpoint kinase-dependent Rad26 phosphorylation in transcription-coupled DNA repair in *Saccharomyces cerevisiae*, Mol. Cell. Biol. 30 (2010) 436–446.
[100] X. Wu, S.M. Shell, et al., Phosphorylation of nucleotide excision repair factor xeroderma pigmentosum group A by ataxia telangiectasia mutated and Rad3-related-dependent checkpoint pathway promotes cell survival in response to UV irradiation, Cancer Res. 66 (2006) 2997–3005.
[101] S.M. Shell, Z. Li, et al., Checkpoint kinase ATR promotes nucleotide excision repair of UV-induced DNA damage via physical interaction with xeroderma pigmentosum group A, J. Biol. Chem. 284 (2009) 24213–24222.
[102] X. Wu, S.M. Shell, et al., ATR-dependent checkpoint modulates XPA nuclear import in response to UV irradiation, Oncogene 26 (2007) 757–764.
[103] M. Praetorius-Ibba, Q.E. Wang, et al., Role of Claspin in regulation of nucleotide excision repair factor DDB2, DNA Repair (Amst) 6 (2007) 578–587.
[104] M.A. El-Mahdy, Q. Zhu, et al., Cullin 4A-mediated proteolysis of DDB2 protein at DNA damage sites regulates in vivo lesion recognition by XPC, J. Biol. Chem. 281 (2006) 13404–13411.
[105] D.E. Brash, J.A. Rudolph, et al., A role for sunlight in skin-cancer – UV-induced p53 mutations in squamous-cell carcinoma, Proc. Natl. Acad. Sci. U.S.A. 88 (1991) 10124–10128.
[106] S. Tornaletti, G.P. Pfeifer, Slow repair of pyrimidine dimers at p53 mutation hotspots in skin-cancer, Science 263 (1994) 1436–1438.

Published paper III

Lazzaro, F., Novarina, D., Amara, F., Watt, D. L., Stone, J. E., Costanzo, V., Burgers, P. M., Kunkel, T. A., Plevani, P. and Muzi-Falconi, M.

RNase H and Postreplication Repair protect cells from ribonucleotides incorporated in DNA.

Published in: Molecular Cell, **2012**, 45, 99–110.

Molecular Cell
Article

RNase H and Postreplication Repair Protect Cells from Ribonucleotides Incorporated in DNA

Federico Lazzaro,[1] Daniele Novarina,[1] Flavio Amara,[1] Danielle L. Watt,[2] Jana E. Stone,[2] Vincenzo Costanzo,[3] Peter M. Burgers,[4] Thomas A. Kunkel,[2] Paolo Plevani,[1,*] and Marco Muzi-Falconi[1,*]
[1]Dipartimento di Scienze Biomolecolari e Biotecnologie, Università degli Studi di Milano, 20133 Milano, Italy
[2]Laboratory of Structural Biology and Laboratory of Molecular Genetics, National Institute of Environmental Health Sciences, National Institutes of Health, DHHS, Research Triangle Park, NC 27709, USA
[3]Genome Stability Unit, Clare Hall Laboratories, London Research Institute, Cancer Research UK, South Mimms, Hertfordshire EN6 3LD, UK
[4]Department of Biochemistry and Molecular Biophysics, Washington University School of Medicine, St. Louis, MO 63110, USA
*Correspondence: paolo.plevani@unimi.it (P.P.), marco.muzifalconi@unimi.it (M.M.-F.)
DOI 10.1016/j.molcel.2011.12.019

SUMMARY

The chemical identity and integrity of the genome is challenged by the incorporation of ribonucleoside triphosphates (rNTPs) in place of deoxyribonucleoside triphosphates (dNTPs) during replication. Misincorporation is limited by the selectivity of DNA replicases. We show that accumulation of ribonucleoside monophosphates (rNMPs) in the genome causes replication stress and has toxic consequences, particularly in the absence of RNase H1 and RNase H2, which remove rNMPs. We demonstrate that postreplication repair (PRR) pathways—*MMS2*-dependent template switch and Pol ζ-dependent bypass—are crucial for tolerating the presence of rNMPs in the chromosomes; indeed, we show that Pol ζ efficiently replicates over 1–4 rNMPs. Moreover, cells lacking RNase H accumulate mono- and polyubiquitylated PCNA and have a constitutively activated PRR. Our findings describe a crucial function for RNase H1, RNase H2, template switch, and translesion DNA synthesis in overcoming rNTPs misincorporated during DNA replication, and may be relevant for the pathogenesis of Aicardi-Goutières syndrome.

INTRODUCTION

The integrity of the eukaryotic cellular genome is preserved by surveillance mechanisms that coordinate DNA replication, repair, and recombination with cell-cycle progression (Muzi-Falconi et al., 2003; Lazzaro et al., 2009). The DNA nature of the chromosomes provides for an intrinsic stability as opposed to the fragility of RNA, which is due to the higher reactivity of ribose compared to deoxyribose. The incorporation of ribonucleotides (rNTPs) in place of deoxyribonucleotides (dNTPs) within genomic DNA is generally avoided by the high selectivity of DNA polymerases, largely due to a steric gate residue in the polymerase active site (Joyce, 1997). However, there are occasions when rNTPs can be linked to DNA chains, such as during the synthesis of Okazaki fragments or possibly during repair of double strand DNA breaks in G1 (Nick McElhinny and Ramsden, 2003; Zhu and Shuman, 2008). Recent work indicates that during normal DNA replication, DNA polymerases can also incorporate rNTPs in place of dNTPs (Nick McElhinny et al., 2010b). rNMPs embedded in DNA are expected to represent a problem for cycling cells, sensitizing the DNA backbone to spontaneous and/or enzymatic nicking. Indeed, the presence of rNMPs in the yeast genome elevates the rate of short deletions in repeated sequences through a mechanism depending on topoisomerase I (Nick McElhinny et al., 2010a; Clark et al., 2011; Kim et al., 2011). Furthermore, the presence of rNMPs alters DNA helix parameters. For example, structural studies (Egli et al., 1993; Jaishree et al., 1993; Ban et al., 1994a; Ban et al., 1994b; Wahl and Sundaralingam, 2000) indicate that rNMPs in dsDNA alter global conformation from B- to A-form, with most of the sugars adopting C3′-endo or closely related conformations. rNMPs must be removed prior to the next cell cycle or they will pose problems during subsequent rounds of replication; in fact, efficient and accurate synthesis by replicative DNA polymerases strongly depends on helix geometry, such that changes in sugar pucker could render a primer terminus more difficult to extend. Indeed, a recent study has shown that single rNMPs in DNA templates impede DNA synthesis by the yeast replicases (Watt et al., 2011). Altered helix geometry may be less problematic for polymerases specialized for translesion synthesis, e.g., DNA polymerase ζ, which can efficiently extend aberrant primer termini (Prakash et al., 2005). An important question is thus how cells cope with replicating chromosomes containing rNMPs that escape repair.

RNase H is a family of enzymes that cleave the RNA moiety in RNA:DNA hybrids, allowing the reconstruction of a dsDNA molecule. Eukaryotic cells possess RNase H1 and RNase H2 activities that have partially overlapping substrate specificity. While RNase H1 requires at least a tract of four rNMPs to cleave, RNase H2 can incise 5′ to a single rNMP incorporated within a DNA molecule (Cerritelli and Crouch, 2009). The in vivo roles of RNase H in eukaryotic cells are still not fully understood. In mammalian cells, RNase H1 is essential for mitochondrial DNA replication (Cerritelli et al., 2003); such function is not conserved in budding yeast cells. The role of the nuclear population of RNase H1 is still not clear. RNase H2 represents the major

RNase H activity in eukaryotic cells and is involved in several cellular processes (Cerritelli and Crouch, 2009). Evidence indicates that these enzymes can process Okazaki fragments during replication although, at least in budding yeast, such activity is redundant and Okazaki fragment processing can be carried out by Rad27 and Dna2 (Rydberg and Game, 2002; Ayyagari et al., 2003). Furthermore, removal of R-loops, which accumulate when a transcription bubble collides with a replication fork, can be achieved by overexpressing RNase H (Huertas and Aguilera, 2003). Mutations in any of the three subunits of human RNase H2 are the molecular cause of a human genetic syndrome known as Aicardi-Goutières syndrome (AGS) (Crow et al., 2006a). The mechanism(s) involved in the pathogenesis of AGS is under intense investigation but still uncertain (Crow et al., 2006b; Yang et al., 2007; Stetson et al., 2008; Rice et al., 2009; Crow and Rehwinkel, 2009).

Another enzyme that processes rNMPs in DNA is topoisomerase I. It was recently reported that, in the absence of RNase H2, rNTPs incorporated in DNA are targeted by topoisomerase I, which cleaves but fails to rejoin the DNA backbone, generating a ssDNA break (Sekiguchi and Shuman, 1997; Kim et al., 2011). Interestingly, not all genomic rNMPs are topoisomerase I targets (Kim et al., 2011), and cells lacking RNase H2 do not exhibit growth defects, suggesting that cells must have other pathways allowing them to replicate rNMP-containing chromosomes.

In this work, we investigate the processes permitting yeast cells to survive in the presence of elevated rNTPs incorporated within genomic DNA. We show that both RNase H1 and RNase H2 play a critical role in repairing rNMPs incorporated by replicative polymerases, and in the absence of RNase H activity residual genomic rNMPs cause replication problems in the following cell cycle. When the replicative DNA polymerases encounter rNMPs in the template strand, endogenous replication stress is generated, which sensitizes cells to mild treatments with exogenous replication stress-inducing agents. In this situation, postreplication repair mechanisms are effectively responsible for the survival of RNase H defective cells. We provide genetic and biochemical evidence that rNMPs-containing chromosomes can be fully replicated through the action of template switch and DNA polymerase ζ, which efficiently bypasses rNMPs in a DNA template.

Our data show unexpected mechanisms that preserve genome integrity in normally replicating cells, extend the role of PRR, and particularly that of Pol ζ, to the replication of rNMPs in genomic DNA, and reveal a synthetic interaction between PRR, RNase H activities, and replication stress that may have relevant consequences for human disease, identifying a possible family of modifier genes that may influence the penetrance of a set of AGS mutations.

RESULTS

Unrepaired rNMPs Incorporated in Genomic DNA during Replication Sensitize Cells to Replication Stress-Inducing Agents

The preferential incorporation of dNTPs over that of rNTPs is at least partially provided by a steric gate that prevents replicative DNA polymerases from using rNTPs during the elongation step (Joyce, 1997). Nonetheless, budding yeast DNA polymerase ε has been demonstrated (Nick McElhinny et al., 2010b) to incorporate large numbers of rNTPs into DNA. This effect is exacerbated in a Pol ε variant, Pol2-M644G, where a methionine adjacent to the steric gate residue (Y645) has been changed to glycine (Nick McElhinny et al., 2010a). A *pol2-M644G rnh201Δ* strain, where the mutation in Pol ε is combined with inactivation of RNase H2, which has been implicated in processing of rNMPs incorporated during DNA synthesis, exhibits slower progression through S phase (Nick McElhinny et al., 2010a), coupled to phosphorylated Rad53 checkpoint kinase (Figure S1C), suggestive of increased replication stress.

Low levels of replication stress-inducing agents (HU or MMS) are known to be toxic for cells with replication problems. To test whether the presence of rNMPs in the template strand affected DNA replication, we plated *pol2-M644G rnh201Δ* cells on medium containing low doses of HU or MMS, which in wild-type cells only mildly slow down cell-cycle progression. Figure 1A shows that a combination of the *pol2-M644G* and *rnh201Δ* mutations, leading to accumulation of elevated levels of rNMPs in genomic DNA, causes high sensitivity to low levels of HU and MMS (see also Figure S5 for quantitative survival data). Interestingly, loss of RNase H1 alone does not sensitize *pol2-M644G* cells to HU or MMS (Figure 1A). These phenotypes can be explained by the fact that, even though the substrate specificity of RNase H1 partially overlaps with that of RNase H2, and both enzymes cleave DNA containing four or more consecutive rNMPs, only RNase H2 cleaves at single rNMPs (Cerritelli and Crouch, 2009). These observations suggest that the presence of large amounts of single rNMPs within chromosomal DNA generates endogenous replication stress. When both RNase H1 and H2 enzymes are inactivated, virtually all single and multiple rNMPs incorporated during DNA synthesis will persist until the next round of replication. Strikingly, *pol2-M644G rnh201Δ* is synthetic lethal with the absence of RNase H1 (Figure 1B), indicating that RNase H1 plays an important role in repairing the rNTPs incorporated by Pol ε.

RNase H1 Cooperates with RNase H2 in the Removal of rNMPs from the Chromosomes Preserving Genome Integrity

The critical role of both RNase H enzymes is supported by the fact that double mutant *rnh1Δ rnh201Δ*, *rnh1Δ rnh202Δ*, and *rnh1Δ rnh203Δ* cells (*RNH202* and *RNH203* encode the two noncatalytic subunits of RNase H2) are sensitive to low levels of replication stress even in the presence of normal replicases (Figure 1C). Microscopic observation revealed that *rnh1Δ rnh201Δ* cells form small and irregular microcolonies on plates containing 25 mM HU while wild-type cells generate a regular colony (Figure 1D). FACS analysis of synchronous cultures incubated with low levels of HU or MMS shows that cells lacking RNase H arrest in G2-M after the bulk of genome replication has been completed (Figures 1E and S1A), and western blot analysis of Rad53 kinase revealed that mutant cells accumulate hyperphosphorylated Rad53 (Figures 1F and S1B). It is worth noting that cycling cells of mutants that accumulate elevated rNMP levels in the genome exhibit a constitutively phosphorylated Rad53, indicative of

Molecular Cell

RNase H and PRR Protect from Chromosomal rNMPs

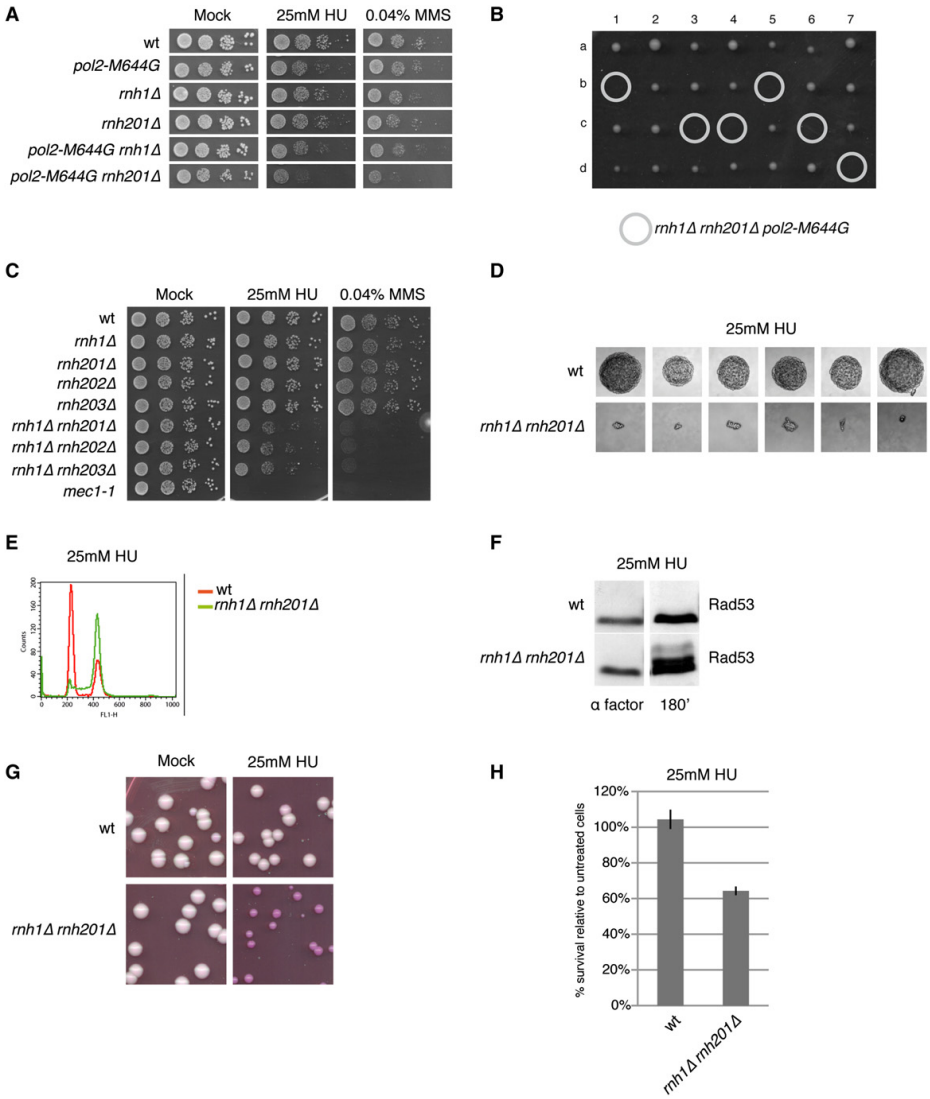

Figure 1. Abundant Incorporation of rNTPs into DNA Sensitizes Cells to Replication Stress and Is Lethal in Cells Lacking RNase H

(A) To test sensitivity to sublethal doses of HU or MMS, 10-fold serial dilutions of the indicated mutant strains were plated on YPD, YPD + 25 mM HU and YPD + 0.04% MMS. Pictures were taken after 3 days of incubation.

(B) Tetrads derived from a cross between *rnh1Δ rnh201Δ* and *rnh1Δ pol2-M644G* were dissected on YPD plates. Seven tetrads (1–7) are shown. The circles on the figure indicate the position of the original *rhn1Δ rnh201Δ pol2-M644G* spores.

(C) Sensitivity to HU and MMS of the indicated strains was tested as described in (A). A checkpoint-defective *mec1-1* strain was included as a positive control.

(D) Single cells were isolated on YPD plates and grown for 22 hr in the presence of 25 mM HU; colonies were visualized by microscopic analysis.

(E and F) wild-type and *rnh1Δ rn201Δ* cells were released in 25 mM HU after α factor arrest. After 180 min, cultures were analyzed by FACS, for DNA contents, and cell extracts were tested by western blotting with anti-Rad53 antibodies.

(G) Wild-type and *rnh1Δ rnh201Δ* cells were plated on YPD with or without 25 mM HU in the presence of Phloxine B, which stains in red colonies containing dead cells.

(H) Quantification of cell survival was obtained by plating G1 synchronized cells (100 cells per plate) on dishes containing 25 mM HU or mock. Colonies were counted after 3 days of incubation. The graph is representative of three independent experiments. Error bars describe standard deviation.

chronic replication stress (Figure S1C). These findings indicate that low doses of HU lead *rnh1Δ rnh201Δ* cells to block at the mitotic checkpoint and cause massive cell lethality, as suggested by the rugged shape of the microcolonies (Figure 1D) and further demonstrated by the fact that the small colonies eventually growing on 25 mM HU contain a large proportion of dead cells, which are stained by Phloxine B (Figure 1G). To estimate the extent of such lethality, we plated wild-type and *rnh1Δ rnh201Δ* cells in the absence or presence of 25 mM HU and calculated the percent survival on HU. Three independent experiments confirmed 40% lethality in cells lacking RNase H and exposed to low doses of HU (Figure 1H). Quantitative survival data for all the strains used throughout this study are shown in Figure S5. To test whether Rad53 phosphorylation and loss of cell viability derive from enzymatic processing of rNMP-containing DNA followed by chromosome breakage, we monitored phosphorylation of histone H2A on S129, a marker of DNA damage. Figure S1D shows that exposure of *rnh1Δ rnh201Δ* cultures to 25 mM HU does not induce H2A phosphorylation, suggesting that these cells do not accumulate double strand breaks, even when challenged with HU.

The sensitivity to HU observed upon loss of RNase H is unlikely to be due to the role of RNase H in Okazaki fragment processing or to a possible involvement in R-loop metabolism. Indeed, *rad27* mutated cells, which accumulate unprocessed Okazaki fragments (Ayyagari et al., 2003), are not sensitive to replication stress (Figure S2A). Moreover, combining *rnh1Δ rnh201Δ* with a mutation in *HPR1* gene, which leads to the accumulation of R-loops (Huertas and Aguilera, 2003), does not increase sensitivity to 25 mM HU and actually seems to mildly suppress the *rnh1Δ rnh201Δ* phenotype at this low dose, even though the mechanism is not known (Figure S2B). These findings strongly support the notion that RNase H activity is important to keeping genomic DNA free from rNMPs incorporated by DNA polymerases during replication and that sensitivity to replication stress-inducing drugs is a valid assay to track this process.

Survival of Cells with rNMPs-Containing Chromosomes Requires Translesion DNA Synthesis and Template Switch PRR Pathways

The survival of cells lacking RNase H activities indicates that yeast must have additional mechanisms to cope with the incorporation of rNTPs into the genome.

We investigated whether nucleotide excision repair (NER) or base excision repair (BER) play a role in the removal of rNMPs from the chromosomes. Abolishing NER (*rad14Δ*) or deleting *APN1*, which is responsible for $\geq$97% of AP endonuclease and 3′-diesterase activities required for BER (Popoff et al., 1990), does not sensitize *rnh1Δ rhn201Δ* cells to replication stress-inducing agents (Figure 2A). This result is consistent with data showing that rNMPs-containing DNA cannot be processed by NER and BER nucleases (Rydberg and Game, 2002). The observation that deletion of *APN2* in a *rnh1Δ rnh201Δ apn1Δ* causes an increase in sensitivity to 25 mM HU can be explained by the fact that simultaneous deletion of *APN1* and *APN2* causes an accumulation of elevated levels of endogenous lesions, increasing cellular stress (Leroy et al., 2001). We cannot exclude, though, that a secondary BER pathway may be able to process a minority of rNMPs.

Given that rNMPs in DNA templates impede DNA synthesis by the yeast replicases Pols ε and δ (Watt et al., 2011), lethality may result from failure to complete DNA replication. We thus investigated whether postreplication repair (PRR) mechanisms may allow full genome replication in *rnh1Δ rnh201Δ* cells. When DNA polymerases encounter replication-blocking lesions, PCNA is monoubiquitylated by Rad6-Rad18 triggering translesion DNA synthesis (TLS), while polyubiquitylation, carried out by Mms2-Ubc13-Rad5, promotes template switch (Ulrich, 2011).

We checked by spot assay whether deleting either branch of PRR would affect DNA replication in cells that do not remove rNMPs from genomic DNA, and cell lethality was quantitated as in Figure 1. Loss of only the template switch pathway (*mms2Δ*) or only translesion DNA synthesis (TLSΔ: corresponding to deletions of *REV1*, *REV3*, *REV7*, and *RAD30* genes encoding all TLS polymerases in budding yeast) does not sensitize cells lacking RNase H to HU. On the other hand, concomitant elimination of TLS and template switch results in almost no growth of *rnh1Δ rhn201Δ* cells in 25 mM HU, due to cell lethality (Figures 2B and 2C). These findings show that when *rnh1Δ rnh201Δ* cells are subjected to a low level of replication stress, survival depends almost entirely on either PRR pathway. This effect, although striking in the presence of HU, can also be detected in unperturbed conditions (bottom line, Figure 2B; see also Figures S3A and S3B). We conclude that cells devoid of RNase H1 and H2 can use TLS and template switch pathways to completely replicate their rNMPs-containing genome. Consistently, deletion of *RAD51*, which is required for a recombination-dependent PRR pathway (Gangavarapu et al., 2007), increases the sensitivity to HU of *rnh1Δ rnh201Δ* cells, while loss of *RAD52* is lethal in this genetic background (Figures 2D and 2E). These phenotypes may be influenced by defects in the additional processes that involve homologous recombination.

DNA Polymerase ζ Is the TLS Polymerase Replicating rNMPs-Containing DNA

To identify which translesion DNA polymerase allows the bypass of rNMPs, we combined mutations in genes coding each of the three yeast TLS polymerases, *REV1*, *REV3*/*REV7* (the catalytic and noncatalytic subunits of Pol ζ, respectively), and *RAD30* (Pol η) in *rnh1Δ rnh201Δ* cells. The experiment was performed in the absence of the *MMS2*-dependent template switch pathway, so that *rnh1Δ rnh201Δ* cells rely only on TLS to complete replication. The spot tests shown in Figure 3A reveal that *rnh1Δ rnh201Δ mms2Δ* cells carrying a deletion of *REV1* or direct inactivation of DNA polymerase ζ *(rev3Δ rev7Δ)* do not survive HU treatment and are less viable even in untreated conditions, recapitulating the total absence of TLS activities. Deletion of *RAD30* does not increase cell lethality under these conditions; on the contrary, we reproducibly observed that loss of Pol η confers an unexpected growth advantage when genomic DNA contains unrepaired rNMPs (Figure 3A), consistently with the phenotype observed in *rnh1Δ rnh201Δ TLSΔ* (Figures 2B and 2C). This unpredicted observation may be

Molecular Cell
RNase H and PRR Protect from Chromosomal rNMPs

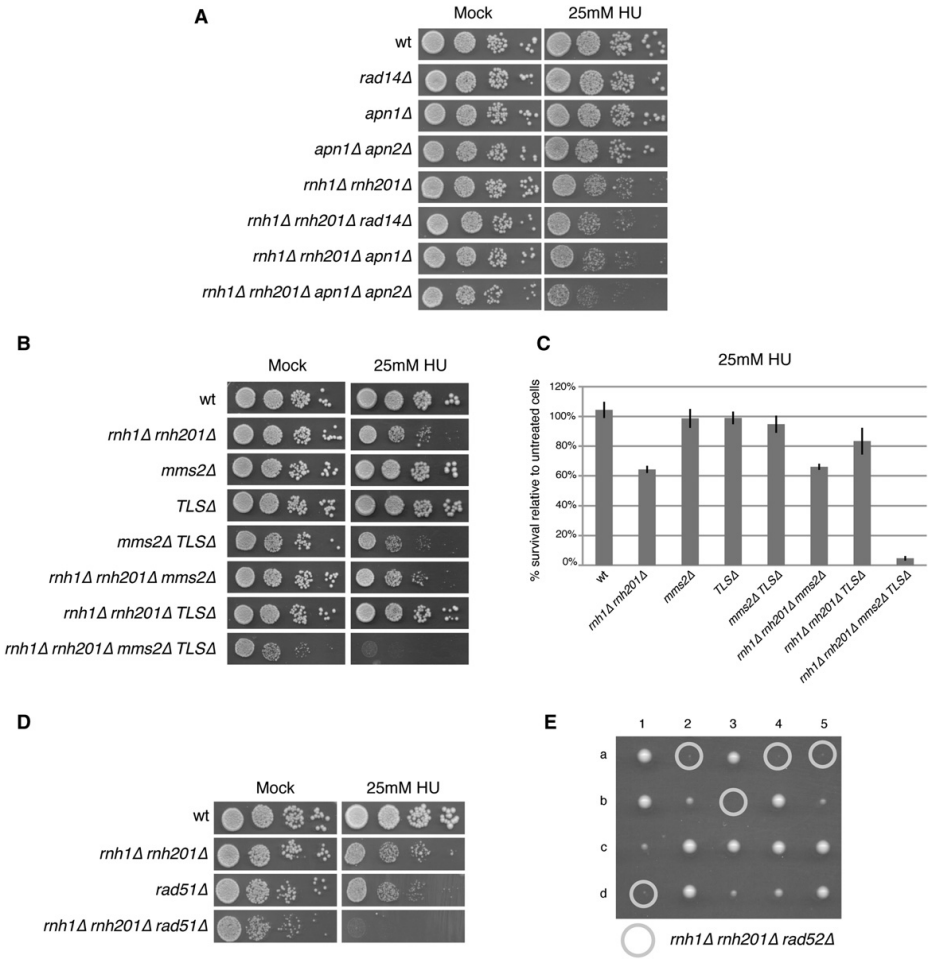

Figure 2. Postreplication Repair Is Specifically Required to Tolerate rNMPs-Containing Chromosomes

Sensitivity to sublethal doses of HU was assayed as described in Figure 1. Pictures were taken after 3 days of incubation. The contribution of NER (A), BER (A), the two branches of PRR (B), and *RAD51* (D) was tested. In (C), Quantification of cell survival was obtained as described in Figure 1H. The graph is representative of three independent experiments. Error bars describe standard deviation. It is worth noting that *mms2Δ TLSΔ* cells, despite being sensitive to HU in the spot tests, do not exhibit increased cell lethality, suggesting that the HU sensitivity derives from a very slow cell-cycle progression. In (E), tetrads derived from a cross between *rnh1Δ rnh201Δ* and *rad52Δ* were dissected on YPD plates. Five tetrads (1–5) are shown.The circles on the figure indicate the position of the original *rhn1Δ rnh201Δ rad52Δ* spores. Cells derived from such microcolonies do not grow when restreaked, revealing that a *rad52Δ* mutation is synthetic lethal with deletion of the *RNH1* and *RNH201* genes. *TLSΔ* comprises *rev1Δ rev3Δ rev7Δ rad30Δ*.

justified envisioning a competition between noneffective pol η and other PRR pathways.

Rev1 plays a noncatalytic role in supporting Pol ζ function (Lawrence and Hinkle, 1996; Lawrence, 2002) and also has a deoxycytidyl transferase activity (Nelson et al., 1996) that could insert a dCTP opposite a rNMP, allowing Pol ζ to extend. Figure 3B shows that, contrary to what was observed with *rev1Δ*, inactivating the polymerase activity of Rev1 does not significantly affect the HU sensitivity of *rnh1Δ rnh201Δ mms2Δ*. Altogether, these data indicate that cells can use Pol ζ to replicate rNMPs-containing templates in vivo and that Rev1 most likely plays a noncatalytic role to promote Pol ζ activity.

To confirm biochemically that DNA polymerase ζ is capable of bypassing rNMPs in DNA templates, we measured the rNMP bypass efficiency of purified yeast Pol ζ in vitro. Labeled substrates containing one, four, or sixteen consecutive rNMPs (Figure 4A) were incubated with purified DNA polymerase ζ or δ, and bypass efficiency was calculated after quantifying the

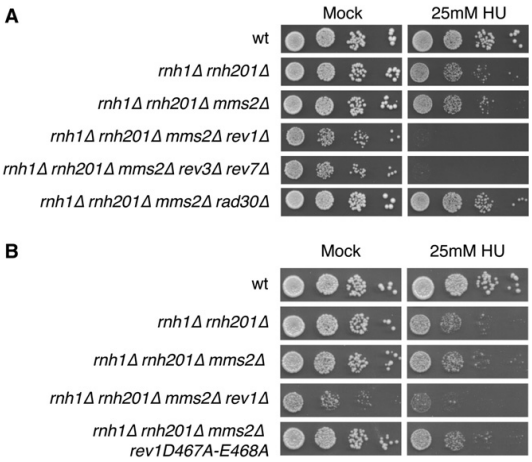

Figure 3. Pol ζ Allows Cells to Cope with Unrepaired rNMPs

The sensitivity to HU was measured as described in Figure 1: the specific contribution of each TLS polymerase (A) and the requirement of the catalytic activity of Rev1 (B) were tested.

primer extension products resulting from a single cycle of processive elongation (Figures 4B and 4D), as previously described (Nick McElhinny et al., 2010b). Consistently with the genetic observations (Figure 3A), the data indicate that Pol ζ bypasses ribonucleotides incorporated in DNA, efficiently copying DNA templates containing one (Figures 4B and 4D) or four rNMPs (Figures 4C, right, and 4D). This is in contrast with Pol δ which is somewhat less efficient in copying templates containing rC and much less efficient at copying templates containing rG, rA, rU, or four consecutive rNMPs (Watt et al., 2011) (Figures 4C and 4D). Pol δ bypass of rA or four consecutive rNMPs was stimulated several fold by adding PCNA to the reactions (see asterisks in Figure 4D), but in neither case was bypass as efficient as for Pol ζ.

We previously showed that, compared to RNase H2-proficient cells, *pol2-M644G rnh201Δ* strains (Nick McElhinny et al., 2010a) and *rnh201Δ* strains (Clark et al., 2011) have elevated rates of 2–5 base pair deletions in repetitive sequences and, recently, these deletions were shown to depend on topoisomerase 1 (Kim et al., 2011). This led to a model wherein topoisomerase 1 incises unrepaired rNMPs to create nicks in DNA with 3′-P and 5′-O ends that must be processed to allow ligation, and this processing may provide the opportunity for strand misalignments in repetitive sequences that yield the observed deletions. To determine if Pol ζ, which is relatively inaccurate (Zhong et al., 2006), might also contribute to this deletion mutagenesis, we measured the effect of deleting *REV3* on mutagenesis in the *pol2-M644G rnh201Δ* strain. Mutagenesis rates were estimated by measuring frequencies of formation of 5-FOA resistant clones, indicative of mutations leading to uracil auxotrophy. The results (Figure 4E) reveal that deleting *REV3* does not significantly (at p = 0.05; see figure legend) affect the overall rate of mutations to 5-FOA resistance, or the rates for total 2–5 base pair deletions or deletions of CA from a previously observed CACA hotspot sequence in the *URA3* gene. The lack of an effect of *rev3Δ* on mutagenesis suggests that Pol ζ does not contribute to topoisomerase 1-dependent mutagenesis resulting from unrepaired ribonucleotides incorporated during replication by Pol2-M644G. When the rate of base substitutions that might be explained by misincorporation of dCTP by Rev1p was calculated, no significant difference was observed between the *pol2-M644G* (from Pursell et al., 2007, and unpublished data), *pol2-644G rnh201Δ* (from Nick McElhinny et al., 2010a) and *pol2-M644G rnh201Δ rev3Δ* strains (from Figures 3 and S6). This supports the notion that the requirement for *REV1* in rNMPs bypass is structural rather dependent on its deoxycytidyltransferase activity.

RNase H-Defective Cells Exhibit Chronically Activated PRR Pathways

The relevance of PRR in coping with rNMPs in chromosomal DNA is evident by analyzing unperturbed mutant cells, which lack RNase H activities. FACS analysis of cycling cells suggests that *rnh1Δ rnh201Δ* cultures contain a higher fraction of S phase cells, and further inactivation of PRR pathways leads to a very sick phenotype (Figures 5A, S3A, and S3B). Indeed, these cells exhibit G2-M arrest coupled to cell lethality, as seen by Phloxine B staining of mutant colonies (Figure 5B).

Affinity-purified HIS-tagged PCNA from exponentially growing *rnh1Δ rnh201Δ* cells revealed a striking increase in PCNA ubiquitylation, compared to wild-type cells. Figure 5C shows that both mono- and polyubiquitylated forms of PCNA are abundant in cells that cannot remove rNMPs from genomic DNA. Conversely, no significant effect is observed in PCNA sumoylation (Figure 5D). Accordingly, deletion of *RAD18*, coding for the ubiquitin ligase responsible for conjugating ubiquitin to PCNA, has a synthetic effect when combined with the loss of RNase H: *rnh1Δ rnh201Δ rad18Δ* cells are exquisitely sensitive to 25 mM HU and exhibit cell lethality even in untreated conditions (Figure S3C).

All these results indicate that cells lacking RNase H have constitutively active PRR, which is crucial to tolerating the presence of rNMP-containing genomic DNA.

DISCUSSION

Yeast Cells Can Insert rNTPs into Genomic DNA

In eukaryotic cells the size of cellular dNTP pools is tightly controlled, and altered dNTP levels are responsible for increased mutagenesis and genome instability (Chabes and Stillman, 2007). Because the pools of rNTPs are much higher, DNA polymerases must be selective to correctly polymerize dNTPs during genome replication. Recent evidence has shown that during normal DNA replication in yeast, DNA polymerases incorporate rNTPs into genomic DNA. The *pol2-M644G* mutation affecting the steric gate of Pol ε increases rNTPs incorporation 10-fold (Nick McElhinny et al., 2010b). Genomic DNA isolated from *rnh201Δ* cells has a high number of alkali-sensitive sites, indicating that RNase H2 is involved in removing rNMPs from DNA (Nick McElhinny et al., 2010a).

Unrepaired rNMPs in genomic DNA will impact on cell-cycle progression since, at the next round of DNA replication, replicative polymerases must duplicate a RNA-containing DNA template. It has been shown that replicative polymerases cannot effectively replicate a template containing rNMPs (Nick McElhinny et al., 2010a; Watt et al., 2011), and this situation generates replication stress, detectable as a higher fraction of cells in S phase (Nick McElhinny et al., 2010a and Figure S1C). Combining a deletion in *RNH201*, coding for the catalytic subunit of RNase H2, with a *pol2-M644G* mutation, we found that cells became sensitive to low doses of replication stress inducing agents (i.e., HU or MMS). These data suggest that the short RNA tracts, which cannot be processed in the absence of RNase H2, cause replication stress when the cell tries to replicate them. Low levels of HU and MMS increase such stress leading to cell lethality.

Since loss of RNase H2 activity from *pol2-M644G* mutated cells does not cause cell lethality per se, additional pathways repairing rNMPs-containing chromosomes must exist. In this work we describe different mechanisms that are involved in allowing cells to cope with the presence of rNMPs in their genome.

RNase H1 Participates in the Removal from the Genome of rNMPs Introduced during DNA Replication

RNase H1 has some overlapping substrates with RNase H2 and is the preferential enzyme for processing RNA:DNA hybrids where more than four rNMPs are present. Double mutant cells, combining *rnh1Δ* with the deletion of any of the RNase H2 subunits, exhibit hypersensitivity to low levels of HU or MMS, a cell-cycle delay in G2-M, and activation of the Rad53 checkpoint kinase.

Strikingly, deletion of *RNH1*, the gene coding for RNase H1, is synthetic lethal when combined with the *pol2-M644G* mutation and RNase H2 inactivation (*rnh201Δ*), demonstrating that RNase H1 also plays a crucial role in the repair of rNMPs incorporated by replicative DNA polymerases. Our genetic analysis excludes a contribution of NER in correcting rNMPs, while a minor involvement of BER in repairing rNMP-containing chromosomes cannot be completely ruled out.

The observation that cells lacking RNase H activities are sensitive to low doses of replication stress-inducing agents may have consequences for cancer chemotherapy. In fact, many cancer cells are characterized by elevated levels of endogenous replication stress (Negrini et al., 2010) and may be thus sensitized to inhibitors of RNase H activity, which could selectively kill cells experiencing replication stress.

Recently, topoisomerase 1 has been reported to be able to process rNMPs-containing DNA and generate ssDNA breaks, which can be easily converted to chromosome breaks. We believe it unlikely that *rnh1Δ rnh201Δ* lethality in HU is due to such chromosome fragmentation, since in our experiments the *rnh1Δ rnh201Δ* double mutant and the wild-type strains exhibit a similar level of phosphorylated histone H2A (Figure S1D), suggesting the absence of double-strand breaks. Altogether, these findings indicate that high levels of unrepaired rNMPs in the chromosome hinder DNA synthesis blocking replication forks, leading to replication stress.

Either One of the PRR Pathways Is Sufficient for Tolerating rNTPs Incorporated by Replicative DNA Polymerases, and DNA Polymerase ζ Is the Enzyme Replicating rNMPs-Containing DNA

When replication-blocking lesions are present in the DNA template, replication forks stall at the site of damage and cannot proceed. Completion of replication is facilitated by PRR mechanisms, namely error-prone translesion DNA synthesis (TLS) and error-free template switch, a recombination-like pathway, requiring, respectively, mono- and polyubiquitylation of PCNA.

Strikingly, exponentially growing *rnh1Δ rnh201Δ* cells exhibit high levels of constitutive mono- and polyubiquitylated PCNA, indicative of chronic PRR activation. Either TLS or template switch can be used to complete replication over rNMPs. Indeed, a strong synthetic effect is observed when both PRR pathways are inactivated or when PCNA ubiquitylation is prevented in cells lacking RNase H activities: these cells are exquisitely sensitive to mild replication stress and are also extremely sick in untreated conditions, indicating a novel role for PRR in tolerating RNA-containing DNA templates (Figure 6).

How cells can replicate a chromosome containing rNMPs is not known. Yeast cells contain three TLS polymerases, Pol η, Pol ζ, and Rev1 (Friedberg et al., 1995). Our data show that, in the absence of a functional template switch pathway, rNMPs-containing DNA can only be replicated by the concerted action of Rev1 and Pol ζ. The fact that a catalytic *rev1* mutant is capable of rescuing the phenotype imparted by a *rev1Δ* mutation indicates that the role of Rev1 is likely to help Pol ζ to replicate rNMPs containing templates. Indeed, untreated *rnh1Δ rnh201Δ* cells lacking the template switch pathway and missing Pol ζ form fewer and smaller colonies. A similar synthetic phenotype is observed in *pol2-M644G* mutant cells lacking PRR pathways (Figure S4). In conclusion, template switch and Pol ζ are crucial to allow replication of endogenous, unrepaired rNMPs (Figure 6), and mutations increasing the rNMPs load, such as *pol2-M644G*, may saturate PRR pathways so that cell survival relies on RNase H1 and RNase H2. The crucial role of Pol ζ for replicating rNMP-containing chromosomes may be performed either by adding a dNTP opposite the rNMP, or by elongating, downstream of the damaged site, a chain created by a replicative polymerase. In vitro data confirm the genetic findings and demonstrate that Pol ζ can efficiently insert a nucleotide opposite the lesion, bypassing 1 or 4 rNMPs in the DNA template, revealing a new cognate, endogenous substrate for this essential, specialized TLS polymerase.

Recombination-dependent PRR mechanisms are less understood. Rad51 and Rad52 are involved in PRR (Gangavarapu et al., 2007) and in other recombination events and, in general, *rad52Δ* strains are more recombination defective than *rad51Δ* cells. We found that deletion of *RAD52* is synthetic lethal with loss of RNase H1 and RNase H2, and *rad51Δ* has a synthetic effect on HU sensitivity, supporting a role for recombination-dependent PRR in tolerating chromosomal rNMPs. However, defects in other recombination-dependent processes can contribute to these effects: for example, restart of blocked replication forks can proceed through recombination mechanisms (Heller and Marians, 2006; Petermann et al., 2010). Furthermore, RNase H enzymes may have diverse cellular targets in addition

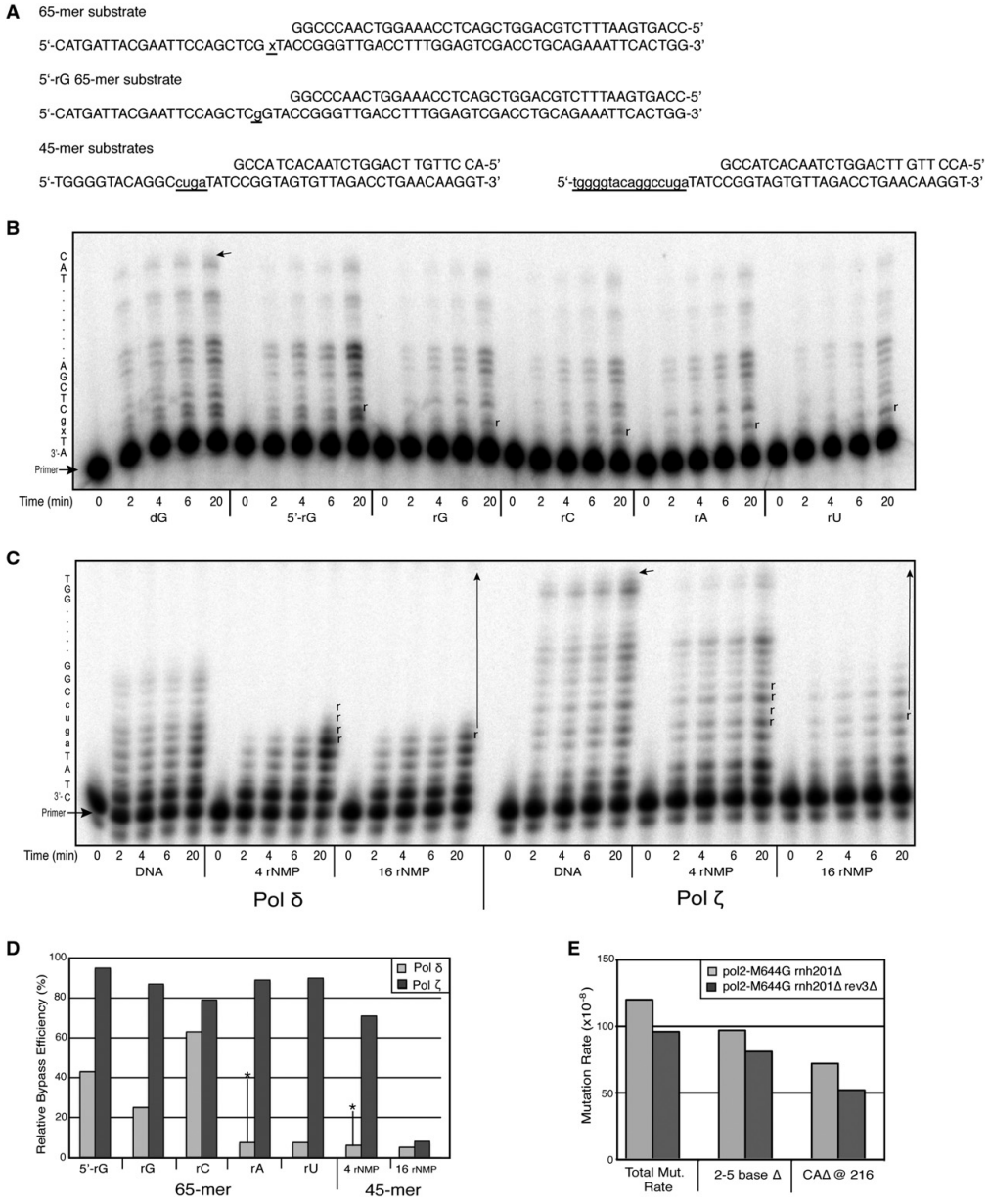

Figure 4. DNA Polymerase ζ Efficiently Bypasses rNMPs in the Template Strand

(A) Primer-template sequences. In the 65-mer substrate, "x" is the position of the single rNMP (rG, rC, rA, or rU) and "g" is the position of the 5′-rG in the DNA template. In the 45-mer substrate, the underlined lowercase nucleotides indicate the position and sequence of the rNMPs in 4- and 16-rNMP substrates, respectively.

(B and C) Phosphorimages of products generated during bypass of a single rNMP (B) and tracts of rNMPs by Pol δ and ζ (C). The template sequence is shown on the left, the arrow depicts the location of full-length product, and "r" represents the position of the rNMPs in the template. No enzyme was added to the unextended primer reaction (0 min).

Molecular Cell

RNase H and PRR Protect from Chromosomal rNMPs

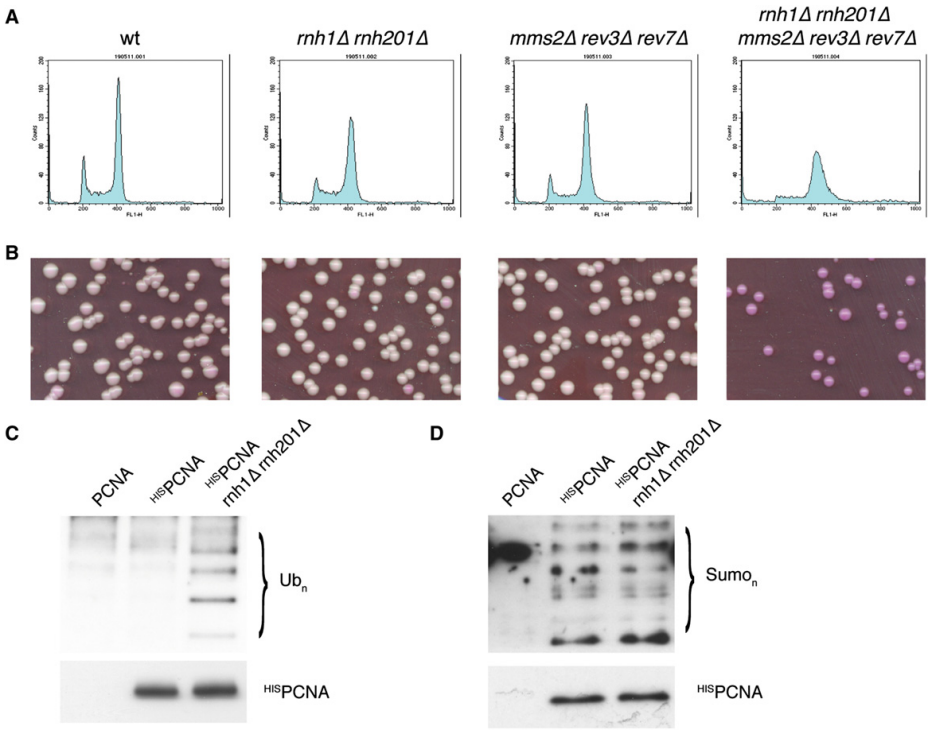

Figure 5. In the Absence of RNase H, the PRR Pathway Is Constitutively Activated and Promotes Cell Survival in an Unperturbed Cell Cycle
The role of PRR was assessed in unperturbed *rnh1Δ rnh201Δ* cultures. Exponentially growing cells lacking RNase H and defective in PRR were analyzed by FACS (A), to monitor cell cycle distribution, and by Phloxine B staining (B), to evaluate cell lethality. PCNA was affinity purified from exponentially growing unperturbed wild-type cells or from cells lacking RNase H activity. PCNA levels were estimated by western blotting with anti-HIS Ab. PCNA ubiquitylation was monitored by western blotting with anti-ubiquitin Ab (C), and PCNA sumoylation was monitored by western blotting with anti-SUMO Ab (D).

to rNTPs incorporated in genomic DNA. Among these are R-loops and Okazaki fragments; the accumulation of both these structures can have lethal outcomes and is prevented by recombination processes (Huertas and Aguilera, 2003; Ii and Brill, 2005).

Given the involvement of RNase H2 in the pathogenesis of the Aicardi-Goutières syndrome, the data reported in this work may help to understand the mechanisms underlying the disease. The reported synthetic effects between RNase H mutations, inducers of replication stress, and postreplication repair alterations, may facilitate the identification of modifier genes, whose alterations may be responsible for the phenotypic variability observed in different AGS patients carrying identical RNase H2 mutations.

EXPERIMENTAL PROCEDURES

Yeast Strains

Strains are derivatives of W303, unless otherwise indicated in Table S1, and were generated by standard genetic procedures (Adams et al., 1998). YFL1449 and YFL1376 were obtained by crossing and backcrossing five times *pol2-M644G* (Nick McElhinny et al., 2010a) or ^{HIS}PCNA (Ulrich and Davies, 2009) with SY2080.

(D) Relative bypass efficiencies for Pols δ and ζ. Images of reaction products shown in (B) and (C) were quantified, and relative bypass efficiencies were calculated as described (Stone et al., 2009). The values for Pol δ with the 65-mer substrates in the absence of PCNA have been reported previously (Watt et al., 2011) and are shown here for comparison. The asterisks indicate the relative bypass values for Pol δ for reaction mixtures containing 200 nM PCNA.
(E) Mutation rates for the *pol2-M644G rnh201Δ* and *pol2-M644G rnh201Δ rev3Δ* strains. The total mutation rates for resistance to 5-FOA were determined as described in Experimental Procedures. The 95% confidence intervals for the *pol2-M644G rnh201Δ* and *pol2-M644G rnh201Δ rev3Δ* strains were 110 to 200 and 57 to 140, respectively. For the *pol2-M644G rnh201Δ* strain, the rates for total 2–5 base pair deletions and for CA deletions at position 216–219 in *URA3* are from Clark et al. (2011). For the *pol2-M644G rnh201Δ rev3Δ* strain, rates for short deletions were calculated after sequencing the *ura3* gene in 163 independent 5-FOA resistant clones. Of these, 136 harbored 2–5 base pair deletions, 88 of which were CA deletions at the CACA hotspot at position 216–219 in *URA3* (see spectrum in Figure S6).

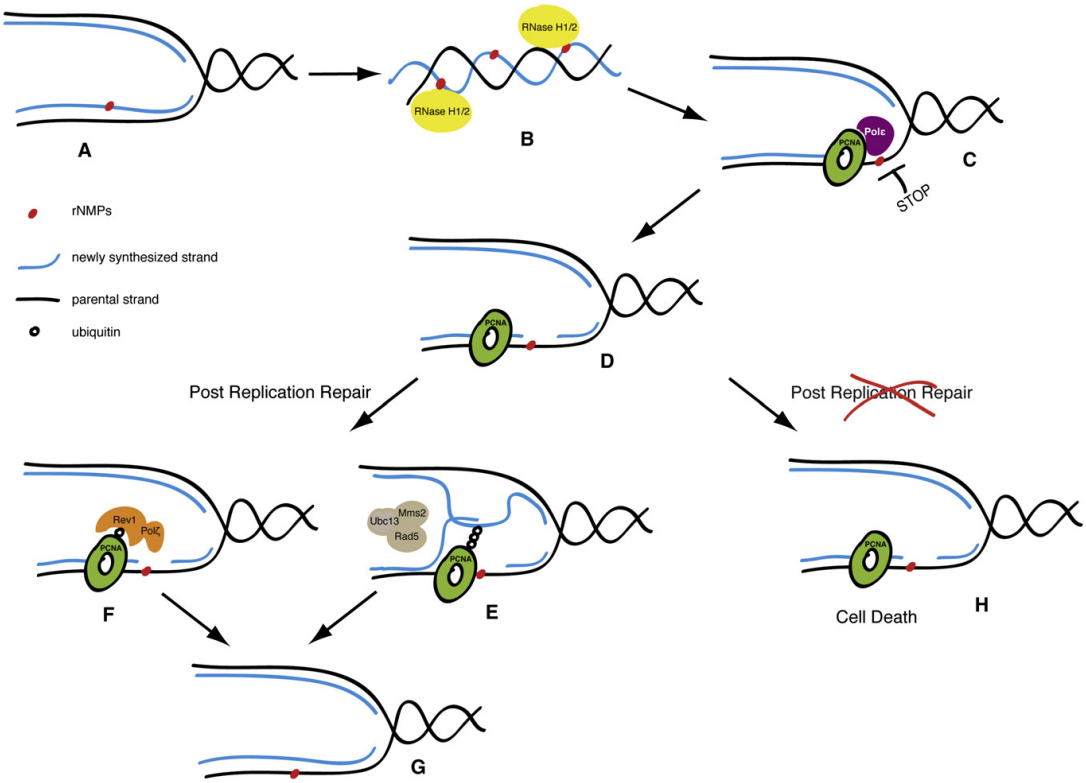

Figure 6. RNase H and Postreplication Repair Protect Cells from rNMPs Incorporated in Chromosomal DNA

During DNA synthesis, replicative polymerases can incorporate rNTPs (red dot) in place of dNTPs (A). RNase H1 and RNase H2 are required to remove rNMPs from newly replicated DNA (blue line) (B). If rNMPs persist until the following cell cycle, they will create problems at during the DNA synthesis step (C), since replicative polymerases cannot efficiently elongate the nascent strand opposite rNMPs in the template strand (black line). Replication fork restart downstream of the lesions leaves incomplete replication products for postreplication repair (D). PCNA is ubiquitylated. Either MMS2-dependent template switch mechanisms (E) or Pol ζ-dependent translesion synthesis (F) allow bypass of rNMPs and completion of replication (G). Under these conditions, inactivation of PRR causes cell lethality (H).

FACS Analysis

Cells were fixed in 70% ethanol and treated with RNase A and proteinase K. DNA was stained with Sytox Green and cell-cycle distribution was estimated by cytofluorimetric analysis with a FACScan.

SDS-PAGE and Western Blotting

To monitor protein levels and phosphorylation, TCA protein extracts were prepared and analyzed by SDS-PAGE (Sabbioneda et al., 2007); western blots were performed with anti-Rad53, anti-H2A, and anti-γH2AX antibodies.

To study PCNA posttranslational modifications, HIS-tagged PCNA was pulled down from denaturing extracts as described (Ulrich and Davies, 2009), separated on 10% SDS-Urea-PAGE, and transferred to nitrocellulose membranes. PCNA ubiquitylation and sumoylation were analyzed by western blotting with anti-ubiquitin and anti-SUMO antibodies.

Sensitivity Assay

To assess cell survival in HU and MMS, overnight yeast cultures were diluted to 1×10^6 cfu/ml, and 10-fold serial dilutions were spotted on plates containing HU or MMS at the indicated concentrations. Images were captured after 3 days' incubation at 28°C. To obtain quantitative data, exponentially growing cells were arrested in G1 with 6 μg/ml α-factor. Cultures were diluted and 100 cfu were distributed on each of three independent YPD plates (mock or 25 mM HU). After 3 days' incubation colonies were counted. The experiments were repeated three times. The graphs show the percentage of surviving cells with respect to the mock sample. Standard deviations were used to obtain error bars.

Cell Lethality Assay

Overnight yeast cultures were diluted as above, and ~100 cfu were plated on YPD containing 20 mg/l Phloxine B, with or without 25 mM HU. Images were captured after 3 days' incubation at 28°C.

Microcolony Assays

Yeast cells were grown to a concentration of 5×10^6 cells/ml and arrested in G1 with α-factor (6 μg/ml). Diluted samples were spread on YPD plates containing 25 mM HU, and single cells were separated using a micromanipulator. Plates were then incubated at 28°C and photographs were taken after 22 hr; thirty individual cells were followed for each experiment. The experiment was repeated four times, and a representative example is shown.

Cell-Cycle Analysis

Yeast cultures were grown to a concentration of 5 × 10^6 cells/ml and arrested in G1 with α-factor (6 μg/ml). Cells were released in YPD supplemented with 25 mM HU or 0.04% MMS or mock. Ninety minutes after, the release α-factor (6 μg/ml) was added back to the culture to avoid re-entry in S phase, allowing the analysis of a complete single cell cycle. Samples were collected for SDS-PAGE and FACS analysis and processed as described above. Growth curves were obtained by measuring cell concentration microscopically and normalizing each read to the initial concentration. Generation time was calculated by interpolating the growth curves.

rNMP Bypass, Mutation Rates, and Spectra

S.cerevisiae two-subunit wild-type Pol ζ (Rev3 –Rev7) and three-subunit Pol δ were expressed in yeast and purified as previously described (Burgers and Gerik, 1998; Garg et al., 2005). Oligonucleotide primer templates were prepared as described (Nick McElhinny et al., 2010b). The polymerase was added to initiate the reaction and aliquots were removed at 2, 4, 6, and 20 min. The DNA products were separated by electrophoresis through an 8% denaturing polyacrylamide gel containing 25% formamide for the 65-mer and 12% denaturing polyacrylamide gel for the 45-mer substrates. A PhosphorImager was used to visualize and quantify the DNA products. The efficiency of insertion opposite individual template positions and the bypass probability were calculated as previously described (Kokoska et al., 2003; Stone et al., 2009; Watt et al., 2011). Mutation rates and spectra were determined as described (Nick McElhinny et al., 2010a); in the relevant strains, the *URA3* reporter was inserted at the *AGP1* locus in orientation 2 as previously described (Nick McElhinny et al., 2010a).

SUPPLEMENTAL INFORMATION

Supplemental Information contains six figures, one table, and Supplemental References and can be found with this article online at doi:10.1016/j.molcel.2011.12.019.

ACKNOWLEDGMENTS

We thank H. Ulrich, A. Aguilera, and C. Santocanale for strains and reagents; J. Williams and A. Clark for comments on the manuscript; S. Sabbioneda, S. Carnevali, F. Spadaro, and the members of our laboratories for discussions. This work was supported by grants from AIRC, MIUR, and Fondazione Cariplo to P.P. and M.M.-F. and MIUR (FIRB RBFR10S3UQ) to F.L. The financial support of Telethon-Italy (grant number GGP11003) is gratefully acknowledged. F.L. was partially supported by a fellowship from Fondazione Buzzati-Traverso. Part of this work was supported by Project Z01ES065070 to T.A.K. from the Division of Intramural Research of the NIH and grant NIHGM32431 to P.M.B. Cancer Research UK, an ERC start-up grant (206281), the Lister Institute of Preventive Medicine, and the EMBO Young Investigator Program supported V.C.

Received: August 9, 2011
Revised: October 28, 2011
Accepted: December 6, 2011
Published: January 12, 2012

REFERENCES

Adams, A., Gottschling, D.E., Stearns, T., and Kaiser, C.A. (1998). Methods in yeast genetics: a Cold Spring Harbor Laboratory course manual (Plainview, NY: Cold Spring Harbor Laboratory Press).

Ayyagari, R., Gomes, X.V., Gordenin, D.A., and Burgers, P.M. (2003). Okazaki fragment maturation in yeast. I. Distribution of functions between *FEN1* AND *DNA2*. J. Biol. Chem. *278*, 1618–1625.

Ban, C., Ramakrishnan, B., and Sundaralingam, M. (1994a). A single 2′-hydroxyl group converts B-DNA to A-DNA. Crystal structure of the DNA-RNA chimeric decamer duplex d(CCGGC)r(G)d(CCGG) with a novel intermolecular G-C base-paired quadruplet. J. Mol. Biol. *236*, 275–285.

Ban, C., Ramakrishnan, B., and Sundaralingam, M. (1994b). Crystal structure of the highly distorted chimeric decamer r(C)d(CGGCGCCG)r(G).spermine complex—spermine binding to phosphate only and minor groove tertiary base-pairing. Nucleic Acids Res. *22*, 5466–5476.

Burgers, P.M., and Gerik, K.J. (1998). Structure and processivity of two forms of Saccharomyces cerevisiae DNA polymerase delta. J. Biol. Chem. *273*, 19756–19762.

Cerritelli, S.M., and Crouch, R.J. (2009). Ribonuclease H: the enzymes in eukaryotes. FEBS J. *276*, 1494–1505.

Cerritelli, S.M., Frolova, E.G., Feng, C., Grinberg, A., Love, P.E., and Crouch, R.J. (2003). Failure to produce mitochondrial DNA results in embryonic lethality in Rnaseh1 null mice. Mol. Cell *11*, 807–815.

Chabes, A., and Stillman, B. (2007). Constitutively high dNTP concentration inhibits cell cycle progression and the DNA damage checkpoint in yeast Saccharomyces cerevisiae. Proc. Natl. Acad. Sci. USA *104*, 1183–1188.

Clark, A.B., Lujan, S.A., Kissling, G.E., and Kunkel, T.A. (2011). Mismatch repair-independent tandem repeat sequence instability resulting ribonucleotide incorporation by DNA polymerase ε. DNA Repair (Amst.) *10*, 476–482.

Crow, Y.J., and Rehwinkel, J. (2009). Aicardi-Goutieres syndrome and related phenotypes: linking nucleic acid metabolism with autoimmunity. Hum. Mol. Genet. *18* (R2), R130–R136.

Crow, Y.J., Leitch, A., Hayward, B.E., Garner, A., Parmar, R., Griffith, E., Ali, M., Semple, C., Aicardi, J., Babul-Hirji, R., et al. (2006a). Mutations in genes encoding ribonuclease H2 subunits cause Aicardi-Goutières syndrome and mimic congenital viral brain infection. Nat. Genet. *38*, 910–916.

Crow, Y.J., Hayward, B.E., Parmar, R., Robins, P., Leitch, A., Ali, M., Black, D.N., van Bokhoven, H., Brunner, H.G., Hamel, B.C., et al. (2006b). Mutations in the gene encoding the 3′-5′ DNA exonuclease TREX1 cause Aicardi-Goutières syndrome at the AGS1 locus. Nat. Genet. *38*, 917–920.

Egli, M., Usman, N., and Rich, A. (1993). Conformational influence of the ribose 2′-hydroxyl group: crystal structures of DNA-RNA chimeric duplexes. Biochemistry *32*, 3221–3237.

Friedberg, E.C., Walker, G.C., and Siede, W. (1995). DNA repair and mutagenesis (Washington, DC: ASM Press).

Gangavarapu, V., Prakash, S., and Prakash, L. (2007). Requirement of RAD52 group genes for postreplication repair of UV-damaged DNA in Saccharomyces cerevisiae. Mol. Cell. Biol. *27*, 7758–7764.

Garg, P., Stith, C.M., Majka, J., and Burgers, P.M. (2005). Proliferating cell nuclear antigen promotes translesion synthesis by DNA polymerase ζ. J. Biol. Chem. *280*, 23446–23450.

Heller, R.C., and Marians, K.J. (2006). Replisome assembly and the direct restart of stalled replication forks. Nat. Rev. Mol. Cell Biol. *7*, 932–943.

Huertas, P., and Aguilera, A. (2003). Cotranscriptionally formed DNA:RNA hybrids mediate transcription elongation impairment and transcription-associated recombination. Mol. Cell *12*, 711–721.

Ii, M., and Brill, S.J. (2005). Roles of SGS1, MUS81, and RAD51 in the repair of lagging-strand replication defects in *Saccharomyces cerevisiae*. Curr. Genet. *48*, 213–225.

Jaishree, T.N., van der Marel, G.A., van Boom, J.H., and Wang, A.H. (1993). Structural influence of RNA incorporation in DNA: quantitative nuclear magnetic resonance refinement of d(CG)r(CG)d(CG) and d(CG)r(C)d(TAGCG). Biochemistry *32*, 4903–4911.

Joyce, C.M. (1997). Choosing the right sugar: how polymerases select a nucleotide substrate. Proc. Natl. Acad. Sci. USA *94*, 1619–1622.

Kim, N., Huang, S.N., Williams, J.S., Li, Y.C., Clark, A.B., Cho, J.E., Kunkel, T.A., Pommier, Y., and Jinks-Robertson, S. (2011). Mutagenic processing of ribonucleotides in DNA by yeast topoisomerase I. Science *332*, 1561–1564.

Kokoska, R.J., McCulloch, S.D., and Kunkel, T.A. (2003). The efficiency and specificity of apurinic/apyrimidinic site bypass by human DNA polymerase eta and Sulfolobus solfataricus Dpo4. J. Biol. Chem. *278*, 50537–50545.

Lawrence, C.W. (2002). Cellular roles of DNA polymerase zeta and Rev1 protein. DNA Repair (Amst.) *1*, 425–435.

Lawrence, C.W., and Hinkle, D.C. (1996). DNA polymerase zeta and the control of DNA damage induced mutagenesis in eukaryotes. Cancer Surv. *28*, 21–31.

Lazzaro, F., Giannattasio, M., Puddu, F., Granata, M., Pellicioli, A., Plevani, P., and Muzi-Falconi, M. (2009). Checkpoint mechanisms at the intersection between DNA damage and repair. DNA Repair (Amst.) *8*, 1055–1067.

Leroy, C., Mann, C., and Marsolier, M.C. (2001). Silent repair accounts for cell cycle specificity in the signaling of oxidative DNA lesions. EMBO J. *20*, 2896–2906.

Muzi-Falconi, M., Liberi, G., Lucca, C., and Foiani, M. (2003). Mechanisms controlling the integrity of replicating chromosomes in budding yeast. Cell Cycle *2*, 564–567.

Negrini, S., Gorgoulis, V.G., and Halazonetis, T.D. (2010). Genomic instability—an evolving hallmark of cancer. Nat. Rev. Mol. Cell Biol. *11*, 220–228.

Nelson, J.R., Lawrence, C.W., and Hinkle, D.C. (1996). Thymine-thymine dimer bypass by yeast DNA polymerase ζ. Science *272*, 1646–1649.

Nick McElhinny, S.A., and Ramsden, D.A. (2003). Polymerase mu is a DNA-directed DNA/RNA polymerase. Mol. Cell. Biol. *23*, 2309–2315.

Nick McElhinny, S.A., Kumar, D., Clark, A.B., Watt, D.L., Watts, B.E., Lundström, E.B., Johansson, E., Chabes, A., and Kunkel, T.A. (2010a). Genome instability due to ribonucleotide incorporation into DNA. Nat. Chem. Biol. *6*, 774–781.

Nick McElhinny, S.A., Watts, B.E., Kumar, D., Watt, D.L., Lundström, E.B., Burgers, P.M., Johansson, E., Chabes, A., and Kunkel, T.A. (2010b). Abundant ribonucleotide incorporation into DNA by yeast replicative polymerases. Proc. Natl. Acad. Sci. USA *107*, 4949–4954.

Petermann, E., Orta, M.L., Issaeva, N., Schultz, N., and Helleday, T. (2010). Hydroxyurea-stalled replication forks become progressively inactivated and require two different RAD51-mediated pathways for restart and repair. Mol. Cell *37*, 492–502.

Popoff, S.C., Spira, A.I., Johnson, A.W., and Demple, B. (1990). Yeast structural gene (APN1) for the major apurinic endonuclease: homology to Escherichia coli endonuclease IV. Proc. Natl. Acad. Sci. USA *87*, 4193–4197.

Prakash, S., Johnson, R.E., and Prakash, L. (2005). Eukaryotic translesion synthesis DNA polymerases: specificity of structure and function. Annu. Rev. Biochem. *74*, 317–353.

Pursell, Z.F., Isoz, I., Lundström, E.B., Johansson, E., and Kunkel, T.A. (2007). Yeast DNA polymerase epsilon participates in leading-strand DNA replication. Science *317*, 127–130.

Rice, G.I., Bond, J., Asipu, A., Brunette, R.L., Manfield, I.W., Carr, I.M., Fuller, J.C., Jackson, R.M., Lamb, T., Briggs, T.A., et al. (2009). Mutations involved in Aicardi-Goutières syndrome implicate SAMHD1 as regulator of the innate immune response. Nat. Genet. *41*, 829–832.

Rydberg, B., and Game, J. (2002). Excision of misincorporated ribonucleotides in DNA by RNase H (type 2) and FEN-1 in cell-free extracts. Proc. Natl. Acad. Sci. USA *99*, 16654–16659.

Sabbioneda, S., Bortolomai, I., Giannattasio, M., Plevani, P., and Muzi-Falconi, M. (2007). Yeast Rev1 is cell cycle regulated, phosphorylated in response to DNA damage and its binding to chromosomes is dependent upon MEC1. DNA Repair (Amst.) *6*, 121–127.

Sekiguchi, J., and Shuman, S. (1997). Site-specific ribonuclease activity of eukaryotic DNA topoisomerase I. Mol. Cell *1*, 89–97.

Stetson, D.B., Ko, J.S., Heidmann, T., and Medzhitov, R. (2008). Trex1 prevents cell-intrinsic initiation of autoimmunity. Cell *134*, 587–598.

Stone, J.E., Kissling, G.E., Lujan, S.A., Rogozin, I.B., Stith, C.M., Burgers, P.M., and Kunkel, T.A. (2009). Low-fidelity DNA synthesis by the L979F mutator derivative of Saccharomyces cerevisiae DNA polymerase zeta. Nucleic Acids Res. *37*, 3774–3787.

Ulrich, H.D. (2011). Timing and spacing of ubiquitin-dependent DNA damage bypass. FEBS Lett. *585*, 2861–2867.

Ulrich, H.D., and Davies, A.A. (2009). In vivo detection and characterization of sumoylation targets in Saccharomyces cerevisiae. Methods Mol. Biol. *497*, 81–103.

Wahl, M.C., and Sundaralingam, M. (2000). B-form to A-form conversion by a 3′-terminal ribose: crystal structure of the chimera d(CCACTAGTG)r(G). Nucleic Acids Res. *28*, 4356–4363.

Watt, D.L., Johansson, E., Burgers, P.M., and Kunkel, T.A. (2011). Replication of ribonucleotide-containing DNA templates by yeast replicative polymerases. DNA Repair (Amst.) *10*, 897–902.

Yang, Y.G., Lindahl, T., and Barnes, D.E. (2007). Trex1 exonuclease degrades ssDNA to prevent chronic checkpoint activation and autoimmune disease. Cell *131*, 873–886.

Zhong, X., Garg, P., Stith, C.M., Nick McElhinny, S.A., Kissling, G.E., Burgers, P.M.J., and Kunkel, T.A. (2006). The fidelity of DNA synthesis by yeast DNA polymerase zeta alone and with accessory proteins. Nucleic Acids Res. *34*, 4731–4742.

Zhu, H., and Shuman, S. (2008). Bacterial nonhomologous end joining ligases preferentially seal breaks with a 3′-OH monoribonucleotide. J. Biol. Chem. *283*, 8331–8339.

Molecular Cell, Volume *45*

Supplemental Information

RNase H and Postreplication Repair Protect Cells from Ribonucleotides Incorporated in DNA

Federico Lazzaro, Daniele Novarina, Flavio Amara, Danielle L. Watt, Jana E. Stone, Vincenzo Costanzo, Peter M. Burgers, Thomas A. Kunkel, Paolo Plevani, and Marco Muzi-Falconi

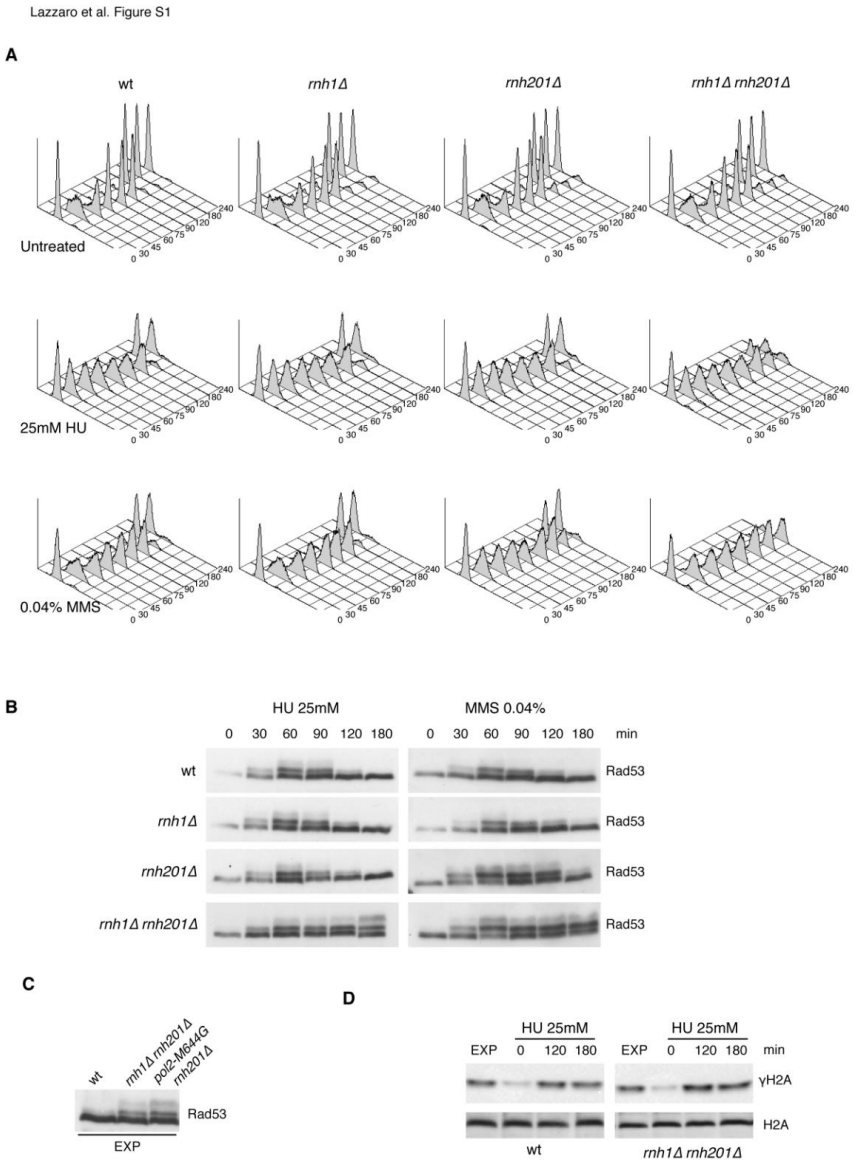

Figure S1, Related to Figure 1. Lack of RNase H Causes Replication Stress and a G2-M Delay

(A) Exponentially growing yeast cultures were arrested in G1 phase with α-factor. Cells were released in the presence of 25 mM HU, 0.04% MMS or fresh medium, and cell cycle progression was analyzed by FACS. The figure shows the number of cells in relation to the DNA content.

(B–D) The same cultures were used to verify checkpoint activation at the indicated time-points after the release. Total cell extracts were analyzed by western blotting to monitor Rad53, H2A and H2A phosphorylation, using specific antibodies.

Lazzaro et al., Figure S2

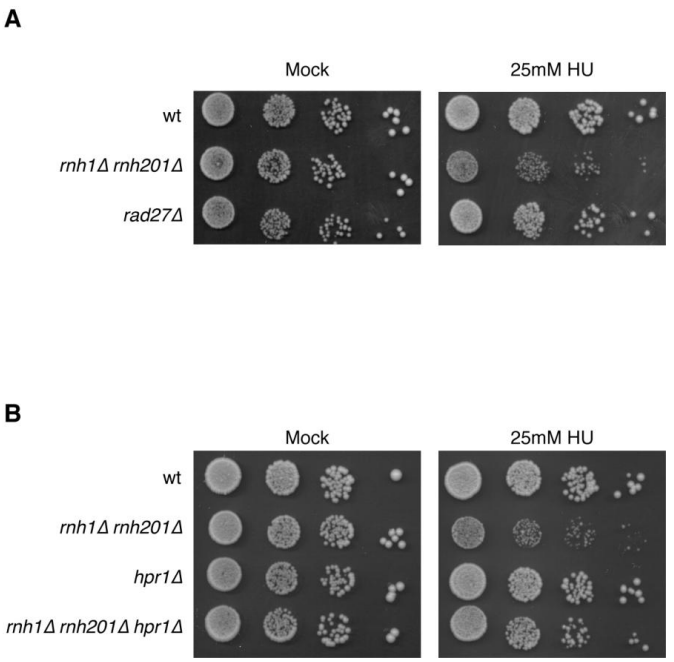

Figure S2, Related to Figure 1. Sensitivity to Replication Stress in RNase H Mutant Cells Is Unlinked from Defective Okazaki Fragments or R-Loops Processing

To verify the effect of mutants defective in processing of Okazaki fragments (A) or R-loops (B) on HU sensitivity, ten-fold serial dilutions of yeast overnight cultures were spotted on YPD plates containing a sublethal HU dose or mock. Ability to grow was analyzed after 3 days incubation.

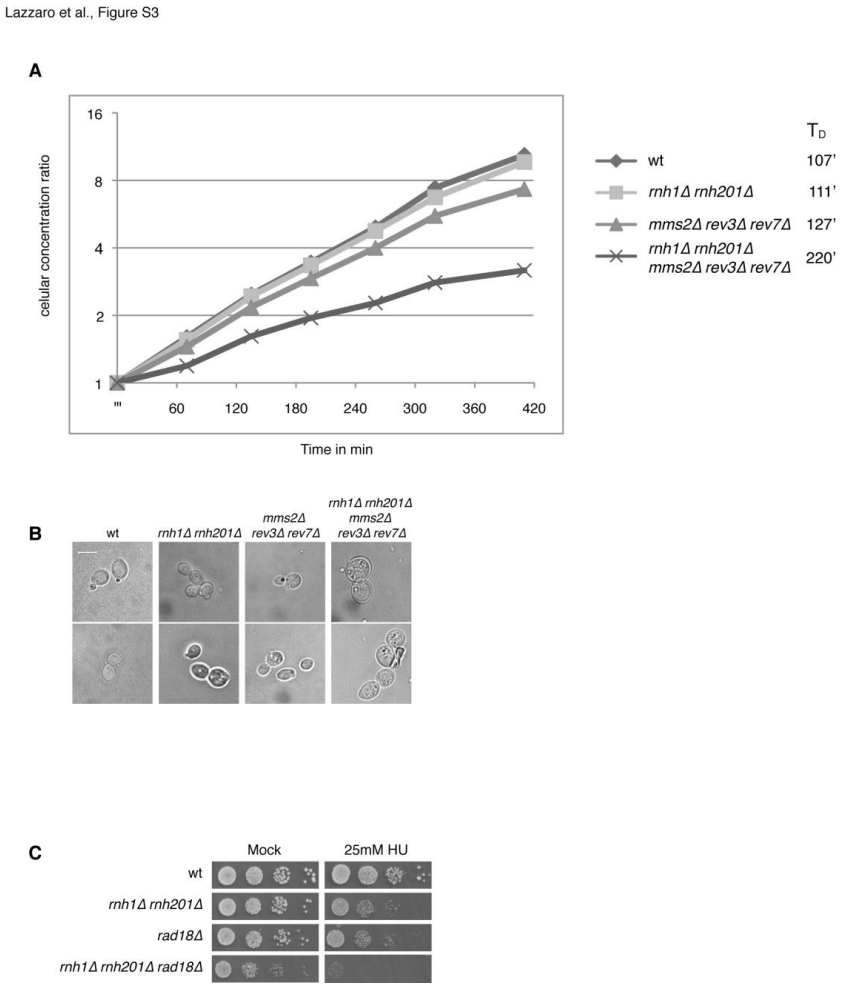

Figure S3, Related to Figure 5. PRR Pathways Play a Crucial Role in the Survival of RNase H-Defective Cells

(A) Growth curves and duplication times (T_D) for exponentially growing cells of the indicated strains were obtained by measuring cell concentrations at different time-points.

(B) The shape and size of wt and mutant cells form exponentially growing cultures were visualized by microscopic analysis. The white bar represents 5µm.

(C) To test the effect on HU sensitivity of a mutation eliminating Rad18, the enzyme responsible for conjugation of ubiquitin to PCNA, ten-fold serial dilutions of yeast overnight cultures were spotted on YPD plates containing a sublethal HU dose or mock. Ability to grow was analyzed after 3 days incubation.

Lazzaro et al. Figure S4

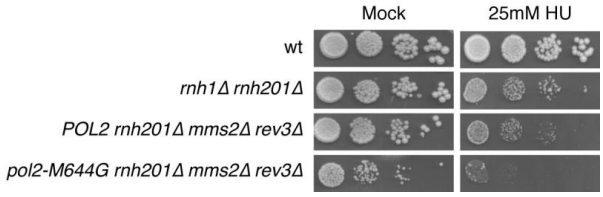

Figure S4, Related to Figure 5. PRR Is Crucial for Cells that Accumulate rNMP in Their Chromosomes

To verify the effect of PRR dysfunction in strains where a mutated DNA polymerase ε incorporates elevated levels of rNMPs in genomic DNA, ten-fold serial dilutions of yeast overnight cultures were spotted on YPD plates containing a sublethal HU dose or mock. Ability to grow was analyzed after 3 days incubation.

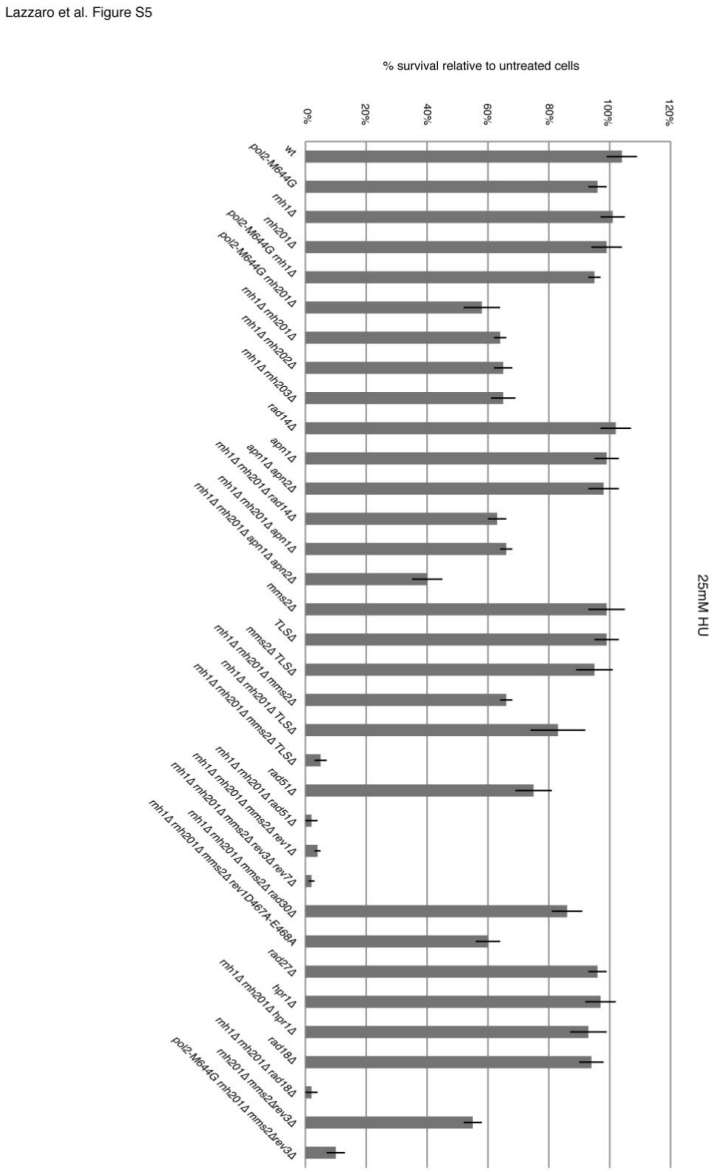

Figure S5, Related to Figures 1–3. Quantitative Survival Assays

To obtain quantitative data on survival upon treatment with 25 mM HU of the yeast strains used throughout this work, survival assays were performed as described in the legend to Figure 1H.

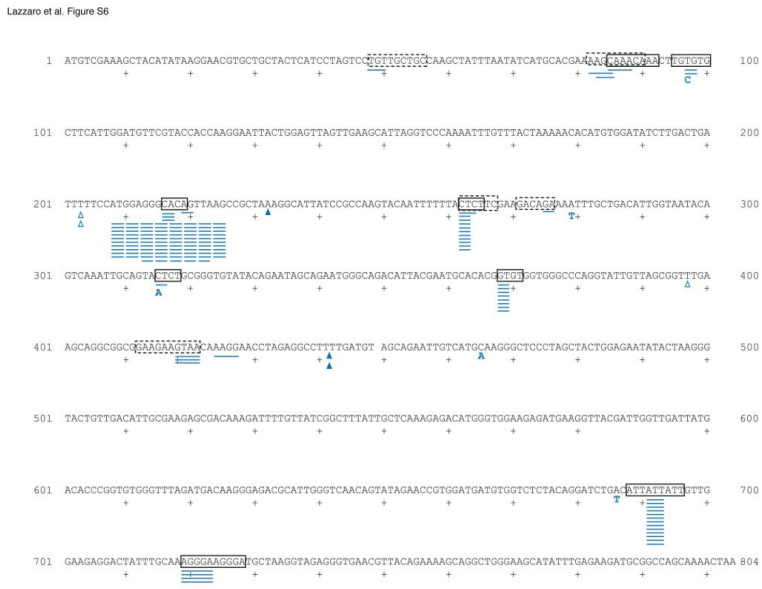

Figure S6, Related to Figure 4. Mutational Spectrum in *pol2-M644G rnh201*△ *rev3*△ Strain

The coding strand of the 804-base-pair *URA3* open reading frame is shown. The sequence changes observed in independent 5-FOA resistant mutants are depicted in blue below coding sequence, for *URA3* in orientation 2 as described in (Nick McElhinny, 2010a]. Letters indicate single-base substitutions, closed triangles indicate single-base additions, open triangles indicate single-base deletions and short lines below the coding sequence indicate 2–5-base deletions. Solid boxes enclose perfect direct repeat sequences, and dashed boxes enclose imperfect direct repeat sequences. Among 163 total mutants sequenced, a few contained other sequences changes not depicted here.

Table S1. Strains Used in This Study

Strain name	Genotype	Source/ Reference
SY2080	*MATa ade2-1 trp1-1 leu2-3,112 his3-11,15 ura3-1 can1-100 RAD5*	M. Foiani
YFL1208	(SY2080) *rnh1::HIS3*	This study
YFL1191	(SY2080) *rnh201::KanMX6*	This study
YFL1193	(SY2080) *rnh202::KanMX6*	This study
YFL1196	(SY2080) *rnh203::KanMX6*	This study
YFL1213	(SY2080) *rnh1::HIS3 rnh201::KanMX6*	This study
YFL1216	(SY2080) *rnh1::HIS3 rnh202::KanMX6*	This study
YFL1218	(SY2080) *rnh1::HIS3 rnh203::KanMX6*	This study
YMIC5A3	*MATa ade2-1 trp1-1 leu2-3,112 his3-11,15 ura3-1 can1-100 rad5-535 mec1-1 sml1*	Sabbioneda, 2007
YFL1449	(SY2080) p*ol2M644G*	This study
YFL1474	(SY2080) p*ol2M644G rnh201::KanMX6*	This study
YMG1146	(SY2080) *mms2::HPH*	This study
YMG1082	(SY2080) *rad30::KanMX6 rev1::KanMX6 rev3::TRP1 rev7::HIS3*	Giannattasio, 2010
YMG1149	(SY2080) *rad30::KanMX6 rev1::KanMX6 rev3::TRP1 rev7::HIS3 mms2::HPH*	This study
YFL1265	(SY2080) *rnh1::HIS3 rnh201::KanMX6 mms2::HPH*	This study
YFL1271	(SY2080) *rad30::KanMX6 rev1::KanMX6 rev3::TRP1 rev7::HIS3 rnh1::HIS3 rnh201::KanMX6*	This study
YFL1294	(SY2080) *rad30::KanMX6 rev1::KanMX6 rev3::TRP1 rev7::HIS3 rnh1::HIS3 rnh201::KanMX6 mms2::HPH*	This study
YFL1331	(SY2080) *rev1::KanMX6 rnh1::HIS3 rnh201::KanMX6 mms2::HPH*	This study
YFL1330	(SY2080) *rev3::TRP1 rev7::HIS3 rnh1::HIS3 rnh201::KanMX6 mms2::HPH*	This study
YFL1341	(SY2080) *rad30::KanMX6 rnh1::HIS3 rnh201::KanMX6 mms2::HPH*	This study
YFL1574	(SY2080) *rev1::KanMX6 rnh1::HIS3 rnh201::KanMX6 mms2::HPH ura3:REV1:URA3*	This study
YFL1575	(SY2080) *rev1::KanMX6 rnh1::HIS3 rnh201::KanMX6 mms2::HPH ura3:rev1-D467A-D468A:URA3*	This study
YFL1376	(SY2080) *leu2::^{6xHIS}POL30:LEU2*	This study
YFL1377	(SY2080) *leu2::^{6xHIS}POL30:LEU2 rnh1::HIS3 rnh201::KanMX6*	This study
YMG649	(SY2080) *rad27::KanMX6*	This study
YNOV59	(SY2080) *hpr1::HIS3*	This study
YNOV61	(SY2080) *rnh1::HIS3 rnh201::KanMX6 hpr1::HIS3*	This study
YFL1671	(SY2080) *rnh201::KanMX6 mms2::HPH rev3::TRP1*	This study

YFL1687	(SY2080) *rnh201::KanMX6 mms2::HPH rev3::TRP1 pol2-M644G*	This study
YFL1580	(SY2080) *rad18::KanMX6*	This study
YFL1629	(SY2080) *rad18::KanMX6 rnh1::HIS3 rnh201::KanMX6*	This study
(Δ|(-2) |-7B-YUNI300)	MATa CAN1 his7-2 leu2::kanMX ura3-Δ trp1-289 ade2-1 lys2-ΔGG2899-2900	Nick McElhinny, 2010a
SNM77	(Δ|(-2) |-7B-YUNI300) URA3-OR2 *pol2-M644G*	Nick McElhinny, 2010a
SNM127	(Δ|(-2) |-7B-YUNI300) URA3-OR2 *pol2-M644G rnh201::HPH*	Nick McElhinny, 2010a
JES184	(Δ|(-2) |-7B-YUNI300) URA3-OR2 *pol2-M644G rnh201::HPH rev3::LEU2*	This study
YFL1541	(SY2080) *rad14::NATr*	This study
YFL1545	(SY2080) *rad14::NATr rnh1::HIS3 rnh201::KanMX6*	This study
YFL1511	(SY2080) *apn1::HPH*	This study
YFL1537	(SY2080) *apn1::HPH apn2::TRP1*	This study
YFL1531	(SY2080) *apn1::HPH apn2::TRP1 rnh1::HIS3 rnh201::KanMX6*	This study
YNOV162	(SY2080) *rad51::HPH*	This study
YFL1451	(SY2080) *pol2-M644G rnh1::HIS3*	This study
YFL1677	(SY2080) *rad51::HPH rnh1::HIS3 rnh201::KanMX6*	This study

Part III

Manuscript in preparation

A Screen for Genome Stability Genes in *Saccharomyces cerevisiae* Identified *VID22* as a New Player in the Genome Integrity Landscape

Daniele Novarina[1], Federico Lazzaro[1], Muthu K. Shanmugam[1], Giulio Pavesi[1], Paolo Plevani[1]* and Marco Muzi-Falconi[1]*

[1]Dipartimento di Bioscienze, Università degli Studi di Milano, Via Celoria 26, 20133 Milano, Italy.

*Corresponding authors

Email: marco.muzifalconi@unimi.it Tel +39 02 50315034 Fax +39 02 50315044

Email: paolo.plevani@unimi.it Tel +39 02 50315032 Fax +39 02 50315044

Abstract

A better understanding of the mechanisms through which eukaryotic cells maintain the integrity of the genome is of capital importance, since failure of these mechanisms leads to genome instability, which is known to be a driving force in tumorigenesis. We took advantage of the Synthetic Genetic Array (SGA) technology to develop a new approach aimed at identifying genome stability genes in *Saccharomyces cerevisiae*: the screening is based on the sensitivity to overexpression of *DDC2* – a DNA damage checkpoint gene – as a readout for the genome instability phenotype in the deletion mutant collection. Among the genes not previously implicated in genome integrity maintenance, we identified the transcription factor *VID22*. We show that *vid22* mutants exhibit both spontaneous genome instability and increased sensitivity to genotoxic agents. The observation that Vid22-deficient cells have a defect in G1/S transition, accompanied and likely caused by decreased expression of G1 cyclin and replication genes, suggests that the various phenotypes observed in *vid22* mutants may arise from deregulation of DNA replication in the absence of the Vid22 transcription factor. Taken together, our findings described *VID22* as a new player in preserving genome integrity.

Introduction

DNA molecules are characterized by intrinsic instability [1] and are also subjected to the action of a series of endogenous and exogenous genotoxic agents [2]. Given the importance of faithfully duplicating and transferring the genetic material at each cell division, eukaryotic cells possess a number of evolutionary conserved mechanisms which preserve genome integrity by handling problems or errors arising during DNA replication, repairing DNA lesions, monitoring chromosome segregation and ensuring proper coordination of all these processes with cell cycle progression [3, 4, 5]. If any of these DNA integrity pathways fail, cells undergo a condition known as "genomic instability", characterized by the presence of many genetic alterations, ranging from point mutations, insertions/deletions of a few nucleotides, or expansion/contraction of repeated sequences, to gross chromosomal rearrangements and aneuploidy [6]. In recent years, compelling experimental evidence indicates that genomic instability acts as a driving force during tumorigenesis [7, 8, 9]. Therefore, the knowledge of the mechanisms preserving genome integrity is of basic importance to better understand the carcinogenic process.

Despite the increasing amount of data obtained in the field of genome stability maintenance, the picture is still far from being complete. To identify new genes involved in the maintenance of genome integrity, we developed a screen based on the overproduction of the Ddc2 checkpoint protein, which sensitizes yeast cells to spontaneous or induced DNA damage. Ddc2 (ATRIP in human) is a binding partner and regulator of the apical DNA damage checkpoint kinase Mec1 (human ATR) [10, 11, 12]. In response to DNA damage, Ddc2 binds to RPA-covered ssDNA and recruits Mec1 to the lesion, thus enabling its activation [13]. Furthermore, Ddc2 mediates the interaction between Mec1 and its activating protein Dpb11 [14]. It was shown that yeast cells overexpressing *DDC2* are very sensitive to DNA damage, as a consequence of checkpoint hyperactivation and permanent cell cycle arrest [15]. Therefore, mutant strains with increased genomic instability are expected to be sensitive to high levels of Ddc2, due to elevated levels of endogenous DNA damage.

Among the recently developed genetic technologies that can be used in the *Saccharomyces cerevisiae* model system, one of the most informative in terms of unraveling the biological function of a given gene is the Synthetic Genetic Array (SGA). This automated approach allows to uncover genetic interactions on a genome-wide scale by individually combining a given mutation with the deletions of all non-essential yeast genes [16]. We adapted the SGA technology to systematically overexpress the *DDC2* gene under a

galactose-inducible promoter in the collection of yeast viable deletion mutants, screening for strains whose growth is impaired in these conditions. This approach allowed the identification of deletion mutants experiencing genome instability on the basis of accumulation of spontaneous DNA damage. We found many genes involved in peroxisome dynamics, mitochondrial metabolism, chromatin remodeling and protein sorting, as well as genes implicated in DNA damage or oxidative stress response, cell cycle progression, control of transcription, ribosome biogenesis, regulation of proteasome assembly and functioning, cytoskeleton organization cell wall integrity and aminoacid biosynthesis, together with previously uncharacterized genes. In particular we indentified *VID22*, and explored its role in genome integrity maintenance: a *vid22* mutant exhibits genome instability phenotypes and sensitivity to DNA-damaging agents. Moreover, it has a defect in G1/S transition and in S-phase progression. We demonstrated that Vid22 regulates expression of the G1 cyclin genes, as well as of some key replication genes. It is possible that decreased cyclin levels in a *vid22* mutant may alter CDK1 activity and/or specificity, leading to defects in S-phase initiation and progression. We propose that altered CDK1 regulation, possibly connected to reduced pre-RC and pre-IC formation are the key factors explaining the genome instability occurring in the absence of Vid22.

Our work identified numerous genes and pathways responsible for maintaining genome stability and characterized a previously unknown contribution of *VID22* in preserving the integrity of the genome. These results and further characterization of the roles of the identified genes may shed new light on the events leading to genome instability, thus contributing to a better knowledge of the carcinogenic process.

Results

A genome-wide screen to identify new genes affecting genome stability. *S. cerevisiae* Ddc2 is the binding partner and activator of the DNA damage checkpoint apical kinase Mec1 (homolog of human ATR) [10]. It was shown that *DDC2* overexpression, despite having no detectable effect on unperturbed cells, causes hyperactivation of the checkpoint response after DNA damage, resulting in prolonged cell cycle arrest and cell death [15]. After verifying (Fig. S1-A) that *DDC2* overexpression increases sensitivity to low doses of DNA damaging agents, we speculated that it might also sensitize yeast cells to endogenous DNA damage. We confirmed this observation by testing the viability in conditions of *DDC2* overexpression

of some yeast strains deleted for genes coding for well known players in genome integrity maintenance, such as *RAD18* [17], *RAD27* [18], *MRE11 [18]* and *SLX8* [19]. These mutated strains accumulate spontaneous DNA damage and, as expected, their growth is severely compromised by high levels of Ddc2 (Fig. S1-B,C).

This observation urged us to develop a new screen to identify genes and pathways involved in genome integrity maintenance, based on the sensitivity to *DDC2* overexpression. By exploiting the Synthetic Genetic Array (SGA) automated approach [16], we overexpressed *DDC2* under a galactose-inducible promoter on a multicopy plasmid in the yeast haploid deletion collection and scored for those mutants whose fitness was reduced on galactose medium compared to the control experiment with the empty vector (Fig. 1A). We chose a multicopy plasmid instead of a centromeric plasmid to produce higher levels of Ddc2, thus increasing the sensitivity of the screen in strains with moderate levels of DNA damage (compare for instance the behavior of *rad18*Δ strain in figures S1-B and S1-C).

We found about 300 genes involved in different cellular pathways, namely DNA damage response, oxidative stress response, cell cycle progression, chromatin remodeling, regulation of transcription, mitochondria and peroxisomes metabolism, protein sorting, autophagy, proteasome function, ribosome biogenesis, aminoacid biosynthesis, meiosis, cytoskeleton, cell wall integrity (Fig. 1B). Importantly, about 20% of the ORFs identified are still uncharacterized. Unespectedly, our screen also identified some strains which show increased fitness after Ddc2 overexpression, but this class of genes needs further investigation.

Vid22 is important for maintenance of genome stability. Among the genes identified, our attention was captured by *VID22*, a gene that, despite its identification in another genome instability screen [20], was never characterized as a genome integrity gene. First, we confirmed by spot test that a *vid22* mutant is sensitive to *DDC2* overexpression (Fig. 1C). We then decided to examine Vid22 localization, since conflicting data have been reported in literature: in fact, Brown et al. described Vid22 as a plasma membrane protein [21], while Huh et al. localized Vid22 in the nucleus [22], a finding which is more compatible with a role in genome stability control. We assessed by immunofluorescence the localization of an HA-tagged version of Vid22 in exponentially growing cells, and we observed a clear colocalization of anti-HA antibody signal with DAPI (Fig. S2): therefore, in agreement with Huh et al. [22], Vid22 is a nuclear protein.

Next we scored for phenotypes directly linked to genome instability.

On the basis of previous observations in strains experiencing spontaneous DNA damage [23, 24, 19], we expected that the DNA damage checkpoint should be to a certain extent active in a *vid22* mutant, even in the absence of any genotoxic insult. We thus examined by western blot the phosphorylation state of the Rad53 checkpoint effector kinase (homolog of human Chk2), which is a marker of checkpoint activation, in an unperturbed cell cycle in wild-type and *vid22*Δ strains (Fig 2A). In a wt yeast strain partial Rad53 phosphorylation is observed 60' after release from the α-factor block, which is likely the consequence of few cells in the population experiencing some problems during DNA replication. Conversely, in a *vid22*Δ strain, Rad53 is partially phosphorylated during the whole cell cycle (for analysis of S-phase progression by flow cytometry see Fig. 4A). It is worth noting, however, that this phosphorylation is clearly distinguishable from full Rad53 phosphorylation observed when checkpoint cascade is fully activated as a consequence of genotoxic treatment (compare the western blots in figures 2A and S4). We interpret this finding by assuming that the checkpoint response is chronically alerted in a *vid22* mutant because these cells undergo continuous endogenous DNA damage as a consequence of some kind of genome instability. Consistently, in the *vid22*Δ strain we also observed increased levels of phosphorylated histone H2A (γH2A) especially at 60' and 90' time-points after release from the G1 block, which persist to a lesser extent throughout the cell cycle (Fig 2A). Mec1- and Tel1- dependent phosphorylation of H2A is one of the first events occurring in response to different types of DNA damage, and this modification has a key role in DNA damage repair and full activation of the checkpoint cascade [25, 26, 27, 28]. Intrestingly, these elevated γH2A levels are most evident at time-points corresponding to the end of S-phase, suggesting that in the absence of *VID22* yeast cells may encounter some problems during DNA replication.

To examine more directly the *VID22* role in preserving genome integrity, we performed some classical genome instability assays. First, we examined forward mutation rates at the *CAN1* locus and found that *vid22* cells have a modest, but statistically significant, increase in spontaneous mutation rate ($\sim$1.5 fold higher than the wt, Fig. 2B). Next, we assessed genome stability at the rDNA locus, which is one of the most fragile regions of the genome [29]. We tested the recombination rates by measuring spontaneous loss of the *ADE2* marker integrated into the rDNA array: indeed, we observed a $\sim$3 fold higher rate in the *vid22* mutant compared to the wt (Fig. 2C). Altogether these data strongly support the notion that *VID22* is involved in genome integrity maintenance.

Genetic interactions and DNA damage sensitivity of a *vid22*Δ mutant. In the attempt to gain further insights in the role of *VID22* in genome integrity, we decided to take advantage of the data available on the genetic interactions in *S. cerevisiae* ([30] and Charlie Boone unpublished data). Through a GO-enrichment analysis – which identifies the biological characteristics (Gene Ontology terms) over-represented in a particular subset of genes, compared to what would be expected by chance [31, 32] – we found that *VID22* negatively interacts with many genes involved in recombination / resolution of replication intermediates, as well as chromatin remodeling, cell cycle checkpoint, cytoskeleton organization, mitochondrial maintenance and distribution, and Golgi vesicle transport (Fig. S3-A). Among the positive interactors we observed an enrichment for chromatin remodeling factors mainly involved in chromatin silencing, the RNA splicing machinery, genes responsible for the formation of RNA polymerase II transcriptional preinitiation complex, DNA repair genes, and some protein complexes, namely cohesins, septing ring components and protein phosphatase type 2A (PP2A) complex members (Fig. S3-B).

We also tested the viability of a *vid22*Δ strain in response to a variety of genotoxic agents. Interestingly, this strain is sensitive to the double-strand breaks (DSBs) inducing agent Bleomicin, to chemicals perturbing replication fork progression, such as the DNA alkylating agent methyl metanesulphonate (MMS) and the ribonucleotide reductase (RNR) inhibitor hydroxyurea (HU), and to hydrogen peroxide (H_2O_2) which is a source of oxidative stress (Fig. 3). Strikingly, the same mutant is not sensitive to UV damage up to a dose of 90 J/m^2 nor to the anticancer agent camptothecin (CPT) which triggers the formation of genotoxic topoisomerase-DNA adducts.

In order to rule out the possibility that the DNA damage sensitivity observed in the absence of *VID22* is due to defective checkpoint activation, we monitored Rad53 phosphorylation after the genotoxic treatments listed above. *vid22*Δ mutant cells exhibit normal checkpoint activation after Bleomicin (Fig. S5-A,B), HU (Fig. S5-C) or MMS (Fig. S5-D) treatments. We also examined the switch-off of the checkpoint response after release from HU: no difference was found in a *vid22*Δ mutant compared to wt (Fig. S5-E). Altogether, these observations indicate that *vid22*Δ cells are sensitive only to certain types of genotoxic insults.

Vid22 is involved in the control of G1/S transition. Among the mechanisms preserving genome integrity, those ensuring proper cell cycle progression, and especially timely and correct DNA replication, are partic-

ularly important [33, 6]. After the observation that spontaneous checkpoint activation in the absence of *VID22* is especially evident in S-phase (Fig 2A), we decided to monitor cell cycle progression of the *vid22*Δ strain by flow cytometry upon release from an α-factor block (Fig. 4A). Intriguingly, while wt cells enter and progress through S-phase synchronously, a certain fraction of *vid22*Δ cells, corresponding to ∼15% of the total population, fail to enter S-phase, as shown by a peak corresponding to 1C DNA content which persists until the rest of the cell population exits form mitosis and starts a new cell cycle. This G1-arrested subpopulation is made up of unbudded cells (data not shown). Note that this phenotype is not due to a defective recovery from the α-factor block, because the same 1C peak persists when exponentially growing cells are treated for 3 hours with the microtubule-depolimerizing agent nocodazole, which arrests cells in M phase (Fig. 4B). Moreover, a slight defect in S-phase progression is visible at 30 to 40 min after release from α-factor in the *vid22*Δ strain (Fig. 4A). These observations are indicative of possible defects in initiating and/or in carrying on DNA replication.

VID22 has been described as a promoter-binding protein, and a bona fide transcription factor [34]. To test this hypothesis and identify putative genes whose expression may be regulated by *VID22*, we performed an RNA-Seq analysis in wt and *vid22*Δ cells. Notably, among the downregulated genes found in the *vid22*Δ mutant we found many cyclins involved in the control of cell cycle progression, namely *CLN1*, *CLN2*, *CLB1*, *CLB6*, *PCL1*, *PCL5,* as well as the essential replication genes *CDC6* and *CDC45* (Fig. 4C). This findings support the hypothesis that a *vid22*Δ strain is defective in G1/S transition and replication initiation. This scenario, beside explaining the cell cycle defects observed in the *vid22*Δ mutant, also provides a possible mechanism for the genomic instability phenotype observed in the absence of *VID22* (see Discussion).

Discussion

Genomic instability is a hallmark of cancer [7, 9] and it has been proposed as a key driving force in tumorigenesis [8, 35]. Taking advantage of the high conservation of the DNA integrity pathways, multiple screens were performed in *S. cerevisiae* which allowed the identification of key genes in the integrity pathways [36, 37, 38, 17, 39, 40, 41, 20, 42, 43, 44, 45, 46, 47]. However, likely due to the different approaches used, the results of these screens are only partially overlapping, and each study provides a different perspective of the genome stability network. Here we used a modified version of

the SGA technology [16] to screen the *S. cerevisiae* deletion collection for genes implicated in genome integrity maintenance, on the basis of chronic accumulation of spontaneous DNA damage. This approach was based on the sensitivity of cells to high levels of Ddc2, which by hyperactivating the DNA damage checkpoint in strains experiencing endogenous DNA damage, results in impaired growth ([15] and Fig. S1). It is worth noting that, differently from previous studies [36, 37, 38, 17, 39, 41, 20, 42, 43, 44, 45, 46, 47], we exploited the sensitivity to Ddc2 overexpression as a readout for spontaneous accumulation of any kind of DNA lesion capable to activate the DNA damage checkpoint, thus broadening the range of genomic instability marks taken into consideration in a single screen.

Multiple pathways contribute to maintenance of genome stability. In our screen we identified genes involved in several cellular processes (Fig. 1B), consistent with multiple mechanisms impacting on genome stability. Beside some already known DNA damage response genes, we found many genes involved in protecting cells from oxidative stress, in regulating peroxisome biogenesis, number and function, and implicated in mitochondrial metabolism. Given that mitochondria and peroxisomes are key players in reactive oxigen species (ROS) metabolism [48, 49], the gene category "safeguarding against oxidative stress" accounts for about 15% of the total identified genes. This finding supports the notion that endogenous accumulation of oxidative damage is a serious challenge to genome integrity [50, 38, 51]. Interestingly, previous screens for genes impacting on genome stability identified only few genes related to oxidative stress [36, 37, 38, 17, 39, 40, 41, 20, 42, 43, 44, 45, 46, 47], likely because of the different experimental approach we used in the screening.

Other representative genes identified in the screen belong to the following pathways: chromatin remodeling, modulation of transcription, cell cycle control, regulation of cytoskeleton dynamics, proteasome assembly and function and autophagy. Most of these pathways have been previously implicated in genome integrity maintenance. Other pathways were more unexpected, such as protein sorting (mainly vesicular trafficking to vacuole or Golgi), ribosome biogenesis, aminoacid biosynthesis or cell wall integrity and composition. As predicted, none of the genes directly implicated in DNA damage checkpoint activation were identified in our analysis: in fact, mutations in these genes are expected to be insensitive to *DDC2* overexpression, despite accumulation of DNA damage. It is worth noting that about 20% of the genes identified in the screen are still uncharacterized, leaving the way open for future studies.

Surprisingly, our analysis also yielded some strains whose growth was improved when *DDC2* was overexpressed. This observation needs further investigation, but may suggest that in some conditions a hyperactive checkpoint can enhance cell viability. Alternatively, it is possible that Ddc2 might have cellular roles other than Mec1 activation. Lastly, we must recognize that some known genome stability genes were not identified in our screen: it is possible that in some strains high levels of genome instability can favour the occurrence of mutations suppressing the original phenotype, which will be likely selected due to growth advantage.

***VID22* is a new player in genome stability.** Among the genes identified, we were intrigued by *VID22* (*YLR373C*), which was not expected to have a role in genome stability maintenance, due to its annotation as "Glycosylated integral membrane protein localized to the plasma membrane" which "plays a role in fructose-1,6-bisphosphatase (FBPase) degradation; involved in FBPase transport from the cytosol to Vid (vacuole import and degradation) vesicles" (Saccharomyces Genome Database). In the existing literature two lines of evidence link *VID22* to genome integrity. First, *VID22* was simultaneously identified in two screens for genome stability genes based on marker inactivation in haploid or diploid yeast cells [20]. Second, Bellaoui et al. found *VID22* among the negative genetic interactors of *MUS81* and *MMS4*, whose products form a protein complex with endonuclease activity involved in the resolution of recombination intermediates [52]. In both papers *VID22* was only mentioned without any further investigations or additional comments.

Despite its annotation as a "plasma membrane protein" (Saccharomyces Genome Database), published data [22] and our observations (Fig. S2) demonstrate that Vid22 is a nuclear protein, consistent with a role in genome stability maintenance. Moreover, Vid22 and its paralog Env11 (encoded by *YGR071C*) were found in a complex with the transcription factor and telomere silencing regulator Tbf1 [53], and it was shown that Vid22 directly binds some gene promoters [34].

Direct observation of genome instability hallmarks in a *vid22*Δ strain allows us to conclusively include *VID22* among the genes required for genome integrity maintenance. First, partial Rad53 phosphorylation and increased γH2A levels (Fig. 2A) are indicative of chronic accumulation of DNA damage. This assumption is also corroborated by a higher spontaneous mutation rate at the *CAN1* locus (Fig. 2B), and a greater recombination rate at the rDNA locus in *vid22*Δ cells (Fig. 2C). Moreover, the absence of Vid22 makes yeast cells sensitive to a number of genotoxic agents (Fig. 3). Inter-

estingly, these defects are at least partially independent from Vid22's role in the Vid22-Env11-Tbf1 complex, since an *env11*Δ mutant was not found sensitive to any genotoxic agent examined, and did not display hallmarks of genomic instability (data not shown). However, we cannot exclude that a Vid22-Tbf1 subcomplex might play a role in genome integrity maintenance, since Tbf1 is an essential gene and therefore damage sensitivity cannot be tested in a *tbf1*Δ mutant.

We ruled out the possibility that these phenotypes are caused by a defect in checkpoint activation after endogenous or exogenous DNA damage (Fig. S5). In fact, *vid22*Δ cells were expected to be checkpoint-proficient, due to the observation of a chronically alerted checkpoint in an unperturbed cell cycle (Fig. 2A) and to the sensitivity to high levels of Ddc2 (Fig. 1C), which should not occur in a checkpoint-deficient strain. We also excluded that these phenotypes could be attributable to a defect in checkpoint inactivation (Fig. S5-E).

Various indirect lines of evidence suggest that genomic instability in the absence of Vid22 may be related to defects in S-phase: i) the spontaneous accumulation of γH2A in a *vid22*Δ strain is detectable more clearly at timepoints at the end of S-phase (Fig. 2A and Fig. 4A); ii) a partial defect in S-phase progression in a *vid22*Δ strain is detectable by FACS and it is accompanied by the appearent inability to enter S-phase of a *vid22*Δ subpopulation (Fig. 4A,B); iii) moreover, genome-wide genetic interaction data suggest that deletion of *VID22* is detrimental in cells deprived of genes involved in resolution of replication and recombination intermediates (fig. S3).

A proposed mechanism for the development of genome instability in the absence if *VID22*. Transcriptional profiling of a *vid22*Δ strain indicates that deletion of *VID22* leads to downregulation of a subset of cyclin genes involved in the control of G1/S transition and S-phase progression, namely *CLN1*, *CLN2* and *CLB6* (Fig. 4C). The G1 cyclins Cln1 and Cln2 interact with yeast CDK1 (Cdc28) to induce transcription of the G1/S regulon [54, 55, 56], thus promoting G1/S transition [57]. Instead, Clb6 activates CDK1 to promote replication origin firing and initiation of DNA synthesis [58, 57]. Interestingly, two other factors necessary for replication initiation were found downregulated in a *vid22*Δ mutant: *CDC6* and *CDC45* (Fig. 4C). Cdc6 is a key factor for pre-replicative complex (pre-RC) assembly at origins of replication [59], while Cdc45 is required for pre-initiation complex (pre-IC) formation [60, 61], DNA polymerase α recruiting and subsequent triggering of replication initiation [62, 57].

Recent work showed that the G1/S transition is governed by a positive feedback loop involving Cln1 and Cln2 [63], which ensures proper expression of the ∼200 genes of the G1/S regulon (among which *CLN1* and *CLN2* genes themselves are included). Interestingly, in a *cln1*Δ *cln2*Δ mutant the positive feedback is disrupted, resulting in inefficient expression of the G1/S regulon and stochastic cell cycle arrest at an unbudded stage [63]. The deletion of *VID22* seems to partially mimic this phenotype, as in a *vid22*Δ mutant downregulation of G1 cyclin genes and sporadic failure to enter S-phase is observed. We propose that in the absence of *VID22* CDK activity required for G1/S transition is downregulated, resulting in defective G1/S transition and impaired replication origin firing. This suggestion is reinforced by the finding that *CDC6* and *CDC45*, two genes encoding for key replication initiation factors, are also downregulated in a *vid22*Δ strain. We speculate that, similarly to what was observed in *cln1*Δ *cln2*Δ cells, these defects may stochastically lead to a complete failure of G1/S transition in a subpopulation of a *vid22*Δ mutant. We wish to point out that our transcriptional analysis was carried out in a cellular population and it is therefore the result of an average behaviour. However, the trascriptional defect observed in the absence of *VID22* may be particularly relevant in some cells; single-cell analysis similar to that described in Skotheim et al. [63] could shed some light on this point.

Multiple lines of evidence point at deregulation of G1/S transition, at the level of both CDK/cyclin complexes activity and replication origin firing, as an important source of genome instability in yeast and mammalian cells [64, 65, 66, 67]: i) CDK inhibition in human cells results in accumulation of hallmarks of spontaneous DNA damage [68, 69]; ii) reduced replication origin firing due to *CLN2* overexpression [70], *SIC1* deletion [71], *CDC6* mutation [72] or *CDC45* and other replication factors depletion [73] results in genome rearrangements; iii) finaly, it was suggested that the human fragile site *FRA3B* is linked to a paucity of replication initiation events [74]. These observations suggest the model in Figure 5. Deregulation of G1/S transition, due to attenuated expression of G1 cyclins and key replication factors in the absence of *VID22*, when not leading to unbudded cell cycle arrest, is accompanied by defects in replication origin firing, which may result in perturbed replication and genomic instability. This view might also explain the synthetic lethality/sickness between *vid22*Δ and deletion of genes involved in the resolution of recombination structures during replication (Fig. S3).

Further experiments can be performed in the future to test this model, in particular direct assessment of origin firing efficiency in the absence of

VID22 and detection of the proposed aberrant recombination structures. Moreover, ChIP analysis at the promoters of genes whose expression was found altered in a *vid22*Δ mutant will help to define which genes are directly regulated by Vid22. Finally, the observation of a genomic instability phenotype in *cln1*Δ *cln2*Δ cells might further reinforce our mechanistic explanation for the genomic instability occurring in *vid22*Δ cells.

Altoghether, our analysis provided new information on pathways contributing to genome integrity maintenance, unraveling a new role for *S. cerevisiae VID22* in ensuring proper G1/S transition, indispensable to guarantee faithful transmission of an intact genome at each round of replication.

Materials & methods

Strains and plasmids

Unless differently stated, the strains used in this work are *RAD5* derivatives of W303 [*MAT***a** *ade2-1 trp1-1 can1-100 leu2-3,12 his3-11,15 ura3*]. All the strains used in this study are listed in Table 1. Plasmid pNOV1.4 was produced by inserting the NAT^R marker in multicopy vector pRS426, to allow the first selection steps of the SGA procedure. Plasmid pFL82.4 was obtained by cloning *DDC2* open reading frame under the *GAL1* promoter in plasmid pNOV1.4.

DDC2 overexpression screen

The screen was performed adapting the SGA technology described in [16]. Briefly, a query strain previously transformed with the *DDC2*-overexpressing plasmid was crossed to an ordered array of all the viable yeast deletion strains. Diploid cells were transferred on a sporulation-inducing medium, after which the spores were selected for the simultaneous presence of the gene deletion and the plasmid. The mutants were then transferred on a galactose-containing medium to induce *DDC2* overexpression, and colony size was analyzed as a measure of the mutants' fitness, as described in [75]. The whole procedure was performed in parallel with a control query containing the same vector devoid of the *GAL-DDC2* gene.

FACS analysis

Cells were fixed in 70% ethanol and treated with RNase A and proteinase K. DNA was stained with Sytox Green and cell-cycle distribution was estimated by cytofluorimetric analysis with a FACScan.

SDS-PAGE and western blotting

TCA protein extracts were separated by SDS-PAGE in 10% (to monitor Rad53) or 15% (to detect H2A) acrylamide gels. Western blotting was performed with anti-Rad53, anti-γH2A and anti-H2A antibodies.

DNA damage sensitivity assays

To assess cell survival after genotoxic treatment, overnight yeast cultures were diluted to an OD of 0.06, and 10-fold serial dilutions were spotted on YPD plates containing Bleomicin, HU, MMS or CPT at the indicated

concentrations. To assess cell survival after H_2O_2 treatment, overnight yeast cultures were diluted to OD 0.06, and treated with the indicated doses of H_2O_2 for 30', after which 10-fold serial dilutions were spotted on YPD plates. To assess cell survival after UV irradiation, overnight yeast cultures were diluted to OD 0.06, and 10-fold serial dilutions were spotted on YPD plates, which were irradiated with the indicated UV doses. Images were captured after 3 days' incubation at 28°C.

Genome instability assays

Measurements of the Can^R spontaneous mutation rate. Forward mutation to canavanine resistance was determined by fluctuation tests using the median method [76]. Single colonies were inoculated in 5 ml YPD and grown up to saturation (∼2 days at 28°C). A 100-µl drop of an appropriate dilution was plated onto canavanine-containing medium (1–2 × 10^7cells/plate) to identify forward mutations in *CAN1* and an appropriate dilution was plated onto SD medium to count viable cell number (∼100 cells/plate). Colonies appearing after 5 days of growth at 28°C were counted. The number of Can^R colonies per 10^7viable cells among 9 parallel cultures was calculated and the median value from each set of 9 cultures was used to determine the spontaneous mutation rate of a given strain by the method of the median [77].

Measurements of the rDNA recombination rate. The loss of an *ADE2* marker integrated into the rDNA array was used to measure recombination, as described in [78]. Cells were grown overnight and then plated onto solid YPD added with 12.5 µg/ml adenine. Colonies were grown 3 days at 28°C, and then transferred at 4°C for 3 days prior to analysis. The number of half-red/half-white colonies was determined; each was assumed to represent a marker loss event during the first cell division after plating. The number of half-sectored colonies divided by the total number of colonies (excluding entirely red colonies) was reported as the rate of marker loss. About 10000-15000 colonies were examined for each strain in each experiment.

RNA-seq

Total RNA from ∼10^8 exponentially growing cells was extracted with RiboPure™-Yeast Kit (Ambion) and treated for 30 min at 37°C with RNAse free DNase I (Ambion). Quality control on RNA samples were performed with the following kits: Agilent RNA 6000 Nano Kit (Agilent) and Qubit™

RNA Assay Kits (Invitrogen), according to the manufacturer's instructions. Equimolar pools of 5 independent RNA extractions were used for the Illumina library preparation (an overall amount of 8 μg RNA). Poly(A) RNA purification, cDNA synthesis and Illumina library preparation were performed with the TruSeq RNA Sample Prep Kit v2 - Set A (Illumina), according to the manufacturer's instructions. The library was controlled with the following kits: Agilent DNA 1000 Kit (Agilent) and Qubit™ ds-DNA HS Assay Kits (Invitrogen). Clusters were generated in triplicate with the Illumina cBot Cluster Generation System, using the TruSeq SR Cluster Kit v2–cBot–GA (Illumina); equimolar amounts of the different libraries were pulled together (at a final concentration of 8pM for each library) and the pool was loaded on 3 lanes of the flowcell. The libraries were then sequenced on a Genome Analizer IIx (Illumina) with the TruSeq SBS Kit v5 GA (36-cycle) (Illumina), performing 36 sequencing cycles.

Sequence reads were mapped on the yeast genome (version April 2011 S288c assembly) using Bowtie [79], allowing up to two substitutions, and keeping for further analyses only reads mapping at unique positions of the genome. Sequence reads were assigned to ORF annotations of the SGD database (version August 2011). Read mapping on overlapping ORFs were discarded from further analysis. For all the annotated ORFs, differential transcript abundance was estimated by performing a t-test between average and standard deviation of the normalized read counts assigned to the gene in the three replicates of each mutant versus average and standard deviation of the wild type. P-values returned from the t-test were modified to accomodate for multiple testing by using a Bonferroni correction. Fold ratios were obtained from average read counts computed as above.

Acknowledgments

We thank L. Guarente for the gift of strains and C. Santocanale for antibodies.

All the members of our laboratory are acknowledged for stimulating discussion.

References

[1] Lindahl T (1993) Instability and decay of the primary structure of DNA. *Nature* 362:709–715.

[2] Hoeijmakers JHJ (2009) DNA damage, aging, and cancer. *N Engl J Med* 361:1475–1485.

[3] Ciccia A, Elledge SJ (2010) The DNA damage response: making it safe to play with knives. *Mol Cell* 40:179–204.

[4] Suijkerbuijk SJE, Kops GJPL (2008) Preventing aneuploidy: The contribution of mitotic checkpoint proteins. *Biochim Biophys Acta*.

[5] Bartek J, Lukas J (2007) DNA damage checkpoints: from initiation to recovery or adaptation. *Curr Opin Cell Biol* 19:238–245.

[6] Aguilera A, Gómez-González B (2008) Genome instability: a mechanistic view of its causes and consequences. *Nat Rev Genet* 9:204–217.

[7] Lengauer C, Kinzler KW, Vogelstein B (1998) Genetic instabilities in human cancers. *Nature* 396:643–649.

[8] Loeb LA (2001) A mutator phenotype in cancer. *Cancer Res* 61:3230–3239.

[9] Hanahan D, Weinberg RA (2011) Hallmarks of cancer: the next generation. *Cell* 144:646–674.

[10] Paciotti V, Clerici M, Lucchini G, Longhese MP (2000) The checkpoint protein Ddc2, functionally related to *S. pombe* Rad26, interacts with Mec1 and is regulated by Mec1-dependent phosphorylation in budding yeast. *Genes Dev* 14:2046–2059.

[11] Rouse J, Jackson SP (2000) LCD1: an essential gene involved in checkpoint control and regulation of the MEC1 signalling pathway in *Saccharomyces cerevisiae*. *EMBO J* 19:5801–5812.

[12] Wakayama T, Kondo T, Ando S, Matsumoto K, Sugimoto K (2001) Pie1, a protein interacting with Mec1, controls cell growth and checkpoint responses in *Saccharomyces cerevisiae*. *Mol Cell Biol* 21:755–764.

[13] Zou L, Elledge SJ (2003) Sensing DNA damage through ATRIP recognition of RPA-ssDNA complexes. *Science* 300:1542–1548.

[14] Mordes DA, Nam EA, Cortez D (2008) Dpb11 activates the Mec1-Ddc2 complex. *Proc Natl Acad Sci U S A* 105:18730–18734.

[15] Clerici M, et al. (2001) Hyperactivation of the yeast DNA damage checkpoint by TEL1 and DDC2 overexpression. *EMBO J* 20:6485–6498.

[16] Baryshnikova A, et al. (2010) Synthetic genetic array (SGA) analysis in *Saccharomyces cerevisiae* and *Schizosaccharomyces pombe*. *Methods Enzymol* 470:145–179.

[17] Smith S, et al. (2004) Mutator genes for suppression of gross chromosomal rearrangements identified by a genome-wide screening in *Saccharomyces cerevisiae*. *Proc Natl Acad Sci U S A* 101:9039–9044.

[18] Chen C, Kolodner RD (1999) Gross chromosomal rearrangements in *Saccharomyces cerevisiae* replication and recombination defective mutants. *Nat Genet* 23:81–85.

[19] Zhang C, Roberts TM, Yang J, Desai R, Brown GW (2006) Suppression of genomic instability by SLX5 and SLX8 in *Saccharomyces cerevisiae*. *DNA Repair (Amst)* 5:336–346.

[20] Yuen KWY, et al. (2007) Systematic genome instability screens in yeast and their potential relevance to cancer. *Proc Natl Acad Sci U S A* 104:3925–3930.

[21] Brown CR, McCann JA, Hung GGC, Elco CP, Chiang HL (2002) Vid22p, a novel plasma membrane protein, is required for the fructose-1,6-bisphosphatase degradation pathway. *J Cell Sci* 115:655–666.

[22] Huh WK, et al. (2003) Global analysis of protein localization in budding yeast. *Nature* 425:686–691.

[23] Duro E, Vaisica JA, Brown GW, Rouse J (2008) Budding yeast Mms22 and Mms1 regulate homologous recombination induced by replisome blockage. *DNA Repair (Amst)* 7:811–818.

[24] Driscoll R, Hudson A, Jackson SP (2007) Yeast Rtt109 promotes genome stability by acetylating histone H3 on lysine 56. *Science* 315:649–652.

[25] Downs JA, Lowndes NF, Jackson SP (2000) A role for *Saccharomyces cerevisiae* histone H2A in DNA repair. *Nature* 408:1001–1004.

[26] Moore JD, Yazgan O, Ataian Y, Krebs JE (2007) Diverse roles for histone H2A modifications in DNA damage response pathways in yeast. *Genetics* 176:15–25.

[27] Javaheri A, et al. (2006) Yeast G1 DNA damage checkpoint regulation by H2A phosphorylation is independent of chromatin remodeling. *Proc Natl Acad Sci U S A* 103:13771–13776.

[28] Hammet A, Magill C, Heierhorst J, Jackson SP (2007) Rad9 BRCT domain interaction with phosphorylated H2AX regulates the G1 checkpoint in budding yeast. *EMBO Rep* 8:851–857.

[29] Kobayashi T (2011) Regulation of ribosomal RNA gene copy number and its role in modulating genome integrity and evolutionary adaptability in yeast. *Cell Mol Life Sci* 68:1395–1403.

[30] Costanzo M, et al. (2010) The genetic landscape of a cell. *Science* 327:425–431.

[31] Ashburner M, et al. (2000) Gene ontology: tool for the unification of biology. The Gene Ontology Consortium. *Nat Genet* 25:25–29.

[32] Eden E, Navon R, Steinfeld I, Lipson D, Yakhini Z (2009) GOrilla: a tool for discovery and visualization of enriched GO terms in ranked gene lists. *BMC Bioinformatics* 10:48.

[33] Sidorova JM, Breeden LL (2003) Precocious G1/S transitions and genomic instability: the origin connection. *Mutat Res* 532:5–19.

[34] Preti M, et al. (2010) The telomere-binding protein Tbf1 demarcates snoRNA gene promoters in *Saccharomyces cerevisiae*. *Mol Cell* 38:614–620.

[35] Negrini S, Gorgoulis VG, Halazonetis TD (2010) Genomic instability–an evolving hallmark of cancer. *Nat Rev Mol Cell Biol* 11:220–228.

[36] Ouspenski II, Elledge SJ, Brinkley BR (1999) New yeast genes important for chromosome integrity and segregation identified by dosage effects on genome stability. *Nucleic Acids Res* 27:3001–3008.

[37] Myung K, Chen C, Kolodner RD (2001) Multiple pathways cooperate in the suppression of genome instability in *Saccharomyces cerevisiae*. *Nature* 411:1073–1076.

[38] Huang ME, Rio AG, Nicolas A, Kolodner RD (2003) A genomewide screen in *Saccharomyces cerevisiae* for genes that suppress the accumulation of mutations. *Proc Natl Acad Sci U S A* 100:11529–11534.

[39] Measday V, et al. (2005) Systematic yeast synthetic lethal and synthetic dosage lethal screens identify genes required for chromosome segregation. *Proc Natl Acad Sci U S A* 102:13956–13961.

[40] Pan X, et al. (2006) A DNA integrity network in the yeast *Saccharomyces cerevisiae*. *Cell* 124:1069–1081.

[41] Storchová Z, et al. (2006) Genome-wide genetic analysis of polyploidy in yeast. *Nature* 443:541–547.

[42] Andersen MP, Nelson ZW, Hetrick ED, Gottschling DE (2008) A genetic screen for increased loss of heterozygosity in *Saccharomyces cerevisiae*. *Genetics* 179:1179–1195.

[43] Strome ED, Wu X, Kimmel M, Plon SE (2008) Heterozygous screen in *Saccharomyces cerevisiae* identifies dosage-sensitive genes that affect chromosome stability. *Genetics* 178:1193–1207.

[44] Ungar L, et al. (2009) A genome-wide screen for essential yeast genes that affect telomere length maintenance. *Nucleic Acids Res* 37:3840–3849.

[45] Alabrudzinska M, Skoneczny M, Skoneczna A (2011) Diploid-specific genome stability genes of *S. cerevisiae*: genomic screen reveals haploidization as an escape from persisting DNA rearrangement stress. *PLoS One* 6:e21124.

[46] Stirling PC, et al. (2011) The complete spectrum of yeast chromosome instability genes identifies candidate CIN cancer genes and functional roles for ASTRA complex components. *PLoS Genet* 7:e1002057.

[47] Zhang Y, et al. (2012) Genome-wide Screen Identifies Pathways that Govern GAA/TTC Repeat Fragility and Expansions in Dividing and Nondividing Yeast Cells. *Mol Cell* 48:254–265.

[48] Bonekamp NA, Völkl A, Fahimi HD, Schrader M (2009) Reactive oxygen species and peroxisomes: struggling for balance. *Biofactors* 35:346–355.

[49] Moldovan L, Moldovan NI (2004) Oxygen free radicals and redox biology of organelles. *Histochem Cell Biol* 122:395–412.

[50] Klaunig JE, Kamendulis LM (2004) The role of oxidative stress in carcinogenesis. *Annu Rev Pharmacol Toxicol* 44:239–267.

[51] Ragu S, et al. (2007) Oxygen metabolism and reactive oxygen species cause chromosomal rearrangements and cell death. *Proc Natl Acad Sci U S A* 104:9747–9752.

[52] Bellaoui M, et al. (2003) Elg1 forms an alternative RFC complex important for DNA replication and genome integrity. *EMBO J* 22:4304–4313.

[53] Krogan NJ, et al. (2006) Global landscape of protein complexes in the yeast *Saccharomyces cerevisiae*. *Nature* 440:637–643.

[54] Cho RJ, et al. (1998) A genome-wide transcriptional analysis of the mitotic cell cycle. *Mol Cell* 2:65–73.

[55] Spellman PT, et al. (1998) Comprehensive identification of cell cycle-regulated genes of the yeast *Saccharomyces cerevisiae* by microarray hybridization. *Mol Biol Cell* 9:3273–3297.

[56] Ferrezuelo F, Colomina N, Futcher B, Aldea M (2010) The transcriptional network activated by Cln3 cyclin at the G1-to-S transition of the yeast cell cycle. *Genome Biol* 11:R67.

[57] Enserink JM, Kolodner RD (2010) An overview of Cdk1-controlled targets and processes. *Cell Div* 5:11.

[58] Schwob E, Nasmyth K (1993) CLB5 and CLB6, a new pair of B cyclins involved in DNA replication in *Saccharomyces cerevisiae*. *Genes Dev* 7:1160–1175.

[59] Cocker JH, Piatti S, Santocanale C, Nasmyth K, Diffley JF (1996) An essential role for the Cdc6 protein in forming the pre-replicative complexes of budding yeast. *Nature* 379:180–182.

[60] Owens JC, Detweiler CS, Li JJ (1997) CDC45 is required in conjunction with CDC7/DBF4 to trigger the initiation of DNA replication. *Proc Natl Acad Sci U S A* 94:12521–12526.

[61] Zou L, Mitchell J, Stillman B (1997) CDC45, a novel yeast gene that functions with the origin recognition complex and Mcm proteins in initiation of DNA replication. *Mol Cell Biol* 17:553–563.

[62] Zou L, Stillman B (2000) Assembly of a complex containing Cdc45p, replication protein A, and Mcm2p at replication origins controlled by S-phase cyclin-dependent kinases and Cdc7p-Dbf4p kinase. *Mol Cell Biol* 20:3086–3096.

[63] Skotheim JM, Talia SD, Siggia ED, Cross FR (2008) Positive feedback of G1 cyclins ensures coherent cell cycle entry. *Nature* 454:291–296.

[64] Dershowitz A, Newlon CS (1993) The effect on chromosome stability of deleting replication origins. *Mol Cell Biol* 13:391–398.

[65] Spruck CH, Won KA, Reed SI (1999) Deregulated cyclin E induces chromosome instability. *Nature* 401:297–300.

[66] Bielinsky AK (2003) Replication origins: why do we need so many? *Cell Cycle* 2:307–309.

[67] Enders GH, Maude SL (2006) Traffic safety for the cell: influence of cyclin-dependent kinase activity on genomic stability. *Gene* 371:1–6.

[68] Zhu Y, et al. (2004) Intra-S-phase checkpoint activation by direct CDK2 inhibition. *Mol Cell Biol* 24:6268–6277.

[69] Maude SL, Enders GH (2005) Cdk inhibition in human cells compromises chk1 function and activates a DNA damage response. *Cancer Res* 65:780–786.

[70] Tanaka S, Diffley JFX (2002) Deregulated G1-cyclin expression induces genomic instability by preventing efficient pre-RC formation. *Genes Dev* 16:2639–2649.

[71] Lengronne A, Schwob E (2002) The yeast CDK inhibitor Sic1 prevents genomic instability by promoting replication origin licensing in late G(1). *Mol Cell* 9:1067–1078.

[72] Bruschi CV, McMillan JN, Coglievina M, Esposito MS (1995) The genomic instability of yeast cdc6-1/cdc6-1 mutants involves chromosome structure and recombination. *Mol Gen Genet* 249:8–18.

[73] Cheng E, et al. (2012) Genome Rearrangements Caused by Depletion of Essential DNA Replication Proteins in *Saccharomyces cerevisiae*. *Genetics* 192:147–160.

[74] Letessier A, et al. (2011) Cell-type-specific replication initiation programs set fragility of the FRA3B fragile site. *Nature* 470:120–123.

[75] Baryshnikova A, et al. (2010) Quantitative analysis of fitness and genetic interactions in yeast on a genome scale. *Nat Methods* 7:1017–1024.

[76] Foster PL (2006) Methods for determining spontaneous mutation rates. *Methods Enzymol* 409:195–213.

[77] Lea DE, Coulson CA (1949) The distribution of the numbers of mutants in bacterial populations. *J Genetics* 49:264–285.

[78] Kaeberlein M, McVey M, Guarente L (1999) The SIR2/3/4 complex and SIR2 alone promote longevity in *Saccharomyces cerevisiae* by two different mechanisms. *Genes Dev* 13:2570–2580.

[79] Langmead B, Trapnell C, Pop M, Salzberg SL (2009) Ultrafast and memory-efficient alignment of short DNA sequences to the human genome. *Genome Biol* 10:R25.

Figure legends

Figure 1. A new screen for genome stability genes based on *DDC2* overexpression.

A Overview of the screen procedure using the SGA technology. See the Results and Material and Methods sections for details.

B Overview of the classes of genes identified in the screen. The assignment of identified genes to functional categories is manually curated, based on the descriptions found in Saccharomyces Genome Database.

C Ten-fold serial dilutions of strains YNOV920 (wt, vector), YNOV921 (wt, *GAL-DDC2*), YNOV922 (*vid22*Δ, vector) and YNOV923 (*vid22*Δ, *GAL-DDC2*) were were spotted on YPGal/Raff medium to induce *DDC2* overexpression and on YPD as a control. Pictures were taken after 3 days of incubation at 28°C.

Figure 2. Yeast cells deleted for *VID22* experience spontaneous genome instability.

A A *vid22*Δ strain shows spontaneous Rad53 phosphorylation and persistent levels of γH2A. Exponentially growing cultures of strains SY2080 (wt) and YNOV108 (*vid22*Δ) were synchronized in G1 phase with 5 μg/ml α-factor and then released in fresh medium. Samples were taken every 30'. The phosphorylation status of Rad53 and histone H2A was analyzed by SDS-page and western blotting with antibodies anti-Rad53 and anti-γH2A respectively; total levels of H2A were monitored with anti-H2A antibodies.

B Spontaneous mutation rate in wt (BY4741) and *vid22*Δ (DMA3420) cells. Forward mutation rate at the *CAN1* locus rate was determined in three fluctuation tests of nine independent colonies each for each strain. The average and standard deviation of the three fluctuation tests is plotted.

C Spontaneous recombination rates at the rDNA array in wt (W303R) and *vid22*Δ (YNOV352) cells. All the strains carry an *ADE2* marker integrated into the rDNA array. Recombination rates were calculated by assessing the loss of the *ADE2* marker in the first generation after plating (half sector assay). The average and standard deviation of the three independent experiments is plotted.

Figure 3. Yeast cells deleted for *VID22* are sensitive to DNA damage.

Ten-fold serial dilutions of strains SY2080 (wt) and YNOV108 (*vid22*Δ) were spotted on YPD, Bleomicin, HU, MMS and H_2O_2 plates at the indicated concentrations. Pictures were taken after 3 days of incubation at 28°C.

Figure 4. *VID22* is implicated in the control of G1/S transition.

A Cell cycle progression of wt (SY2080) and *vid22*Δ (YNOV108) strains. Cells were were synchronized in G1 phase with 5 μg/ml α-factor and then released in fresh medium. Samples were taken every 5' and analyzed by flow cytometry. The blue arrow shows the 1C peak which persists in the *vid22*Δ mutant; the red arrow shows the delay in S-phase progression of the *vid22*Δ mutant. To better visualize the S-phase defect of the *vid22*Δ mutant, overlay of the DNA content profiles of the two strains at the crucial timepoints are also shown.

B Cell cycle profile after nocodazole arrest. Exponentially growing cultures of strains SY2080 (wt) and YNOV108 (*vid22*Δ) were arrested in M phase with 4 μg/ml nocodazole for 3h and analyzed by flow cytometry.

C List of genes involved in G1/S transition and replication initiation which were found downregulated in a *vid22*Δ strain.

Figure 5. A proposed model for the mechanism leading to genome instability in the absence of *VID22*.

A In a wt strain, Vid22 ensures (directly or indirectly) proper expression of genes promoting G1/S transition. A positive feedback loop regulates the expression of *CLN1* and *CLN2* genes, which in turn are responsible for timely and robust expression of the so-called G1/S regulon, among which are many genes governing replication initiation. In particular, this ensures proper levels of Cdc45, a key component of the pre-initiation complex (pre-IC). Vid22 is also required for the adequate expression of *CDC6*, encoding for another key factor involved in replication origin licencing. Finally, efficient G1/S regulon expression provides enough CDK1/Clb6 complex, which controls replication origin firing by phosphorylating key replication factors. Altoghether, these mechanisms ensure timely and efficient G1/S transition.

B In a *vid22*Δ strain, G1/S regulon expression is incoherent and insufficient. The positive feedback involving G1 cyclins is likely abrogated; *PCL1*, which could partially compensate for Cln1 and Cln2 reduced levels, is poorly expressed; lower amounts of Cdc6 and Cdc45 are available for pre-replicative complex (pre-RC) and pre-initiation complex (pre-IC) formation; moreover, defective expression of *CLB6* gene results in reduced activity of CDK1/Clb6 complex. Depending on the stochastic cell-to-cell variability, these defects may result in absolute impairment of origin firing and subsequent unbudded arrest at the G1/S transition (bottom left), or in perturbed and insufficient origin firing, leading to genomic instability (bottom right).

Tables

Table 1. Strains used in this study

Strain name	Relevant genotype	Source
YNOV42	*MATα can1Δ::MFA1pr-HIS3 mfα1Δ::MFα1pr-LEU2 lyp1Δ leu2Δ0 his3Δ1 ura3Δ0 met15Δ0 LYS2*$^{+}$pFL82.4 [*GAL-DDC2*]	This study
YNOV46	*MATα can1Δ::MFA1pr-HIS3 mfα1Δ::MFα1pr-LEU2 lyp1Δ leu2Δ0 his3Δ1 ura3Δ0 met15Δ0 LYS2*$^{+}$pNOV1.4 [vector]	This study
BY4741	*MAT***a** *his3Δ1 leu2Δ0 met15Δ0 ura3Δ0*	Euroscarf
YNOV920	BY4741 pRS426 [vector]	This study
YNOV921	BY4741 pFL60.1 [*GAL-DDC2*]	This study
YNOV922	BY4741 *vid22Δ::KANMX6* pRS426 [vector]	This study
YNOV923	BY4741 *vid22Δ::KANMX6* pFL60.1 [*GAL-DDC2*]	This study
SY2080	*MAT***a** wt	M. Foiani
YNOV108	*MAT***a** *vid22Δ::KANMX6*	This study
DMA3420	BY4741 *vid22Δ::KANMX6*	This study
W303R	*MAT***a** *RDN1::ADE2*	L. Guarente
YNOV352	*MAT***a** *RDN1::ADE2 vid22Δ::KANMX6*	This study

Figure 1

A

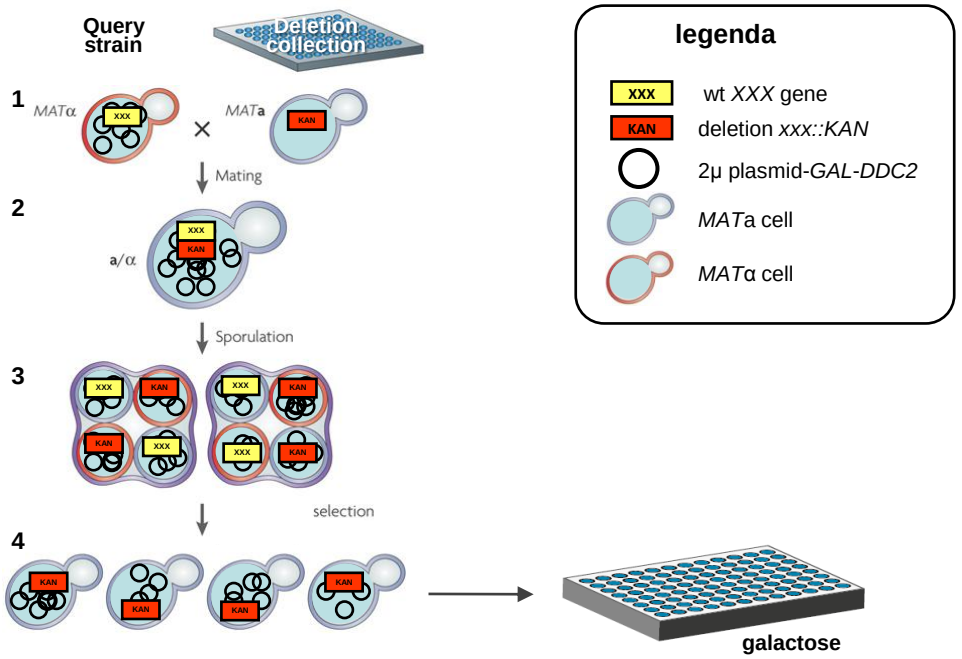
Query strain
Deletion collection
1
MATα
MATa
Mating
2
a/α
Sporulation
3
selection
4
galactose
legenda
wt XXX gene
deletion xxx::KAN
2µ plasmid-GAL-DDC2
MATa cell
MATα cell

B

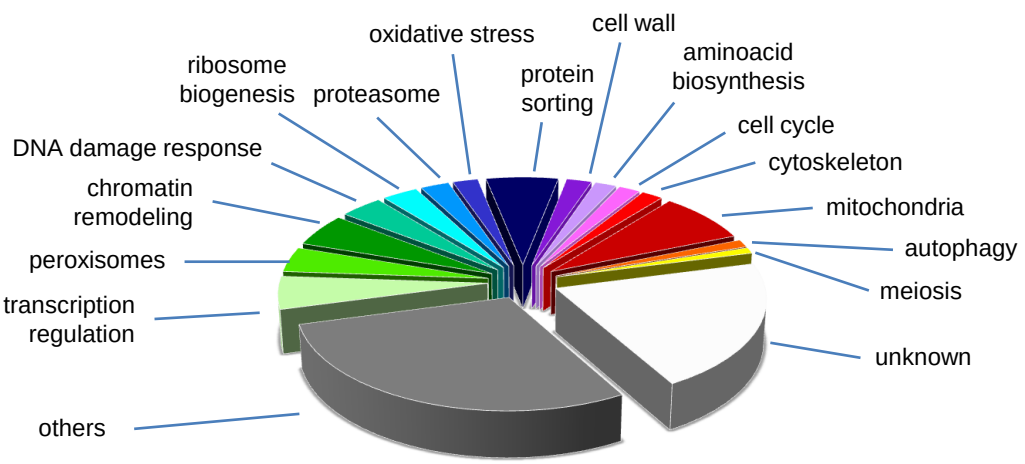
oxidative stress
cell wall
ribosome biogenesis
proteasome
protein sorting
aminoacid biosynthesis
DNA damage response
cell cycle
chromatin remodeling
cytoskeleton
mitochondria
peroxisomes
autophagy
meiosis
transcription regulation
unknown
others

C

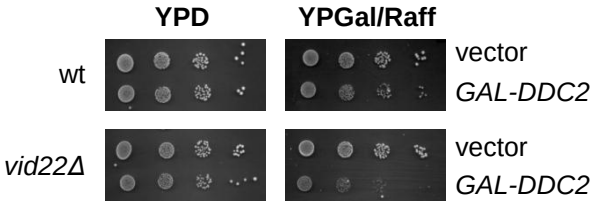
YPD
YPGal/Raff
wt
vector
GAL-DDC2
vid22Δ
vector
GAL-DDC2

Figure 2

A

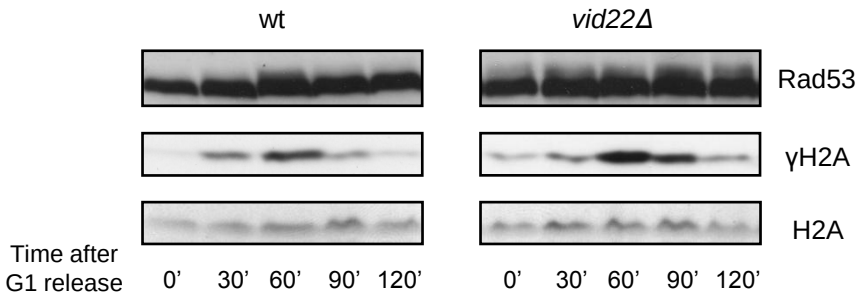
wt
vid22Δ
Rad53
γH2A
H2A
Time after
G1 release
0’ 30’ 60’ 90’ 120’
0’ 30’ 60’ 90’ 120’

B

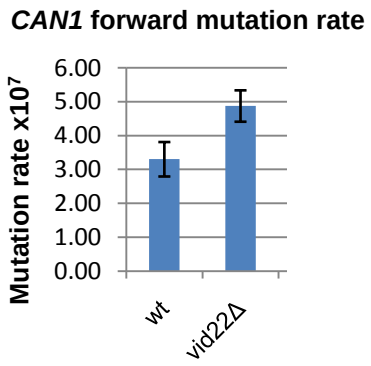
CAN1 forward mutation rate
Mutation rate x10⁷
6.00
5.00
4.00
3.00
2.00
1.00
0.00
wt
vid22Δ

C

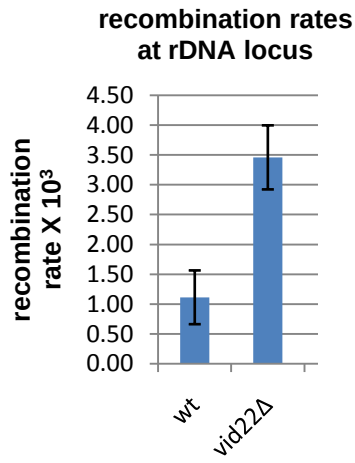
recombination rates
at rDNA locus
recombination
rate X 10³
4.50
4.00
3.50
3.00
2.50
2.00
1.50
1.00
0.50
0.00
wt
vid22Δ

Figure 3

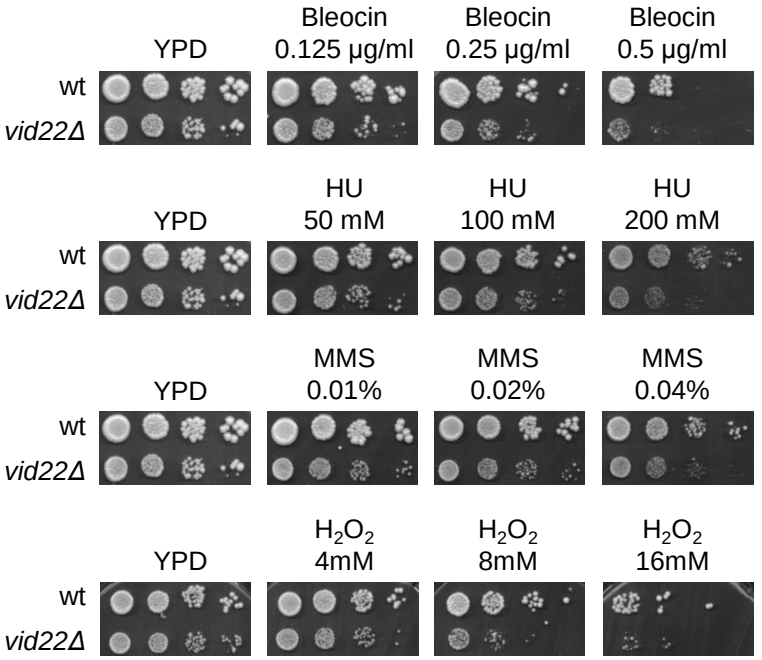
YPD
Bleocin 0.125 µg/ml
Bleocin 0.25 µg/ml
Bleocin 0.5 µg/ml
wt
vid22Δ
YPD
HU 50 mM
HU 100 mM
HU 200 mM
wt
vid22Δ
YPD
MMS 0.01%
MMS 0.02%
MMS 0.04%
wt
vid22Δ
YPD
H2O2 4mM
H2O2 8mM
H2O2 16mM
wt
vid22Δ

Figure 4

A

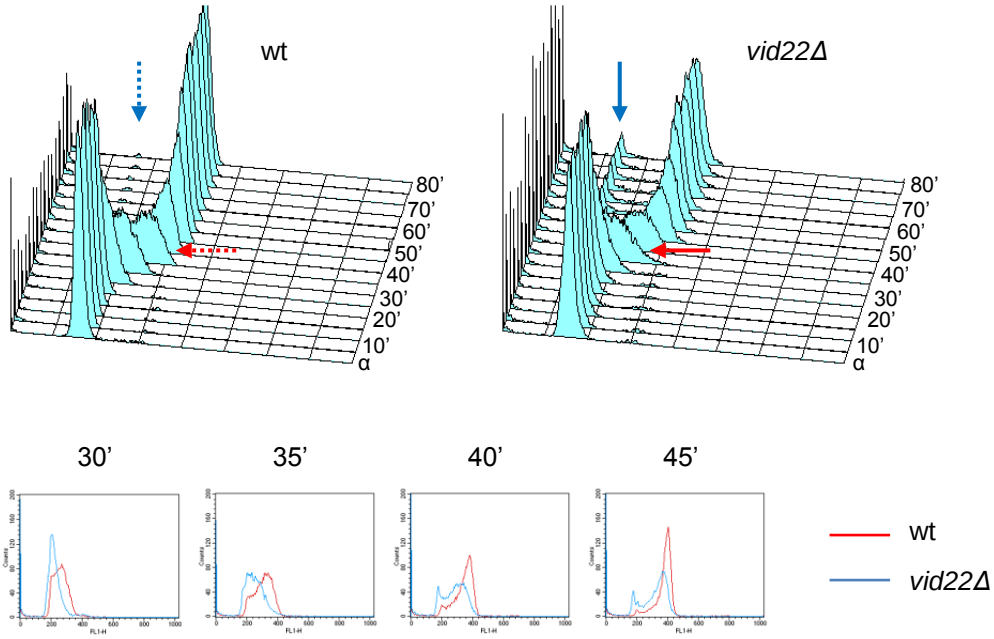

B

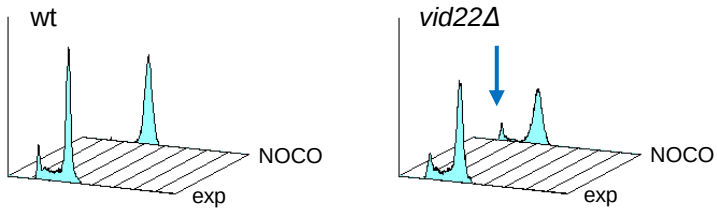

C

ORF	Gene	SGD description
YMR199W	**CLN1**	G1 cyclin involved in regulation of the cell cycle; activates Cdc28p kinase to promote the G1 to S phase transition
YPL256C	**CLN2**	G1 cyclin involved in regulation of the cell cycle; activates Cdc28p kinase to promote the G1 to S phase transition
YNL289W	**PCL1**	Cyclin, interacts with cyclin-dependent kinase Pho85p; member of the Pcl1,2-like subfamily, involved in the regulation of polarized growth and morphogenesis and progression through the cell cycle
YGR109C	**CLB6**	B-type cyclin involved in DNA replication during S phase; activates Cdc28p to promote initiation of DNA synthesis
YJL194W	**CDC6**	Essential ATP-binding protein required for DNA replication, component of the pre-replicative complex (pre-RC)
YLR103C	**CDC45**	DNA replication initiation factor; recruited to MCM pre-RC complexes at replication origins; promotes release of MCM from Mcm10p, recruits elongation machinery

Figure 5

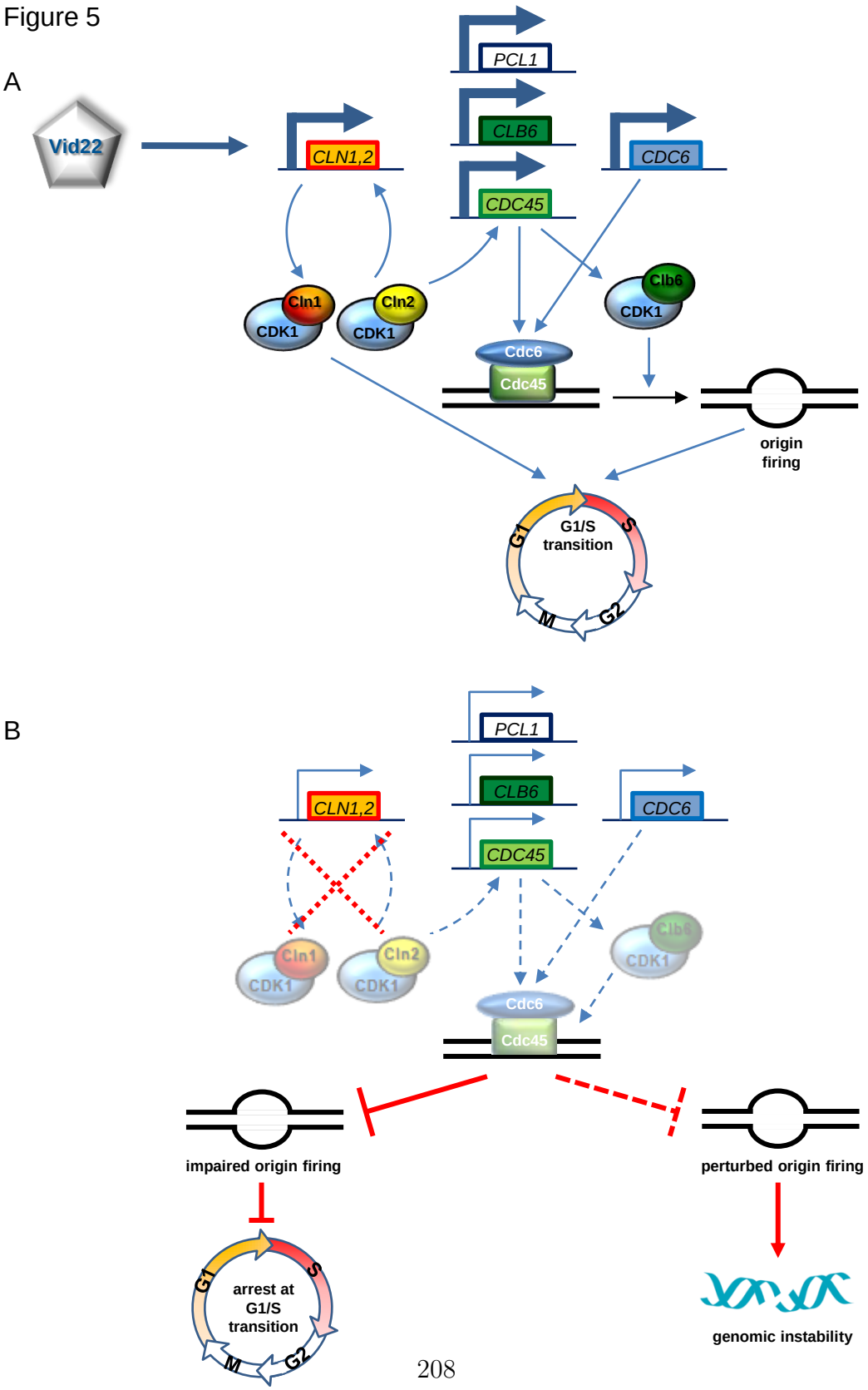
A
Vid22
CLN1,2
PCL1
CLB6
CDC6
CDC45
Cln1
CDK1
Cln2
CDK1
Clb6
CDK1
Cdc6
Cdc45
origin
firing
G1
G1/S
transition
S
M
G2
B
CLN1,2
PCL1
CLB6
CDC6
CDC45
Cln1
CDK1
Cln2
CDK1
Clb6
CDK1
Cdc6
Cdc45
impaired origin firing
perturbed origin firing
G1
arrest at
G1/S
transition
S
M
G2
genomic instability

Supporting information

Supplementary figures

Figure S1. Overexpression of *DDC2* increases sensitivity to exogenous or endogenous DNA damage.

A Ten-fold serial dilutions of strains YNOV46 (wt, vector) and YNOV42 (wt, *GAL-DDC2*), were were spotted on YPGal/Raff medium to induce *DDC2* overexpression and on YPD as a control. The plates were either mock or UV irradiated (50 J/m^2). Pictures were taken after 4 days of incubation at 28°C.

B *rad18*Δ, *rad27*Δ, *mre11*Δ and *slx8*Δ strains were transformed with centromeric plasmid pFL57.1 (*GAL-DDC2*) or pRS314 (vector) and cell viability after of *DDC2* overexpression was tested as described in Fig. 1C.

C *rad18*Δ, *mre11*Δ and *slx8*Δ strains were transformed with multicopy plasmid pFL58.1 (*GAL-DDC2*) or pRS424 (vector) and cell viability after of *DDC2* overexpression was tested as described in Fig. 1C.

Figure S2. Vid22 protein localizes in the nucleus.

Immunolocalization of Vid22-3HA in exponentially growing cells: Vid22-3HA was detected with an anti-HA antibody, while DAPI staining marks the nucleus.

Figure S3. Overview of the genetic interactions of *VID22*.

Negative (**A**) and positive (**B**) genetic interactions of *VID22* obtained from genome wide SGA experiments ([30] and Charlie Boone, unpublished data) are shown. Colors and labels display the results of GO-enrichment analysis.

Figure S4. Yeast cells deleted for *VID22* are not sensitive to UV or camptothecin.

A Ten-fold serial dilutions of strains SY2080 (wt) and YNOV108 (*vid22*Δ) were spotted on YPD and mock or UV-irradiated at the indicated doses. Pictures were taken after 3 days of incubation at 28°C.

B Ten-fold serial dilutions of strains SY2080 (wt) and YNOV108 (*vid22*Δ) were spotted on YPD/DMSO or CPT plates at the indicated concentrations. Pictures were taken after 3 days of incubation at 28°C.

Figure S5. Yeast cells deleted for *VID22* are not defective in DNA damage checkpoint activation and switch-off.

A Exponentially growing cultures of strains SY2080 (wt) and YNOV108 (*vid22*Δ) were arrested in G1 phase with 10 µg/ml α-factor and then 50 µg/ml Bleomicin was added to the cultures. Checkpoint activation was monitored at the indicated timepoints by SDS-page and western blotting with antibodies anti-Rad53.

B Exponentially growing cultures of strains SY2080 (wt) and YNOV108 (*vid22*Δ) were arrested in M phase with 20 µg/ml nocodazole; Bleomicin treatment and checkpoint activation was analyzed as described in Fig. S5-A.

C Exponentially growing cultures of strains SY2080 (wt) and YNOV108 (*vid22*Δ) were synchronized in G1 phase with 5 µg/ml α-factor and then released in 25 mM HU. Checkpoint activation at the indicated timepoints was monitored as described in Fig. S5-A.

D Exponentially growing cultures of strains SY2080 (wt) and YNOV108 (*vid22*Δ) were synchronized in G1 phase with 5 µg/ml α-factor and then released in 0,02% MMS. Checkpoint activation at the indicated timepoints was monitored as described in Fig. S5-A.

E Exponentially growing cultures of strains SY2080 (wt) and YNOV108 (*vid22*Δ) were synchronized in G1 phase with 5 µg/ml α-factor and then treated with 200 mM HU for 1h, after which they were released in fresh medium. Checkpoint activation status was monitored as described in Fig. S5-A.

Figure S1

A

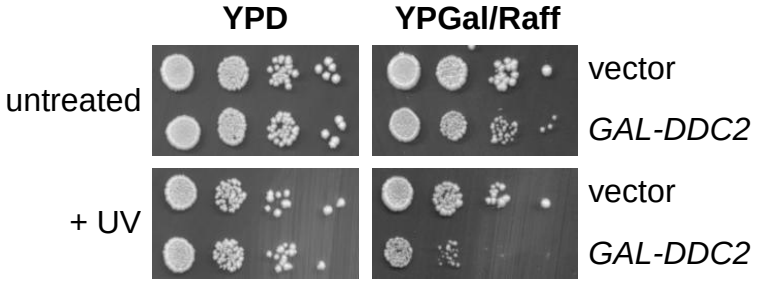

B

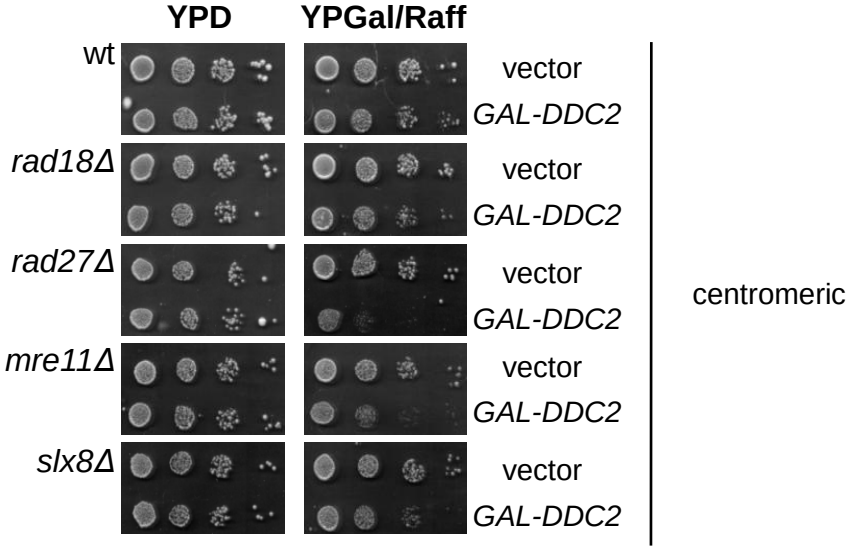

C

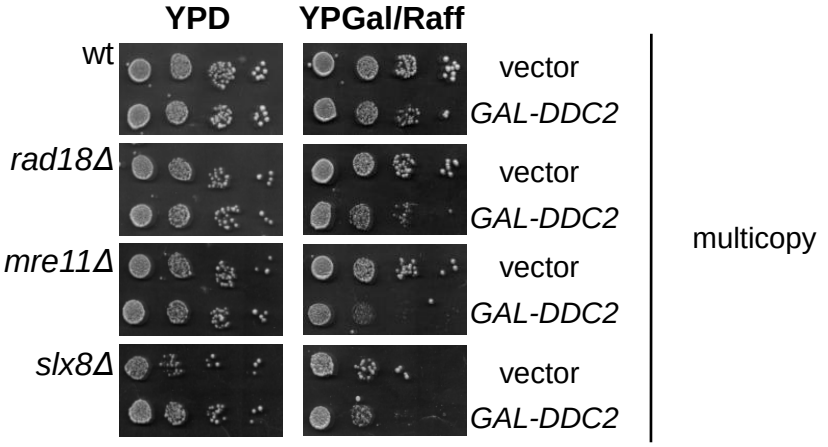

Figure S2

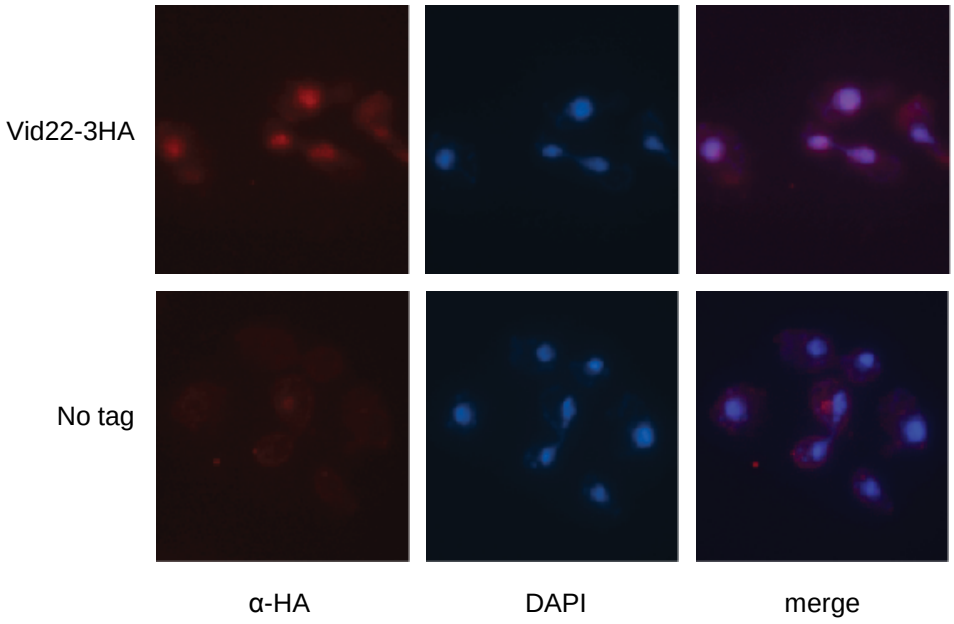

Figure S3

A

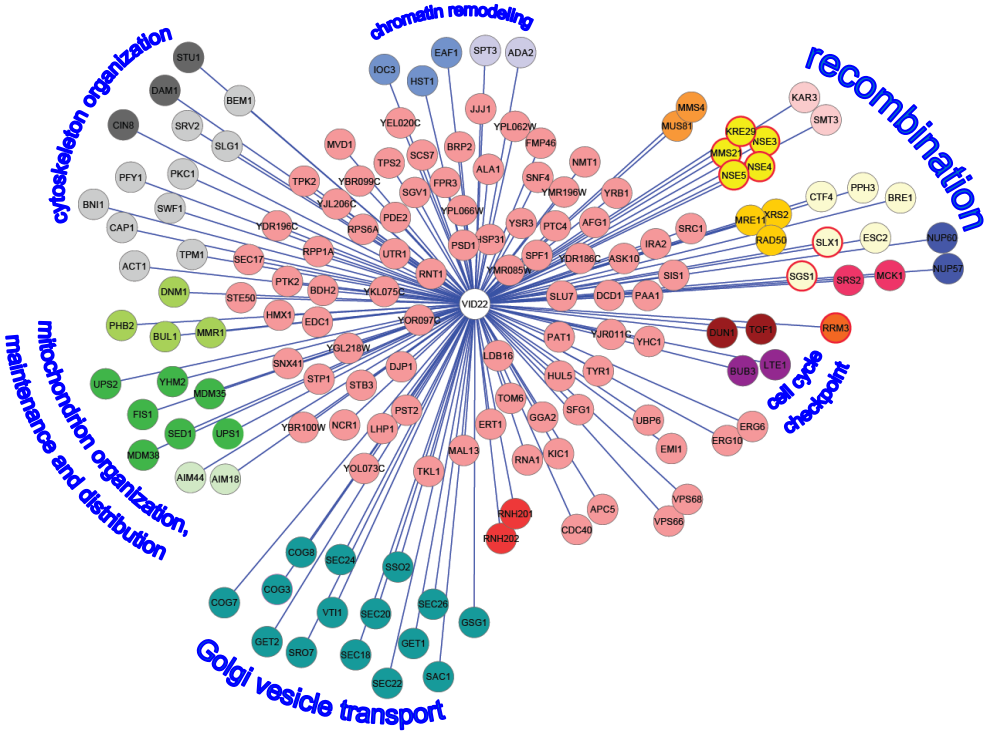
chromatin remodeling
recombination
cytoskeleton organization
mitochondrion organization, maintenance and distribution
cell cycle checkpoint
Golgi vesicle transport
VID22

B

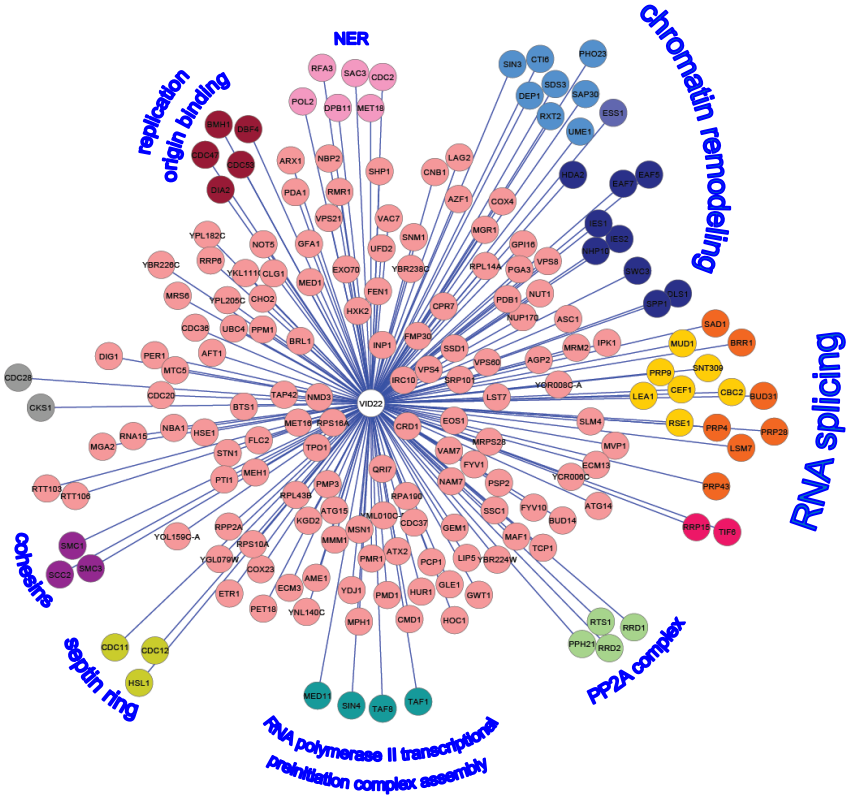
NER
chromatin remodeling
replication origin binding
RNA splicing
cohesine
septin ring
PP2A complex
RNA polymerase II transcriptional preinitiation complex assembly
VID22

Figure S4

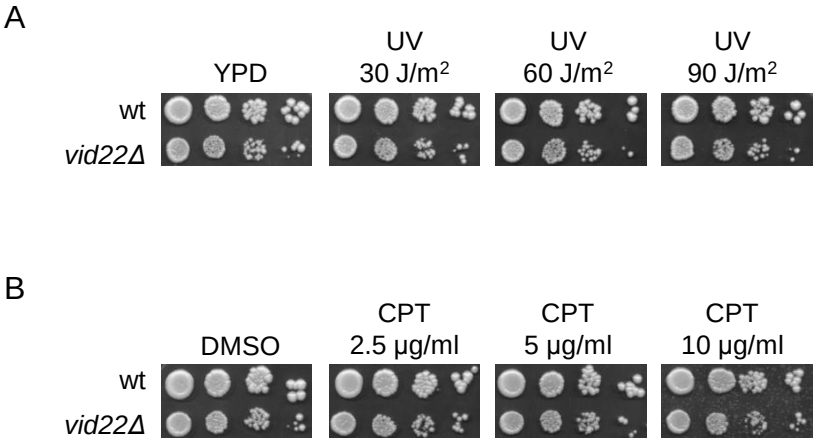
A
YPD
UV
30 J/m2
UV
60 J/m2
UV
90 J/m2
wt
vid22Δ
B
DMSO
CPT
2.5 µg/ml
CPT
5 µg/ml
CPT
10 µg/ml
wt
vid22Δ

Figure S5

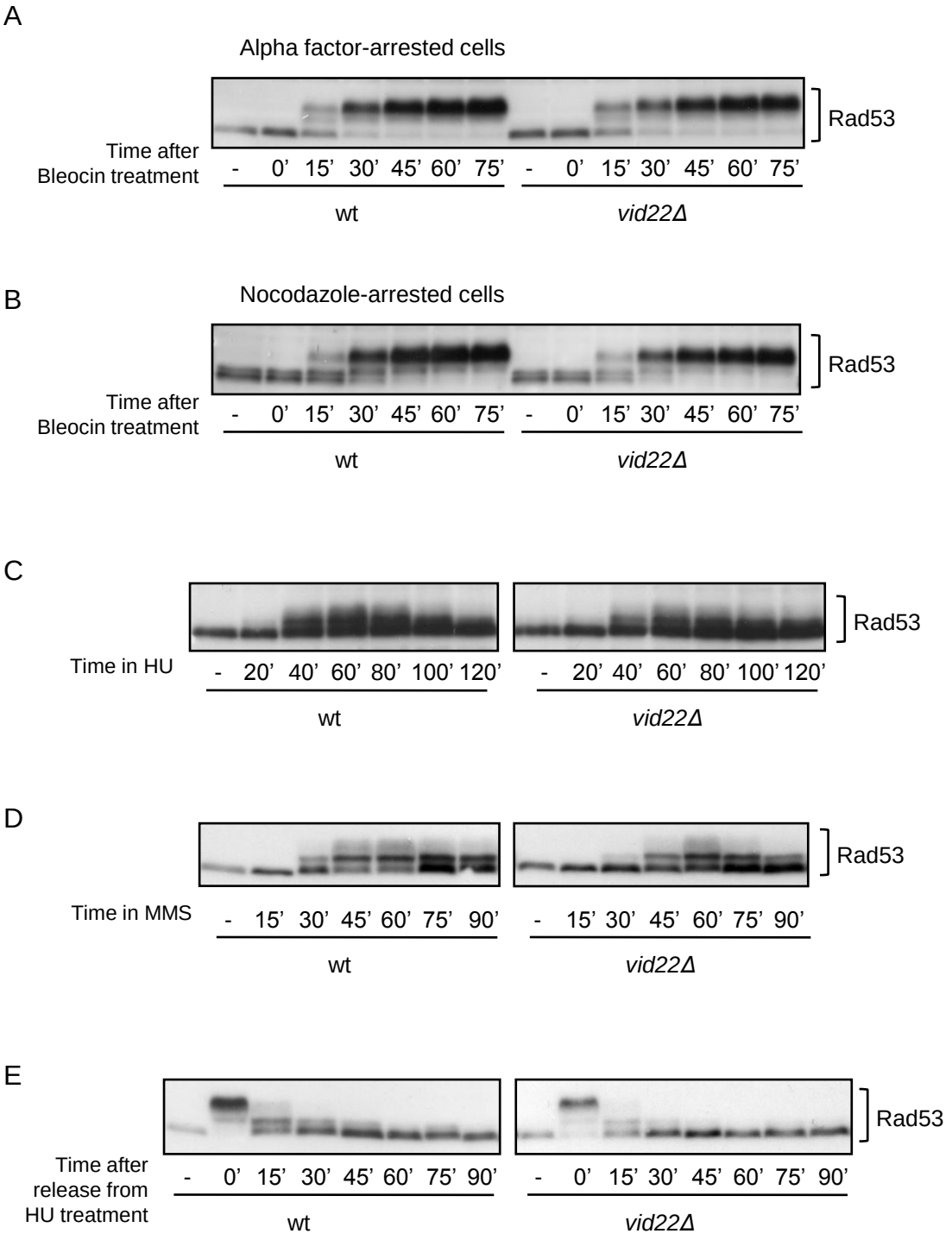
A
Alpha factor-arrested cells
Rad53
Time after Bleocin treatment
- 0' 15' 30' 45' 60' 75' - 0' 15' 30' 45' 60' 75'
wt
vid22Δ
B
Nocodazole-arrested cells
Rad53
Time after Bleocin treatment
- 0' 15' 30' 45' 60' 75' - 0' 15' 30' 45' 60' 75'
wt
vid22Δ
C
Rad53
Time in HU
- 20' 40' 60' 80' 100' 120' - 20' 40' 60' 80' 100' 120'
wt
vid22Δ
D
Rad53
Time in MMS
- 15' 30' 45' 60' 75' 90' - 15' 30' 45' 60' 75' 90'
wt
vid22Δ
E
Rad53
Time after release from HU treatment
- 0' 15' 30' 45' 60' 75' 90' - 0' 15' 30' 45' 60' 75' 90'
wt
vid22Δ

Supplementary materials & methods

Supplementary strains and plasmids

Supplementary strains are listed in Table S1.

Plasmid pFL57.2 and pFL58.2 were obtained by cloning *DDC2* open reading frame under the *GAL1* promoter in centromeric vector pRS314 and multicopy vector pRS324, respectively.

In situ immunofluorescence of yeast cells

1 ml cells were fixed 15' at room temperature with fixation buffer (3.7% formaldehyde, 0.1 M K-phosphate pH 6.4, 0.5 mM $MgCl_2$); samples were washed three times with wash buffer (0.1 M K-phosphate pH 6.4, 0.5 mM $MgCl_2$) and one time with spheroplasting solution (1.4 M sorbitol, 0.1 M K-phosphate pH 6.4, 0.5 mM $MgCl_2$), after which they were resuspended in 200 µl of the same buffer. Spheroplasts were prepared using 5 µl of 1 mg/ml zymolyase at 37°C, monitoring spheroplastization by microscopic observation, and then washed one time with spheroplasting solution. Spheroplasts were used to prepare a multi-well glass slide for immunofluorescence. For immunodetection, slides were incubated o/n at 4°C with anti-HA primary antibody, and then 2 hours at room temperature with secondary antibody. DNA was stained with DAPI.

Table S1. Supplementary strains

Strain name	Relevant genotype	Source
YFL747	*MAT***a** pRS314 [vector]	This study
YFL741	*MAT***a** pFL57.2 [*GAL-DDC2*]	This study
YFL749	*MAT***a** *rad18*Δ*::KANMX6* pRS314 [vector]	This study
YFL743	*MAT***a** *rad18*Δ*::KANMX6* pFL57.2 [*GAL-DDC2*]	This study
YFL750	*MAT***a** *rad27*Δ*::KANMX6* pRS314 [vector]	This study
YFL744	*MAT***a** *rad27*Δ*::KANMX6* pFL57.2 [*GAL-DDC2*]	This study
YFL751	*MAT***a** *mre11*Δ*::KANMX6* pRS314 [vector]	This study
YFL745	*MAT***a** *mre11*Δ*::KANMX6* pFL57.2 [*GAL-DDC2*]	This study
YFL752	*MAT***a** *slx8*Δ*::KANMX6* pRS314 [vector]	This study
YFL746	*MAT***a** *slx8*Δ*::KANMX6* pFL57.2 [*GAL-DDC2*]	This study
YNOV375	*MAT***a** pRS424 [vector]	This study
YFL783	*MAT***a** pFL58.2 [*GAL-DDC2*]	This study
YNOV359	*MAT***a** *rad18*Δ*::KANMX6* pRS424 [vector]	This study
YFL785	*MAT***a** *rad18*Δ*::KANMX6* pFL58.2 [*GAL-DDC2*]	This study
YNOV361	*MAT***a** *mre11*Δ*::KANMX6* pRS424 [vector]	This study
YFL787	*MAT***a** *mre11*Δ*::KANMX6* pFL58.2 [*GAL-DDC2*]	This study
YNOV362	*MAT***a** *slx8*Δ*::KANMX6* pRS424 [vector]	This study
YFL788	*MAT***a** *slx8*Δ*::KANMX6* pFL58.2 [*GAL-DDC2*]	This study
YNOV120	*MAT***a** *VID22-3HA::HIS3MX6*	This study

Supplementary data

Supplementary figure 1

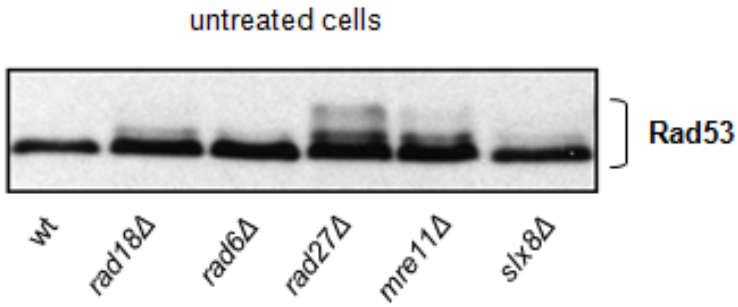

Yeast strains deleted for genes known to be involved in genome stability display a chronic Rad53 psopshorylation.
Protein extracts were prepared from exponentially growing cultures of the indicated strains and the phosphorylation status of Rad53 was analyzed by SDS-page and western blotting with antibodies anti-Rad53.

Supplementary figure 2

The key catalytic Asp residues do not seem to be conserved in the RNase H fold of Vid22. Secondary structure-based aligment of the RNase H fold of Vid22 and Hermes transposase was performed with the Phyre2 server. The key catalytic Asp residues of Hermes are highlighted with red circles; blue arrows mark the corresponding positions on Vid22 sequence.

Supplementary figure 3

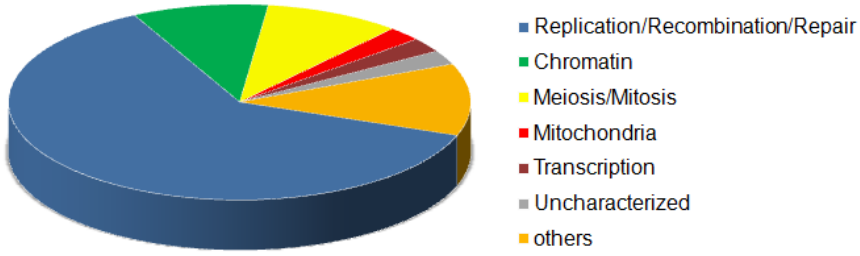

Overview of the negative trigenic genetic interactions involving yeast RNase H1 and RNase H2.
The SGA technology was used to identify the genetic interactors of a *rnh1Δ rnh201Δ* query strain, both in unperturbed conditions and with 10mM or 25 mM HU treatment. A summary of the biological functions of the interactions overall identified is shown.